UNIVERSITY OF BIRMINGHAM

A Tale of Nitrogen Cycling in Two Free Air CO_2 Enrichment (FACE) Experiments: BIFoR-FACE and EucFACE

By

Manon Rumeau

A Thesis Submitted to the University of Birmingham for the degree of

DOCTOR OF PHILOSOPHY

School of Geography, Earth and Environmental Sciences

College of Life and Environmental Sciences

University of Birmingham

October 2024

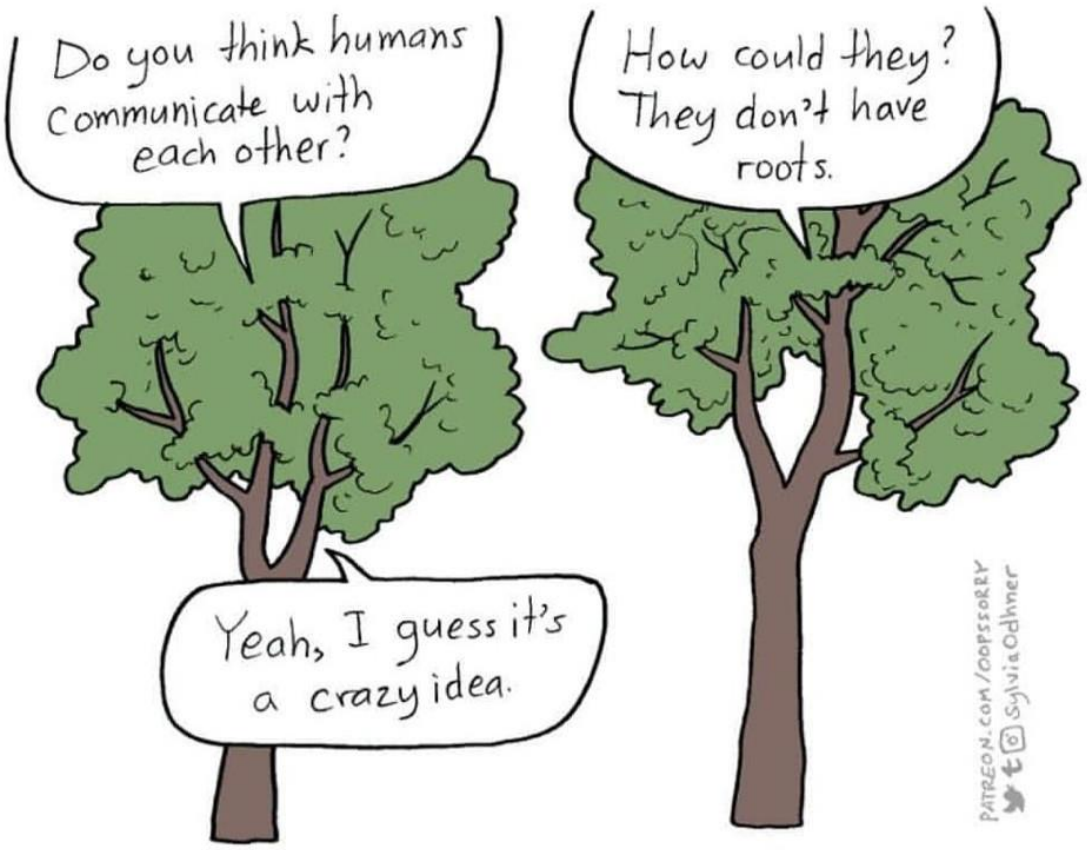
Do you think humans communicate with each other?
How could they? They don't have roots.
Yeah, I guess it's a crazy idea.
PATREON.COM/OOPSSORRY
SylviaOdhner

Abstract

The constraint of tree growth under elevated atmospheric CO_2 (eCO_2) concentration by limiting soil nutrients, particularly nitrogen (N) in temperate ecosystems, can reduce projected carbon (C) storage from 25% to 75%. This uncertainty arises from the lack of experimental data on mature forests that experience stronger nutrient limitation than young forest ecosystems which have been studied to date. Therefore, it is essential to evaluate how eCO_2 will affect nutrient transformations and availability in mature forest soils to assess if tree N demands can be met under eCO_2. The purpose of this research was to evaluate the response of soil N cycling processes to eCO_2 in two contrasting mature forests; in a N-limited deciduous temperate forest dominated by 180-year-old oak (*Quercus robur* L.) trees in the UK, and in a phosphorus (P)-limited Eucalyptus (*Eucalyptus* L.) dominated forest in Australia. This study seeks to identify the mechanisms by which forest ecosystems may modulate N availability under eCO_2, understand the interactions between C, N and P cycling and provide experimental data to predict nutrient constraints to the CO_2 fertilization effect under future CO_2 enriched atmospheres.

The research was conducted in two Free Air Carbon Dioxide Enrichment (FACE) facilities: Birmingham Institute of Forest Research (BIFoR) FACE located near Birmingham, UK, and EucFACE in New South Wales, Australia. Furthermore, EucFACE was fertilized with P to momentarily alleviate/reduce P limitation. We employed a ^{15}N labelling approach to measure N transformations (i.e. gross mineralization, depolymerization, N fixation, nitrification and denitrification). When possible, methods were adapted for *in-situ* measurements to preserve roots and soil structure whilst introducing newly adopted ^{15}N labelling techniques.

At BIFoR-FACE, we found a ~30% increase in net and gross *in-situ* N mineralization, delivering an extra 26 kg N ha^{-1} y^{-1}, meeting the higher N uptake from trees estimated at 10 kg N ha^{-1} y^{-1}. Organic and inorganic N-mining via primed microbial activity were especially enhanced in

the rhizosphere suggesting a stronger rhizosphere priming effect (RPE) under eCO_2. Furthermore, the tenfold difference in N mineralization rates between rhizosphere and bulk soils suggests that by expanding the rhizosphere relative volume, trees under eCO_2 may be able to meet higher N demand. Conversely, gross nitrification was downregulated at the macro-scale due to higher fine root biomass reducing nitrification hot-spots, and, at the micro-scale of the rhizosphere suggesting a N conservation strategy by trees. Moreover, an additional experiment simulating changes in root exudate composition highlighted that N-mining enhancement under eCO_2 was driven by the increase in exudate C:N ratio rather than the amount of C added, challenging the original theory focusing RPE mainly on C input. Therefore, at BIFoR-FACE, a faster and tighter N cycle facilitated by plant-soil interactions and N conservation strategies at the ecosystem scale supported C biomass gains under eCO_2 after six years of enrichment. However, with declining N deposition and a high soil C:N ratio, BIFOR FACE sits at a tipping point where microbes could start outcompeting trees for N resources with a likelihood of N limitation in the long run.

In contrast, nutrient cycling at EucFACE, in a highly P-limited forest, showed a very different response. No sign of a higher C allocation belowground was detected as root biomass was lower under eCO_2 in the 0-10 cm layer. N-mining remained largely unaffected under eCO_2 despite the observed accumulation of soil nitrate. C, N and P mining were coupled together and slowed down with P fertilization. But this decrease was partly offset under eCO_2 suggesting that P fertilization initiated a faster C, N, P cycling under eCO_2.

Taken together, results from this research indicate that the response of mature forests to eCO_2 is not consistent but rather depends on which nutrient is limiting forest growth and likely the degree of nutrient limitation. These diverging responses highlight that predicting global C storage of mature forests requires either the multiplication of such experimental facilities to cover the diversity of forests worldwide; or a deeper understanding of the mechanisms behind forest response to eCO_2; or both.

Acknowledgment

First, I would like to thank all my supervisors. To Sami Ullah who has been following me from the start, from helping me in the field to reading my papers repeatedly. To Rob MacKenzie, who despite not being a “nitrogen person” followed my work and challenged my thinking. To Fotis Sgouridis who even though wasn’t in the original project, stepped up and allowed this work to happen – thanks for your time and patience to analyse my hundreds and hundreds of samples. To Michaela Reay, for all your help at the beginning of my PhD, and for teaching me good lab practices. And finally, thanks to Yolima Carrillo, for your warm welcome in Australia and your supervision during this project.

Thanks to all the technicians at BIFOR FACE facility, Kris Hart, Peter Miles, Gael Denny, Tom Downes and Nick Harper, who make our work possible in such an amazing facility and to all principal investigators of the QUINTUS team, Ian P. Hartley, Andy Smith, Emma Sayer and Liz Hamilton who provided a lot of support in the writing phase. I also want to thank the QUINTUS lab technicians, Robert Grzesik, James Gore and Georges Fereday, for all your help and assistance in the lab and for making the lab such a lively and friendly environment that is hard to leave to go write! And special shout out to James, for going out of your way and training us over and over on the lab instruments. I also want to thank the Biosciences side of BIFOR, thanks for welcoming me in your lab and thanks Vanja for almost making me a microbiologist! Thanks to all the people within BIFOR who make BIFOR such a dynamic institute, with a special thanks to Deanne Brettle for all your support and Samantha Dobbie for giving me so many fun public outreach opportunities.

But my PhD journey wasn’t just about fieldwork and labwork and repeat; it was also about the amazing people I shared it with. To PhD family who made this experience feel like a second ERASMUS adventure, from our Mojito Mondays to our different trips across the UK and abroad. To all the Bratby’s drinks for every time someone went on holiday, had a paper

accepted or rejected or just because it was time for a drink Thank you for sharing this journey with me and for being there every time I cried because my experiment failed (again) (Gianni tmtc). Thanks to Adria (our partying Spanish), Lisa (literally our mom!), Gianni (the bestie, nitrogen buddy and so much more), Andrea (our always busy Italian), Alex (our only-by-look homeless guy), Aaron (my favourite bee guy), Jess (our crazy story Jess'), Grace (second mom ?), Annabelle (our UoB migrant). And so much more who shared this journey with me!

Thanks to my family, to my parents, to my sisters especially who never asked but always have to listen to me talking about my research. Thanks for supporting through anything and despite my choices and always telling me that I was smart enough!

Despite ups and downs, my PhD felt like an awesome experience which made me fall in love with the world of science and research! So, thanks again Sami for choosing me and trusting me with this amazing project.

Declaration

This thesis has not been submitted for a degree at this or in any other institution. This thesis is the result of my own work with the help of my supervisors or collaborators which names figure in the appropriate chapters. This work was funded by the UKRI NERC Large grants- Quinquennial (half-decadal) carbon and nutrient dynamics in temperate forests: Implications for carbon sequestration in a high carbon dioxide world (QUINTUS; NE/S015833/1), a NERC Discovery grants- FACE underground: can trees in mature forests gain greater access to soil nutrients under elevated atmospheric CO2? (NE/T000449/1) and a Royal Society International Exchange grant (IES\R3\213025).

Contents

Chapter 1. Introduction 22

1.1. Forests, powerful allies for climate change mitigation 22

1.2. Progressive nitrogen limitation under eCO_2 24

1.3. Nitrogen cycling in temperate forest ecosystem 25

1.4. Nitrogen external flux 26

1.4.1. New nitrogen in the ecosystem 26

1.4.2. Nitrogen losses 28

1.4.3. Nitrogen recycling within the ecosystem 29

1.4.4. Tree control of nitrogen cycling in the rhizosphere 31

1.5. How might eCO_2 influence the nitrogen cycle? 32

1.5.1. Diverging responses of N mining to eCO_2 32

1.5.2. Knowledge gaps on the response of free-living nitrogen fixation, nitrification, and denitrification to eCO_2 33

1.5.3. Effect of eCO_2 on rhizosphere priming effect 34

1.6. Experimental sites: BIFOR FACE and EucFACE 35

1.7. Assessment of N cycling processes: methods based on ^{15}N stable isotope 38

1.8. Aims and thesis layout 39

1.9. Key hypotheses 40

Chapter 2. Enhanced soil nitrogen transformation supports biomass C gains in a mature forest under elevated CO_2 42

2.1. Introduction 45

2.2. Material and Methods 47

2.2.1. Experimental set-up 47
2.2.2. Soil nutrient pools 48
2.2.3. Net nitrogen mineralisation 49
2.2.4. *In-situ* gross mineralization and N_2O emissions 49
2.2.5. Lab measurement of N_2 flux under artificial atmosphere 51
2.2.6. Nitrogen fixation 51
2.2.7. Nitrogen mass balance 52
2.2.8. Statistical analyses 52
2.3. Results & Discussion 53
2.3.1. Upregulation of N mineralization 53
2.3.2. Seasonal effects of eCO_2 on N mineralization 56
2.3.3. A faster yet tighter N cycle under eCO_2 58
2.4. Conclusion 59
2.5. Supplementary materials 61
Chapter 3. The role of rhizosphere in enhancing N availability in a mature forest under eCO_2 67
3.1. Introduction 70
3.2. Material & Methods 73
3.2.1. Experimental set up 73
3.2.2. Soil sampling 74
3.2.3. Nutrient standing pools analysis 75
3.2.4. ^{15}N isotopic pool dilution combined with the ^{15}N Gas Flux method 77
3.2.5. Enzyme assays 80

3.2.6. Net N mineralisation 82
3.2.7. Statistical analyses 82
3.3. Results 83
3.3.1. Soil nutrient standing pools 83
3.3.2. Nitrogen and carbon fluxes 85
3.3.3. Soil enzyme activities and stoichiometries 89
3.4. Discussion 90
3.5. Conclusion 93
3.6. Supplementary materials 95
Chapter 4. Root exudate stoichiometry has a stronger effect on N cycling than root exudate quantity 103
4.1. Introduction 106
4.2. Methods 109
4.2.1. Experimental design 109
4.2.2. Exudate solutions and delivery 110
4.2.3. Soil sampling 111
4.2.4. Nutrient contents 111
4.2.5. Potential gross N transformations 112
4.2.6. Statistical analyses 113
4.3. Result 114
4.3.1. Organic and inorganic soil N concentrations 114
4.3.2. Effect of exudates on N cycling rates 115
4.3.3. Effect of microbial exclusion on N cycling rates 116

4.3.4. Comparison of the effect of exudate quantity vs quality 117

4.4. Discussion 118

4.5. Conclusion 121

Chapter 5. Soil microbial limitation shifts in response to elevated CO_2 and P fertilization in a Eucalyptus forest 123

5.1. Introduction 126

5.2. Materials and Methods 128

5.2.1. Experimental site 128

5.2.2. Phosphorus fertilization treatment 128

5.2.3. Sampling 129

5.2.4. Soil and microbial nutrient pools 130

5.2.5. ^{15}N pool dilution assays 131

5.2.6. Soil enzyme activities and microbial C and P use efficiency 133

5.2.7. Ion-exchange resins 134

5.2.8. Statistical analyses 135

5.3. Results 136

5.3.1. Effect of eCO_2 136

5.3.2. Effect of P fertilization 139

5.4. Discussion 144

5.4.1. eCO_2 increases soil nitrate pool in the top 10 cm 144

5.4.2. P fertilization reduce SOM and N availability 145

5.4.3. Faster nutrient cycling under eCO_2 after P addition 146

5.5. Conclusion 147

5.6. Supplementary materials 149

Chapter 6. Conclusion and outlook 155

6.1. Aims and hypothesis 155

6.2. Limitation and future work 160

References 162

List of figures

Figure 1.1: Schematic of C input and losses in a forest ecosystem to calculate the net C uptake. Blue arrows represent C fixation and transport in plant and soil and red arrows represent respiration fluxes. 23

Figure 1.2: Simplified schematic of the N cycle in a deciduous forest ecosystem. All nitrogen fluxes are represented with a blue arrow. Full arrows represent N internal cycling and dashed arrows represent external N cycling. 26

Figure 1.3: A) Conceptual figure showing the enrichment and depletion of bacterial community taxa in the rhizosphere compared to bulk soil from Ling et al. (2022). B) Conceptual figure depicting the direct and indirect pathways of SOM decomposition as driven by exudate composition from Jilling et al. (2018). 31

Figure 1.4: Schematic of the (A) BIFoR-FACE and (B) EucFACE sites. Fumigated arrays are represented in orange and ambient arrays are in blue. 37

Figure 2.1: Nitrogen mass balance under eCO_2 and aCO_2 for the year 2022 in the O-organic layer (depth = 7.5 cm on average). All fluxes are expressed in kg ha^{-1} y^{-1}, positive fluxes are the N inputs and negatives fluxes are the N outputs. 53

Figure 2.2: Soil nutrient pools and gravimetric moisture measured monthly from February 2022 to November 2022. Error bars represent the standard error between replicates (n=15). Green and red bars represent positive and negative eCO_2 effect, respectively, over a period. 55

Figure 2.3: A) Net nitrogen mineralization measured monthly from February 2022 to November 2022. Error bars represent the standard error between replicates (n=15). B) Correlation between net mineralization rate and soil DOC content per season of the year. . 57

Figure 2.4: A) Response ratio of soil CO_2 flux, gross ammonification, gross nitrification, soil N_2O flux and fine root biomass to eCO_2 with p-value of the eCO_2 effect (P_{eCO2}). B) Correlation network using the Pearson correlation index (threshold = 0.5) summarizing correlation over

the 3 campaigns. C) Principal Component Analysis (PCA) plot representing the variable distribution along the dimensions 1 and 2 explaining together 44.7% of the total variability. Variable contributions (contrib) are represented by the darkness of the arrows. 58

Figure 3.1: Schematic of the BIFoR-FACE site from (Hart et al., 2020). Fumigated arrays are represented in orange and ambient arrays are in blue. 74

Figure 3.2: Response ratio (lnRR mean with standard error) of the eCO_2 effect in the bulk (brown) and rhizosphere soil (red) relative to aCO_2 calculated for each variable (gross rates, N_2O emissions and CO_2 respiration are measured from soil incubated with 15N label). A negative response ratio means that eCO_2 decreased that specific variable and a positive value means that eCO_2 increased that variable. 85

Figure 3.3: Ammonium and nitrate dynamics under aCO_2 (blue) and eCO_2 (orange) in rhizosphere and bulk soils. A) Gross mineralization, gross nitrification, ammonium and nitrate consumption where errors bars represent the standard error between replicates (n=9) in August. B) Net mineralization and nitrification in June and August (n=15). C) Rhizosphere relative mass expressed in percentage. Significant differences between treatments, types, or interactions are indicated with an asterisk above the respective groups..... 87

Figure 3.4: A) N_2O emission source partitioned (i.e. denitrification and nitrification and other). Errors bars represent the standard error between replicates (n=9). An asterisk indicates significant differences (p-value <0.05) between treatment for that soil fraction. B) Total N_2O emission correlation with microbial biomass carbon (MBC)..... 88

Figure 3.5: Enzyme activities in nmol g^{-1} h^{-1} in bulk and rhizosphere soils in function of treatments. Error bars represent standard error between replicates (n=9). LAP = leucine amino-peptidase, BG = B-glucosidase, NAG = 1,4-N-acetyl-glucosaminidase, AP = acid phosphatase, PEROX = peroxidase, PHENOX = phenol oxidase. An asterisk indicates significant differences (p-value <0.05) between treatment for that soil fraction. Note the very different magnitudes of activity (i.e., y-axis ranges)..... 90

Figure 4.1: Experimental design's schematics and picture. a) Schematic of one experimental block with the three root exudate treatment plots, showing the location of soil sampling and exclusion bags, b) Picture of one of the automated root exudation systems (ARES), c) Schematical diagram representing the ARES system from Lopez-Sangil et al. (2017)..... 110

Figure 4.2: Nitrogen concentrations in experimental exudate treatments a) in the O-horizon soil and b) in exclusion bags. Letters (a,b) indicate significant difference between treatment for this type soil micro-habitat. Values are means ± SE for n = 4 per treatment. Note the difference in y axis ranges among panels..... 115

Figure 4.3: Ammonium and nitrate production rates, immobilization rates and mean residence time in experimental exudate treatments and exclusion bags. A dashed line separates the O-horizon and exclusion bag soils. Gross nitrification and NO_3^- residence time were not detectable in the O-horizon. Significant effects of treatment, exclusion bags or their interaction at $p < 0.05$ are indicated by an asterisk. Values are mean ± SE for n = 4 per treatment. ... 116

Figure 4.4: Ratio between consumption and production rates for NH_4^+ (NH_4^+ immobilization / gross mineralization) and NO_3^- (NO_3^- immobilization / gross nitrification). A dash line separates the O-horizon soil and the exclusion bag soils. Significant effect of treatment, exclusion bags or their interactions are indicated by a p-value below 0.05 with an asterisk. Values are mean (n=4) ± SE. 117

Figure 4.5: Response ratio of N availability and processes to exudate quantity change (low C:N vs control) and to exudate quality change (high C:N vs low C:N). 118

Figure 5.1: Schematic of A) P addition and sampling time across the three months of the experiment B) the sampling and processing for one FACE ring. 129

Figure 5.2: (A) Nitrate, (B) ammonium and (C) phosphate availabilities measured by IER from December 2021 to June 2023 in the six rings under eCO_2 (orange) and aCO_2 (blue) in both unfertilized (─P) and fertilized (+P) areas. ANOVA p-values are detailed for the effect of eCO_2, time and P-fertilization (Ferti) their interactions. Number in subscript indicate the number of time points considered in the ANOVA. Data are means + SE (n=12). 137

Figure 5.3: Fine root biomass, soil dissolved organic carbon (DOC), soil microbial biomass C (MBC) and N (MBN), gravimetric moisture and inorganic nitrogen content (NH_4^+ and NO_3^-) measured at three times: before fertilization (March), 10 days after fertilization (April) and two months after fertilization (May). ANOVA p-values for the effect of eCO_2 (eCO_2), fertilization (Ferti) and significant interactions are provided for each variable. Number in subscripts indicate the number of time points considered in the ANOVA. Data are means + SE (n=8). 138

Figure 5.4: A) Bray-P concentration, microbial biomass P concentration at three collection times (means +SE). B) Difference in P pools between fertilized and unfertilized plots calculated per plot (ΔBray-P, ΔMBP). C) Microbial biomass ratios: C:N, C:P and N:P. ANOVA p-values for the effect of eCO_2 (eCO_2), fertilization (Ferti) and significant interactions are provided for each variable. Number in brackets indicate the number of time points considered in the ANOVA. 139

Figure 5.5: A) Concentration of 13 amino acids in April and total of the 13 amino acids on the upper right part of the figure (data are means + SE). B) ANOVA test results where asterisk indicate level of significance for each amino acid. 140

Figure 5.6: Ammonium and amino acids production, immobilization, microbial retention and microbial N use efficiency (NUE) in P-fertilized (+P) and non-P-fertilized (-P) plots under aCO_2 (blue) and eCO_2 (yellow) in March, April and May. Data are means + SE (n=8). Min = Mineralization, Imm= Immobilization, Depol = Depolymerization and n.d. = non dimensional. 142

Figure 5.7: Compound specific depolymerization and AA immobilization rates in April. Data are means + SE (n=4). C. S. = compound specific. 143

Figure 5.8: Soil enzymatic activities associated with C (BG, AG, CB, Bxyl), N (NAG, LAP) and P (Pho) cycling before (April) and after P-fertilization (April and May) in P-fertilized (+P) and non-P-fertilized (-P) plots under aCO_2 and eCO_2. Data are means + SE (n=8). 144

Figure 6.1: Conceptual representation of C allocation and feedback on nutrient cycling between at BIFoR-FACE and EucFACE. 158

Figure 6.2: Conceptual diagram representing the growth response of trees depending on N and P availability. EucFACE is located on severely low P soil constraining plant growth while BIFoR-FACE is located on low N soils only preventing optimal growth. 159

List of tables

Table 3.1: Soil nutrient content and microbial biomass in bulk soil and rhizosphere soil under aCO_2 (ambient) and eCO_2 (elevated) and ANOVA test results with p-value below 0.1 highlighted in bold. Mean values and standard errors are indicated for each soil fraction and treatment (n=9). 84

Table 3.2: Primed C and N calculated as the difference in CO_2 respiration and gross mineralization respectively between rhizosphere and bulk soil (mean ± se). ANOVA results for treatment are described on the right part of the table. 87

Table 3.3: Soil microbial respiration and microbial metabolic quotient (qCO_2) (mean ± se). ANOVA results for soil fraction, treatment and the interaction effects are described on the right part of the table. 89

Table 4.1: Exudate cocktail composition expressed in mg L^{-1}. Water treatment contain none of the compounds in the table but contained calcium chloride (0.18 g L^{-1} $CaCl_2$) to maintain consistent ionic strength across treatments. 111

Table 4.2: Statistics from two-way analyses of variance testing the effects of exclusion bag (O-horizon, 41-micron and 1-micron exclusion bags), exudate treatment (low C:N, high C:N, control) and their interactions on soil N pools and transformation rates. Bold typing indicates a significant effect ($P < 0.05$) and underline indicates a marginal effect ($0.1 > P > 0.05$)..... 118

List of abbreviations

N: Nitrogen

C: Carbon

P: Phosphorus

CO_2: Carbon Dioxide

FACE: Free Air Carbon Dioxide Enrichment

BIFoR FACE: Birmingham Institute of Forest Research Free Air Carbon Dioxide Enrichment

EucFACE: Eucalyptus Free Air Carbon Dioxide Enrichment

ARES: Automated Root Exudation System

eCO_2: elevated carbon dioxide concentration

PNL: Progressive Nitrogen Limitation

SOM: Soil Organic Matter

POM: Particulate Organic Matter

MAOM: Mineral Associated Organic Matter

RPE: Rhizosphere Priming Effect

BNF: Biological Nitrogen Fixation

NO_3^-: Nitrate

NH_4^+: Ammonium

FAA: Free Amino Acids

N_2O: Nitrous Oxide

NO: Nitric Oxide

N_2: Dinitrogen

Nr: Reactive Nitrogen

DOC; DON: Dissolve Organic Carbon; Nitrogen

MBC; MBN; MBP: Microbial Biomass Carbon; Nitrogen; Phosphorus

CUE; NUE; PUE: Carbon; Nitrogen; Phosphorus use efficiency

AM: Arbuscular Mycorrhiza

ECM: Ectomycorrhiza

ANOVA: Analysis of Variance

Atom %: atom percentage

APE: 15N atom percentage excess

δ15N: ratio of the two stable isotopes of N (15N/14N) in parts per thousand

GC: Gas Chromatography

EA: Elemental Analyser

IRMS: Isotope Mass Ratio Spectrometry

LC-MS: Liquid Chromatography – Mass Spectrometry

ppm: part per million

RSD: Relative Standard Deviation

QC: Quality Control

lnRR: logarithm of the response ratio

w/v: weight to volume ratio

IER: Ion Exchange Resin

PO_4^{3-}: Phosphate

BG: β-glucosidase

AG: α-glucosidase

Bxyl: β-xylosidase

CB: β-d-cellubiosidase

LAP: leucine amino-peptidase

NAG: β-N-acetyl-glucosaminidase

AP: Acid Phosphatase

PHENOX: Phenol oxidase

PEROX: Peroxidase

Chapter 1. Introduction

1.1. Forests, powerful allies for climate change mitigation

The rise in atmospheric carbon dioxide (CO_2) concentration, from pre-industrial values of about 280 ppm to ~ 415 ppm as of 2024 (NOAA, 2024), is primarily due to fossil fuel consumption and is driving global temperature increases (Lacis et al., 2010). In response to these alarming levels, recent reports from the Intergovernmental Panel on Climate Change (IPCC) emphasized the importance of reducing CO_2 emissions but also the importance of mitigating or offsetting them (IPCC, 2022). Therefore, scientists are turning to nature-based solutions, relying on marine and terrestrial carbon (C) sinks to mitigate unavoidable CO_2 emissions and its build up in atmosphere (Hanson et al., 2020). The main two C sinks are terrestrial plants and oceans, which absorb approximatively 30% and 25%, respectively, of anthropogenic CO_2 emissions (Friedlingstein et al., 2022). These C sinks rely largely on photosynthesis by plant or plankton/algae as well as on CO_2 dissolution in water in the case of ocean ecosystems. Forests contribute to ~ 62% of C sequestration among terrestrial C sinks, making them key players in climate change mitigation (Friedlingstein et al., 2022). Understanding, optimizing, and promoting these natural C sinks has become a new and crucial area of research with the ambition of attenuating and slowing down critical temperature rise (Griscom et al., 2017).

One area of research on optimizing the forest C sink focuses on the "CO_2 fertilization effect" which posits that, as CO_2 is often a limiting reactant of photosynthesis, increased CO_2 concentration enhances photosynthesis which could potentially lead to an increase in C storage of forests (Gardner et al., 2021; Hamilton et al., 2002; Norby et al., 2002). This "CO_2 fertilization effect" triggered a lot of interest in recent decades and has been studied in various ecosystems to understand its potential for its contribution to mitigating climate change as reviewed by Luo et al. (2006). It is now widely recognized that elevated CO_2 (eCO_2) concentration can indeed enhance plant photosynthesis in the short-term (Larcher, 2003).

However, increased photosynthesis may not be sustained on the long term or may not translate in increased productivity (Ellsworth et al., 2017; Norby et al., 2010). Increasing photosynthesis is a necessary condition to increase C storage but it may not be sufficient. Nutrient and/or water availability may prevent direct assimilation of C into biomass (Jiang et al., 2020) or; increased plant respiration rates may indirectly offset the biomass gains (Fig. 1.1) (Hickler et al., 2015; Körner et al., 2005). Therefore, whether rising CO_2 will accelerate forest growth and increase C storage as wood aboveground and/or belowground remains an open question (Hamilton et al., 2002; Norby et al., 2002; Terrer et al., 2021).

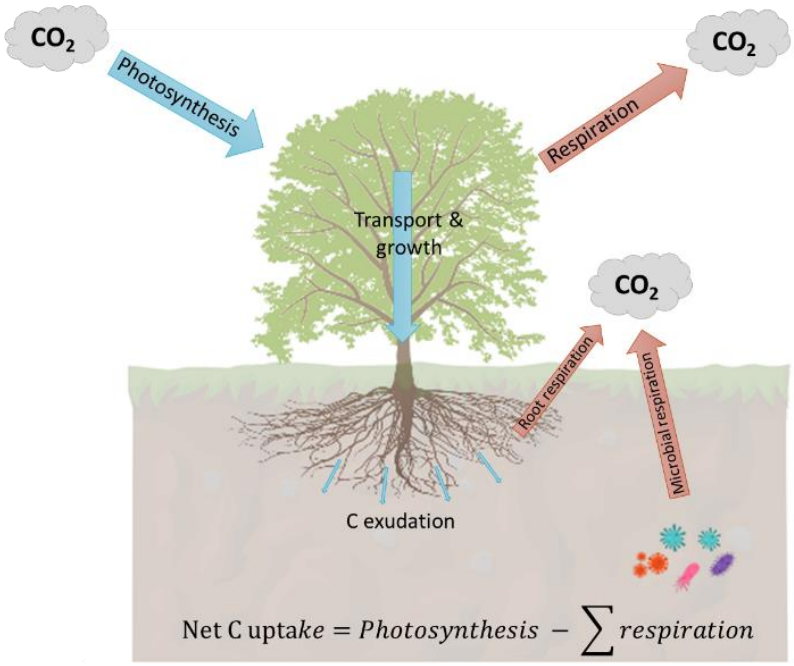

Figure 1.1: *Schematic of C input and losses in a forest ecosystem to calculate the net C uptake. Blue arrows represent C fixation and transport in plant and soil and red arrows represent respiration fluxes.*

Whether eCO_2 increases soil C storage is even more uncertain (Terrer et al., 2021). Soil C storage is a result of the balance between inputs from both aboveground and belowground biomass, and losses due to the decomposition of soil organic matter residues and root respiration, both components likely increased by eCO_2 (Kuzyakov et al., 2019) (Fig. 1.1). A meta-analysis gathering observations from Free-Air CO_2 Enrichment (FACE), open-top chamber, and growth chamber experiments under eCO_2, revealed that eCO_2 concentration led

to an average stimulation of plant biomass by 21%, and a notable increase in soil C storage by 5.6% (Luo et al., 2006). However, other studies have reported either marginal increases (Kuzyakov et al., 2019) or, conversely, a depletion of C stocks in soils due to SOM mining for nutrient supply to trees (Carney et al., 2007; Terrer et al., 2021). The divergent outcomes regarding the effects of eCO_2 on soil C stocks can be attributed to the dynamics of soil organic matter (SOM) decomposition (Pendall et al., 2011; Terrer et al., 2021). When SOM decomposition is enhanced by eCO_2 to a greater extent than the enhanced biomass inputs, the SOM pool progressively declines (Pendall et al., 2011). In fact, according to Terrer et al. (2021), there is an inverse relation between aboveground biomass increase and soil C storage under eCO_2 in ectomycorrhizal forests specifically suggesting that as aboveground biomass increases, soil C storage declines in response to eCO_2. This hypothesis carries major implications for the predicted C storage of forest under future climates and need to be verified by experimental manipulations.

1.2. Progressive nitrogen limitation under eCO_2

Furthermore, mature forest productivity is generally limited by soil nutrient availability, especially N and P for which bioavailable forms for trees are present in low concentration in soils. Northern hemisphere forests are more often limited by N which is mainly released through SOM decomposition. Southern hemisphere forest, often grown on older soils, are more limited by P that can either be released through SOM decomposition or through desorption from soil minerals. Thereby, while eCO_2 can initiate an enhancement of forest production, this enhancement is projected to be shortly truncated by nutrient limitation in soils and especially N, and P due to higher sequestration of these nutrients in long-term biomass pools (De Graaff et al., 2006; Luo et al., 2006; van Groenigen et al., 2006). Indeed, when N availability is considered in models, C storage predictions can be reduced between 25% to 74% (Meyerholt et al., 2016; Thornton et al., 2007) and yet this constrain might have been underestimated as these predictions are based on young forests which are less nutrient-limited

than mature forests. The progressive N limitation (PNL) hypothesis under eCO_2 was supported by one of the first Free Air Carbon dioxide Enrichment (FACE) experiments involving young Sweet Gum plantation at Oak Ridge FACE, where the initially enhanced NPP decreased after a few years of eCO_2 treatment indicating that N limited the growth enhancement (Iversen and Norby, 2008). Yet, outcomes from a similar FACE experiment (Duke FACE) challenged the PNL hypothesis as enhanced NPP was maintained over 11 years suggesting that N supply in soils was sustained via enhanced decomposition of SOM (Phillips et al., 2011; U.S. DOE, 2020). These disparities between different FACE manipulations and biogeochemical models shed light on the significant gap in our understanding of N cycling, particularly in the context of climate change (Iversen and Norby, 2008). Thereby, addressing the question of PNL requires a comprehensive understanding of the effect of eCO_2 on the N cycle including N inputs, N outputs and N recycling within the system.

1.3. Nitrogen cycling in temperate forest ecosystem

N availability in soils is a function of all the N process kinetics involved in the N cycle. N in ecosystems undergoes a continuous, partially open, loop, transitioning from inert to reactive forms, organic to inorganic states, and non-available to plant-available forms (Galloway et al., 2003) (Fig. 1.1). Soil microbes play a pivotal role in orchestrating these transformations and supplying N to meet microbe and plant N demands (Li et al., 2019). *New N* is provided by biological N fixation (BNF) and atmospheric reactive N deposition (Galloway et al., 2008). Once in the ecosystem, N can be recycled between the plant and the soil biomass or can be lost through processes such as nitrate (NO_3^-) leaching or nitrification and denitrification emitting nitrous oxide (N_2O), nitric oxide (NO) and dinitrogen (N_2) into the atmosphere (Davidson et al., 2000). The *openness* of the N cycle is determined by the N recycling efficiency where an *open* N cycle is characterized by significant N losses from the ecosystem, contributing to groundwater pollution and greenhouse gas emissions and can cause the ecosystem to transition from N-abundant to N-limited (Rastetter et al., 2021). The balance between N

turnover, inputs, and outputs governs the N availability within a system (Fowler et al., 2013; Vitousek et al., 1998). Therefore, estimating the kinetics and drivers of these processes is crucial for predicting N availability and characterizing the *openness* of the N cycle.

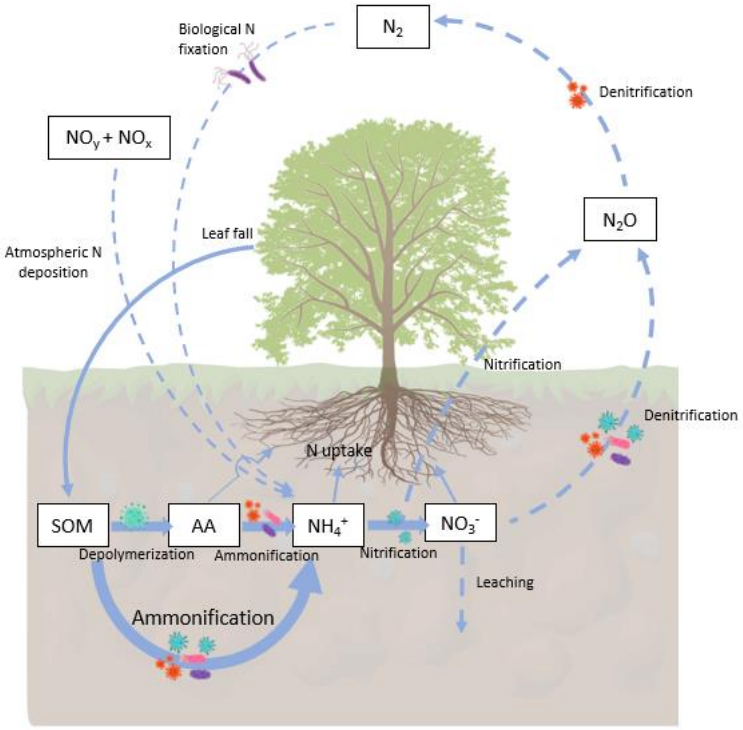

Figure 1.2: *Simplified schematic of the N cycle in a deciduous forest ecosystem. All nitrogen fluxes are represented with a blue arrow. Full arrows represent N internal cycling and dashed arrows represent external N cycling.*

1.4. Nitrogen external flux

1.4.1. New nitrogen in the ecosystem

In natural ecosystems with little to no anthropogenic N deposition, BNF is the main source of new N (Melillo, 1981). BNF is carried out by a group of prokaryotes that carry genes able to code for the nitrogenase enzyme. This enzyme catalyses the breaking of the dinitrogen molecule (N_2) and the addition of three hydrogen atoms to each N atom. However, this reaction requires substantial amounts of energy: 16 moles of ATP for the reduction of one mol of N (Reed et al., 2011). Microorganisms provide this energy either by photosynthesis (phototrophic

bacteria) or by the oxidation of other organic C molecules (heterotrophic bacteria) (Vitousek et al., 2013). Alternatively, in the case of symbiotic N fixation, the host plant provides the necessary organic C substrates as an essential energy source (Mylona et al., 1995). While symbiotic N fixation has been extensively characterized due to its significance in agricultural systems, free-living N fixation remains understudied (Smercina et al., 2019). This lack of attention in temperate forests is attributed to its minor contribution to the N budget i.e. delivering only 2 to 3 kgN ha^{-1} y^{-1} due to the energy limitation (Cleveland et al., 1999; Son, 2001). However, in natural ecosystems and over the long-term, free-living N fixation may be of considerable importance (Dynarski and Houlton, 2018) especially in root-dense soils as it energy limitation can be alleviated in the rhizosphere (Smercina et al., 2019).

However, over the last century, anthropogenic N deposition has also become a significant source of *new N* due to the drastic doubling of reactive N (Nr) in the biosphere (Galloway and Cowling, 2021). N deposition can occur in oxidised N form, known as NOy (NO, HNO_3, NO_2^-) or in reduced form known as NHx (NH_3, NH_4^+) and can be deposed as dry or wet deposition. Some N compounds, like NH_3, can engage in a two-way exchange between plant and atmosphere (Zhang et al., 2021). N deposition is unequally distributed globally but can provide more than 30 kg N ha^{-1} y^{-1} near industrial or agricultural areas (Rubin et al., 2023) and inhibit N fixation in such areas (Saiz et al., 2021; Zheng et al., 2019). In N-limited natural ecosystems, N deposition boosted plant productivity and soil C storage (Fleischer et al., 2019; Tipping, 2017) but unlike N fixation, N deposition lacks self-regulation and may lead to excessive and harmful N levels associated with soil acidification, reduced plant and microbial diversity and increased N_2O emissions (Nadelhoffer et al., 1999; Zheng et al., 2020). Moreover, N deposition is not uniformly distributed worldwide, with hot spots concentrated around urban areas (Decina et al., 2020) contributing to an uneven distribution of nutrients worldwide (Steffen et al., 2015). However, effective environmental policies succeeded in decreasing N deposition by half

between 1990 and 2015 (EMEP 2017) and should lead to further decrease in the coming years according to the Clean Air scenario (Amann et al., 2020).

1.4.2. Nitrogen losses

N losses can be of two types in a natural ecosystem: nitrate leaching or N gas emissions (N_2O or N_2). In temperate forest, nitrification serves as a precursor process for N losses as it converts ammonium (NH_4^+) or organic N into NO_3^- through an autotrophic or a heterotrophic process (Prosser, 2005). Additionally, nitrification also produces significant amount of N_2O as a by-product, contributing to N losses and greenhouse gas emissions (Inatomi et al., 2019). While NO_3^- can be a primary N source for some plants, mature trees preferentially take up organic N or NH_4^+ over NO_3^- (Schimel and Bennett, 2004; Stadler et al., 1993). Consequently, NO_3^-, being a soluble and mobile anion, is prone to leaching below the root horizons or is prone to reduction into N_2O by denitrifying microbes (Groffman and Tiedje, 1989). In forest ecosystems, processes such as NO_3^- leaching, N_2O and N_2 emissions typically occur at low rates during dry months. However, during intense precipitation events, a significant amount of N can be lost through these mechanisms within a short period of time (Garcia-Montiel et al., 2003; L. Yu et al., 2022).

Furthermore, while nitrification and the first stage of denitrification can be relatively easy to measure (see Chap. 2; Methods), the second stage of denitrification converting N_2O into N_2 is more difficult to measure using isotopes or other methods (Micucci et al., 2023). Due to this missing part of the N budget, it is often difficult to accurately estimate N losses of an ecosystem. A theoretical ratio of 8% is often used to estimate the ratio (N_2O/N_2O+N_2) but this ratio is highly dependent on the composition of the soil denitrifying communities as only bacteria (and not fungi) can reduce N_2O into N_2. Therefore it may vary from one ecosystem to another or, within an ecosystem following shifts in microbial community composition (Scheer et al., 2020). In

acidic forest soils where fungal denitrification prevails using the theoretical ratio of 8% may lead to significant overestimation of N_2 emissions (Rütting et al., 2013; Zheng et al., 2022).

Finally, N can also be transported in and out of natural ecosystems by mobile organisms, especially animals referred as *mobile link* (Lundberg and Moberg, 2003). *Mobile links* can redistribute significant amount of N between or within ecosystems by consuming organic biomass and depositing N waste (urea, faeces). However, predicting N flow patterns via *mobile links* requires an in-depth understanding of their behaviour and interactions (McInturf et al., 2019). While these flows are important to acknowledge, in our study we assume a net balance of 0 via *mobile links*.

1.4.3. Nitrogen recycling within the ecosystem

Unlike agricultural systems, which are characterized by an *open* N cycle in order to supply human populations with food, forest ecosystems are characterized by a nearly *closed* N cycle where high N demands are met though a fast and efficient turnover of SOM (Rennenberg and Dannenmann, 2015). SOM in soils is commonly categorized into two groups: particulate organic matter (POM) which is easily accessible to microbes and mineral associated organic matter (MAOM), which is a more resistant form that may necessitate abiotic destabilization before microbial depolymerization of organic N can occur (Lavallee et al., 2020). As POM is readily available for microbial decomposition, POM-N may serve as the primary N source, but it will lead to an increased microbial respiration due to its higher C:N ratio. Conversely, MOAM having a low C:N ratio, its decomposition will produces less CO_2 (Jilling et al., 2018; W. Yu et al., 2022) but may impact the long-term C pools as it will destabilize soil overall C stores. When the ecosystem experiences N or P limitation, microbial decomposition of SOM of either pool can be intensified to release low molecular weight N or P compounds but depending on which pool is targeted it will impact the C cycle and stores differently (Craine et al., 2007; Feng and Zhu, 2021).

The most well-known process releasing available N is called ammonification which is the conversion of low or high molecular weight organic N into NH_4^+ (Fig. 1.2). This reaction is performed by a large spectrum of microbes generally called *ammonifiers* (Bottomley et al., 2012) that breakdown organic matter, utilize as much N as they need and release the excess in the environment as NH_4^+ (Norton and Schimel, 2011; Strock, 2008). Based on this observation, traditional thinking believed that plants were poor competitors for N as plant nutrition seemed to rely solely on the excess mineralized by microbes. However, scientific consensus now acknowledges that plants can also uptake organic N in the forms of free amino acids (FAA) making them better competitors (Schimel and Bennett, 2004). This recent discovery also underscored the significance of the protein depolymerization process in regulating N availability to plants. High-molecular-weight organic N polymers (i.e. proteins, peptides, chitin) are the largest N soil pool (Maxwell et al., 2022) thereby the depolymerization of such compounds into low-molecular-weight organic N compounds (amino acids, oligopeptides) is currently considered the bottleneck in the N cycle for providing available N (Noll et al., 2019; Schimel and Bennett, 2004).

1.4.4. Tree control of nitrogen cycling in the rhizosphere

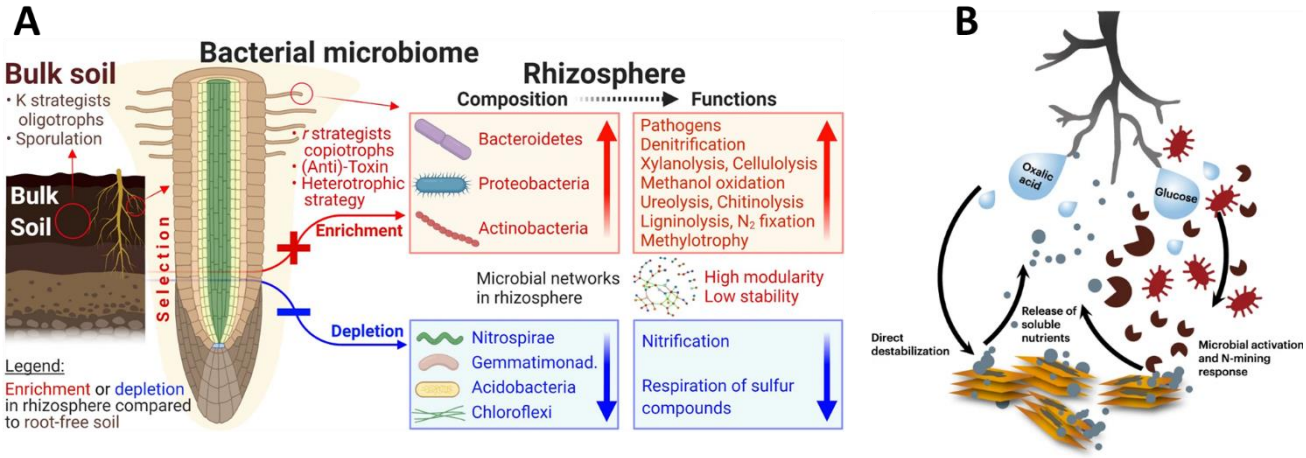

Figure 1.3: *A) Conceptual figure showing the enrichment and depletion of bacterial community taxa in the rhizosphere compared to bulk soil from Ling et al. (2022). B) Conceptual figure depicting the direct and indirect pathways of SOM decomposition as driven by exudate composition from Jilling et al. (2018).*

Why trees are not more N-limited is puzzling, given that soil N availability is mainly regulated by microbial activity (Rennenberg and Dannenmann, 2015). However, trees have evolved alongside soil microbes, developing mechanisms such as symbiotic or non-symbiotic partnerships with soil microbes, to enhance N availability in their rhizospheres or to acquire nutrients through their symbionts. Notably, around 60% of trees on Earth have formed symbiotic relationships with ectomycorrhizal (ECM) fungi (Steidinger et al., 2019). These partnerships enable trees to thrive because ECM fungi possess the unique ability to access otherwise inaccessible N sources (Anthony et al., 2022). Another consequence of this co-evolution is root exudation, acting as a communication tool from trees to microbes (Bais et al., 2006). Root exudation enables trees to influence N cycling in their rhizosphere either indirectly by priming rhizosphere microbial activity (Dijkstra et al., 2013) or directly by abiotic destabilization of SOM (e.g. oxalic acid release; Jilling et al., 2018) or by inhibiting processes (e.g. biological nitrification inhibitor release; Nardi et al., 2020) (Fig. 1.3). Through root exudation, trees influence the microbial community structure in their rhizosphere, favouring beneficial microbes (Fig. 1.3). Together these mechanisms help our understanding of tree N

nutrition and reveal that, while N availability is regulated by microbial activity, microbial activity itself is at least partially regulated by tree physiology.

1.5. How might eCO_2 influence the nitrogen cycle?

1.5.1. Diverging responses of N mining to eCO_2

As discussed above, the N cycle is strongly regulated by tree N demand and tree N acquisition strategies. Different tree N acquisition strategies may be one of the drivers behind different responses of N cycling to eCO_2. For instance, N fixing trees may be less affected by N limitation under eCO_2 as N fixing activity can be adjusted to tree N demand (Norby, 1987; Rogers et al., 2009). Similar mechanisms could occur with trees associated with specific mycorrhizae fungi or rhizosphere bacteria as these beneficial partners can mine for N in soils to increase N availability to trees (Meier et al., 2015; Terrer et al., 2018). Hence, depending on the symbiotic relationship's robustness and the properties of the beneficial microbe, trees may be able to alleviate N limitation (Franklin et al., 2014). Notably, differences in ecological function between arbuscular mycorrhizal (AM) and ectomycorrhizal (ECM) fungi play a crucial role in forests' response to eCO_2 (Terrer et al., 2016). ECM-associated trees are less likely to be N-limited due to ECM fungi ability to decompose SOM, while AM fungi can only transfer available N to trees (Phillips et al., 2013).

But N availability is also influenced by the soil C:N:P nutrient status due to the existing C:N:P stoichiometry in the microbial biomass and the SOM pool (Cleveland and Liptzin, 2007). Due to this stoichiometry, soil nutrient ratios dictate which nutrient microbes will retain more tightly (i.e. immobilization) rather than releasing it for plant uptake (Xu et al., 2015). This means that under eCO_2, where C availability increases in soils, microbe nutrient limitation may shift from C to N (Norby et al., 2004; Phillips et al., 2011). This will likely result in a microbial N limitation and an increase in microbial N use efficiency (NUE; Mooshammer et al., 2014), calculated as the ratio of amino acids (AA) used for growth over AA immobilized. In that case, an increase

in gross depolymerization and mineralization may not translate in a higher amount of inorganic N being released for plant uptake (Mooshammer et al., 2014). Results from various experimental manipulations often show an acceleration of N uptake, N ammonification, and N immobilisation under eCO_2 (Kuzyakov et al., 2019), but it is not always certain if this acceleration translates into higher net mineralization (i.e. higher N availability for trees). Conversely, a few studies have reported lower decomposition rate under eCO_2 and explained it by an increase of the leaf litter C:N ratio and lignin content making the organic matter more recalcitrant (Berntson and Bazzaz, 1997; Hu et al., 1999; Karnosky, 2003; Kuzyakov et al., 2019) while other studies did not detect any effects of eCO_2 on N mineralization (Gahrooee, 1998; Zak et al., 2003). The response of N mineralization or, more generally, SOM decomposition under eCO_2 seems to vary according to several identified drivers: the duration of the exposure to eCO_2, the initial nutrient statue (Andresen et al., 2020; Rütting and Andresen, 2015), the type of trees or their symbiotic associations (Terrer et al., 2021). However, except for studies conducted at EucFACE (a P-limited mature forest), most studies were conducted on young tree plantations or in greenhouse settings for which responses may deviate strongly from what could happen in mature forest (Jiang et al., 2020) where trees and soil microbes have had decades to build beneficial associations and therefore may use and recycle N more efficiently (Norby et al., 1999).

1.5.2. Knowledge gaps on the response of free-living nitrogen fixation, nitrification, and denitrification to eCO_2

Another way for ecosystems to meet the increased demand for N would be to increase N fixation and reduce N losses; however very little attention has been paid to these processes.

While N-fixing trees have been shown to increase N fixation activity to sustain the higher N demand under eCO_2 (Li et al., 2017; Rogers et al., 2009; Tobita et al., 2016), most forest (especially temperate forests) relies on biological N fixation (BNF) by free-living N fixers. Yet, the effects of eCO_2 on BNF are not well understood. Measurements from various experiments

show very contrasting results (Hofmockel and Schlesinger, 2007; Hungate et al., 2014; Ullah et al., 2020) suggesting that, despite the higher C availability under eCO_2, BNF is not systematically enhanced as it may be limited by other nutrients such as P, Mo and Zn that can become scarce under eCO_2. Moreover, out of the four studies that conclude that eCO_2 elicits N fixation, only one was conducted in a forest ecosystem (Ullah et al., 2020) emphasizing the need for further studies in mature forests.

In addition, the regulation of N losses under eCO_2 remained understudied, to our knowledge, no study has focused on N_2 losses or NO_3^- leaching under eCO_2. Several studies on young trees have generally reported no overall effect of eCO_2 on N_2O emission despite some seasonal variations (Ambus and Robertson, 1999; Barnard et al., 2005; Phillips et al., 2001). However, the only study on mature forest reported higher N_2O potential rates due to higher microbial activity in soils incubated without plant roots (Sgouridis et al., 2023). Furthermore, nitrification, denitrification and NO_3^- leaching are highly dependent on soil moisture (Morley and Baggs, 2010; Zheng et al., 2021) so their response might depend upon the water budget response to eCO_2. Yet, recent models indicate that the anticipated increase in soil water under eCO_2 may not be as significant as initially assumed (Ward et al., 2018), with other factors potentially exerting a greater influence on the water budget in a mature forest (Medlyn et al., 2001). Therefore, exploring the impact of eCO_2 on soil moisture and its implications for N losses in a mature forest calls for additional research.

1.5.3. Effect of eCO_2 on rhizosphere priming effect

More generally, plant-microbe interactions in the rhizosphere has been identified as a key mechanism for increasing N supply to plants under eCO_2 (Meier et al., 2015; Phillips et al., 2012, 2011). The rhizosphere priming effect (RPE) defined as the stimulation or retardation of SOM decomposition by root presence and exudation (Carrillo et al., 2014; Dijkstra et al., 2013), which can both increases or decreases N availability depending primarily on root exudate quality and quantity but also on other factors (soil nutrient statue, microbial communities)

(Craine et al., 2007; Gaudel et al., 2024; Kuzyakov, 2002). Therefore, understanding to what extent tree and soil microbe interactions via exudation/RPE are able to enhance rhizosphere N availability is a key aspect in forecasting future N limitation. However, before addressing the latter question, several knowledge gaps must be bridged. The first step is to determine how eCO_2 will affect root exudates quality and quantity and the second is to determine how this will in turn affect soil N cycling and N availability for tree uptake in the long-term. Research has established that, under eCO_2, root exudation quantity increases (Phillips et al., 2011) and the composition in the main groups (amino acids, sugars, organic acids) changes (Dong et al., 2021; Johansson et al., 2009; Phillips et al., 2009). For instance, organic acids were found to be released in higher quantity under eCO_2 (Hasegawa et al., 2023), which could directly destabilize SOM and mobilise nutrients in the rhizosphere (Jilling et al., 2018). A recent study conducted at BIFoR-FACE highlighted that root exudate C:N ratio increases under eCO_2 from 13 to 17 (Reay et al, *in prep*). Whether such change impact RPE towards an enhancement of SOM decomposition to meet the higher tree nutrient demands remain to be confirmed (Terrer et al., 2021). In addition, the effects of eCO_2 on root exudate secondary metabolites remain to be assessed as secondary metabolites can serve multiple functions, such as phenols enhancing SOM decomposition (Zwetsloot et al., 2018) or biological nitrification inhibitor (BNI) suppressing nitrification (Nardi et al., 2020).

1.6. Experimental sites: BIFOR FACE and EucFACE

N processes are highly dynamic and respond to different drivers, with vegetation playing a significant role. Therefore, relying on young tree plantations to forecast the response of C and N cycling in mature forests worldwide is insufficient and may result in erroneous predictions regarding the global C budget. **The present research aims at enhancing our understanding of N cycling under eCO_2 to improve future C storage predictions using two natural mature forests as experimental sites: BIFoR-FACE and EucFACE.**

BIFoR-FACE and EucFACE sites are currently the only “second generation forest FACE facilities”, so called because the facilities are implanted inside existing mature forests. First generation FACE experiments such as Duke FACE and Oak Ridge FACE provided foundational data on the response of planted young forest to climate change. However, these data need to be complemented with data from mature and complex forest ecosystems, hence the construction of these two second generation FACE facilities. BIFoR FACE and EucFACE consist in a similar experimental design: three patches of forest exposed to +150 ppm CO_2 (i.e., the projected global norm by mid-21st-century) and three control patches exposed to ambient air (Fig. 1.4). BIFoR FACE started the CO_2 enrichment treatment in April 2017 and EucFACE started in 2013. Both forests are expected to continue delivering +150 ppm of CO_2 for at least ten years in order to address the long-term questions. Both forests are in the category of temperate forests, with BIFoR-FACE characterized as a deciduous temperate maritime forest and EucFACE as a dry perennial forest. BIFoR-FACE is located in Staffordshire, UK and is dominated by 180 year-old oak (*Quercus robur L.*), hazel (*Corylus avellana L.*) and sycamore (*Acer pseudplatanus L.*) trees (Hart et al., 2020). EucFACE experiment is located in a remnant Cumberland plain woodland in Sydney’s Hawkesbury district with 90 year-old Eucalyptus tree (*Eucalyptus L.*) dominance (Drake et al., 2016).

After a few years of enrichment, the two forests showed diverging response to eCO_2. At BIFoR-FACE, evidence of increases in photosynthetic rate (Gardner et al., 2021), in net primary productivity (NPP; Norby et al., 2024) was detected from the first years of enrichment. Trees also increased yearly N uptake with signs of mild N limitation as indicated by an increase in leaf C:N ratio and leaf N resorption (Mayoral et al., *in prep*). At EucFACE, despite an increase in the photosynthetic rate of the dominant tree species, NPP did not increase even after ten years of enrichment (Jiang et al., 2024; Pathare et al., 2017). EucFACE, located in a nutrient and water limited system, is believed to be particularly constrained by P, which limits the ecosystem's response to eCO_2 (Ellsworth et al., 2017). Consequently, to disentangle the

nutrient limitation effect on microbial and plant processes under eCO_2, EucFACE was fertilized with 1.75 kg P ha^{-1} in April 2023. The subsequent response of C-N-P cycling to eCO_2 post P-fertilization was monitored to gauge the extent to which the forest would respond to eCO_2 once P is no longer limiting.

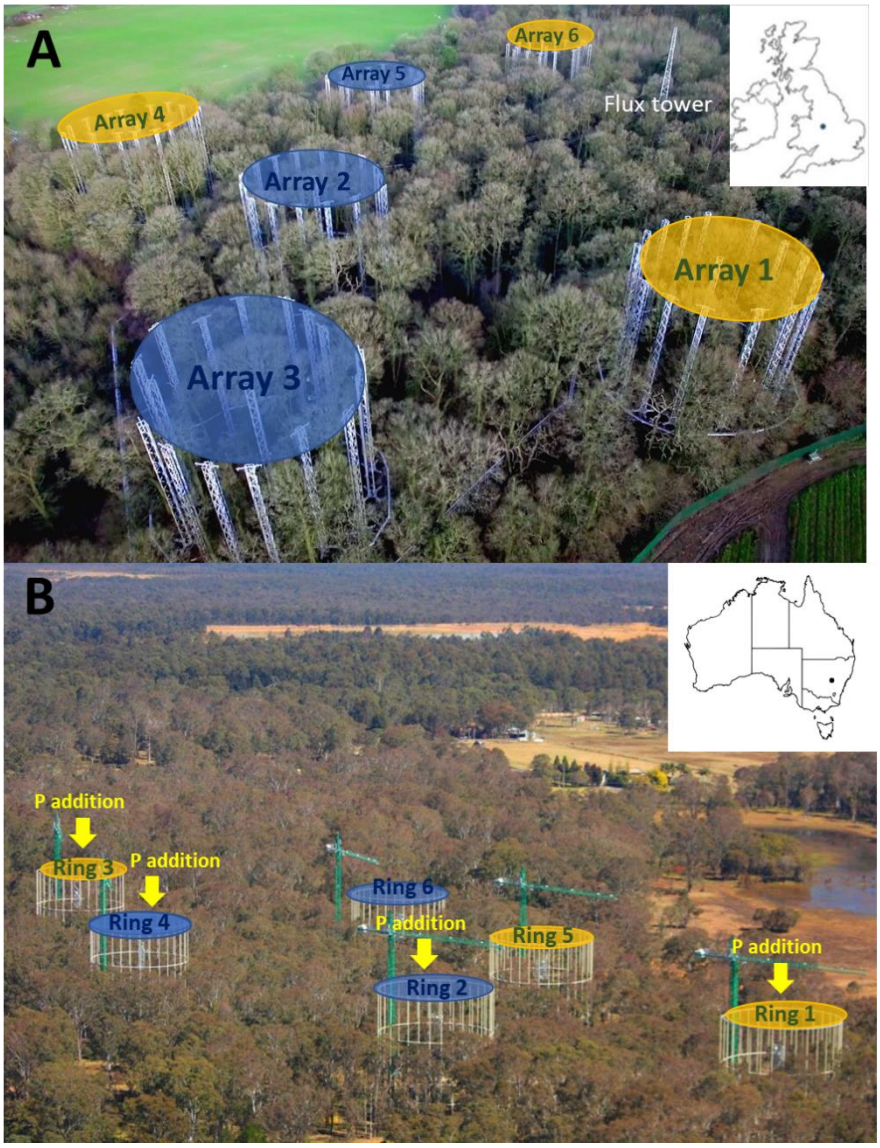

Figure 1.4: *Schematic of the (A) BIFoR-FACE and (B) EucFACE sites. Fumigated arrays are represented in orange and ambient arrays are in blue.*

1.7. Assessment of N cycling processes: methods based on ^{15}N stable isotope

^{15}N is a stable N isotope with low natural abundance (0.364% of ^{15}N in atmospheric N_2; Webb, 1999), making it a valuable tool for tracing N processes. It is commonly employed to track the movement of N from one pool to another using either a tracing approach or a pool dilution approach.

The tracing method using enriched ^{15}N provision is used in the determination of N fixation and N_2O emissions from nitrification and denitrification. In the case of N fixation, the atmospheric N_2 pool is enriched with ^{15}N-N_2 gas and after 24 h of incubation the ^{15}N that has been *fixed* is recovered from the total soil N pool. In the case of determining the contribution of nitrification and denitrification to N_2O emissions, either NH_4^+ or NO_3^- pool is enriched, and after 24 h, the ^{15}N that has been converted into N_2O is detected in the N_2O pool. However, the significant drawback in using ^{15}N as a tracer is that enriching a N pool can stimulate its consumption causing an overestimation of the rate measured.

Conversely, ^{15}N isotope pool dilution method is a powerful method conceptualized in 1954 (Kirkham and Bartholomew, 1954) that allows the determination of gross mineralisation rates without stimulating these processes. The principle is to enrich a specific N soil pool (NH_4^+ or NO_3^-) and monitor the decline of the enrichment over time to determine a rate of production and a rate of consumption. Unlike the net mineralisation method which measure the absolute difference between pool sizes, gross rates can inform on the mechanisms behind changes in net rates (Verchot et al., 2001). More recently this principle has been extended to assess protein depolymerization rates (Wanek et al., 2010). In this method, we enrich the pool of free amino acids (FAA) in soil and monitor the production of FAA through ^{15}N pool dilution. However, challenges in measuring the $^{15}N/^{14}N$ ratio of the FAA pool have limited the adoption of this method despite its ecological relevance (Schimel and Bennett, 2004). In this thesis, we

made significant efforts to contribute to the development of a reliable and straightforward method for assessing protein depolymerization rates in forest soils using recent methodological literature (Warren, 2019).

Combining these methods together offers a robust assessment of the N cycle; however, these methods are typically employed in laboratory settings using sieved and homogenized soil samples; thus, only allowing the assessment of potential rates. **In this research a particular effort was put to measure N processes in-situ on intact cores of soil to assess *real* rates and preserve the effect of roots and soil structure**.

1.8. Aims and thesis layout

The purpose of this research is to explore the effects of eCO_2 on N availability in soils by estimating the kinetics of N processes governing N availability in two temperate forests under the Birmingham Institute of Forest Research Free Air Carbon Dioxide Enrichment facility (BIFoR-FACE), in the UK and the Eucalyptus FACE (EucFACE) facility, in Australia. **Chapter 2** focuses on assessing the N cycle dynamics under eCO_2 at BIFoR-FACE using stable isotopic methods and continuous monitoring of inorganic N dynamic in soils. The aim is to calculate the forest soil N pools and fluxes and determine how, and, if changes in soil process rates sustain the higher tree N demand under eCO_2. **Chapter 3** aims to elucidate the role of the rhizosphere in alleviating N limitation under eCO_2. This was accomplished by comparing N processes and more broadly C, N and P metabolisms using soil enzymatic activity methods along with isotopic methods in both bulk and rhizosphere soils. **Chapter 4** delves deeper into the mechanisms involved in rhizosphere priming effect under eCO_2 by looking at the specific effect of root exudates C:N ratio on N gross mineralization. In addition, to identify which microbial communities primed SOM decomposition under eCO_2, gross mineralization was assessed in root exclusion bags (41 µm mesh) and root and fungi exclusion bags (1 µm mesh). **Chapter 5** concentrates on the response of the N cycling to eCO_2 at EucFACE, a P-limited forest, and how alleviating P limitation affects this N cycling response. In this chapter, the short-term

microbial response to P-fertilization under aCO_2 and eCO_2 was assessed using several methods mentioned above: isotopic dilution methods, soil enzymatic activity assessment and continuous monitoring of inorganic N and P pools. Finally, the **chapter 6** answer the key scientific questions of this research:

1. Does eCO_2 increase C allocation belowground?
2. Are N supplies via N fixation and mineralization fluxes enhanced under eCO_2?
3. Does increased C availability belowground under eCO_2 enhance nitrification and denitrification leading to greater N losses?
4. What mechanisms are behind the response of N cycling to eCO_2?
5. Is the N response to eCO_2 consistent among ecosystems with different nutrient limitation status?

The final chapter compare the ecosystemic response of BIFoR and EucFACE and discuss the potential causes of divergence. This chapter also discuss the limitation of the present work and the directions for future work.

1.9. Key hypotheses

We hypothesized that both forests will increase leaf CO_2 uptake under eCO_2 and redistribute a portion of this C belowground to alleviate nutrient limitations. At BIFoR-FACE, we expect that the increased belowground C allocation will stimulate N cycling, particularly enhancing N-mining from SOM. In contrast, at EucFACE, we hypothesize that the increased C allocation belowground will primarily target P cycling, driving P-mining from SOM and possibly promoting P desorption from minerals. Therefore, our central hypothesis is that while both forests will increase C uptake, nutrient limitations specific to each site will influence subsequent soil processes.

More specifically, at BIFoR-FACE, we propose that increased soil C availability will stimulate N mineralization and free-living N fixation to meet the higher N demands of trees and microbes.

However, this increase in C and N availability may also accelerate N losses through nitrification and denitrification. Consequently, we hypothesize that although increased N availability will initially support enhanced CO_2 uptake and NPP, N will become progressively limiting in the long-term due to increased losses and the depletion of easily accessible SOM.

Conversely, at EucFACE, we hypothesized that N cycling will be little to not affected by eCO_2 enrichment, as the increased C allocation will primarily focus on mobilizing available P from SOM. However, we hypothesized that by fertilizing EucFACE with P, we will shift the limiting nutrient from P to N, which will result in similar dynamics as observed in BIFoR-FACE with a stimulation of N mining but also of N losses.

Chapter 2. Enhanced soil nitrogen transformation supports biomass C gains in a mature forest under elevated CO_2

Enhanced soil nitrogen transformation supports biomass C gains in a mature forest under elevated CO_2

Manon Rumeau[1,2*], Fotis Sgouridis[3], Carolina Mayoral[1,2], Michaela K. Reay[4], Yolima Carrillo[5], Richard J. Norby[1,6], Liz Hamilton[1,2], Iain P. Hartley[7], Gianni Micucci[8], Rob MacKenzie[1,2] and Sami Ullah[1,2]

[1]*Birmingham Institute of Forest Research, University of Birmingham, Birmingham, B15 2TT, UK*

[2]*School of Geography, Earth and Environmental Science, University of Birmingham, B15 2TT, UK*

[3]*School of Geographical Sciences, University of Bristol, Bristol, UK*

[4]*Organic Geochemistry Unit, School of Chemistry, University of Bristol, UK*

[5]*Hawkesbury Institute for the Environment (HIE), Western Sydney University Richmond, Australia*

[6]*Department of Ecology and Evolutionary Biology, University of Tennessee, Knoxville, TN, USA*

[7]*Geography, Faculty of Science, Environment and Economy, University of Exeter, Exeter, UK*

[8]*Department of Civil Engineering, McGill, University, Montreal H3A 0C3, Canada*

Corresponding author (*): Manon Rumeau, MLR094@student.bham.ac.uk

Additional corresponding author: Sami Ullah, s.ullah@bham.ac.uk

Abstract

The constraint of tree growth under elevated atmospheric CO_2 (eCO_2) in future by soil nitrogen (N) availability is projected to reduce carbon (C) capture by 25 to 75% over the next century. This uncertainty, emanates from insufficient data on specific N processes' response to eCO_2 in mature forests, thus hampering a more accurate climate prediction. This research investigates key soil N transformations and pools in a mature English Oak-dominated temperate forest in central England after six years of Free Air CO_2 Enrichment (FACE). Here we show that C biomass gains under eCO_2 are supported by enhanced N mineralization and a conservation of N at the ecosystem scale. *In-situ* net N mineralization was enhanced by 29% with a pronounced effect at oak budburst period. *In-situ* gross ammonification was up-regulated (+30%) and correlated with higher soil CO_2 flux and higher fine root biomass measured in intact soil cores. Despite increased N mining, gross nitrification was suppressed suggesting a faster but tighter N cycle under eCO_2. Yet, with declining atmospheric N deposition and exhaustible soil organic matter, enhanced N mining may only temporarily alleviate progressive N limitation before microbes outcompete trees for N resources.

Keywords: FACE experiment, nitrogen mineralization, nitrous oxide, nitrogen fixation, carbon-nitrogen coupling

2.1. Introduction

The anticipated rise in atmospheric CO_2 is projected to boost terrestrial plant growth through the "CO_2 fertilization" effect, mitigating a portion of anthropogenic CO_2 emissions (Haverd et al., 2020; Le Quéré et al., 2018). However, CO_2 enrichment of forests may exacerbate progressive nitrogen (N) limitation (PNL) due to higher photosynthetic N demands and N sequestration in long-term biomass pools (Johnson, 2006; Luo et al., 2004). When N availability is considered in the CO_2 fertilization models for forests, C capture predictions are reduced by 25 to 75% (Meyerholt et al., 2020; Thornton et al., 2007). These predictions are based on experimental data from young forest Free-Air CO_2 Enrichment (FACE) experiments, which were less nutrient-limited than mature forests and yet they experienced N limitation after several years of exposure to eCO_2 (Iversen and Norby, 2008). In mature forests, stronger nutrient limitation, may result in negligible C capture responses (Norby et al., 1999) as observed in the mature Eucalyptus forest FACE experiment in Australia (EucFACE) where C capture remained unaffected due to severe phosphorus (P) limitation (Jiang et al., 2020). While southern hemisphere forests are generally P-limited, northern hemisphere forests are considered N-limited but decades of atmospheric N deposition may have alleviated N constraint on optimal growth (Tipping, 2017). Hence, it became uncertain if the response of mature northern forest to eCO_2 will be constrained by N availability. Therefore, it is critical to assess how N cycling and availability regulate the response of northern mature forest to eCO_2 to reduce uncertainties in future climate predictions (Medlyn et al., 2015).

Investigating N availability in soils under eCO_2 is challenging as it requires integrating internal N cycling with external N fluxes and with the ecosystem's N demands. Yet, research to date has primarily focused on the stimulation of gross mineralization through increased C allocation belowground under eCO_2. However, while enhanced gross mineralization was observed at Aspen-FACE (Holmes et al., 2006) and during the first four years at BIFoR-FACE (Sgouridis et al., 2023), no effects were detected in the young pine and sweet gum forests at Duke FACE

and Oak Ridge FACE (Iversen et al., 2011; Phillips et al., 2011), respectively, nor at EucFACE (Andresen et al., 2020). These contrasting responses suggest that the effect of eCO_2 on mineralization depend upon the initial nutrient limitation and upon tree N acquisition strategies (Rütting and Andresen, 2015; Terrer et al., 2018). Furthermore, an enhancement of SOM decomposition may only delay N limitation as easily accessible SOM may become exhaustible with time given that more N will be sequestered in long-term biomass pools (Phillips et al., 2011; Terrer et al., 2021). On the contrary, higher *new N* inputs or a reduction of ecosystem N losses have the potential to alleviate N limitation in the long term (Johnson, 2006). Asymbiotic biological N fixation (BNF) in non-N-fixing forests provide usually low to negligible input of *new N* in these northern temperate forests, but, could theoretically be upregulated under eCO_2 because of higher C availability in soils (Verburg et al., 2004). However, existing data in forest ecosystems have found no overall effect of eCO_2 on BNF (Berthrong et al., 2014; Hungate et al., 2014). *New N* is also provided via atmospheric reactive N deposition, which is declining in the UK due to effective environmental policies limiting N emissions (Matejko et al., 2009). Ecosystem N losses via N gas emissions and leaching especially in temperate forests are poorly estimated. Research on young trees (Duke FACE) has found no significant changes in N_2O emissions despite seasonal variations (Phillips et al., 2001). But, potential N_2O emissions from root-free soils incubated under laboratory conditions were enhanced under eCO_2 at BIFoR-FACE (Sgouridis et al., 2023). To our knowledge, the effects of eCO_2 on N_2 emissions and N leaching have not yet been studied, hindering a comprehensive assessment of soil N availability (Barnard et al., 2005). Hence, there is an urgent need for more exhaustive measurements, particularly in mature forests, to adequately assess N fluxes under eCO_2, crucial for predicting future trends in N availability.

Herein, we comprehensively investigated key internal and external N processes, measured across different periods of the year to capture seasonality effects of eCO_2 (Lauriks et al., 2021; Socci and Templer, 2011), and synthetize them into a one-year N mass balance following six

years of eCO_2 enrichment. Our objective was to address the question of potential future N limitation by estimating soil N supplies and losses, in a mature deciduous forest at the Birmingham Institute of Forest Research (BIFoR) Free Air Carbon Dioxide Enrichment (FACE) facility in the UK. Initial results at BIFoR-FACE have demonstrated an upregulation of photosynthetic capacity (Gardner et al., 2021) leading to a 10% increase in tree dry matter (Norby et al., 2024), an increase in fine root biomass (Ziegler et al., 2023), and in leaf mass per unit area without change in leaf C:N ratio (Gardner et al., 2022). This was coupled with a stimulation of potential N mineralization and N losses from soils in the early years of eCO_2 enrichment (Sgouridis et al., 2023). Given that, higher leaf CO_2 uptake (Gardner et al., 2021) and higher C exudation (Norby et al., 2024) will result in higher C availability in soils under eCO_2, we hypothesized that, 1) N supplies will be upregulated under eCO_2 to sustain higher tree N demand (Gardner et al., 2022); leading to 2) enhanced N losses by coupled nitrification and denitrification processes (N_2O and N_2 gases) resulting in a more *open N* cycle. We assessed rates of belowground N processes *in-situ* using intact soil cores to preserve the influence of roots under short ^{15}N tracing incubations (see Material and Methods, below). Gross mineralization, N_2O emissions and BNF were measured in spring, summer and autumn, and net mineralization was measured monthly throughout 2022, a year with a hot and dry summer in central England and across Europe (Van Der Woude et al., 2023).

2.2. Material and Methods

2.2.1. Experimental set-up

The study was performed at the BIFoR-FACE facility, in a mature deciduous forest in Staffordshire (52º 48’ 3.6” N, 2º 18’ 0”W), UK. The forest is dominated by oak (*Quercus robur* L.), hazel (*Corylus avellana* L.) and sycamore (*Acer pseudoplatanus* L.) trees and include holly (*Ilex aquifolium L.*) and hawthorn (*Crataegus monogyna* L.) in the understorey and fern (Dryopteris sp.), brumble (*Rubus fruticosus agg.)* and bluebell (*Hyacinthoides sp.)* in the ground coverage. The soil is classified as a Ortic Luvisol (Hart et al., 2020) with a sandy loam

texture and a pH around 4.5 (Hollis et al., 2021). The organic layer (O) is 6 to 9 cm deep and features a high fine root density (1 mg cm^{-3}), a high C content (10%) and a low bulk density (0.45 g cm^{-3}). Minerals layers (A and B) featured mostly coarse roots with a medium packing density and a soil pH around 5 (Hollis et al., 2021).

The BIFoR-FACE facility is composed of six infrastructure arrays (30m diameter), three are fumigated with a target concentration of +150 ppm of CO_2 above the ambient concentration (eCO_2) and three with ambient air (aCO_2) (Fig. S2-1). CO_2 enrichment started in April 2017 and operated in daylight hours from budburst (~1st April) to leaf fall (~1st November). Performance of the system has been reported in Hart et al. (2020); updated in Norby et al. (2024), showing that the system is able to deliver the target concentration precisely given a secure CO_2 supply. The daytime CO_2 enrichment achieved during the 2022 growing season was 135 ± 24 ppm (mean ± SD), due to intermittency in the global CO_2 supply crises. The mean annual air temperature at the site is 10.8°C (sensors HMP155; Helsinki, Finland) and the mean annual precipitation is 1152 mm (rain gauges at site TR-525M; Dallas, Texas). For a detailed description of the site, see Hart et al. (2020), and of the general analytical pipeline, see MacKenzie et al. (2021).

In each array, three sampling plots of 0.5 m x 0.5 m were established, each at approximately one-metre distance from three different oak trees. Among these three plots, five pseudo-replicate locations were defined for this experiment. For each sampling, the leaf litter was first removed (Oi) and the full organic layer was sampled (Oe + Oa). The sampling depth varied from 6 to 9 cm depending on the depth of the O horizon.

2.2.2. Soil nutrient pools

Gravimetric moisture was measured by drying 5 g of soil at 105°C for 48h. Soil NH_4^+ and NO_3^- concentrations were measured by 0.5 M potassium sulphate (K_2SO_4; soil: extractant ratio of 1:5 (*w*/*v*)) extraction and continuous flow colorimetry analysis (Skalar SA 3000 analyser,

Netherlands). The limit of detection was 0.02 mg N L^{-1} for both NH_4^+ and NO_3^-. The concentrations were blank corrected, and the relative standard deviation (RSD) calculated on quality control (QC) samples was below 2%. The soil concentration of DOC and TDN was measured after extraction with 0.5 M K_2SO_4, as described above, and extracts analysed on a TOC/TN analyser after diluting 10-fold with DI water (Multi N/C 2100, Analytik Jena, Germany). Samples were blank corrected and the RSD was below 1% for DOC and below 4% for TDN.

2.2.3. Net nitrogen mineralisation

From February 2022 to November 2022, monthly net N mineralization was measured in the organic layer. Soil samples (O-horizon) were collected from the five pseudo-replicate locations per array, sieved and homogenized on-site, and a subsample was incubated for 28 days in a polyethylene bag buried *in-situ* under the leaf litter. The polyethylene bag was water-tight but air-porous to facilitate gas exchange. Net mineralization was assessed by comparing the inorganic N content (NH_4^+ + NO_3^-) on the sampling day with that after a 28-day incubation period (Ullah and Moore, 2009). Since the soil is isolated from roots, separately estimating net ammonification and nitrification may be misleading due to the absence of root competition with nitrifying bacteria. Therefore, we focused on estimating and interpreting net mineralization only.

2.2.4. *In-situ* gross mineralization and N_2O emissions

Gross rates of N mineralisation were measured using the ^{15}N isotopic pool dilution method adapted for field incubation on intact core soils (Davidson et al., 1991). We further adapted the method to include rate of N_2O emissions from nitrification and denitrification using the ^{15}N Gas Flux method. Within a week prior to the ^{15}N labelling, soil NH_4^+ and NO_3^- content were measured in each pseudo-replicate location to target ~20% enrichment of N pool size during the labelling. A range of labelling solutions were prepared to deal with the different soil concentrations and the solutions were flushed with oxygen-free N_2 to avoid any oxygen introduction in soils during labelling. In each pseudo-replicate location, a pair of O-horizon soil

intact cores (T24 h samples) was sampled with a slide hammer (5 cm diameter) and a pair of disturbed soil samples (T0 h samples) of the same depth was sampled with a hand auger and directly transferred in a cool box for transfer to the lab. The intact soil cores were labelled with $K^{15}NO_3$ or with $^{15}NH_4Cl$ by multiple injections with a long needle into the soil to ensure homogeneous labelling and were incubated *in-situ* for 24 h. After 24 h incubation, samples were homogenized by hand and a subsampled was extracted with KCl 1M (1:5, v:W). Extracts were analysed on continuous flow colorimetry analysis (Skalar SA 3000 analyser, Netherlands) for inorganic N content and the enriched pool of either NH_4^+ or NO_3^- was diffused onto an "acid trap" following the diffusion procedure to measure the ^{15}N atom % of these N pools using an EA-IRMS (elemental analyser-IRMS: Elementar Isoprime Precision; Elementar Analysensysteme GmbH, Hanau, Germany; Sgouridis et al., 2023).

Roots from the soil cores were washed with DIW, dried at 65°C, and fine root biomass (diameter $\leq$ 1 mm) was measured per soil volume. Additionally, a subset of root samples was pulverized and analyzed using the EA-IRMS analyzer to ensure that the root ^{15}N label uptake did not affect gross N transformation rates calculations(Richter et al., 2003).

Concurrently, gas samples were taken immediately before closing the core and after 24 h of incubation with a syringe though the septum and transferred into a pre-evacuated 12 ml gas exetainer vial (Labco, Ceredigion, UK).These samples were analysed for total CO_2, N_2O and CH_4 concentration on a gas chromatograph (GC; Agilent Technologies Ltd, USA) equipped with μECD (electron capture detector) and FID (flame-ionisation detector). The ^{15}N content of the N_2O was determined using a continuous flow isotope ratio mass spectrometer (IRMS; Elementar Isoprime Precision; Elementar Analysensysteme GmbH, Hanau, Germany) coupled with a trace-gas pre-concentrator inlet with autosampler (isoFLOW GHG; Elementar Analysensysteme GmbH, Hanau, Germany).

Gross N mineralisation rates were calculated using the equations developed by Kirkham and Bartholomew (1954) and N_2O emissions from nitrification and denitrification were calculated as described in Sgouridis et al. (2023).

2.2.5. Lab measurement of N_2 flux under artificial atmosphere

As N_2 flux from denitrification was not detectable in intact soil cores under natural atmosphere, a lab incubation was conducted under artificial atmosphere and controlled moisture to measure N_2 losses via denitrification using the ^{15}N Gas Flux method (Micucci et al., 2024). Briefly, soil samples were placed in air-tight 100 ml serum bottles and labelled with $K^{15}NO_3$ targeting simultaneously 25% enrichment of the NO_3^- pool and 65% soil gravimetric moisture. An initial gas sample was taken and transferred into a 12 ml gas exetainer vial before vial closure and vial atmosphere was replaced by an artificial atmosphere depleted in N_2 (5% N_2, 20% O_2, 75% He and 0.11 ppm of N_2O). After 6 h and 24 h, gas samples were taken from the serum bottles. Gas samples were analysed on EA-IRMS coupled with a trace-gas pre-concentrator inlet and the ratio $N_2O/(N_2O+N_2)$ was calculated using the equations described in Micucci et al. (2024).

2.2.6. Nitrogen fixation

In-situ rates of N fixation were assessed by the ^{15}N assimilation method (Saiz et al., 2019). O-horizon soil samples from the six arrays were collected in June 2021, September 2021 and April 2022. Five cores of soils were collected per array, bulked together, sieved (< 2 mm) on site and eight subsamples of 10 g each were weighted into 50 ml dark and air-tight serum bottles. Five replicates out of eight were incubated with an atmosphere enriched at 20% in $^{15}N_2$ by replacing 5 ml of the headspace with $^{15}N_2$ gas (98 atom % ^{15}N, Sigma-Aldrich) and three of the replicates were incubated with ambient air (controls). Negative standards were made of autoclaved soils. All samples were incubated *in-situ* for 24 h before aerating the samples to stop the incubation. Samples were dried at 70 °C for 72 h, pulverized, and analysed on an EA-IRMS. The analytical precision limit of the EA-IRMS (LOD) was determine by doing repetitive

measurement of a bulk soil sample's natural abundance. Nitrogen fixation rate was calculated with Equation 2.1.

$$Y = \left(\frac{atom\%^{15}Nexcess}{100}\right) x \left(\frac{totalN\ x\ 10^{9}}{t\ x\ 28}\right) x \left(\frac{100}{\%^{15}N\ headspace}\right) \quad (2.1)$$

Where Y (nmol N g^{-1} h^{-1}) is the amount of N fixed during the incubation, $atom\%^{15}Nexcess$ is the difference of ^{15}N between enriched and control samples, $totalN$ is the total nitrogen content in the sample in %, t is the incubation time (24 h) and $\%^{15}N\ headspace$ is the amount of $^{15}N_2$ in the serum bottle (20%).

2.2.7. Nitrogen mass balance

The N mass balance of the ecosystem was calculated for the O-horizon layer for the year 2022. Net nitrogen mineralization was used to estimate the supply of available inorganic N assuming that possible N gas emissions during the net mineralization incubations in buried bags were minimal. Net mineralization, N fixation and N gas losses were converted in kg ha^{-1} y^{-1} by considering an average organic layer of 7.5 cm depth and an average bulk density of 0.45 g cm^{-3}. Nitrogen uptake by oak trees was calculated based on the N pools in different tree organs, including the wood increment of 2022, as well as the N pools in the leaves and roots produced during the year. The calculation also subtracted the atmospheric N depositions and the N re-translocated within the canopy from the previous year (Mayoral et al. *in prep*). N atmospheric deposition data at the site was measured by analysing the concentration in reduced and oxidised N collected monthly in 2022 in dry and wet collectors outside the forest (Mayoral et al. *in prep*). The N mass balance was calculated by adding all N inputs (positive fluxes) and N outputs (negative fluxes) and the resulting balance include N leached in the mineral horizons and errors.

2.2.8. Statistical analyses

Statistical analyses were carried out with Rstudio software (version 4.1.0; R Core Team, 2021). Linear mixed effect models were used to detect eCO_2 effects, with eCO_2 set as fixed effect,

and period and array as random effects ("lmer" function, lme4 package; Bates et al., 2015). Due to high variability and low number of replications in FACE experiments we considered that a p-value (*P*) between 0.1 and 0.05 indicate an effect and a $P < 0.05$ indicate a significant effect. When assumptions of normality and homogeneity of variance were not met, log transformations were performed to meet model assumptions. Correlation network was build using the Pearson correlation index with a threshold defined at 0.5. To estimate the eCO_2 effect, we calculated the natural log of the response ratio (RR) as an effect size and its corresponding pooled variance (V) between the eCO_2 and aCO_2 treatments (Hedges et al., 1999).

2.3. Results & Discussion

2.3.1. Upregulation of N mineralization

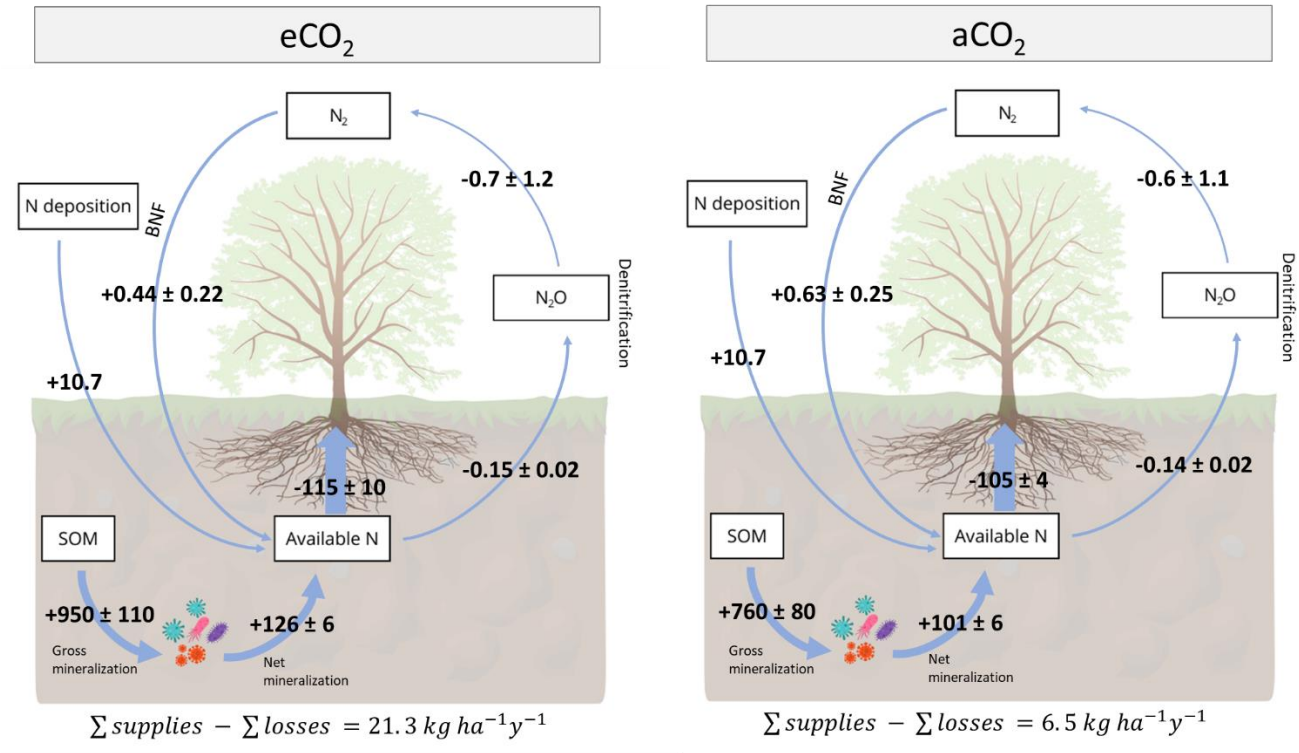

Figure 2.1: *Nitrogen mass balance under eCO_2 and aCO_2 for the year 2022 in the O-organic layer (depth = 7.5 cm on average). All fluxes are expressed in kg ha^{-1} y^{-1}, positive fluxes are the N inputs and negatives fluxes are the N outputs.*

After six years of CO_2 enrichment, higher N demand was sustained by higher net N mineralization delivering an extra 26 kg N ha^{-1} y^{-1} of available N ($P < 0.05$; Table S-1) for an extra 10 kg N ha^{-1} y^{-1} being taken up by the trees under eCO_2 (Fig. 2.1). This resulted in higher ammonium availability (+15%; $P < 0.05$) while nitrate availability was unaffected (Fig. 2.2). Net N mineralization matched the forest trees' N uptake under ambient CO_2 concentration (101 kg N mineralized for 105 kg N taken-up ha^{-1} y^{-1}) underscoring its significance as key N source for trees (Peng and Apps, 1999; Reich et al., 1997; Uri et al., 2003). Thus, supporting that net mineralization can reliably predict forest NPP in N-limited systems (Finzi et al., 2002). However, under eCO_2, net mineralization exceeded N uptake by 15 kg N ha^{-1} y^{-1} (Fig. 2.1), suggesting that the understorey vegetation also absorbed more N over the growing season, as the accumulation of ammonium under eCO_2 accounted for less than 1 kg N ha^{-1}. *In-situ* gross ammonification rates were also higher under eCO_2 over the three-seasons measured (+26%; $P = 0.11$; Fig. 2.4A) but no changes was observed in the microbial immobilization/ammonification balance (~ 87%; Fig. S2-2) supporting the 20% increase in microbial biomass N (Rumeau et al., 2024; Chap 3). Gross ammonification rates were positively correlated with the enhanced soil respiration (+26%; $P < 0.05$) and larger fine root biomass (+39%; $P < 0.05$) measured in the same intact cores during ^{15}N tracing incubations (Fig. 2.4A). These results support that N-mining is stimulated in soils via an expansion of root exploration (Rumeau et al., 2024; Chap 3) and an increase in C availability in soils (+14% in DOC; Fig. 2.2) which primed nutrient mineralization (Dijkstra et al., 2013). However, the positive correlation between ammonification and CO_2 respiration during the ^{15}N incubation suggests a coupling between C and N mineralization due to C and N stoichiometry in SOM (Quan et al., 2014; Tipping et al., 2016). This led to C losses estimated at approximatively 330 kg C ha^{-1} y^{-1} based on the respiration rate in the incubated cores. Such losses match the extra C released by exudation under eCO_2 (Norby et al., 2024) and could offset about 30% of the extra C stored as wood under eCO_2 (Norby et al., 2024). This finding aligns with biogeochemical models forecasting a trade-off between belowground and aboveground C due

to nutrient mining (Terrer et al., 2021). Furthermore, *new N* from BNF remained extremely low at site (0.5 kg N ha^{-1} y^{-1} on average; Table S2-2) and was not upregulated by higher C availability under eCO_2 contrary to our first hypothesis. Atmospheric reactive N (Nr) deposition at site averaging 10.7 kg N ha^{-1} y^{-1} in 2022 (Fig. 2.1) is expected to decline due to UK regulations limiting N emissions (Directive EU, 2024; Matejko et al., 2009). Therefore, it is uncertain how long enhanced N-mining of SOM – augmented by 200 years of high atmospheric Nr deposition (Tipping, 2017) – can be sustained as SOM pool may deplete or become more recalcitrant. With a soil C:N ratio around 17 (Fig. S2-3) suggesting a moderate N limitation and/or a very tightly coupled N cycling between microbes and plants, this forest sits at a tipping point where N limitation could constrain plant response to eCO_2 (Terrer et al., 2021).

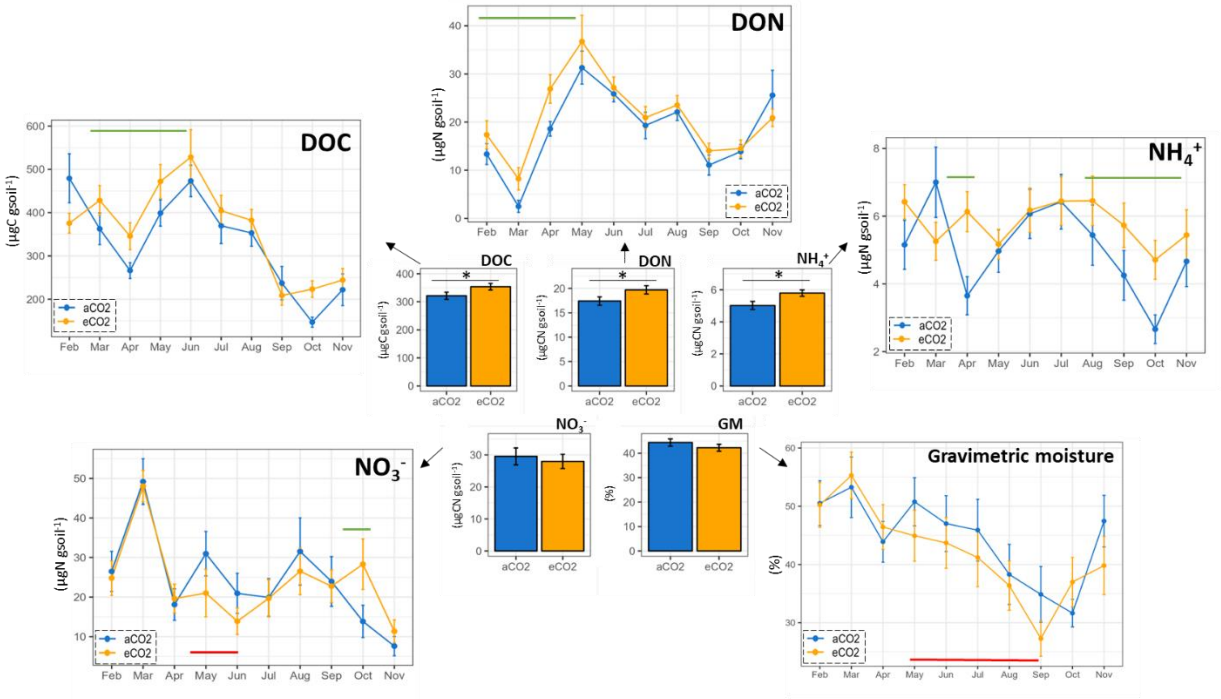

Figure 2.2: *Soil nutrient pools and gravimetric moisture measured monthly from February 2022 to November 2022. Error bars represent the standard error between replicates (n=15). Green and red bars represent positive and negative eCO_2 effect, respectively, over a period.*

2.3.2. Seasonal effects of eCO_2 on N mineralization

The high-frequency monitoring of N transformations undertaken here brings to light a temporal variability in the magnitude of the eCO_2 effect on N mineralization, which is closely linked to soil DOC concentration especially in spring and autumn (R^2 = 0.20 and R^2 = 0.17, respectively; Fig. 2.3B). *In-situ* net mineralization was enhanced in April by 75% (P < 0.05; Fig. 2.2A), coinciding with the onset of tree leaf flushing, higher soil DOC content (+ 44%; Fig. 2.2) and higher root C exudation rate (Norby et al., 2024). From May to July, net mineralization was at its highest, reaching 185 kg ha^{-1} y^{-1}, due to high soil temperature, but eCO_2 had little to no discernible effect (+9%; Fig. 2.3). An indiscernible effect of eCO_2 in summer might have been caused by the drought recorded that summer. Such drought was exacerbated under eCO_2 as gravimetric moisture was ─5 to ─20% lower under eCO_2 (Fig. S2-4 and Fig. S2-5). This is in accordance with long term data suggesting a trend towards drier patches under eCO_2 (MacKenzie et al., 2021). Higher root biomass and thicker/denser leaves (Gardner et al., 2021) likely increased the amount of water residing in the canopy in addition to increasing whole-tree evapotranspiration under eCO_2 (Gardner et al., 2023; Ward et al., 2018). These aboveground changes may explain the soil water depletion during the summer which limited the net mineralization response (Wang et al., 2006). From August to October, net mineralization enhancement under eCO_2 peaked up again (+50% relative to aCO_2) coinciding with the tree nutrient resorption period (Hagen-Thorn et al., 2006), fresh litter decomposition and higher ECM production rates at site (Reay et al., *in prep*). Therefore, the seasonal effect of eCO_2 on mineralization mirrors the seasonal effect on tree C allocation via root exudation and ECM production (Reay et al., *in prep*). This further agrees with studies observing a seasonality in eCO_2 effect on photosynthesis activity (Lauriks et al., 2021; Quentin et al., 2015). Together these findings suggest that trees under eCO_2 can increase C allocation belowground to stimulate N mining at periods when N demand is high to keep up with enhanced photosynthesis (Gardner et al., 2022).

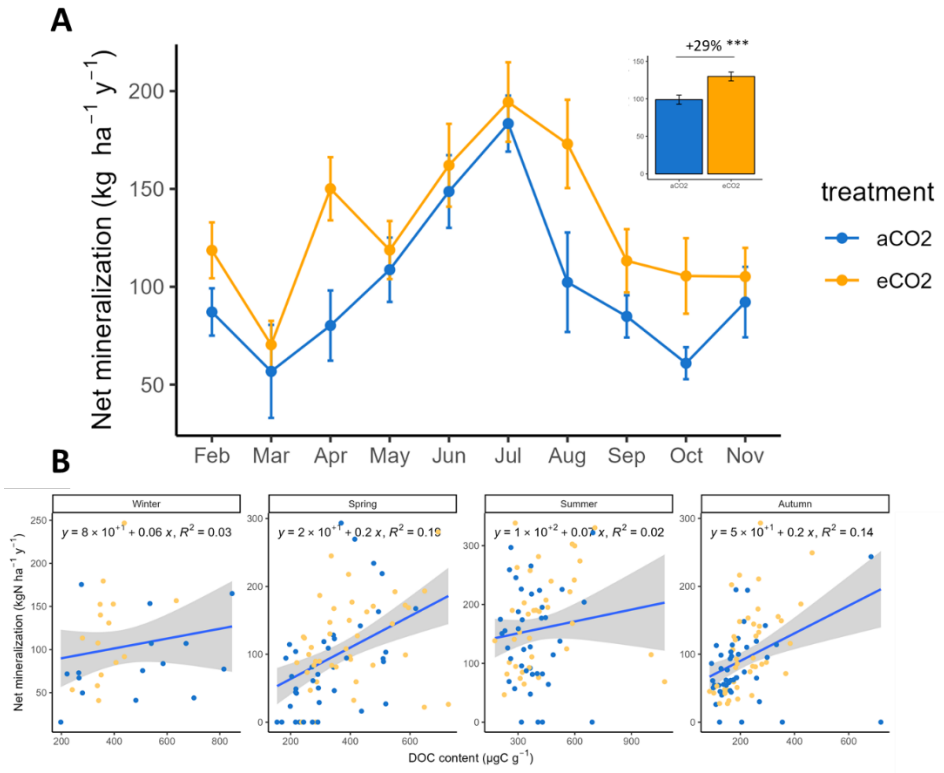

Figure 2.3: *A) Net nitrogen mineralization measured monthly from February 2022 to November 2022. Error bars represent the standard error between replicates (n=15). B) Correlation between net mineralization rate and soil DOC content per season of the year.*

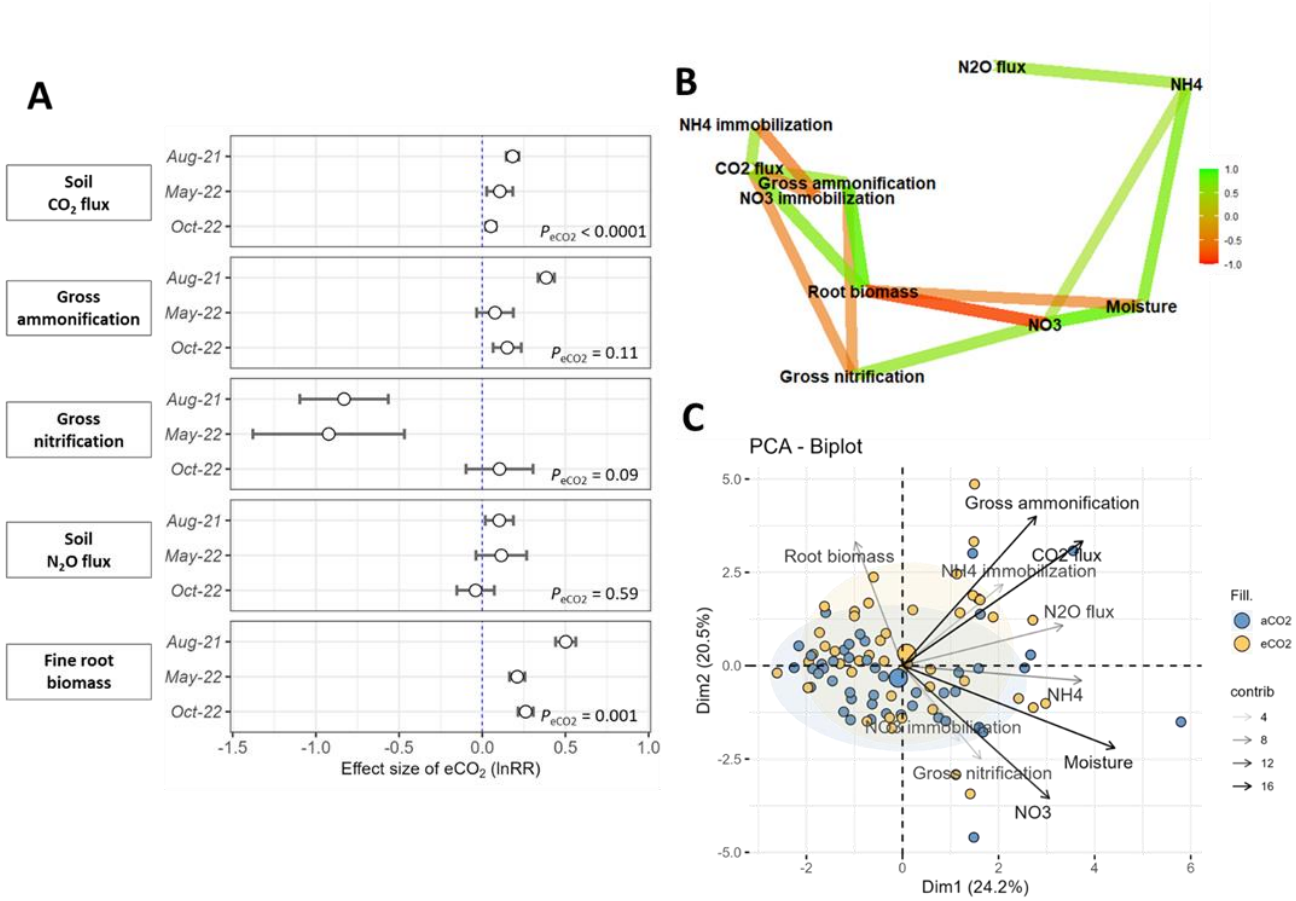

Figure 2.4: *A) Response ratio of soil CO_2 flux, gross ammonification, gross nitrification, soil N_2O flux and fine root biomass to eCO_2 with p-value of the eCO_2 effect (P_{eCO2}). B) Correlation network using the Pearson correlation index (threshold = 0.5) summarizing correlation over the 3 campaigns. C) Principal Component Analysis (PCA) plot representing the variable distribution along the dimensions 1 and 2 explaining together 44.7% of the total variability. Variable contributions (contrib) are represented by the darkness of the arrows.*

2.3.3. A faster yet tighter N cycle under eCO_2

The enhanced N-mining under eCO_2 did not translate in higher N losses contradicting our second hypothesis. Instead, nitrification was suppressed in spring and summer by 60% (P = 0.09), despite the higher DOC and DON availability which typically stimulate nitrification in acidic forest soils (Tang et al., 2019). Nitrate content in the intact cores was negatively correlated with root biomass, suggesting a mitigating effect of root presence on nitrification. A reduction of nitrification and an enhancement of ammonification was also observed in the rhizosphere (Rumeau et al., 2024; Chap 3). Thus, while higher root biomass might reduce

nitrification at the macro-scale by intensifying the competition for ammonium (Dijkstra et al., 2013) and diminishing nitrification microsites (Schimel and Bennett, 2004) (Fig. 2.4B); at the micro-scale of the rhizosphere, nitrification is also suppressed by eCO_2 likely through biological nitrification inhibition mechanisms (Zhu et al., 2021). Discrete N_2O measurements in intact soil cores showed no measurable effect of eCO_2 against natural variability (Fig. 2.4A). However, continuous in-situ measurements detected a 74% reduction in total N_2O emissions (Armstrong et al., 2024). Conversely, laboratory measurements on root-free soils found higher potential N_2O emissions in the bulk soil at site in 2022 ($P < 0.05$; Fig. S2-6) and across previous years (Sgouridis et al., 2023). These contrasting responses suggest that root presence mitigates N_2O emissions as part of a N conservation strategy for trees (Fender et al., 2013). N conservation strategies were also observed at the ecosystem scale, through the higher C:N ratio of the soil leachates and of the root exudates (Reay et al., *in review*), together with the 25% increase in N leaf resorption at leaf fall (Mayoral et al., *in prep).* Together these findings challenge the original paradigm of a uniformly faster N cycle under eCO_2. Instead, they reveal a faster yet tighter N cycle facilitated by complex plant-soil interactions and trees' ability to conserve N. This faster and tighter N cycle may be a crucial factor in delaying N limitation under future climate scenarios but will also intensify competition between microbes and trees, potentially leading to a scenario where microbes outcompete trees for N resources.

2.4. Conclusion

After six years of CO_2 enrichment, enhanced net primary productivity, dominated by 180-year-old oaks, was sustained through enhanced mineralization and a N conservation at the ecosystem scale. Linking C allocation belowground to seasonal enhanced N mineralization supports that trees under eCO_2 are able to increase C allocation belowground to stimulate soil N-mining in time of need. However, with negligible BNF and decreasing atmospheric N deposition, enhanced N mining and increased N conservation may only provide a temporary relief from PNL. Eventually, SOM stocks could deplete or become increasingly resistant to

decomposition, and competition between plants and microbes will intensify which would have implications for constraining the CO_2 fertilization effect in future.

While this study brings to light an adaptability in N cycling allowing trees to adapt to higher N demand. But this study also raises multiples questions on the underlying mechanisms driving this N cycling adaptability: What mechanisms are involved in the enhanced N-mining under eCO_2? Which pool of SOM is being targeted? Why does root biomass have opposite effects on ammonium and nitrate dynamics? The next chapter will address these different questions by zooming onto the rhizosphere processes involved in N and C metabolisms.

2.5. Supplementary materials

Table S 2-1: *Effect of treatment and period and their interactions shown as a model F statistic and P value. Bod typing indicate a significative effect (P <0.05), and a dash line indicate the switch between monthly measured variables (DF = 9) to seasonally measured variables (DF = 2).*

Factors	Treatment		Period		Treatment:Period	
DF	1		9 (or 2)		9 (or 2)	
Analysis of variance	F statistic	*P*	F statistic	*P*	F statistic	*P*
Gravimetric moisture	1.21	0.27	5.5	**<0.0001**	0.53	0.85
DOC	5.03	**0.02**	17.15	**<0.0001**	0.98	0.45
DON	3.95	**0.04**	17.12	**<0.0001**	0.86	0.56
NH_4^+	6.01	**0.01**	2.7	**0.005**	1.49	0.14
NO_3^-	0.01	0.90	7.34	**<0.0001**	0.86	0.55
Net mineralization	6.48	**0.01**	9.39	**<0.0001**	0.54	0.83
Gross mineralization	2.51	0.11	3.0	**0.05**	0.6	0.54
Gross nitrification	2.84	**0.09**	1.84	0.16	1.01	0.36
NH_4^+ immobilization	3.08	**0.08**	0.09	0.91	1.7	0.19
NO_3^- immobilization	3.92	**0.05**	4.01	**0.02**	2.6	**0.08**
Soil CO_2 flux	12.3	**0.0005**	78.3	**<0.0001**	3.9	**0.02**
Root biomass	11.1	**0.001**	1.2	0.3	0.9	0.40
N_2O emissions	0.27	0.59	15.5	**<0.0001**	0.12	0.87
N_2O per nitrification	1.6	0.20	1.1	0.33	0.12	0.88
N_2O per denitrification	0.004	0.98	2.7	**0.07**	0.7	0.49

Table S 2-2: *Nitrogen fixation in the six arrays at three time points (June and September 2021 and April 2022) in nmol g^{-1} d^{-1}. Different letters indicate significant difference between the six arrays. LOD = limit of detection set at 0.14 nmol g^{-1} d^{-1} from repeated IRMS analysis. Data are means + SE (n=5).*

	eCO_2			**aCO_2**		
	A1	A4	A6	A3	A2	A5
June 2021	<LOD a	0.19 ± 0.04 a	0.71 ± 0.56 a	<LOD a	0.31 ± 0.16 a	0.63 ± 0.33 a
September 2021	<LOD a	<LOD a	<LOD a	0.19 ± 0.04 a	0.57 ± 0.42 a	0.28 ± 0.13 a
April 2022	<LOD b	0.22 ± 0.06 b	0.37 ± 0.15 b	<LOD b	0.17 ± 0.02 b	0.66 ± 0.17 a

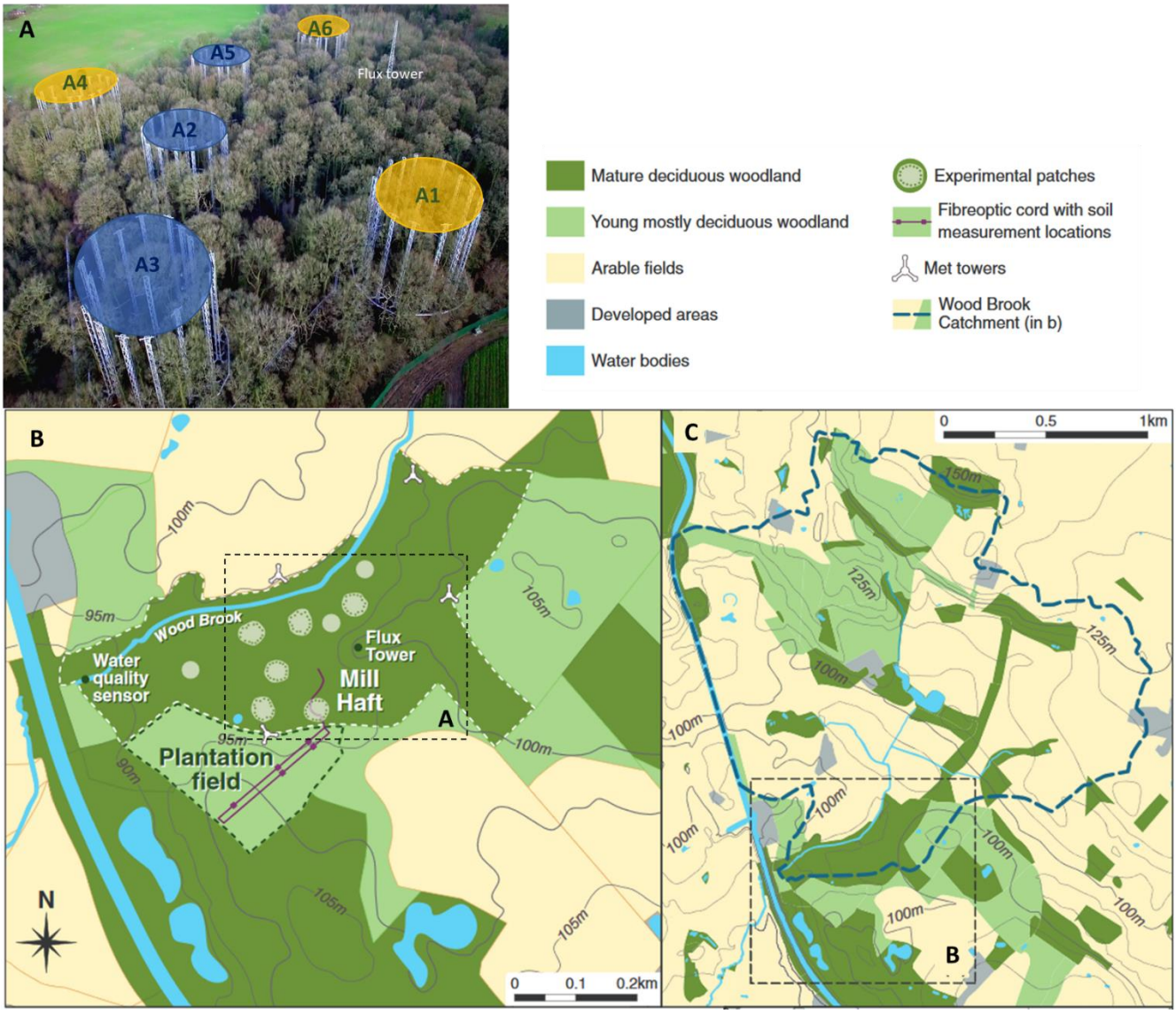

Figure S 2-1: *A) Schematic of the BIFoR-FACE (fumigated arrays are represented in orange and ambient arrays are in blue) B) and C) Maps of BIFoR FACE surrounding from Mackenzie et al. 2021.*

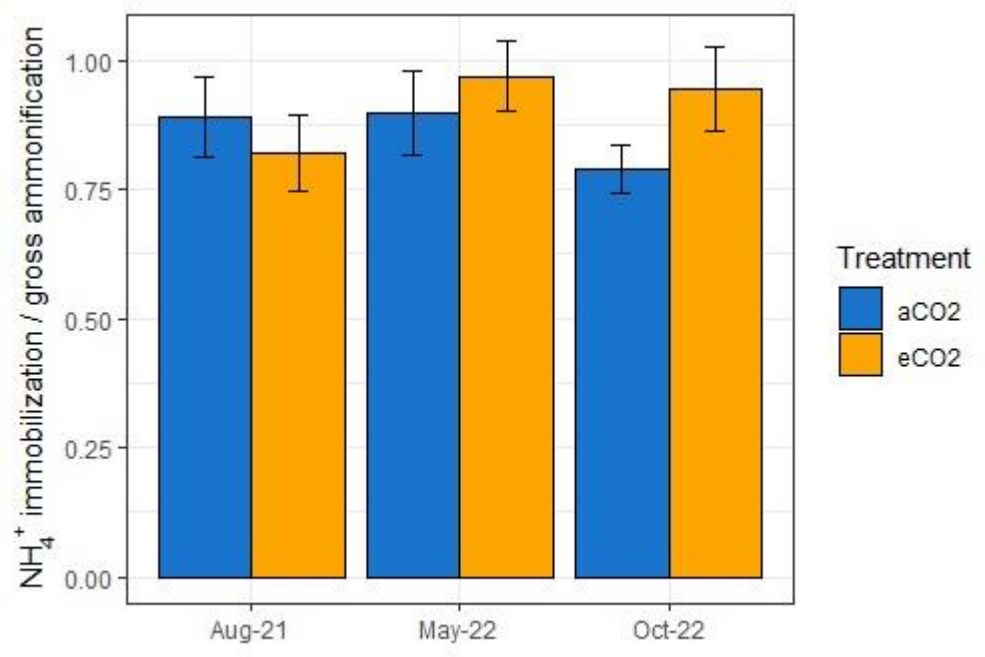

Figure S 2-2: *Ratio of NH_4^+ immobilization over gross mineralization from in-situ incubation in August 2021, May 2022 and October 2022 (mean + se).*

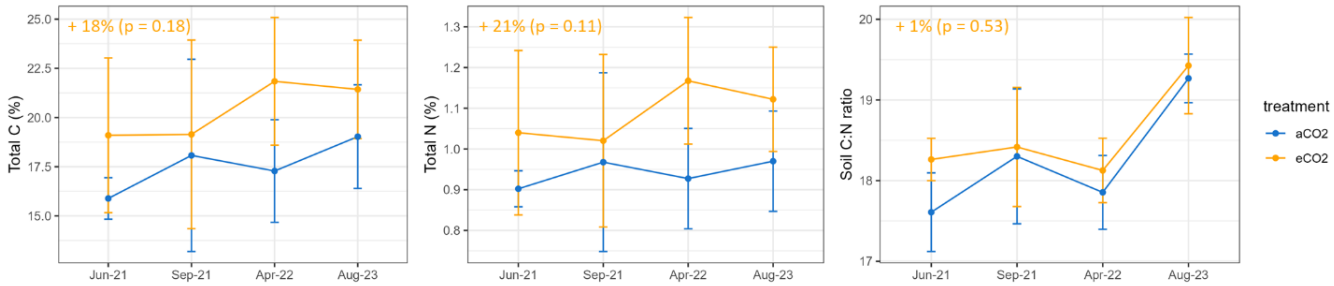

Figure S 2-3: *Soil total C, N and C:N ratio at four sampling times from 2021 to 2023. Errors bars represent the standard errors between arrays (n=3).*

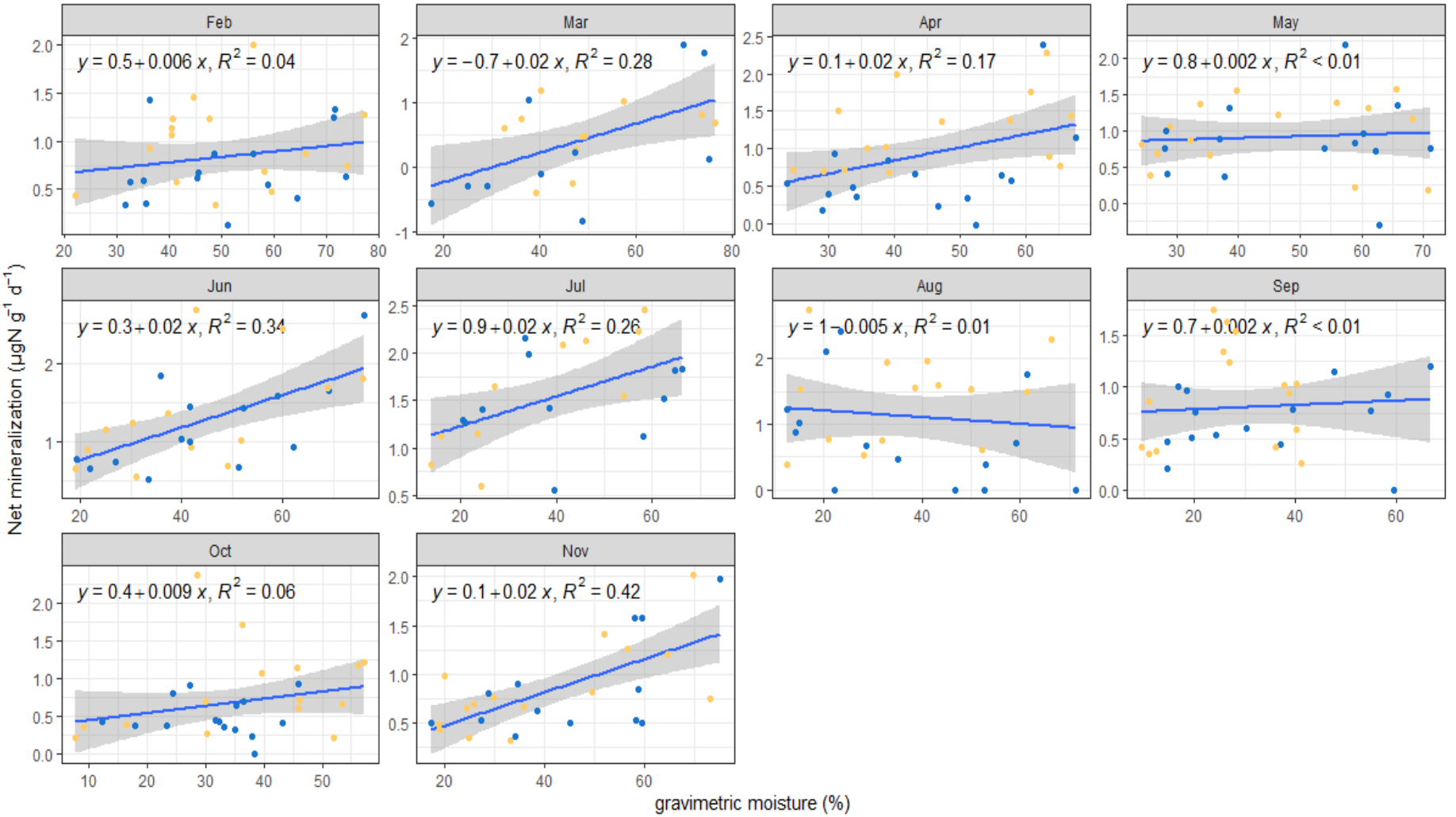
Feb
y = 0.5 + 0.006 x, R2 = 0.04
Mar
y = −0.7 + 0.02 x, R2 = 0.28
Apr
y = 0.1 + 0.02 x, R2 = 0.17
May
y = 0.8 + 0.002 x, R2 < 0.01
Jun
y = 0.3 + 0.02 x, R2 = 0.34
Jul
y = 0.9 + 0.02 x, R2 = 0.26
Aug
y = 1 − 0.005 x, R2 = 0.01
Sep
y = 0.7 + 0.002 x, R2 < 0.01
Oct
y = 0.4 + 0.009 x, R2 = 0.06
Nov
y = 0.1 + 0.02 x, R2 = 0.42
Net mineralization (µgN g−1 d−1)
gravimetric moisture (%)

Figure S 2-4: *Net mineralization correlation with soil gravimetric moisture on a monthly basis from February 2022 to November 2022 (orange= eCO_2, blue = aCO_2).*

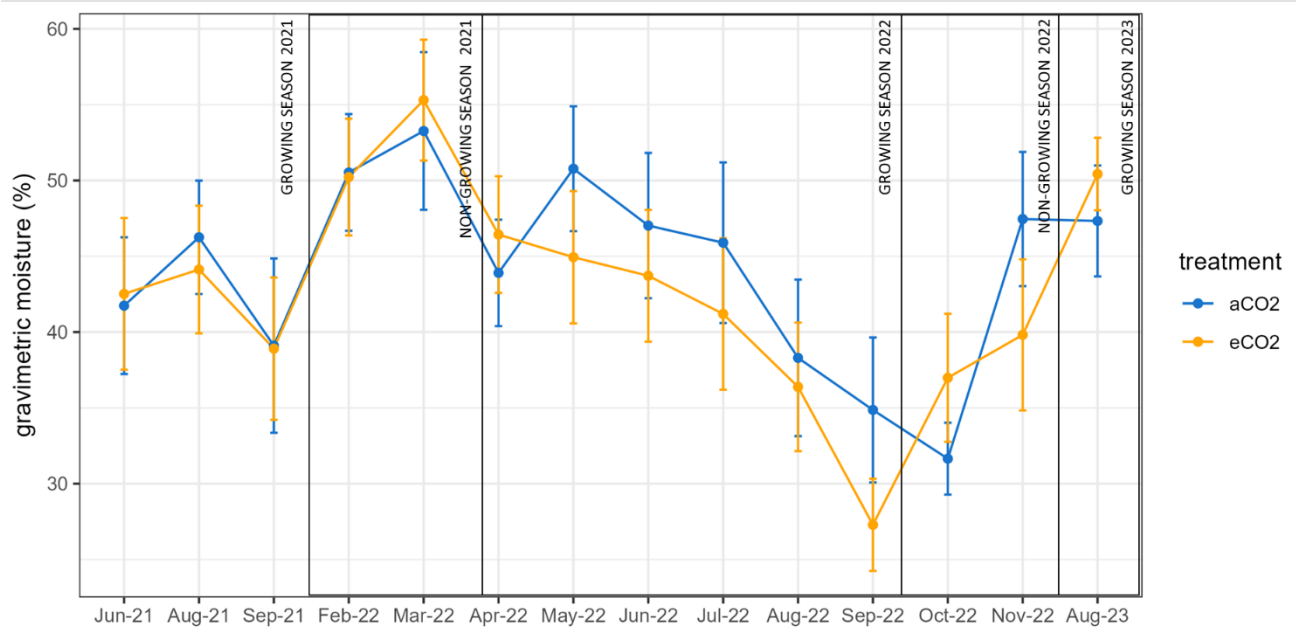

Figure S 2-5: *Soil gravimetric moisture under eCO_2 (orange) and aCO_2 (blue) from June 2021 to August 2023. Error bars represent the standard error between replicates (n=15). Periods are separated between growing and non-growing seasons.*

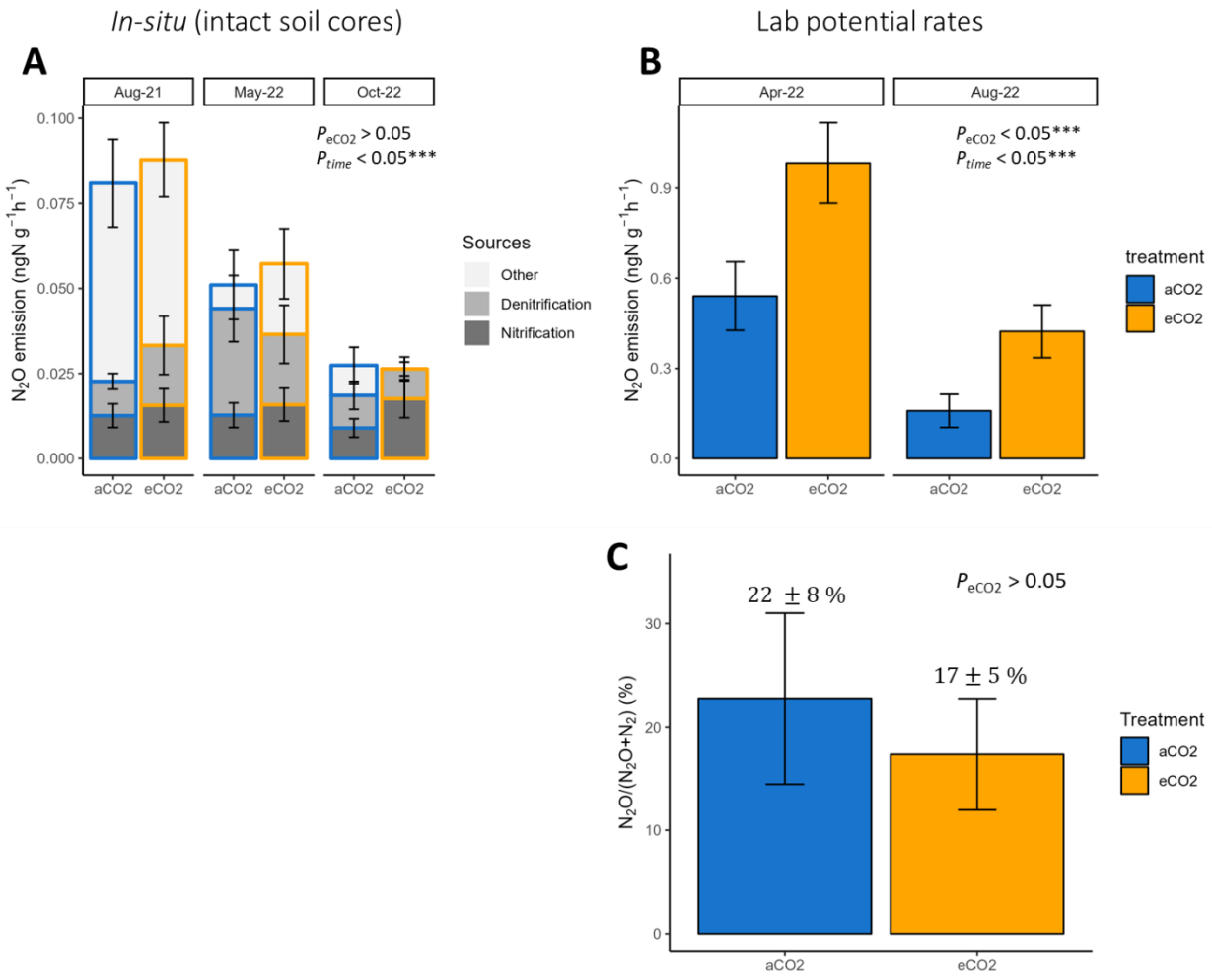

Figure S 2-6: *A) Nitrous oxide emission with source partitioning (from nitrification, denitrification or other sources) at the 3 sampling dates (n=30 replicates). B) Potential total N_2O emissions measured in a laboratory setting in April and August 2022 (n=15). C) Potential denitrification ratio (N_2O/N_2O+N_2) in percentage measured in a laboratory setting (n=5). P-values associated with the effect of eCO_2 and the effect of sampling date are indicated by P_{eCO2} and P_{time} respectively.*

Chapter 3.The role of rhizosphere in enhancing N availability in a mature forest under eCO_2

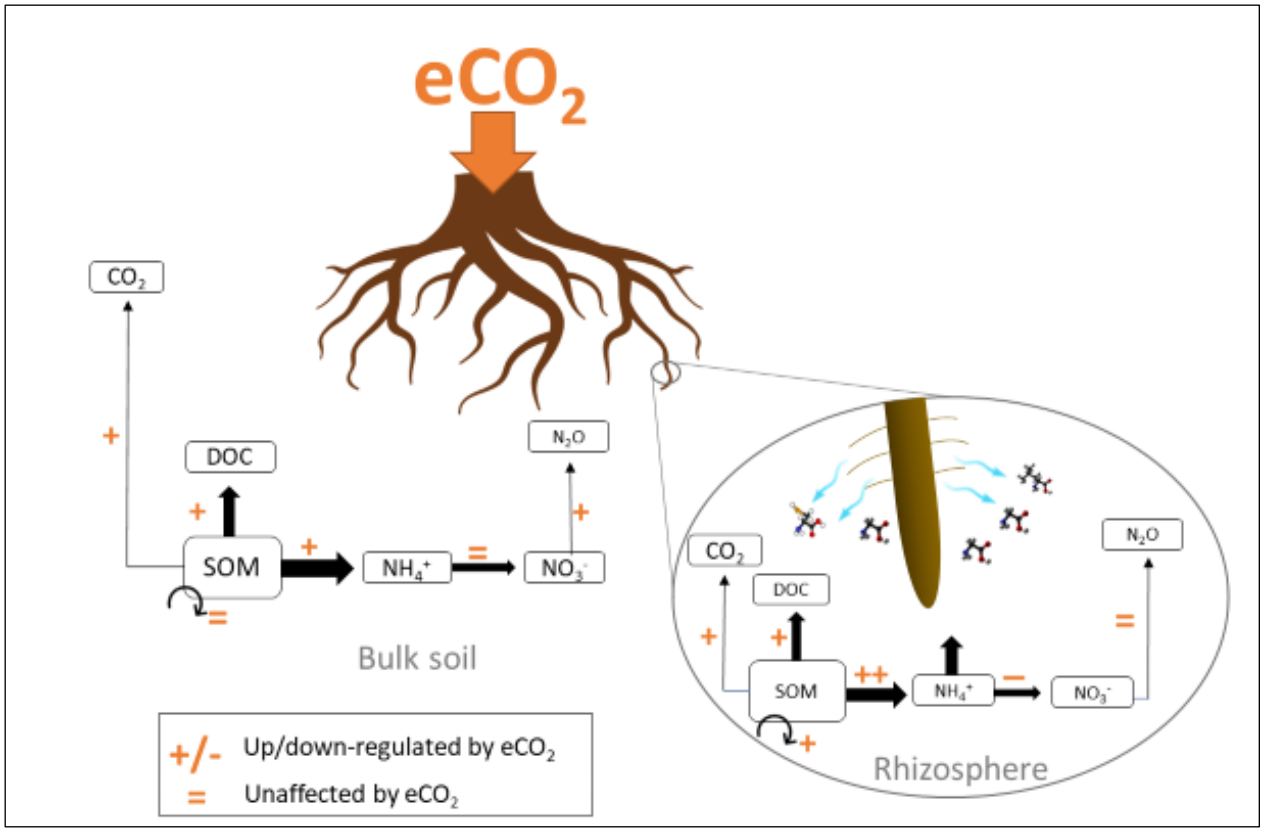

The role of rhizosphere in enhancing N availability in a mature temperate forest under elevated CO_2

Manon Rumeau[1,2,*], Fotis Sgouridis[4], Rob MacKenzie[1,2], Yolima Carrillo[3], Michaela K. Reay[5], Ian P. Hartley[6] and Sami Ullah[1,2]

[1]*Birmingham Institute of Forest Research, University of Birmingham, Birmingham, UK*

[2]*School of Geography, Earth and Environmental Science, University of Birmingham, UK*

[3]*Hawkesbury Institute for the Environment (HIE), Western Sydney University Richmond, Australia*

[4]*School of Geographical Sciences, University of Bristol, Bristol, UK*

[5]*Organic Geochemistry Unit, School of Chemistry, University of Bristol, UK*

[6]*Geography, Faculty of Science, Environment and Economy, University of Exeter, Exeter, UK*

* Corresponding author: MLR094@student.bham.ac.uk (Manon Rumeau).

Additional Corresponding authors: S.ullah@bham.ac.uk (S. Ullah)

This chapter is the last version of the following manuscript published in Soil and Biogeochemistry:

Rumeau, M., Sgouridis, F., MacKenzie, R., Carrillo, Y., Reay, M.K., Hartley, I.P., Ullah, S., 2024. The role of rhizosphere in enhancing N availability in a mature temperate forest under elevated CO2. Soil Biol. Biochem. 197, 109537. https://doi.org/10.1016/j.soilbio.2024.109537

Abstract

Enhanced growth of trees under elevated atmospheric CO_2 concentration ('CO_2 fertilisation') can potentially reduce a fraction of anthropogenic CO_2 emissions but is anticipated to become progressively constrained by nitrogen (N) limitation in temperate ecosystems. However, it is believed that this constraint may be mitigated if trees under elevated CO_2 (eCO_2) prime microbial activity in their rhizosphere to release available N. We assessed whether mature trees under eCO_2 regulate N availability in their rhizosphere to meet increased N demand. We hypothesized that eCO_2 primes N mineralization in the rhizosphere while reducing N losses through nitrification and denitrification. This study was conducted in a mature English-Oak-dominated temperate forest in central England, in the sixth year of Free Air CO_2 Enrichment (FACE). In the summer of 2022, we measured N transformations, enzyme activities, and nutrient pools in the rhizosphere and bulk soil of the organic layer (0-7 cm) under laboratory conditions. While the rhizosphere was found to be inherently more active (i.e. positive N priming) than the bulk soil, the effect of eCO_2 were not consistently stronger in the rhizosphere. Available soil N, dissolved organic carbon and microbial biomass were enhanced under eCO_2 in bulk and rhizosphere soils. Net N mineralization was enhanced under eCO_2 in the bulk and rhizosphere soils while leucine aminopeptidase activity, associated with organic N depolymerization, was enhanced solely in the rhizosphere. Despite higher C and N availability creating potential hot spots, nitrification was reduced under eCO_2 and denitrification remained unaffected in the rhizosphere, demonstrating a more efficient conservation of N under eCO_2. Our findings demonstrate that eCO_2 stimulates N-mining and reduce N losses in the rhizosphere. Furthermore, the tenfold difference in N turnover rates between rhizosphere and bulk soils suggests that expanding rhizosphere mass from increased root biomass may help trees under eCO_2 to meet higher N demand.

Keywords: FACE experiment, mineralization, nitrous oxide, soil enzyme activities, carbon

3.1. Introduction

Temperate forests under elevated atmospheric CO_2 (eCO_2) concentration are expected to require more available nitrogen (N) to be able to sustain the higher net primary productivity (NPP) triggered by the CO_2 fertilisation effect (Gardner et al., 2021; Norby et al., 2002). Biogeochemical simulations and meta-analysis indicate that enhanced photosynthesis under eCO_2 exacerbates progressive N limitation (PNL) of forest ecosystems because more N will be sequestered in long lasting biomass pools (De Graaff et al., 2006; Johnson, 2006; Luo et al., 2004; McMurtrie et al., 2008; van Groenigen et al., 2006). This hypothesis was supported by one of the firsts free air carbon enrichment (FACE) experiments involving young sweetgum plantation at Oak Ridge FACE, where the initially enhanced NPP decreased after a few years of eCO_2 treatment, indicating N limitation of the growth enhancement (Norby et al., 2010). However, outcomes from a similar FACE experiment (Duke FACE) challenged the PNL hypothesis as enhanced NPP was maintained over 11 years, suggesting N supply in soils was sustained via enhanced decomposition of soil organic matter (SOM) (Phillips et al., 2011). This discrepancy between CO_2 manipulation experiments demonstrates our lack of understanding in forest N cycling, especially in the context of climate change and rising atmospheric CO_2 (U.S. DOE, 2020). Furthermore, while most FACE experiments have been conducted in systems with young trees (Norby and Zak, 2011), recent observations in a mature forest (EucFACE) showing lower-than-expected C uptake responses to eCO_2 challenged original thinking on whether mature trees can initiate an enhancement of photosynthesis under eCO_2 (Ellsworth et al., 2017; Jiang et al., 2020). Thereby, it is uncertain whether the way trees regulate biochemical cycles under eCO_2 is similar in mature forests which had decades to interact with soil microbial communities and exhaust soil nutrient resources (Norby et al., 1999).

Tree ability to enhance N availability is largely governed by their interactions with microbes. For instance, under eCO_2, trees in association with ectomycorrhizal fungi (ECM) can acquire

N at low cost due to the fungi's ability to access SOM (Pellitier et al., 2021; Stuart and Plett, 2020; Terrer et al., 2018). More generally, plant-microbe interactions in the rhizosphere have been identified as a key mechanism for increasing N supply to plants under eCO_2 (Meier et al., 2015; Phillips et al., 2012, 2011). However, rhizosphere priming effect (RPE) defined as the stimulation or retardation of SOM decomposition by root presence and exudation (Carrillo et al., 2014; Dijkstra et al., 2013), can both increases or decreases N availability depending on soil nutrient status, soil and/or exudate C:N ratio and microbial nutrient acquisition strategy (Craine et al., 2007; Gaudel et al., 2024; Kuzyakov, 2002); properties likely to be affected by eCO_2. Especially, changes in root exudate composition and quantity observed under eCO_2 (Dong et al., 2021; Johansson et al., 2009; Phillips et al., 2009) are likely to enhance SOM decomposition to meet the higher tree nutrient demands (Meier et al., 2015; Pihlblad et al., 2023; Terrer et al., 2021). For instance, enhanced exudation of dissolved organic carbon was found to stimulate microbial activity and therefore the secretion of N-acquiring enzymes in low-N soils (Phillips et al., 2011). Organic acids were also found to be released in higher quantity under eCO_2 (Hasegawa et al., 2023), which could directly destabilize SOM and mobilise nutrients into bioavailable forms (Jilling et al., 2018).

However, enhanced SOM decomposition for N release could progressively lead to a depletion of soil C pools, offsetting the biomass C sink under eCO_2 (Terrer et al., 2021). This soil-for-plant C offsetting may be especially significant if slow cycling pools of SOM are targeted, as it has been observed by the gradual reduction of mineral associated organic matter (MAOM) pool under eCO_2 (Dorodnikov et al., 2011; Hofmockel et al., 2011) or by the loss of *old C* (Carrillo et al., 2018). Enzyme activity can provide valuable insights into which specific pools of soil organic matter (SOM) are being targeted for decomposition under eCO_2. A shift between oxidative and hydrolytic enzyme activity can indicate which components of SOM are primed, since oxidative enzymes often initiate the first step of complex organic matter break-down or destabilization (Jilling et al., 2018). eCO_2 was found to promote hydrolytic over oxidative

enzyme activity indicating a preference for decomposing simple molecules (Xiao et al., 2018), this preference reversed over time at Duke FACE (Finzi et al., 2006b). Therefore, how eCO_2 influences rhizosphere priming and its subsequent impact on soil C pools over time remains uncertain (Hyvönen et al., 2007; Kuzyakov et al., 2019; Terrer et al., 2021).

In addition, the regulation of N losses via dissimilatory reduction to N gases and leaching into groundwater in the rhizosphere under eCO_2 is poorly understood (Barnard et al., 2005; Rütting and Andresen, 2015). Nitrification and denitrification in the rhizosphere could be enhanced because of the higher C availability and, hence, higher microbial activity (Philippot et al., 2009) or, conversely, trees could exudate higher concentrations of biological nitrification inhibitor (BNI), as a N conservation strategy (Guyonnet et al., 2017; Jilling et al., 2018; Subbarao et al., 2007). Therefore, constraining N availability under eCO_2 requires an understanding of N turn-over and loss regulation in forest rhizosphere of mature trees as well as an understanding of microbial ecological strategies.

In this study, we aimed at understanding the response of N availability in the rhizosphere under eCO_2 in a mature deciduous forest, six years into CO_2 enrichment treatment at the Birmingham Institute of Forest Research (BIFoR) Free Air Carbon Dioxide Enrichment (FACE) facility in the UK. We assessed both potential net and gross N mineralization rates to gain comprehensive insights into the temporal changes in N availability (net mineralization measured in-situ over 28 days) and into the specific N process dynamics (gross mineralization) in the rhizosphere and bulk soils of the organic layer (0-7 cm) under elevated and ambient atmospheric CO_2 conditions after six years of CO_2 enrichment. We also quantified potential N_2O emissions, potential oxidative and hydrolytic extracellular enzyme activities involved in C, N and phosphorus (P) cycling to elucidate nutrient acquisition shifts. Given that eCO_2 can potentially affect exudation quantity and quality, we hypothesised that: 1) eCO_2 will prime N mineralization in the rhizosphere through the decomposition of recalcitrant SOM pools. Inversely, 2) eCO_2

will decrease nitrification and denitrification rates more strongly in the rhizosphere than in the bulk soils as a strategy to conserve N.

3.2. Material & Methods

3.2.1. Experimental set up

The study was performed at the BIFoR-FACE facility, located in a mature deciduous forest in Staffordshire, UK. The forest is dominated by English oak (*Quercus robur* L.) in the upper canopy and common hazel (*Corylus avellana* L.*),* sycamore (*Acer pseudoplatanus* L.), and hawthorn (*Crataegus monogyna* Jacq.) in the understorey. The soil at site, classified as Ortic Luvisol (Hart et al., 2020), set on glacial till and is about 50 cm deep where the organic soil layer (O) of about 7-10 cm depth overlies an A horizon (15 to 25 cm deep) overlying the B horizon transiting into sandstone geology. The O-layer is a sandy loam (41% sand, 43% silt, 16% clay), with a pH of 3.8 and is characterized by a high root density (1 mg cm^{-3} on average, data not shown), a high organic matter (10% of C) and low bulk density (0.45 $g.cm^{-3}$) (Hollis et al., 2021). The mineral layer (A) is also a sandy loam (39% sand, 39% silt, 22% clay), with a pH of 4.7 and a bulk density of 0.79 $g.cm^{-3}$. More detailed soil properties for the first 15 cm can be found in Sgouridis et al. (2023).

The BIFoR-FACE facility is composed of six infrastructure arrays, three are fumigated with a target concentration of +150 ppm of CO_2 above the ambient concentration (eCO_2) and three with ambient air (aCO_2) (Fig. 3.1). CO_2 enrichment started in April 2017 and operated in daylight hours from budburst (~1st April) to leaf fall (~1st November).

Figure 3.1: *Schematic of the BIFoR-FACE site from (Hart et al., 2020). Fumigated arrays are represented in orange and ambient arrays are in blue.*

The towers reach one to three metres above the local canopy top in order to fumigate the forest from ground to canopy level. Air is released from the upwind quadrant of the array through vertical vent pipes (VVPs) placed on the 16 peripheral towers in each array. Performance of the system has been reported in Hart et al. (2020), showing that the system is able to deliver the target concentration precisely; the daytime CO_2 enrichment achieved during the 2022 growing season was of 135 ± 24 ppm (mean ± SD), due to intermittency in the CO_2 supply. The mean annual air temperature at the site was of 10.8°C (sensors HMP155 (Helsinki, Finland)) and the mean annual precipitation was 1152 mm (rain gauges at site TR-525M (Dallas, Texas)). For a detailed site description, see Hart et al. (2020).

3.2.2. Soil sampling

In each array, three sampling plots of 0.5 m x 0.5 m were established, each at approximately one-metre distance from different individual oak trees. On August 13th 2022, three soil cores

of 5 cm diameter comprising exclusively the organic layer (O-horizon: Oe +Oa) after removing the leaf litter (Oi) were collected per sampling plot and bulked together to make-up one sample per sampling plot before analysis. On the day of the sampling, the soil surface temperature was 15°C and the soil gravimetric moisture in the O horizon varied between 10 to 55% (Table S3-1). The depth of the O-horizon varied between 5 to 9 cm between sampling areas (Table S3-1 and Fig. S3-1).

Rhizosphere soil was separated from bulk soil by gently shaking the roots. Soil that remained attached to the roots after shaking was considered as the rhizosphere sample while the rest of the sample constituted the bulk soil and was sieved through a 2 mm sieve. Masses of rhizosphere and bulk soils were recorded to calculate the proportion of rhizosphere. Roots were kept and visually identified as “oak root” or “non-oak root” to determine the relative proportion of oak rhizosphere (Table S3-2). Rhizosphere and bulk soil samples were stored at 5°C until further analysis.

3.2.3. Nutrient standing pools analysis

To determine soil nutrient pools, we quantified soil ammonium ($N\text{-}NH_4^+$), nitrate ($N\text{-}NO_3^-$), free amino acids (FAA), dissolved organic C (DOC), dissolved N (DN), microbial biomass C and N (MBC and MBN) and total C and N contents. All nutrient analyses were performed within a week after field collection. Gravimetric moisture was measured by drying 5 g of soil at 105°C for 48h. Soil pH was determined after mixing 3 g of soil in 30 ml of deionized water using a pH meter (SevenExcellence pH, Mettler Toledo, UK).

Soil NH_4^+ and NO_3^- concentrations were measured by extracting 2 g of soil with 0.5 M potassium sulphate (K_2SO_4; soil: extractant ratio of 1:5 (*w*/*v*)). The extracts were filtered at 0.45 µm and analyzed by continuous flow colorimetry (Skalar SA 3000 analyser, Netherlands). The limit of detection was 0.02 mg N L^{-1} for both NH_4^+ and NO_3^-. The concentrations were blank corrected and the relative standard deviation (RSD) calculated on quality control (QC) samples was below 2%.

Soil free amino acid (FAA) concentration was determined using the OPAME fluorescence assay described by (Jones, 2002) and adapted to a microplate assay by Darrouzet-Nardi et al. (2013). Briefly, 2 g of soil was extracted in 10 ml of 1M KCl, shaken, filtered at 0.45 µm and 50 µl was added to a microplate with 100 µl of OPAME working reagent. As NH_4^+ reacts to fluorescence in the first hour, fluorescence was measured after 1 h of incubation when the fluorescence from reaction with NH_4^+ is negligible.

The soil concentration of DOC and DN was measured after extraction with 0.5 M K_2SO_4, as described above, and extracts analysed on a TOC/TN analyser after a 10-fold dilution (Multi N/C 2100, Analytik Jena, Germany). Samples were blank corrected and the RSD was below 1% for DOC and below 4% for DN.

The dried soils used for soil moisture determination were manually pulverized with a pestle and a mortar and approximatively 8 mg was weighed in a tin capsule. These samples were analysed for total C and N soil concentrations by an elemental analyser (EA; vario PYRO cube; Elementar Analysensysteme GmbH, Hanau, Germany). The EA was calibrated with sulphanilamide (N: 16.26%, C: 41.81%) and the precision was below 5% RSD for both C and N.

C and N in the microbial biomass (MBC and MBN) were measured according to the chloroform extraction method (Brookes et al., 1985). For each soil sample, two subsamples were weighed and one was fumigated with chloroform for 48 h. Blanks without soil were also fumigated. Fumigated and non-fumigated soil subsamples were then extracted with K_2SO_4 (0.5 M) for DOC and DN quantification as above. MBC and MBN were calculated as the difference in the DOC and DN concentrations between the fumigated and the non-fumigated samples and divided by a correction factor of 0.45.

3.2.4. ^{15}N isotopic pool dilution combined with the ^{15}N Gas Flux method

Gross N mineralisation, nitrification rates, soil N_2O emissions from nitrification and denitrification were assessed by a ^{15}N pool dilution method as described by Hart et al. (1994) combined with a ^{15}N Gas flux method as described by Sgouridis et al. (2023) within 2 weeks of sampling.

Labelling and incubation. Rhizosphere soils (5 g) and bulk soils (10 g) were weighed in quadruplets into airtight specimen cups equipped with a septum on the lid to allow gas sampling. Before labelling, all samples were acclimated in the dark at 15°C for 2 days, chosen to match the soil temperature on the sampling day. To achieve a simultaneous 20% enrichment in ^{15}N atom percentage – avoiding the stimulating of microbial activity – (Micucci et al., 2024) and raise the soil moisture to 35% (i.e. average of soil gravimetric moisture in summer) in all samples, various labelling solutions were prepared using $K^{15}NO_3$ (98 at. % ^{15}N, Sigma-Aldrich) or $^{15}NH_4Cl$ (98 at. % ^{15}N, Sigma-Aldrich). The labelling solutions were added dropwise, and soils were gently stirred with a spatula to ensure a uniform distribution of labels before closing the specimen cups. Immediately after labelling and following a 24 h incubation at 15°C in the dark, soil samples were extracted with 1 M KCl. A soil extract aliquot was analysed for extractable $N\text{-}NH_4^+$and $N\text{-}NO_3^-$, as described above, and the rest of the soil extract was used to extract the ^{15}N content in the NH_4^+ and NO_3^- pools using the gas diffusion procedure (Davidson et al., 1991; Hart et al., 1994).

Concurrently, 20 ml of gas was sampled near the soil surface with a syringe before cup closure and transferred into a pre-evacuated 12 ml gas exetainer vial (Labco, Ceredigion, UK). A final set of gas samples were obtained after 24 h of incubation by pumping the headspace (100 ml) with a syringe through the septum and transferring into a 12 ml gas exetainer. These samples were analysed for total CO_2, N_2O and CH_4 concentration on a gas chromatograph (GC; Agilent Technologies Ltd, USA) equipped with μECD (electron capture detector) and FID (flame-ionisation detector). The ^{15}N content of the N_2O was determined using a continuous flow

isotope ratio mass spectrometer (IRMS; Elementar Isoprime Precision; Elementar Analysensysteme GmbH, Hanau, Germany) coupled with a trace-gas pre-concentrator inlet with autosampler (isoFLOW GHG; Elementar Analysensysteme GmbH, Hanau, Germany). Gas samples in the 12 ml exetainer were purged into a He stream through the autosampler and then entered 2 sequential liquid N_2 traps to isolate and cryofocus the N_2O. The gas sample containing the concentrated N_2O was separated from any residual CO_2 via a GC column before passing though the IRMS where the N_2O isotopologues and R45 and R46 ratios were measured at a current of 600 µA. Ten N_2O reference samples were run before any of the samples to ensure instrument stability and a $\delta^{15}N$ standard deviation lower of 0.05‰.

Gas diffusion procedure on enriched soil extracts

The diffusion procedure was performed according to Davidson et al. (1991) and Hart et al. (1994). The aim is to diffuse the enriched pool of either NH_4^+ or NO_3^- onto an "acid trap" to then measure the ^{15}N at% of these N pools by an EA-IRMS (elemental analyser-IRMS: Elementar Isoprime Precision; Elementar Analysensysteme GmbH, Hanau, Germany). Acid traps were prepared with 8 mm diameter Whatman 3 filter discs soaked with 10 µL of 2.5 M $KHSO_4$ and wrapped in sealing PTFE tape. Using 20 to 40 ml of soil extract, NH_4^+ was diffused by simultaneously adding 0.2 g of MgO and an acid trap. To ensure complete diffusion, extracts were shaken at low speed for 7 days. Then, acid traps were retrieved, dried in a desiccator, and encapsulated in tin capsules for EA-IRMS analysis. To diffuse NO_3^-, NH_4^+ was first removed from the solution using the above procedure but the filters were discarded. NO_3^- was then diffused by adding 100 µL of 30 % Brij-35 and 0.4 g of Devarda's alloy, which reduces NO_3^- to NH_4^+. A second acid trap was placed into the specimen cups and samples were let for another 7 days at room temperature on reciprocal shaker. The filters disks were dried, wrapped and analysed for ^{15}N atom % on EA-IRMS.

Calculations

Gross mineralisation fluxes were calculated using the following equations developed by Kirkham and Bartholomew (1954):

$$M\ (\mu g\ g^{-1}\ day^{-1}) = \frac{[NH_4^+]_0 - [NH_4^+]_t}{t} \times \frac{\log\left(\frac{APE_0}{APE_t}\right)}{\log\left(\frac{[NH_4^+]_0}{[NH_4^+]_t}\right)} \quad (3.1)$$

$$C\ (\mu g\ g^{-1}\ day^{-1}) = M - \frac{[NH_4^+]_t - [NH_4^+]_0}{t} \quad (3.2)$$

Where M= gross mineralization rate, C= NH_4^+ consumption rate, t = time elapsed, [NH_4^+] = NH_4^+ soil concentration (µg g^{-1}), APE_τ = ^{15}N atom percent excess of the NH_4^+ pool, τ. Gross rates of nitrification and NO_3^- consumption were calculated by replacing NH_4^+ concentration by NO_3^- concentration, and APE in the NH_4^+ pool by the APE in the NO_3^- pool. NH_4^+ immobilization rate is equal to the difference between NH_4^+ consumption rate and gross nitrification. NO_3^- immobilisation rate is assumed equivalent to the gross NO_3^- consumption rate.

Total N_2O emissions and basal respiration (i.e. CO_2 flux) were calculated using the following equation (CO_2 flux example):

$$CO_2\ flux\ (\mu gC\ g^{-1}\ h^{-1}) = \frac{(\ [CO_2]_t - CO_2]_0) \times H}{m \times t} \quad (3.3)$$

Where $[CO_2]_\tau$ = concentration of CO_2 in µg C L^{-1} in the vial, H = headspace in L, m = mass of dry soil (g), t = time elapsed (h). N_2O flux is calculated in the same way by substituting the concentration in N_2O in µg N L^{-1} in the above equation. N_2O from nitrification and denitrification were calculated as described in Sgouridis et al. (2023)

To assess microbial activity, the microbial metabolic quotient (qCO_2) was calculated by dividing microbial respiration by the microbial biomass C (Anderson and Domsch, 1993).

Finally, primed C and N by rhizosphere effect (Yin et al., 2021) were calculated as follows where R and B represent rhizosphere and bulk soil respectively (Equations 3.4 and 3.5):

$$Primed\ C\ (\mu gC\ g^{-1}\ h^{-1}) = R_{CO_2\ flux} - B_{CO_2\ flux} \quad (3.4)$$

$$Primed\ N\ (\mu gN\ g^{-1}\ h^{-1}) = R_{gross\ mineralization} - B_{gross\ mineralization} \quad (3.5)$$

3.2.5. Enzyme assays

The activities of six soil extracellular enzymes involved in microbial C, N and P cycling were assayed. These enzymes fall into two functional groups based on the type of compounds they are able to decompose. Oxidative enzymes including peroxidase (PEROX) and phenol oxidase (PHENOX) decompose recalcitrant SOM such as lignin. Hydrolytic enzymes involved in several organic compound breakdown such as β-N-acetyl-glycosaminidase (NAG) and leucine aminopeptidase (LAP) for organic N, β-glucosidase (BG) for organic C and acid phosphatase (AP) for organic P.

Fluorometric assays. Hydrolytic enzymes activities were determined by fluorimetry. Within 2 weeks after sampling, soil suspensions were prepared by sonicating 2 g of soil in 125 ml of acetate buffer (pH 5.2). While stirring, 200 µl of soil suspension were added in duplicate to 50 µl of substrate solution of 200 µM (Table S3-2) on a sterile black 96-well microplate. Quenched standard wells received 200 µl of soil suspension and 50 µl of either 4 methylumbelliferone, or 7-amino-4-methyl coumarin at concentrations ranging from 0.025 µM to 50 µM. Reference standard wells received 50 µl of standard (same as above) and 200 µl acetate buffer. Blank wells received 50 µl of acetate buffer and 200 µl of soil suspension and negative control wells received 50 µl of substrate and 200 µl of acetate buffer. Fluorescence was measured at 30°C every 5 minutes for an hour with excitation wavelength of 365 nm and an emission wavelength of 450 nm. Fluorescence intensity after the first 10 minutes of pre-incubation was plotted over time. The slope of the linear regression and coefficient of determination were calculated. Each regression was visually assessed, and any outliers were removed to ensure a satisfactory coefficient of determination ($R^2 > 0.97$). The slope was then used to determine the activity. An example of the linear regression can be found in Fig. S3-2.

Colorimetric assays. Phenol oxidase (PHENOX) and Peroxidase (PEROX) activities were determined by measuring absorbance at 450 nm. Soil suspensions were prepared by sonicating 0.5 g of soil in 125 ml of acetate buffer (pH 5.2). Again, 200 µl of soil suspension were added to 50 µl of substrate solution (25 mM DOPA) (Table S3-2) on a sterile transparent 96-well microplate. For peroxidase assays, 10 µl of 0.3 % H_2O_2 was added to the 50 µl of 25 mM DOPA substrate. Blank wells received 50 µl of acetate buffer and 200 µl of soil suspension, negative control wells received 200 µl of acetate buffer and 50 µl of substrate solution (+ 10 µl of 0.3% H_2O_2 in the case of Peroxidase). Absorbance was measured at 30°C every 5 minutes for 2 hours for Peroxidase, and every few hours for up to 48 h for Phenol oxidase. Similarly, activity was calculated as the slope of absorbance over time.

Calculations of microbial carbon use efficiency (CUE) and nitrogen use efficiency (NUE) from enzyme activities. We calculated microbial CUE and NUE (e.g. amount of nutrient assimilated in microbial cells over the amount taken up) from the elemental stoichiometry of organic matter and microbial biomass, and the ratios of C to N-acquiring eco-enzymatic activities (Sinsabaugh et al., 2016) (Equations 3.6 and 3.7). This method assesses how microbes shift their resource use efficiency in response to substrate stoichiometry (Schimel et al., 2022).

$$CUE_{C:N} = CUE_{max}\left(\frac{S_{C:N}}{(S_{C:N}+K)}\right) \quad where\ S_{C:N} = \frac{1}{EEA_{C:N}} \times \frac{B_{C:N}}{L_{C:N}} \qquad (3.6)$$

$$NUE_{N:C} = NUE_{max}\left(\frac{S_{N:C}}{S_{N:C}+K}\right) \quad where\ S_{N:C} = (1 - EEA_{N:C}) \times \frac{B_{N:C}}{L_{N:C}} \qquad (3.7)$$

where $S_{C:N}$ is a scalar that quantifies how ecoenzymatic activities allocate resources to mitigate differences between the elemental composition of available resources and that of microbial biomass. CUE_{max} is set at 0.6, NUE_{max} is set at 1.0 and K is the half saturation constant set at 0.5 (Sinsabaugh et al., 2016). $EEA_{C:N}$ refers to the enzymatic C:N ratio, $B_{C:N}$ is the microbial C:N ratio and $L_{C:N}$ is the soil DOC:DN ratio.

3.2.6. Net N mineralisation

Nitrogen net mineralisation rates were measured in June 2022 and August 2022. On June 6th and August 2nd, 5 replicates of organic soils (O horizon) were collected per array. On the same day, the rhizosphere soil was separated from the bulk soil as described above. Each bulk and rhizosphere sample were divided into two subsamples; one subsample was left for 28 d incubation in a polyethylene bag buried in-situ under the leaf litter (T28d) and the other (T0) was transported to the laboratory and analysed for extractable N-NH_4^+ and N-NO_3^- (see method description above). After 28 days, incubated T28d samples were retrieved and analysed for extractable N-NH_4^+ and N-NO_3^-. Net mineralization and net nitrification were then calculated as the difference N-NH_4^+ and N-NO_3^- content between the T0 and the T28d samples.

3.2.7. Statistical analyses

Statistical analyses were carried out with Rstudio software (version 4.1.0; R Core Team, 2021). Linear mixed effect models were used to evaluate soil fraction (rhizosphere or bulk soil) and treatment (eCO_2 or aCO_2) effects, with soil fraction and treatment set as fixed effects, and array set as random effects ("lmer" function, lme4 package; Bates et al., 2015). Due to high variability and low number of replications in FACE experiment (n = 3) we considered that a p-value (*p*) between 0.1 and 0.05 indicates an effect and a p-value < 0.05 indicates a significant effect. A Tukey's multi-comparison test was performed when the treatments or soil fraction had a significant effect on the variable ($p < 0.05$). Furthermore, to detect treatment effect independently from the soil fraction, one-way ANOVA models were performed on the rhizosphere data and on the bulk soil data separately (Table S3-3). When the assumptions of normality and homogeneity of variance were not met, log transformations were performed to meet model assumptions (Table S3-3). Correlations between variables were assessed using Pearson correlation tests and R-squared coefficients of determination. To estimate the eCO_2 effect, we calculated the natural log of the response ratio (RR) as an effect size and its

corresponding pooled variance (V) (Hedges et al., 1999) between the eCO_2 and aCO_2 treatment in both the bulk soil and the rhizosphere soil separately (Equations 3.8 and 3.9).

$$lnRR = \ln\left(\frac{Xe}{Xa}\right) \quad (3.8)$$

$$V = \frac{Se^2}{(Ne \times Xe^2)} + \frac{Sa^2}{(Na \times Xa^2)} \quad (3.9)$$

where X_e and X_a are the mean values of a specific variable in the eCO_2 and aCO_2 treatment respectively; N_e and N_a are the sample sizes; and S_e and S_a are the standard deviations.

3.3. Results

3.3.1. Soil nutrient standing pools

Expect of NO_3^-, all nutrient pools showed a positive rhizosphere effect with notably NH_4^+ increasing by 100%, DOC by 13%, free amino acids (FAA) by 18% and C:N ratio by 7% relative to the bulk soil ($p < 0.05$; Table 3.1, Fig. S3-3). Soil total C, N and microbial biomass pools were also higher, though the difference was not significant ($p > 0.05$). Soil NH_4^+ concentration, dissolved organic carbon (DOC) concentration and dissolved nitrogen (DN) were significantly higher under eCO_2 in both rhizosphere and bulk soils while FAA and NO_3^- concentrations remained unaffected by eCO_2 (Table 3.1). MBC was also higher under eCO_2 in both bulk and rhizosphere soils while MBN only increased significantly in the bulk soil (Table 3.1). Consequently, the microbial C:N ratio was increased by 10% under eCO_2 in the rhizosphere ($p > 0.05$). Total C and N were higher under eCO_2 in the bulk soil but lower in the rhizosphere ($p > 0.05$). Overall, most soil nutrient and microbial biomass pools were positively affected by eCO_2 but displayed a stronger eCO_2 effect in the bulk soil ($lnRR_{bulk\text{-}pool}$ = 0.32 on average against $lnRR_{rhizosphere\text{-}pool}$ =0.08; Fig. 3.2). Additionally, while the difference was not significant, the relative proportion of rhizosphere soil was slightly higher under eCO_2 (23.7%) compared to aCO_2 (21.2%; Fig. 3.3C).

Table 3.1: *Soil nutrient content and microbial biomass in bulk soil and rhizosphere soil under aCO_2 (ambient) and eCO_2 (elevated) and ANOVA test results with p-value below 0.1 highlighted in bold. Mean values and standard errors are indicated for each soil fraction and treatment (n=9).*

	Bulk soil		Rhizosphere soil		*ANOVA p-value*		
	aCO_2	eCO_2	aCO_2	eCO_2	*fraction*	*treatment*	*fraction x treatment*
Gravimetric moisture (%)	22 ± 3	25 ± 5	21 ± 3	21 ± 4	***0.08***	*0.83*	*0.48*
pH	3.9 ± 0.2	3.8 ± 0.2	3.8 ± 0.1	3.9 ± 0.2	*0.77*	*0.83*	*0.21*
$N\text{-}NO_3^-$ (µg g^{-1})	15 ± 5	20 ± 7	11 ± 3	13 ± 5	*0.15*	*0.52*	*0.15*
$N\text{-}NH_4^+$ (µg g^{-1})	3.8 ± 0.7	6.9 ± 1.1	9.5 ± 2.2	11.4 ± 1.4	***<0.001***	***<0.001***	*0.24*
N-FAA (µg g^{-1})	2.8 ± 0.2	3.3 ± 0.4	3.4 ± 0.3	3.8 ± 0.3	***0.06***	*0.44*	*0.88*
MBC (µg g^{-1})	695 ± 62	969 ± 79	791 ± 91	914 ± 93	*0.69*	***0.02***	*0.36*
MBN (µg g^{-1})	86 ± 7	119 ± 10	100 ± 13	106 ± 13	*0.85*	*0.45*	***0.08***
MBC:MBN ratio	8.1 ± 0.2	8.2 ± 0.3	8.1 ± 0.3	8.9 ± 0.3	*0.23*	*0.42*	*0.18*
DOC (µg g^{-1})	240 ± 11	311 ± 25	284 ± 7	333 ± 19	***0.05***	***0.06***	*0.52*
DN (µg g^{-1})	33 ± 4	44 ± 8	38 ± 4	43 ± 3	*0.18*	***0.03***	*0.50*
Total C (%)	8.9 ± 1.7	13.0 ± 2.3	13.3 ± 2.5	10.9 ± 1.6	*0.57*	*0.7*	***0.10***
Total N (%)	0.50 ± 0.07	0.67 ± 0.10	0.63 ± 0.12	0.56 ± 0.07	*0.92*	*0.57*	*0.19*
C:N ratio	17.1 ± 0.7	18.5 ± 0.8	19.6 ± 0.6	18.9 ± 0.5	***0.03***	*0.54*	***0.09***

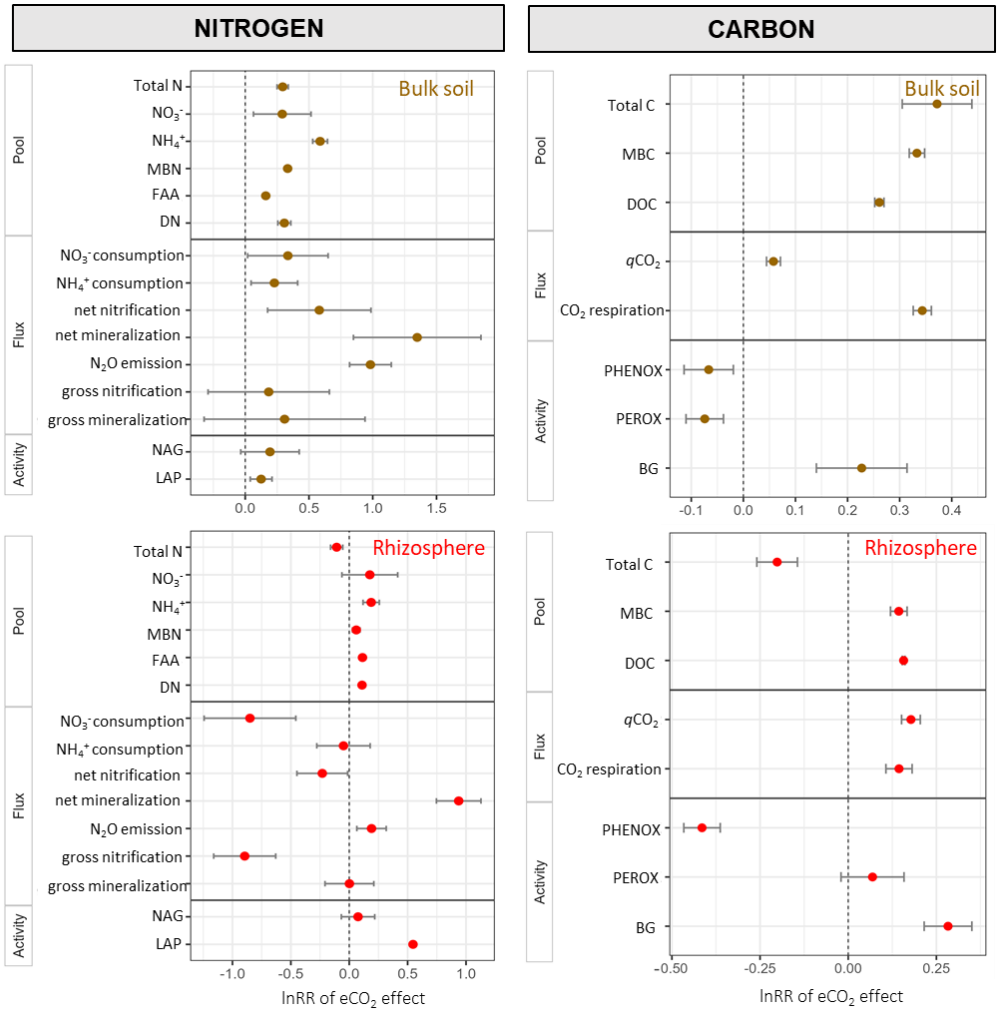

Figure 3.2: *Response ratio (lnRR mean with standard error) of the eCO_2 effect in the bulk (brown) and rhizosphere soil (red) relative to aCO_2 calculated for each variable (gross rates, N_2O emissions and CO_2 respiration are measured from soil incubated with 15N label). A negative response ratio means that eCO_2 decreased that specific variable and a positive value means that eCO_2 increased that variable.*

3.3.2. Nitrogen and carbon fluxes

3.3.2.1. Nitrogen mineralization and nitrification

Gross and net mineralization rates were ten times higher in the rhizosphere compared to bulk soils (Fig. 3.3). However, while eCO_2 had no discernible impact on gross rates or on the amount of primed N (Table 3.2), it increased net rates in both bulk and rhizosphere soils (RR > 0.9; Fig. 3.2), but this enhancement was only significant in the rhizosphere (+150% in August; Fig. 3.3B). Gross nitrification and net nitrification were both enhanced in the

rhizosphere but only under aCO_2 ($p < 0.05$). Consequently, nitrification was lower under eCO_2 compared to aCO_2 in the rhizosphere ($p > 0.05$; Fig. 3.3), this reduction was especially pronounced on the gross rates (RR = ─ 0.80) compared to the net rates (RR = ─ 0.25; Fig. 3.2). Additionally, gross nitrification showed a positive correlation with soil DOC and DN content under aCO_2 but not under eCO_2 (Fig. S3-4) while net nitrification was mostly correlated with soil moisture (Fig. S3-5). Finally, while gross and net mineralization rates were positively correlated (R^2= 0.30), gross and net nitrification showed a poor correlation (R^2=0.03; Fig. S3-6).

NH_4^+ and NO_3^- consumption mirrored the production rates, showing no effect of eCO_2 on NH_4^+ consumption but indicating lower NO_3^- consumption in the rhizosphere (Fig. 3.3A). NO_3^- immobilization by microbes can be approximated by NO_3^- consumption, given that N_2O emission by denitrification is comparatively minimal. NH_4^+ immobilization, approximated by the difference between NH_4^+ consumption and gross nitrification, was higher in the rhizosphere (8.4 ± 13.3 µg g^{-1} d^{-1}; $p > 0.05$) compared to the bulk soil where NH_4^+ immobilization was barely detectable (0.3 ± 1.2 µg g^{-1} d^{-1}). NH_4^+ and NO_3^- mean residence times (MRT) were calculated as the nutrient pool divided by the rate of mineralization or nitrification respectively. NH_4^+ MRT was 3 d in the bulk soil and 0.5 d in the rhizosphere. NO_3^- MRT was faster in the rhizosphere under aCO_2 (from 2 d in the bulk soil to 0.7 d in the rhizosphere) but remained the same between bulk and rhizosphere under eCO_2.

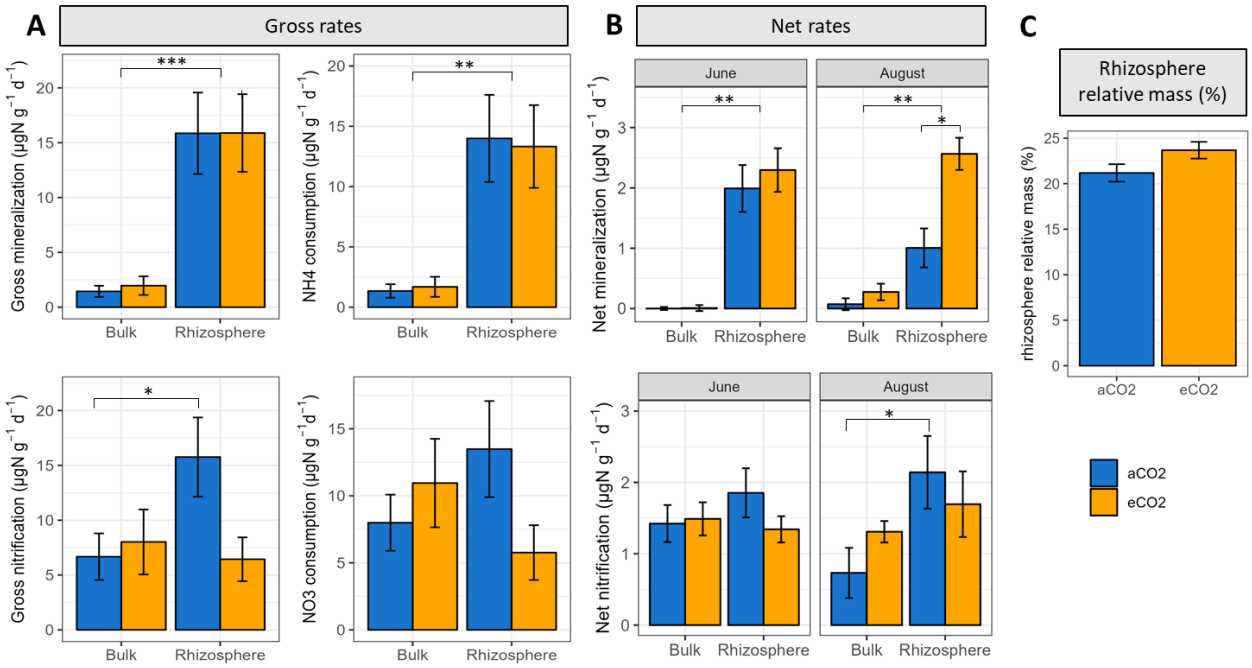

27

28 ***Figure 3.3:*** *Ammonium and nitrate dynamics under aCO_2 (blue) and eCO_2 (orange) in rhizosphere and*
29 *bulk soils. A) Gross mineralization, gross nitrification, ammonium and nitrate consumption where errors*
30 *bars represent the standard error between replicates (n=9) in August. B) Net mineralization and*
31 *nitrification in June and August (n=15). C) Rhizosphere relative mass expressed in percentage.*
32 *Significant differences between treatments, types, or interactions are indicated with an asterisk above*
33 *the respective groups.*

34 ***Table 3.2:*** *Primed C and N calculated as the difference in CO_2 respiration and gross mineralization*
35 *respectively between rhizosphere and bulk soil (mean ± se). ANOVA results for treatment are described*
36 *on the right part of the table.*

Priming effect	aCO_2	eCO_2	*ANOVA p-value treatment*
Primed C ($ugC\ g^{-1}\ h^{-1}$)	0.46 ±0.22	0.46 ±0.32	0.99
Primed N ($ugN\ g^{-1}\ h^{-1}$)	16.4 ±6.1	14.8 ±5.9	0.89

37

38 ### *3.3.2.2. N_2O losses by nitrification and denitrification*

39 Under equal soil moisture, total nitrous oxide emissions were higher under eCO_2 in the bulk
40 soil ($p > 0.05$) but not in the rhizosphere (Fig. 3.4). This enhancement was mainly explained
41 by a higher denitrification activity under eCO_2 in the bulk soil ($p = 0.03$). N_2O emissions from
42 nitrification were not affected by treatments in neither bulk nor rhizosphere soil. Moreover, N_2O

emissions were positively correlated with soil MBC in the bulk soil, whereas this correlation was less pronounced in the rhizosphere (Fig. 3.4B). On average, denitrification and nitrification contributed to approximately 40% and 50% of the total N_2O emissions, respectively, leaving only 10% for other sources or errors. However, this distribution varied considerably among treatments and soil fractions. In the bulk soil, N_2O emissions were predominantly associated with nitrification, whereas in the rhizosphere, the primary source of N_2O emissions was denitrification (Fig. 3.4A).

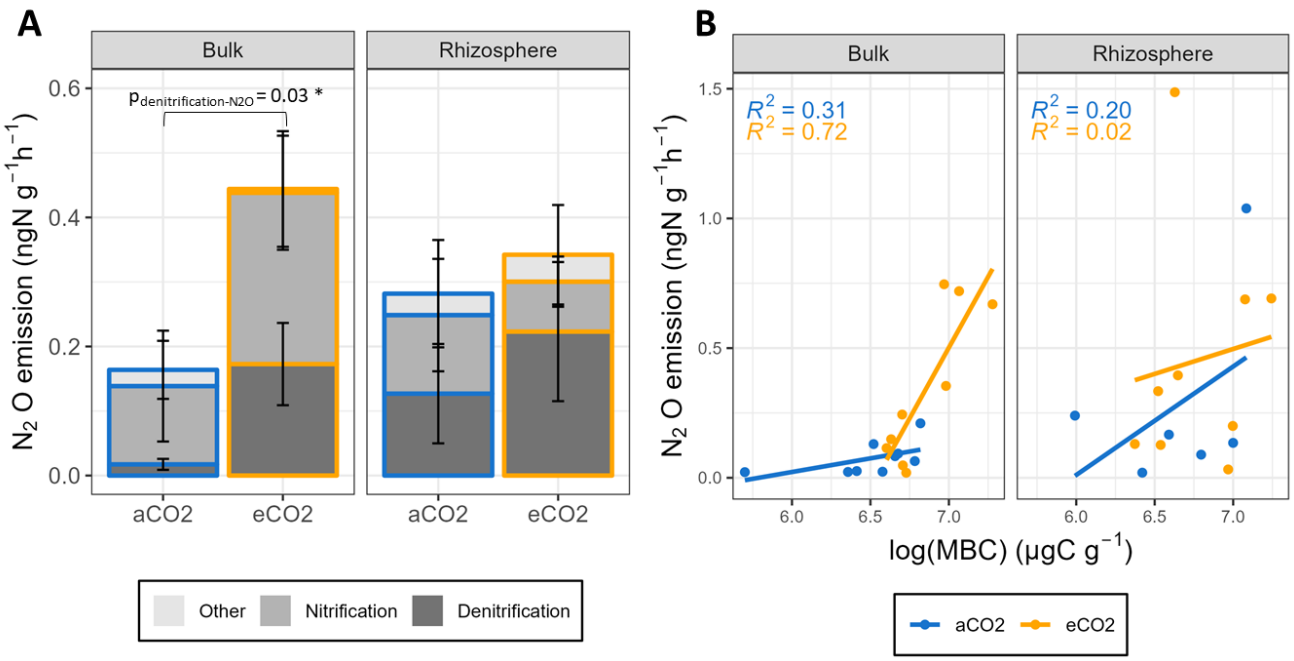

Figure 3.4: *A) N_2O emission source partitioned (i.e. denitrification and nitrification and other). Errors bars represent the standard error between replicates (n=9). An asterisk indicates significant differences (p-value <0.05) between treatment for that soil fraction. B) Total N_2O emission correlation with microbial biomass carbon (MBC).*

3.3.2.3. Microbial carbon respiration

Microbial respiration was influenced by soil fraction and eCO_2 treatment (Table 3.3), but the eCO_2 effect was stronger in the bulk soil (RR = 0.34) compared to the rhizosphere soil (RR = 0.14) leading to no overall effect of eCO_2 on the positive priming effect regarding C (Table 3.2). The microbial metabolic quotient (qCO_2), providing insight into microbial activity was

significantly higher in the rhizosphere ($p < 0.05$), with no significant enhancement under eCO_2 (Table 3.3).

Table 3.3: *Soil microbial respiration and microbial metabolic quotient (qCO_2) (mean ± se). ANOVA results for soil fraction, treatment and the interaction effects are described on the right part of the table.*

Microbial respiration	Bulk soil		Rhizosphere		*ANOVA p-value*		
	aCO_2	eCO_2	aCO_2	eCO_2	*fraction*	*treatment*	*fraction x treatment*
Flux ($ugC\ g^{-1}\ h^{-1}$)	0.71 ±0.14	0.99 ±0.35	1.12 ±0.41	1.39 ±0.62	***0.004***	***0.06***	*0.63*
qCO_2 ($ugC\ gMBC\ h^{-1}$)	1.09 ±0.3	1.15 ±0.23	1.51 ±0.55	1.81 ±0.59	***0.002***	*0.21*	*0.67*

3.3.3. Soil enzyme activities and stoichiometries

eCO_2 had a stronger effect on potential soil enzyme activity in the rhizosphere while trends were less noticeable in the bulk soil. Notably, in the rhizosphere, LAP was significantly enhanced under eCO_2 (+67%), while phenol oxidase activity was downregulated (-34%). BG activity also showed a slight enhancement in both bulk and rhizosphere soils under eCO_2 ($p > 0.05$; Fig. 3.5). Despite these changes, microbial CUE, NUE and enzymatic ratios remained unaffected by soil fraction or eCO_2 (Table S3-4). The ratio of ln(BG):ln(PHENOX) was 14% higher under eCO_2 in the rhizosphere ($p = 0.12$; Table S3-4) suggesting that there was a shift in the type of enzyme utilized under eCO_2 in the rhizosphere from oxidative to hydrolytic. The activities of all the hydrolytic enzymes (LAP, BG, NAG, AP) were positively correlated with each other, and BG especially was positively correlated with gross mineralization and NH_4^+ consumption (Fig. S3-7). Phenol oxidase activity, on the other hand, showed a negative correlation with NH_4^+ consumption, gross mineralization, gross nitrification and NH_4^+ content (Fig S3-7).

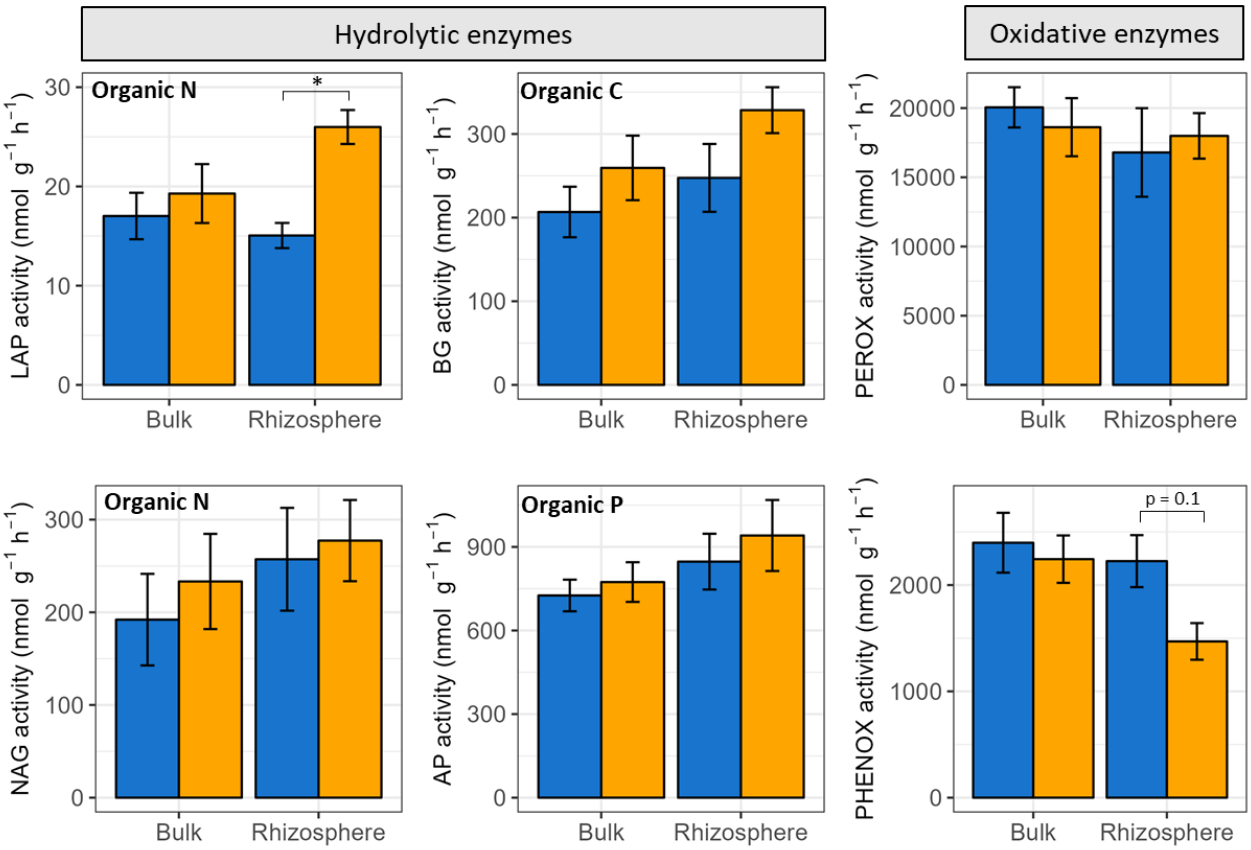

Figure 3.5: *Enzyme activities in nmol g^{-1} h^{-1} in bulk and rhizosphere soils in function of treatments. Error bars represent standard error between replicates (n=9). LAP = leucine amino-peptidase, BG = B-glucosidase, NAG = 1,4-N-acetyl-glucosaminidase, AP = acid phosphatase, PEROX = peroxidase, PHENOX = phenol oxidase. An asterisk indicates significant differences (p-value <0.05) between treatment for that soil fraction. Note the very different magnitudes of activity (i.e., y-axis ranges).*

3.4. Discussion

Nitrogen availability and cycling were enhanced by eCO_2 in the bulk soil and in the rhizosphere as evidenced by the higher net mineralization rates, higher NH_4^+ content and higher LAP activity under eCO_2. The increase of the LAP enzyme activity under eCO_2 in the rhizosphere indicated a potential increase of protein depolymerization activity, as LAP degrades mostly proteins and peptides (Matsui et al., 2006). Higher N-acquiring enzyme production, together with the higher microbial C:N ratio observed in the rhizosphere suggests that higher C availability (i.e. DOC) under eCO_2 triggered a microbial N demand in the rhizosphere (Manzoni et al., 2021; Moorhead et al., 2013). Furthermore, the higher microbial respiration supports the hypothesis of a faster SOM decomposition for N-mining, resulting in increasing NH_4^+

availability. These findings align with studies on young tree plantations suggesting an enhanced N-mining under eCO_2 based on higher N-acquiring enzyme activities (Meier et al., 2015; Phillips et al., 2011) or net mineralization (Finzi et al., 2006a, 2002). However, only few studies have detected signs of gross mineralization enhancement (i.e. prime indicator of N-mining) (Phillips et al., 2011; Sgouridis et al., 2023), indicating that it may only be discernible in highly N-limited systems (Andresen et al., 2020; Rütting and Andresen, 2015). Therefore, net rates, measured *in-situ* on long term incubation periods, may be more sensitive to changes in N availability changes compared to gross rates (Verchot et al., 2001). Yet, further evidence is required to confirm whether the increased net mineralization results from higher SOM decomposition and not only from lower NH_4^+ consumption. Nevertheless, this experiment suggests that after six years of eCO_2 treatment, N availability is not constrained under eCO_2, as NH_4^+ is more available, likely due to increased SOM decomposition, as supported by higher LAP activity, net mineralization and microbial respiration.

Net nitrification and gross nitrification were slightly downregulated under eCO_2 in the rhizosphere despite the positive rhizosphere effect and eCO_2 effect creating hot spots for heterotrophic nitrification (i.e. high DOC and DN content) (Zhang et al., 2019). While high soil DOC can reduce autotrophic nitrification by promoting heterotrophic activity (Strauss and Lamberti, 2002), in acidic forest soils, heterotrophic nitrification primarily dominates (Li et al., 2018). Hence, nitrification was expected to be stimulated by both rhizosphere and eCO_2 effects. Yet, a positive rhizosphere effect solely occurred under aCO_2 where rhizosphere DOC and DN levels drove increased nitrification activity. This suggests that another mechanism is involved in the reduction of nitrification under eCO_2. Earlier research on bulk soils has generated inconsistent results on nitrification (Barnard et al., 2005; Rütting and Andresen, 2015; Sgouridis et al., 2023), generally pointing towards an overall lack of effect. However, a decrease was observed in some cases (Barnard et al., 2005; Rütting and Andresen, 2015), aligning with our observations in the rhizosphere. Nitrification can be downregulated in soils in the presence of roots either due to competition for NH_4^+ (Dijkstra et al., 2013; Zhu et al.,

2021) or due to the release of biological nitrification inhibitor (BNI) compounds by roots as a strategy to conserve N (Subbarao et al., 2007) suggesting that eCO_2 increased the competition between roots and nitrifying bacteria and may alter the concentration of BNI released by roots. Similar mechanisms may have regulated N_2O losses by denitrification in the rhizosphere (Fender et al., 2013). Denitrification was only primed by the higher C in the bulk soil while no eCO_2 effect was detected in the rhizosphere where a higher N demand by trees may have suppressed denitrifying communities (Rummel et al., 2021) and counteracted the C exudation effect. These results collectively suggest that N losses via nitrification and denitrification are reduced under eCO_2 in the rhizosphere, thereby conserving available N for tree uptake. However, further investigation is needed to understand the underlying mechanisms of this downregulation.

Furthermore, shifts in soil enzyme activities observed in the rhizosphere indicate that the higher N-mining activity under eCO_2 primarily targets easily accessible SOM, such as proteins or cellulose, rather than recalcitrant C denoted by the lower phenol activity. Similar shifts were noted in a meta-analysis but were not significant (Xiao et al., 2018) suggesting a small yet tangible effect of eCO_2. Microbes under eCO_2 might shift their nutrient acquisition strategy, acquiring N from easily accessible nutrients provided by the higher rhizodeposition under eCO_2 (Phillips et al., 2009) rather than recalcitrant SOM (Dijkstra et al., 2013). Thereby, while the decrease in phenol oxidase activity under eCO_2 may imply a promotion of C storage (Sinsabaugh, 2010), we hypothesize that the accelerated decomposition of *new carbon* could impede C accumulation under eCO_2 (Phillips et al., 2012), aligning the lower total C found in the rhizosphere and with research suggesting an overall marginal effect of eCO_2 on soil C storage (Carney et al., 2007; Kuzyakov et al., 2019; Terrer et al., 2021).

While the rhizosphere was found to be inherently more *active* (i.e. positive priming of C and N) than the bulk soil, the effects of eCO_2 were not consistently stronger in the rhizosphere, contrary to our initial hypothesis. Increased nutrient availability and N mineralization were observed in both rhizosphere and bulk soils, complicating interpretations on the role of RPE

149 on N availability under eCO_2. This could be due to the dense root distribution in the organic
150 layer (1 mg cm^{-3}) resulting in high exudation quantity of 5 µg cm^{-2} d^{-1} (Reay et al., *in prep*),
151 which likely extended the priming effect into the bulk soil especially under eCO_2 where the fine
152 root biomass is higher. Consequently, even a small addition of C in the bulk soil may trigger
153 more changes than a larger addition in the rhizosphere, an already nutrient-rich environment.
154 Thus, in our study, eCO_2 also influenced the bulk soil, giving it rhizosphere-like characteristics
155 such as higher microbial biomass, respiration and N availability (Kuzyakov and
156 Blagodatskaya, 2015). We cannot exclude the possibility of errors during the separation of
157 bulk and rhizosphere soils where some rhizosphere soil might have fallen into the bulk soil,
158 especially since rhizosphere soil can be attached more loosely to roots in organic soils
159 compared to mineral soils. However, this potential error should have been consistent between
160 eCO_2 and aCO_2.

161 Additionally, by increasing root biomass (Ziegler et al., 2023), eCO_2 likely expanded the
162 proportion of rhizosphere soil as it was observed in our experiment (+ 2%) and to a larger
163 extent at Duke FACE (Meier et al., 2015). Given that N mineralization is ten times faster in the
164 rhizosphere, even a modest expansion of 2% in relative mass can potentially boost N gross
165 mineralization by 18% when scaling-up to soil volume (2.53 µgN cm^{-3} d^{-1} under eCO_2 against
166 2.13 µgN cm^{-3} d^{-1} under aCO_2). Therefore, rhizosphere mass expansion might be a crucial
167 mechanism for enhancing N availability that must not be disregarded when addressing tree N
168 demand under future climates.

169 3.5. Conclusion

170 Collectively, our findings demonstrate that eCO_2 stimulates N cycling in the rhizosphere and
171 bulk soils to meet microbial and tree N demand and reduce N losses in the rhizosphere,
172 through a higher competition for available N. Our study proposes that the promotion of SOM
173 decomposition and the control of N availability through plant and rhizobiome interactions could
174 be a crucial mechanism sustaining plant growth under higher atmospheric CO_2 concentrations.
175 However, long-term studies need to track the trajectories of these processes to understand

whether a shift may happen from abundant N supply to N limitation forcing long term C pool priming and leading to either a limitation of tree growth and/or a depletion of soil organic matter pool.

While this study highlights the role of plant-soil interactions in the rhizosphere in enhancing N availability, it does not explicitly identify the mechanisms underlying the observed changes in rhizosphere processes. Although the role of root exudates is implied, a clear connection needs to be established between changes in exudate quantity/quality and N cycling. The next chapter will delve deeper into the drivers of N cycling under eCO_2 by reproducing the observed changes in root exudation quantity and quality under eCO_2.

3.6. Supplementary materials

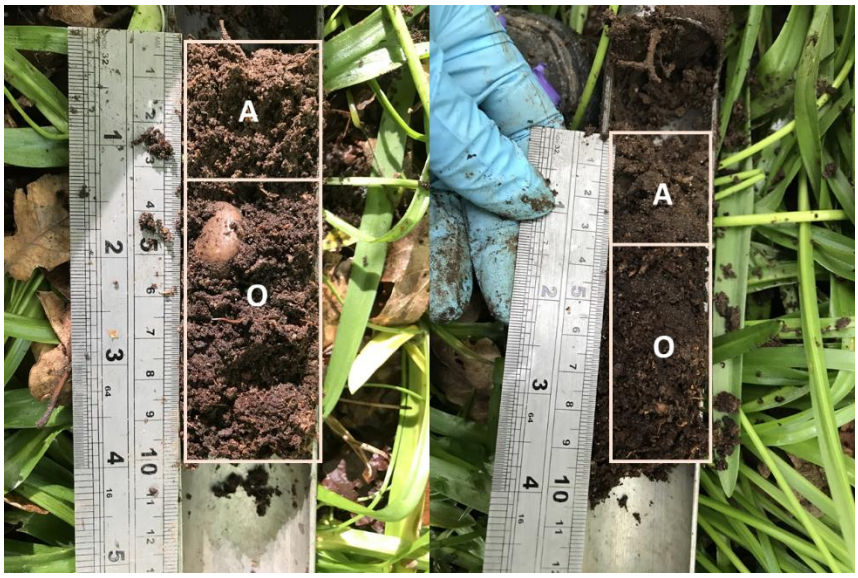

Figure S 3-1*: Two pictures of soil samples with the organic horizon (O) and the beginning of the mineral layer (A).*

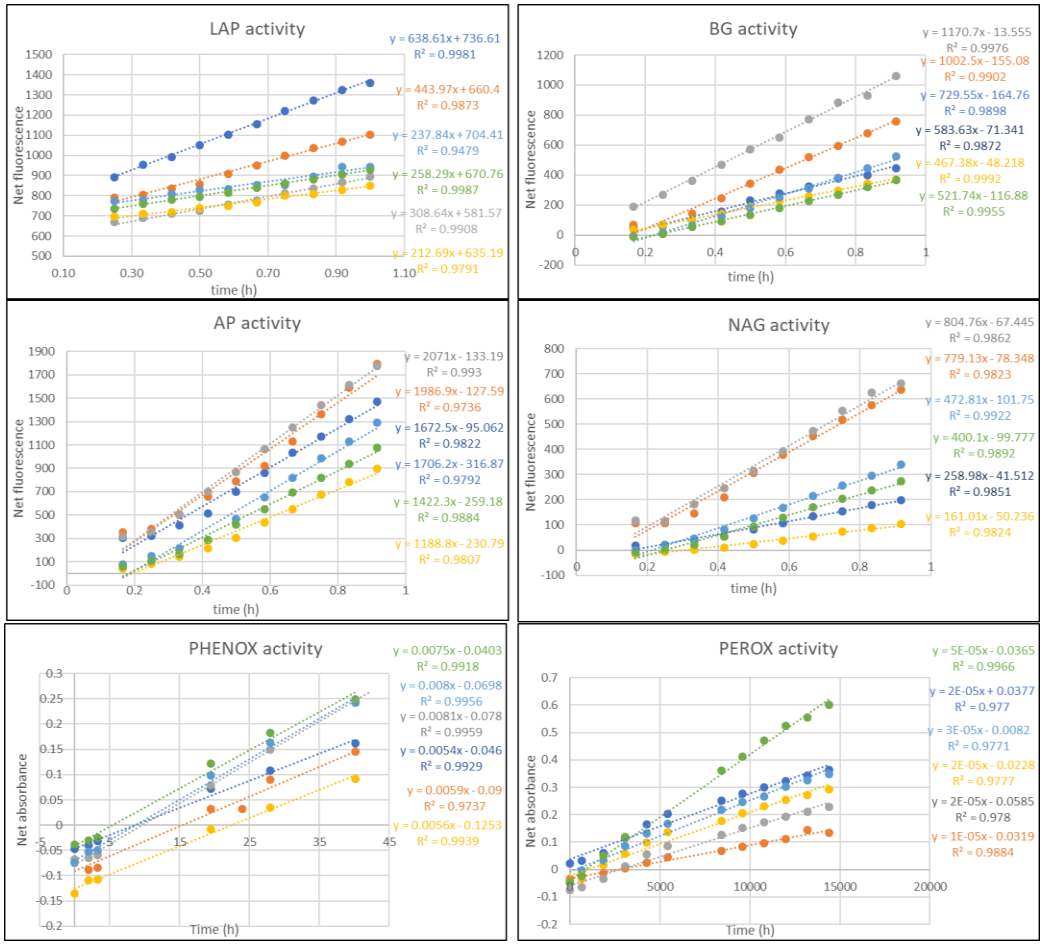

Figure S 3-2: *Fluorescence in function of time plotted for the six enzymes (LAP, BG, AP, NAG, PEROX and PHENOX) for the first six samples. For each regression line the equation and the regression coefficient are detailed.*

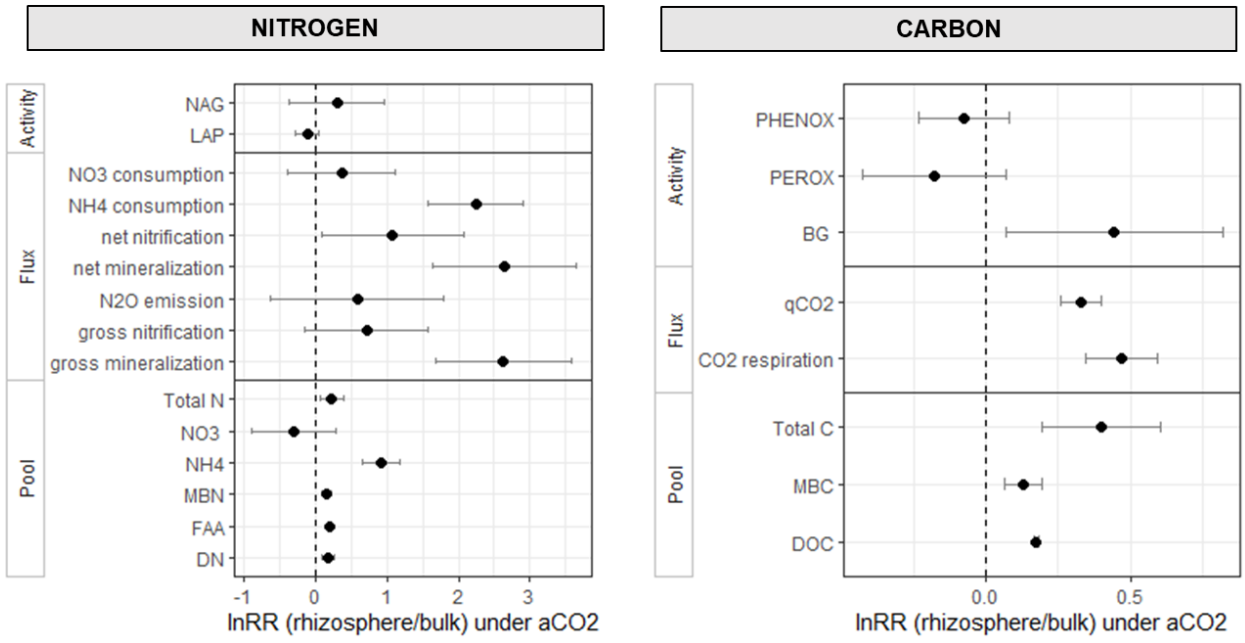

Figure S 3-3: *Response ratio (lnRR mean with standard error) of the rhizosphere effect under aCO_2 calculated for each variable. A negative response ratio means a negative rhizosphere effect for this variable and a positive value means a positive rhizosphere effect.*

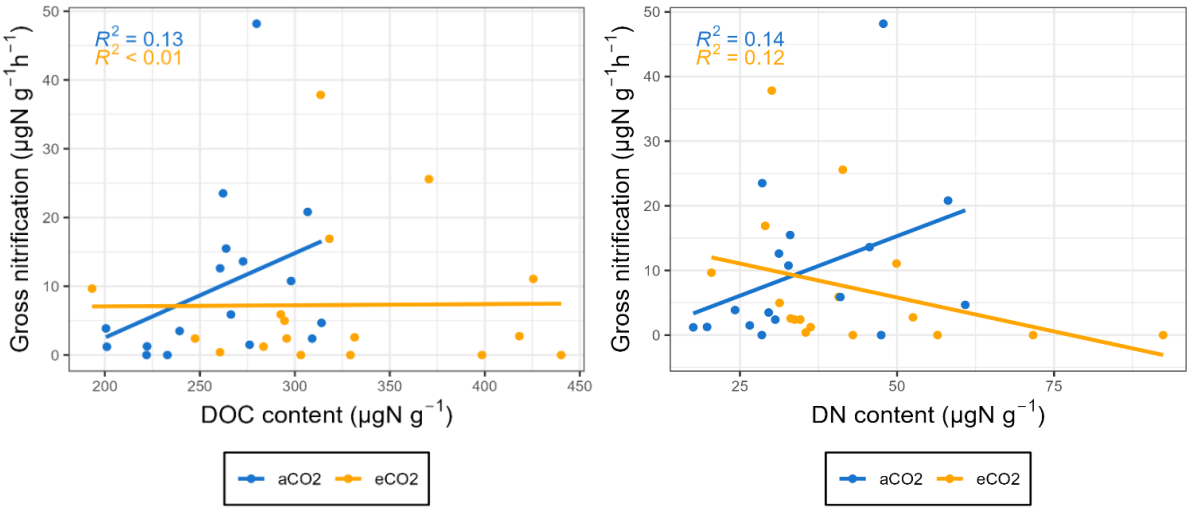

Figure S 3-4: *Correlation between gross nitrification rate expressed in (µg g-1 day-1) and soil DOC and DN content (µg g-1) under aCO2 and eCO2 (n=18).*

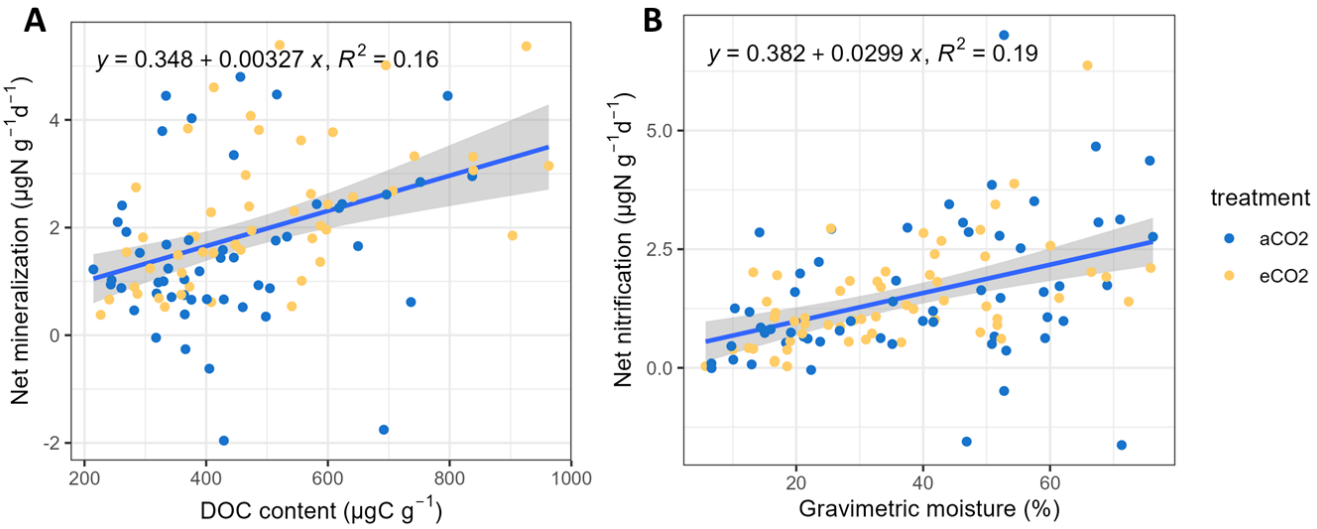

Figure S 3-5: *A) Net mineralization correlation with soil DOC content and B) net nitrification correlation with soil gravimetric moisture.*

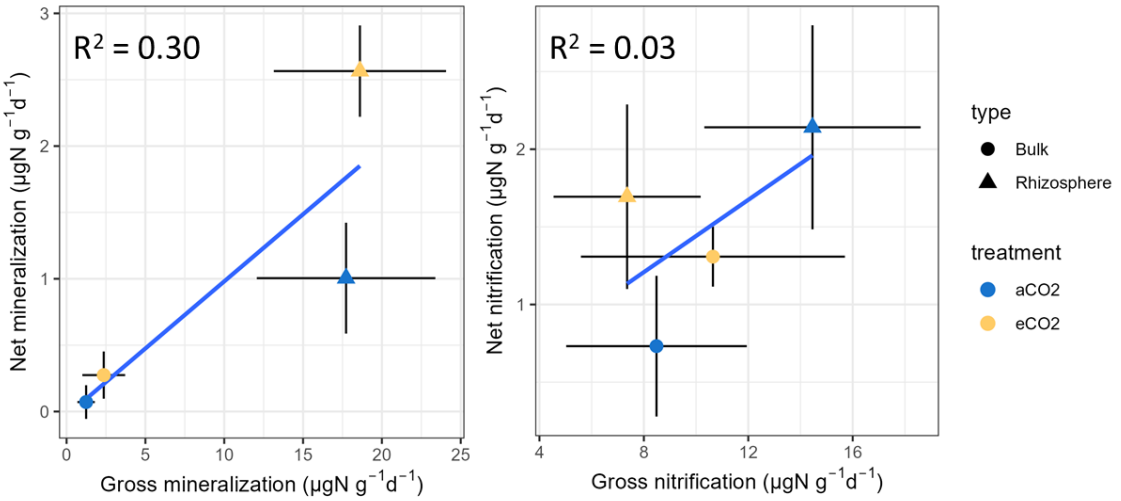

Figure S 3-6: *Correlation between gross and net rates of mineralization and nitrification rate under aCO_2 and eCO_2 (colour) in the bulk and rhizosphere soils (shape) (mean + SD).*

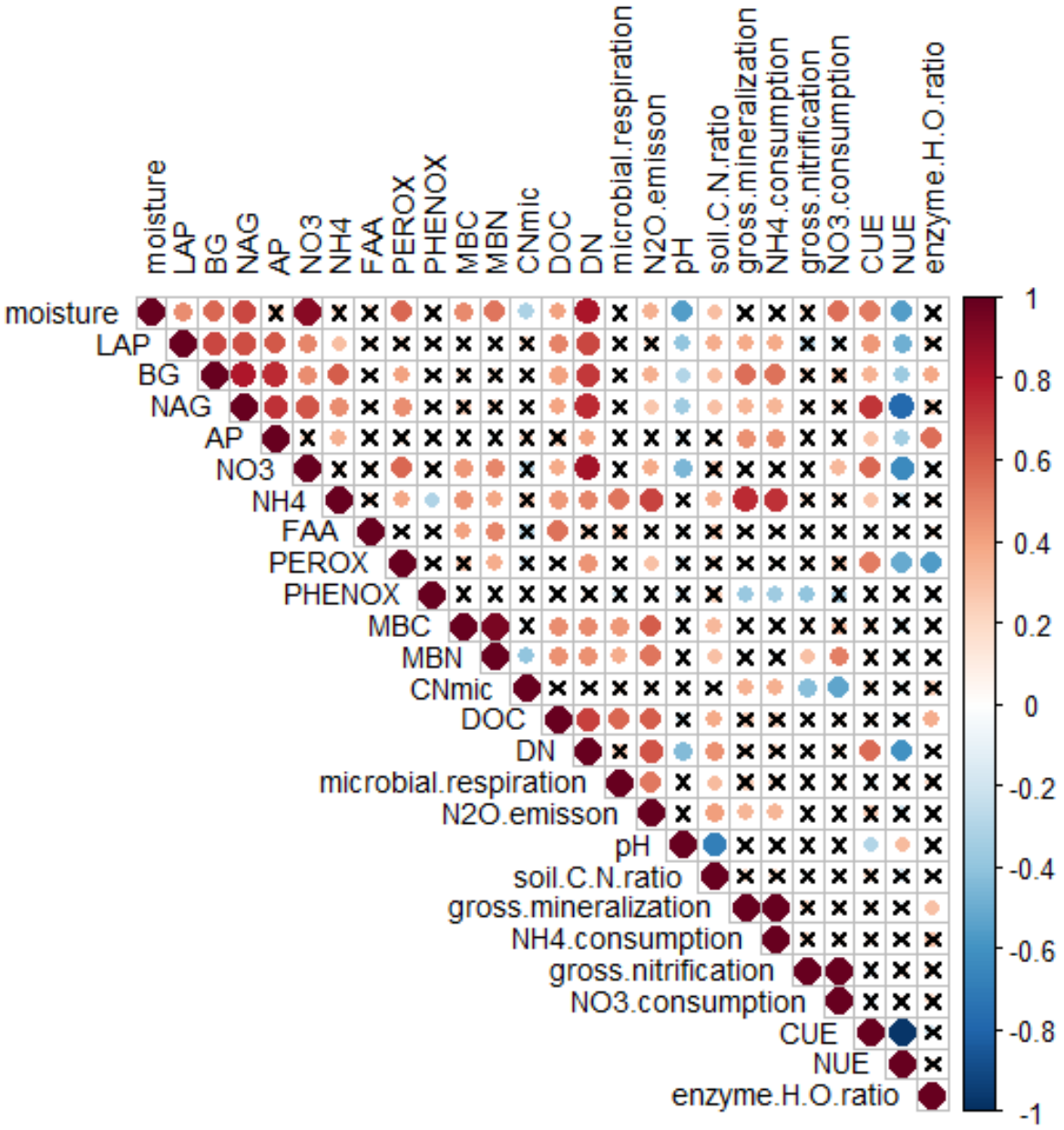

Figure S 3-7: *Correlation matrix figuring most of the variable measured. Correlation is calculated with the Pearson index. Positive correlation is coloured in red, negative correlation is coloured in blue and no correlation is represented by a cross. CNmic = microbial C:N ratio, enzyme.H.O.ratio = ratio hydrolytic: oxidative enzyme.*

***Table S 3-1**: Soil O-horizon depth (cm), soil moisture and root type characterization per array.*

Array	Treatment	O horizon depth (cm) (mean ± sd)	Soil moisture (%) (mean ± sd)	Qualitative estimation of root type
1	eCO_2	7.25 ± 0.67	19 ± 4	Mostly oak roots
2	aCO_2	7.84 ± 0.89	25 ± 7	Mix of oak/non-oak roots
3	aCO_2	7.89 ± 0.73	14 ± 2	Mostly oak roots
4	eCO_2	7.29 ± 0.74	14 ± 3	Mix of oak/non-oak roots
5	aCO_2	6.89 ± 0.49	26 ± 10	Mostly non-oak roots
6	eCO_2	7.74 ± 0.72	37 ± 11	Mostly non-oak roots

***Table S 3-2:** Substrates name and concentration used for each enzyme assessed in this experiment.*

Enzyme	**Abbreviation**	**Substrate**
Hydrolytic enzymes		
β-glucosidase	BG	200 µM 4-methylumbelliferyl β-D-glucosaminide
β-N-acetyl-glucosaminidase	NAG	200 µM methylumbelliferyl β-D-glucopyranoside
Acid phosphatase	AP	200 µM 4-methylumbelliferyl phosphate disodium salt
Leucine aminopeptidase	LAP	200 µM L-leucine-7-amino-4-mehtylcourmarin hydrochloride
Oxidative enzymes		
Phenol oxidase	PHENOX	25 mM L-3,4-dihydroxyphenylalanine
Peroxidase	PEROX	25 mM L-3,4-dihydroxyphenylalanine + 0.3% H_2O_2

Table S 3-3: *On the left side of the table, p-values from two-way ANOVA models with soil fraction (rhizosphere or bulk), treatment (eCO_2 or aCO_2) and the interaction for each variable. On the right side, p-values of one-way ANOVA models with treatment for each variable on the rhizosphere data and on the bulk data separately. Variables are written in italics when log transformations were performed to meet ANOVA assumptions. All variable showing an effect of soil fraction or treatment are in bold, an asterisk indicates a significant effect.*

Fixed effects	**Fraction**	**Treatment**	**Fraction x Treatment**	**Treatment**	
	All data			**Rhizosphere data**	**Bulk data**
Gravimetric moisture	***0.08***	*0.83*	*0.48*	*0.9*	*0.74*
pH	*0.77*	*0.83*	*0.21*	*0.32*	*0.61*
N-NO_3^-	*0.15*	*0.52*	*0.15*	*0.82*	*0.74*
N-NH_4^+	***<0.001****	***<0.001****	*0.24*	*0.46*	***0.008****
N-FAA	***0.06***	*0.44*	*0.88*	0.39	0.30
MBC	*0.69*	***0.02****	*0.36*	0.64	**0.08**
MBN	*0.85*	*0.45*	***0.08***	0.26	**0.01***
MBC:MBN	*0.23*	*0.42*	*0.18*	0.12	0.83
DOC	***0.05***	***0.06***	*0.52*	0.04	0.007
DN	*0.18*	***0.03****	*0.50*	0.28	0.06
Total C	*0.57*	*0.7*	***0.10***	*0.56*	*0.43*
Total N	*0.92*	*0.57*	*0.19*	*0.72*	*0.42*
C:N ratio	***0.03****	*0.54*	***0.09***	*0.37*	*0.17*
Gross mineralization	***<0.001****	*0.94*	*0.94*	*0.99*	*0.71*
NH4 consumption	***<0.001****	*0.96*	*0.88*	*0.92*	*0.80*
Gross nitrification	***0.06***	*0.55*	***0.04****	*0.24*	*0.80*
NO_3^- consumption	*0.87*	*0.12*	*0.25*	*0.25*	*0.65*
Net mineralization	**< 0.001 *** **	**0.20**	0.02	**0.01***	0.23
Net nitrification	**0.05**	0.79	**0.01***	0.17	0.23
N_2O total	*0.24*	*0.32*	*0.21*	*0.63*	*0.36*
N_2O-denitrification	*0.18*	***0.03 *.***	*0.37*	*0.51*	*0.23*
N_2O-nitrification	*0.31*	*0.63*	*0.26*	*0.65*	*0.32*
Microbial respiration	***0.004****	***0.06***	*0.63*	0.37	**0.02 ***
Microbial respiration per unit C	***0.02****	*0.53*	***0.04****	0.20	0.52
Microbial respiration per unit MBC	***0.002****	*0.21*	*0.67*	0.31	0.63
LAP	0.28	**0.02***	0.13	**0.003****	0.67
BG	*0.12*	*0.61*	*0.77*	*0.26*	*0.45*
NAG	*0.44*	*0.66*	*0.88*	*0.84*	*0.68*
AP	0.28	0.59	0.86	0.69	0.71
PHENOX	0.14	0.19	0.37	**0.1**	0.76
PEROX	0.54	0.96	0.67	0.81	0.69

Table S 3-4: *Stochiometric enzymatic ratio, nutrient use efficiency and hydrolytic to oxidative ratio in bulk and rhizosphere soils in function of treatment (aCO_2 = ambient CO_2, eCO_2 = elevated CO_2). Mean value ± se are indicated for soil fraction and treatment (n=9 replicates). ANOVA results for soil fraction, treatment and the interaction effects are described on the right part of the table.*

	Bulk soil		**Rhizosphere soil**		*ANOVA p-value*		
					fraction	*treatment*	*fraction x treatment*
	aCO_2	**eCO_2**	**aCO_2**	**eCO_2**			
Enzymatic C:N	1.2 ± 0.2	1.3 ± 0.2	1.4 ± 0.2	1.3 ± 0.2	*0.62*	*0.93*	*0.69*
Enzymatic C:P	0.26 ± 0.*04*	0.31 ± 0.03	0.32 ± 0.04	0.39 ± 0.05	*0.12*	*0.17*	*0.88*
Enzymatic N:P	0.25 ± 0.06	0.29 ± 0.05	0.28 ± 0.06	0.33 ± 0.04	*0.51*	*0.41*	*0.94*
CUE	0.38 ± 0.03	0.37 ± 0.02	0.36 ± 0.02	0.38 ± 0.02	*0.91*	*0.78*	*0.62*
NUE	0.66 ± 0.05	0.68 ± 0.04	0.69 ± 0.04	0.66 ± 0.03	*0.81*	*0.87*	*0.60*
ln(BG)/ln(PHENOX)	0.67 ± 0.04	0.70 ± 0.02	0.70 ± 0.06	0.80 ± 0.03	*0.11*	*0.12*	*0.50*

Chapter 4. Root exudate stoichiometry has a stronger effect on N cycling than root exudate quantity

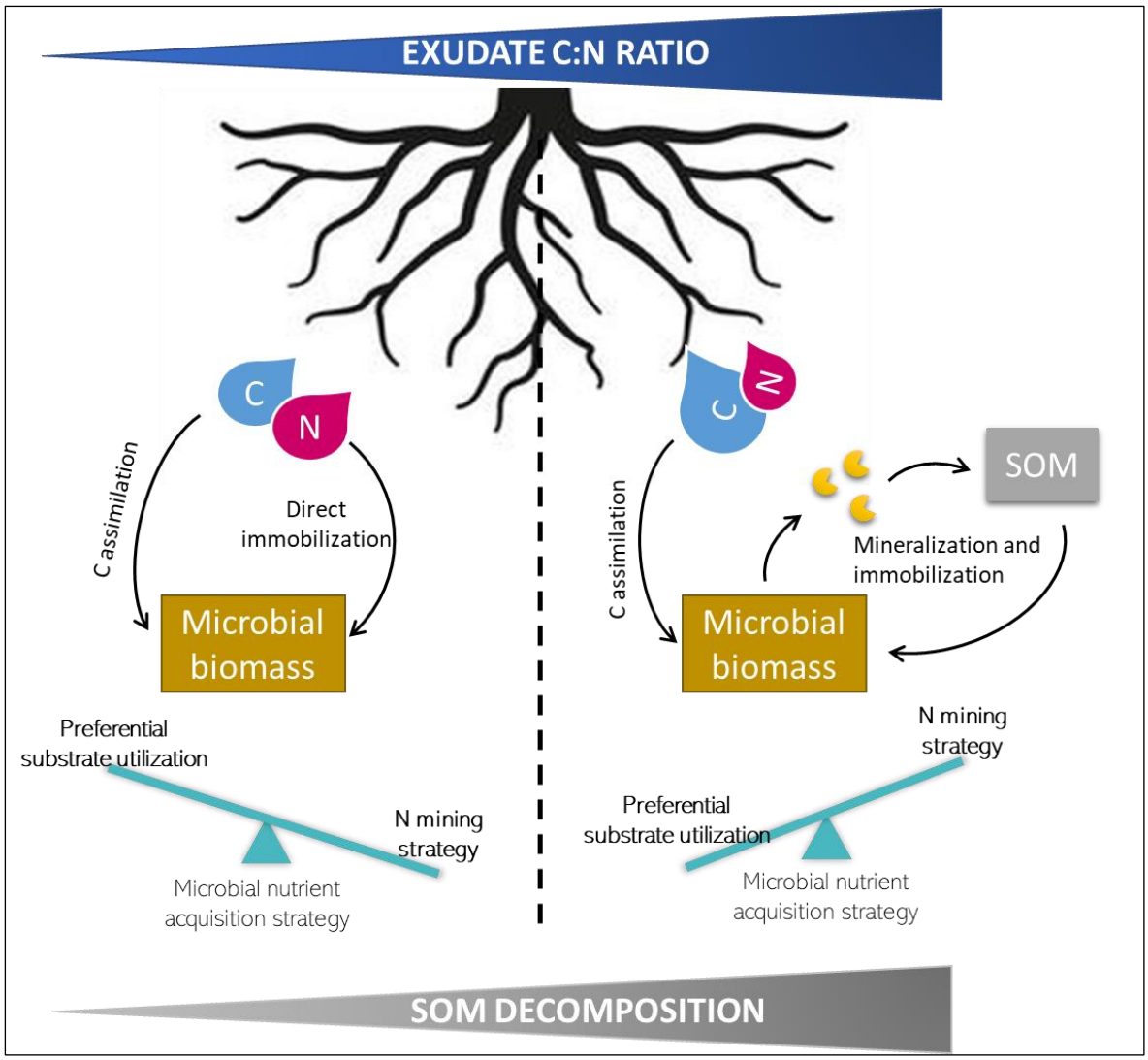

Root exudate stoichiometry has a stronger effect on N cycling than root exudate quantity

Manon Rumeau[1,2,*], Johanna Pihlblad[1,2,3], George Fereday[1,2], Michaela K. Reay[4], Fotis Sgouridis[5], Yolima Carillo[6], Ian P. Hartley[7], Emma Sayer[8], Liz Hamilton[1,2] and Rob Mackenzie[1,2] Sami Ullah[1,2]

[1]*Birmingham Institute of Forest Research, University of Birmingham, Birmingham, UK*

[2]*School of Geography, Earth and Environmental Science, University of Birmingham, UK*

[3]*Lancaster Environment Centre, Lancaster, UK*

[4]*School of Geographical Sciences, University of Bristol, Bristol, UK*

[5]*Organic Geochemistry Unit, School of Chemistry, University of Bristol, UK*

[6]*Hawkesbury Institute for the Environment (HIE), Western Sydney University Richmond, Australia*

[7]Geography, Faculty of Science, Environment and Economy, University of Exeter, Exeter, UK

[8]*Institute of Botany, Ulm University, Germany*

* Corresponding author: MLR094@student.bham.ac.uk (Manon Rumeau).

Additional Corresponding authors: S.ullah@bham.ac.uk (S. Ullah)

This chapter is the last version of a manuscript in review in New Phytologist.

Abstract

Root exudates play a key role in nitrogen (N) release from soil organic matter, making them pivotal in alleviating progressive N limitation under elevated atmospheric carbon dioxide (eCO_2). Exposure to eCO_2 increases the quantity and alters the quality of the exudates, which affects microbial activity and N cycling. However, it is uncertain whether these changes will result in greater N availability for trees. In this field experiment, we used an automated root exudation system to mimic changes in root exudate quantity (increased in C and N content) and quality (higher C:N ratio) in response to eCO_2. After six months of continuous application, we measured N transformation rates in O-horizon soils and in exclusion soil bags to partition the role of roots, fungi and bacteria. Root exclusion inhibited gross N mineralization and enhanced gross nitrification. Increasing exudate C:N ratio stimulated gross mineralization, especially in the rhizosphere microbiome, by shifting microbial nutrient acquisition towards a N-mining strategy. High exudate C:N ratio also increased fungal, but not bacterial, nitrification rates in the absence of roots. These results demonstrate that root exudate stoichiometry has a stronger effect on N cycling than root exudate quantity and thus, must be considered alongside changes in quantity.

Keywords: root exudation; gross N mineralization; gross nitrification; automated root exudate system (ARES); ^{15}N pool dilution; exclusion bags; elevated CO_2; exudate stoichiometry

4.1. Introduction

Root exudation mediates interactions between plants and soil microbes, which are crucial for plant nutrition (Haichar et al., 2014; Shi et al., 2011; Zhalnina et al., 2018). Exudates consist of sugars, amino acids, organic acids (Phillips et al., 2008) and countless secondary metabolites (Salem et al., 2022), which are released both passively and actively by roots (Yan et al., 2023). Root exudates stimulate microbial activity, resulting in the release of bioavailable nutrients, such as nitrogen (N), during the decomposition of plant material and soil organic matter (SOM; Churchland and Grayston, 2014; Jacoby et al., 2017). Plants secrete between 1 to 10% of the carbon (C) assimilated via photosynthesis into the soil as root exudates (Brunn et al., 2022; Chari et al., 2024; Jones et al., 2004; Phillips et al., 2008).

Although much work has focused on quantifying the amount of C released into the soil as root exudates (Brunn et al., 2022; Chari et al., 2024) and its effect on microbial activity, research into root exudate quality (i.e. chemical composition) remains rare. Nonetheless, emerging evidence reveals that root exudate composition influences bacterial diversity (Wen et al., 2022) and SOM dynamics (Bradford et al., 2013; Carrillo et al., 2014; Chari and Taylor, 2022). Thus, the effects of root exudate quantity and quality on microbial processes is complex and not fully understood (Wen et al., 2022). This complexity arises from the diversity of exudate compounds and from the specificity of the microbial response, which in turn depend upon the extant soil microbial communities in the rhizosphere (Chen et al., 2014; Dijkstra et al., 2013; Salem et al., 2022). Knowledge gaps around root exudates are further exacerbated by the limited number of *in-situ* studies (Liu et al., 2024; Lopez-Sangil et al., 2017; Yan et al., 2023). Most research has been performed in laboratory settings, and were mainly restricted to the addition of simple sugars, which limits our understanding under real-world conditions (Yan et al., 2023). However, understanding the role of exudates in plant productivity is a critical aspect of global change research (Dijkstra et al., 2013; Phillips et al., 2009; Zhang et al., 2016).

With climate change, forest productivity is expected to face greater nutrient limitations, which could also influence the forest C sink. The "CO_2 fertilization effect" from rising atmospheric

CO_2 concentration enhances photosynthesis and potentially increases forest C storage, but also induces higher nutrient demands of the trees (De Graaff et al., 2006; van Groenigen et al., 2006). In this context, N limitation of forest productivity is of particular interest, because mature temperate and boreal forests are often N-limited (E. Du et al., 2020). Therefore, understanding to what extent root exudation is able to alleviate soil N limitation by stimulating soil microbial activity is a key aspect in forecasting the future forest C capture (Phillips et al., 2011; Terrer et al., 2016). However, to achieve this, we must first determine how elevated CO_2 (eCO_2) will affect both the quality and quantity of root exudates, and then determine how such changes will affect soil N cycling and availability.

Under eCO_2, the quantity of root exudates, measured as C input to the soil, increases (Norby et al., 2024; Phillips et al., 2011). The increased C input to the soil is thought to accelerate ecosystem N cycling to meet the higher N demands of the trees (Phillips et al., 2011). However, a recent study conducted at BIFoR-FACE – a free-air CO_2 enrichment (FACE) experiment in mature oak woodland – highlighted that root exudation quality also changed under eCO_2, resulting in a higher C:N ratio of the exudates (Reay et al, *in prep*). In addition, studies at BIFoR-FACE have found an enhancement of net and gross N mineralization under eCO_2 but a reduction of dissimilatory losses (nitrification and denitrification) in the rhizosphere despite higher C availability under eCO_2 (Rumeau et al., 2024; Sgouridis et al., 2023). Whether these N cycling response to eCO_2 are triggered by a change in quantity and/or quality in exudates or have other drivers remains unknown. Higher exudate C:N ratio could affect organic and inorganic N transformations, potentially promoting faster N mineralization from SOM (L. Du et al., 2020) and higher microbial retention of free amino acids (FAA) due to scarce N resource for microbes (Mooshammer et al., 2014). Faster N mineralization under eCO_2 is also linked to the ability of ECM fungi to facilitate N mineralization and meet plant demand (Terrer et al., 2016) but could also relies on the rhizosphere bacteria community (Meier et al., 2015). Clear links between exudate quality, ECM activity and N mineralization remains to be demonstrated. Conversely, a higher exudate C:N ratio could also reduce

microbial activity if the lower N availability limits production of exoenzymes (Drake et al., 2013; Liu et al., 2022). Meanwhile, the response of gross nitrification to a change in exudate C:N ratio remains unexplored to our knowledge. Fungal heterotrophic nitrification, predominant in acidic forest soil (Li et al., 2018), may be enhanced by greater C availability (Zhang et al., 2019), leading to higher N losses via leaching or N_2O emissions. Thus, quantifying the response of organic and inorganic N transformation rates and the contribution of bacteria and fungi in these transformations is crucial to assess any changes in N acquisition strategies and/or in the *openness* of the N cycle.

Our study investigated the effects of changes in soil exudate C:N quantity (increased C and N content) and exudate quality (increased C:N ratio) on soil N transformation processes after applying a complex exudate "cocktail" (comprising two sugars, four amino acids and five organic acids) for six months using a novel automated root exudation system (ARES; Lopez-Sangil et al., 2017). The study was conducted adjacent to a FACE experiment in mature oak woodland, and the changes in exudate quantity and quality reflected those of *in-situ* exudation rates by oak roots under eCO_2 enrichment (Reay et al. *in prep*). To determine potential drivers of N transformations and of tree-microbe interactions, we partitioned the contribution of fungi, bacteria and roots to N transformation processes using exclusion bags with different mesh sizes. We hypothesized that 1) gross N mineralization and NH_4^+ immobilization will be enhanced in both exudate treatments compared to control with a more pronounced response in the high C:N ratio treatment due to higher microbial N limitation. And this response will be mainly associated with ECM fungal activity. 2) Gross nitrification will be enhanced by C addition independently from the C:N ratio because C availability stimulates heterotrophic fungal activity in acidic soil. To test our hypotheses, we analysed soil N content and gross N transformations following six months of experimental exudate treatments mimicking exudation quality and quantity under ambient or elevated CO_2, and compared the responses in the soil O horizon, and in soil bags excluding roots or roots and fungi.

4.2. Methods

4.2.1. Experimental design

This experiment was conducted at the Birmingham Institute of Forest Research (BIFOR) facility in Staffordshire (52º 48' 3.6" N, 2º 18' 0"W), adjacent to a Free Air CO_2 Enrichment (FACE) experiment, which was established in 2017 (Hart et al., 2020). The forest is dominated by oak trees (*Quercus robur L.*) with common hazel (*Corylus avellana* L.), sycamore (*Acer pseudoplatanus* L.*)* and hawthorn (*Crataegus monogyna* L.) trees in the understorey and as sub-dominants, respectively. The soil at site, classified as Ortic Luvisol (Hart et al., 2020), set with an organic soil layer (O) of about 7-10 cm depth overlying an A Horizon (15 to 25 cm deep) and a B horizon transiting into sandstone geology. The O-layer is a sandy loam (41% sand, 43% silt, 16% clay), with a pH of 3.8. More details can be found in Rumeau et al. (2024)

The present study consisted of four experimental blocks, each divided into three plots of 0.96 m^2 in which three different exudate treatments (Table 4.1) were administered: control (water + $CaCl_2$ to maintain ionic strength), low C:N (5% of forest NPP as root exudate solution with a C:N ratio of 4.4), high C:N (5% of forest NPP as root exudate solution with a C:N ratio of 7.4). Each block was located near an oak tree to ensure the predominance of oak roots and an automated Root Exudate System (ARES; Lopez-Sangil et al. 2017) was set up in each plot. The ARES comprise a mini drip irrigation system with 24 spikes sunk into the organic horizon to c. 2 cm depth, which cover an area of *c*. 0.96 cm^2.

To determine the role of roots and fungi in N transformation processes, exclusion bags were installed in the organic layer (~8 to 10 cm) of each plot right before the beginning of the experiment. The bags measured 4-cm diameter and 10-cm depth and consisted of 100 g of autoclaved sieved soil from the experiment site with a mesh size of either 41 μm to exclude roots but allow both bacteria and fungal mycelium to access the soil inside the bags, or 1 μm to exclude roots and fungi, allowing only bacteria to access the soil (Fig. 4.1).

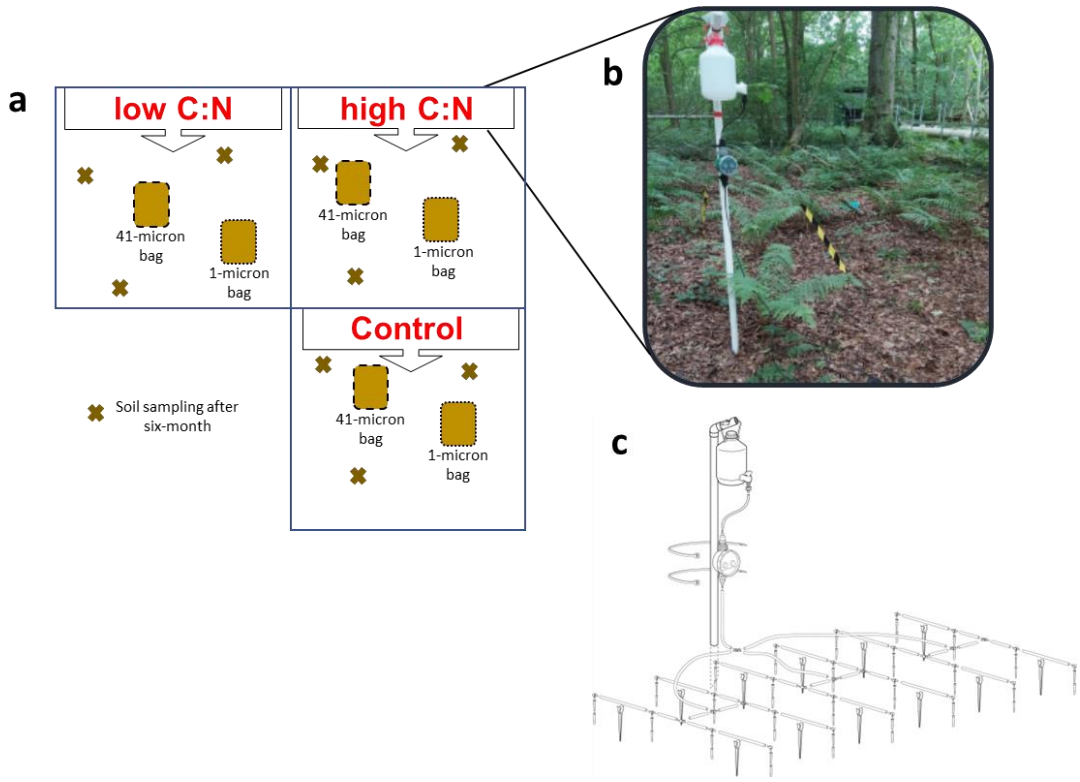

***Figure 4.1**: Experimental design's schematics and picture. a) Schematic of one experimental block with the three root exudate treatment plots, showing the location of soil sampling and exclusion bags, b) Picture of one of the automated root exudation systems (ARES), c) Schematical diagram representing the ARES system from Lopez-Sangil et al. (2017).*

4.2.2. Exudate solutions and delivery

Standard exudation solutions representing control or eCO_2 treatments were prepared weekly by combining sugars, amino acids and organic acids (see composition in Table 4.1). The total C concentration was adjusted to represent approximatively 5% of the forest NPP (i.e. 60 g C m^{-2} y^{-1}; Norby et al., 2024). Exudate treatments were continuously delivered to the soils at a rate of 0.29 L d^{-1} through 24 needles over a 0.96 m^2 area by an automated root exudation system (ARES; Fig. 4.1), which operated for 6 months from May to December 2022. In six months, soils under ARES treatment received an additional 10% of water compared to normal precipitation of 1152 mm per year (rain gauges at site TR-525M; Dallas, Texas). A full description of the ARES can be found in Lopez-Sangil et al. (2017).

Table 4.1: *Exudate cocktail composition expressed in mg L^{-1}. Water treatment contain none of the compounds in the table but contained calcium chloride (0.18 g L^{-1} $CaCl_2$) to maintain consistent ionic strength across treatments.*

Compound	Control	low C:N	high C:N
Sugars			
Glucose	0	260	390
Sucrose	0	260	390
Organic acids			
Oxalic acid	0	220	330
Na Acetate	0	160	240
Fumaric Acid	0	80	120
Citric Acid	0	80	120
Sodium Succinate	0	100	150
Amino acids			
Glutamic acid	0	600	300
Alanine	0	500	250
Glycine	0	500	250
Valine	0	500	250
Total C	0	1166	885
Total N	0	288	144
C:N ratio		4.4	7.4

4.2.3. Soil sampling

In December 2022, after 6 months of exudate treatments, the organic layer (depth *c*. 7- 9 cm) was sampled in three random locations of each plot (pseudo-replicates) and soil samples were sieved and combined to make one composite sample per plot. On the same day, the exclusion bags were retrieved. All samples were brought back to the laboratory on ice and were kept at 4°C for maximum 1 week until analysis.

4.2.4. Nutrient contents

Soil extractable ammonium-N (NH_4^+-N) and nitrate-N (NO_3^--N) concentrations were determined by extracting 2 g of soil with 10 ml 0.5 M potassium sulphate (K_2SO_4). The extracts were filtered at 0.45 µm with syringe filters and analyzed by continuous flow colorimetry using the Berthelot reaction method for NH_4^+-N and the cadmium-reduction reaction method for NO_3^--N (SA 3000 analyser, Skalar Analytical, Breda, Netherlands). The limit of detection was 0.02

mg N L^{-1} for both NH_4^+-N and NO_3^--N. The concentrations were blank corrected, and the relative standard deviation (RSD) calculated on quality control (QC) samples was < 2%.

Soil free amino acid (FAA) concentration was determined using the *o*-phthaldialdehyde and β-mercaptoethanol (OPAME) fluorescence assay described by Jones (2002) and adapted to a microplate assay by Darrouzet-Nardi et al. (2013). Briefly, 2 g of soil was extracted in 10 ml of 1 M potassium chloride (KCl), shaken, filtered at 0.45 µm, and 50 µl was added to a microplate with 100 µl of OPAME working reagent. As NH_4^+-N reacts to fluorescence within 1 hour, fluorescence was measured after 1 h of incubation at ambient temperature when the fluorescence from reaction with soil NH_4^+-N is negligible. Gravimetric soil water content was measured by drying 5 g of soil at 105°C for 48 h in order to mass correct soil nutrient concentration.

4.2.5. Potential gross N transformations

To determine N transformations, gross mineralisation and nitrification rates were assessed by the ^{15}N pool dilution method (Davidson et al., 1991; Hart et al., 1994) within a week of sampling. For this, 10 g of each soil sample was weighed in quadruplet into specimen cups. Before ^{15}N labelling, all samples were acclimated in the dark at 15°C for 2 days, chosen to match summer soil temperature at the field site. To achieve a 20% enrichment in ^{15}N atom percentage (at. % ^{15}N) in all samples within a 5% increase in moisture, a range of labelling solutions were prepared to deal with the different soil concentrations in NO_3^--N and NH_4^+-N. Solutions were prepared using $K^{15}NO_3$ (98 at.% ^{15}N, Merck) or $^{15}NH_4Cl$ (98 at. % ^{15}N, Merck). The labelling solutions were added dropwise, and soils were gently stirred with a spatula to ensure a uniform distribution of labels before closing the specimen cups. Soil subsamples were extracted with 1 M KCl immediately after labelling and again following a 24 h incubation at 15°C in the dark. An aliquot of extract was then analysed for NH_4^+-N and NO_3-N, as described above. The rest of the soil extract was analysed followed the gas diffusion procedure (Brooks et al., 1989) to determine the ^{15}N content in the NH_4^+-N and NO_3^--N pools. Briefly, acid traps were prepared with 8-mm diameter Whatman™ 3 filter discs soaked with 10

µL of 2.5 M $KHSO_4$ and sealed in PTFE tape. NH_4^+-N was diffused by simultaneously adding 0.2 g of MgO and an acid trap to the soil extract. To ensure complete diffusion, extracts were shaken at low speed for 7 days. To diffuse NO_3^--N, NH_4^+-N was first removed from the solution using the above procedure but the filters were discarded. NO_3^- was then diffused by adding 100 µL of 30 % Brij-35 and 0.4 g of Devarda's alloy, which reduces NO_3^--N to NH_4^+-N. A second acid trap was placed into the specimen cups and samples were shaken for another 7 days at room temperature. All acid traps were then dried in a desiccator, encapsulated in tin capsules and analysed via a continuous flow isotope ratio mass spectrometer (IRMS; Elementar Isoprime Precision; Elementar Analysensysteme GmbH, Hanau, Germany) coupled with an elemental analyser (EA) inlet (vario PYRO cube; Elementar Analysensysteme GmbH, Hanau, Germany).

Gross mineralisation fluxes were calculated using the following equations developed by Kirkham and Bartholomew (1954):

$$M\ (\mu g\ g^{-1}\ day^{-1}) = \frac{[NH_4^+]_0 - [NH_4^+]_t}{t} \times \frac{\log\left(\frac{APE_0}{APE_t}\right)}{\log\left(\frac{[NH_4^+]_0}{[NH_4^+]_t}\right)} \quad (4.1)$$

$$C\ (\mu g\ g^{-1}\ day^{-1}) = M - \frac{[NH_4^+]_t - [NH_4^+]_0}{t} \quad (4.2)$$

Where M= gross mineralization rate, C= NH_4^+ consumption rate, t = time elapsed, [NH_4^+] = NH_4^+ soil concentration (µg g^{-1}), APE_τ = ^{15}N atom percent excess of the NH_4^+ pool, τ. Gross rates of nitrification and NO_3^- consumption were calculated by replacing NH_4^+ concentration by NO_3^- concentration, and APE in the NH_4^+ pool by the APE in the NO_3^- pool. NH_4^+ immobilization rate is equal to the difference between NH_4^+ consumption rate and gross nitrification. NO_3^- immobilisation rate is assumed equivalent to the gross NO_3^- consumption rate.

4.2.6. Statistical analyses

Statistical analyses were carried out in R version 4.1.0 (R Core Team, 2021) with Rstudio software (RStudio Team, 2021). The effects of exudate treatment (low C:N and high C:N) and

microbial exclusion (1-micron bag, 41-micron bag, O-horizon) on soil N content and transformations were tested with two-way analysis of variance (ANOVA) followed by Tukey's post-hoc tests for multiple comparisons when the ANOVA indicated a significant treatment effect at $p < 0.05$. The normality of the residuals and homogeneity of variances were inspected for all variables and log transformations were performed for the N cycling rates. To assess the effects of exudate quantity (increased C and N) and exudate quality (increased C:N ratio), we computed the logarithm of the response ratio (lnRR) between control and low C:N ratio treatments, and between low and high C:N ratio treatments, respectively. Response ratio ($lnRR$) and its corresponding pooled variance (V) was determined using the formula in Hedges et al. (1999) (Equations 4.3 and 4.4).

$$lnRR = \ln\left(\frac{X1}{X2}\right) \quad (4.3)$$

$$V = \frac{S1^2}{(N1 \times X1^2)} + \frac{S2^2}{(N2 \times X2^2)} \quad (4.4)$$

where $X_1$and X_2 are the mean values of a specific variable in the different exudate treatments respectively; N_1 and N_2 are the sample sizes; and S_1 and S_2 are the standard deviations.

4.3. Result

4.3.1. Organic and inorganic soil N concentrations

Overall, NH_4^+, NO_3^- and FAA concentrations were consistently higher in the O-horizon followed by the 41 µm bag followed by the 1 µm bag (Fig. 4.2). The concentrations of NH_4^+ and NO_3^- in the O-horizon soils were similar between exudate treatments but both were significantly higher than in the control soils ($P < 0.05$). However, NH_4^+ and NO_3^- concentrations in the exclusion bags were at least 10 times lower than in O-horizon soil and were unaffected by exudate treatments (Fig. 4.2.b). Surprisingly, FAA concentration was lower in the low C:N exudate treatment compared to the high C:N exudate treatment in both O-horizon soil (─50%; $P = 0.09$) and 41 µm bags (─27%; $P < 0.05$), even though the amount of amino acids added in the low C:N exudate treatment was twice as high (Fig. 4.2.a).

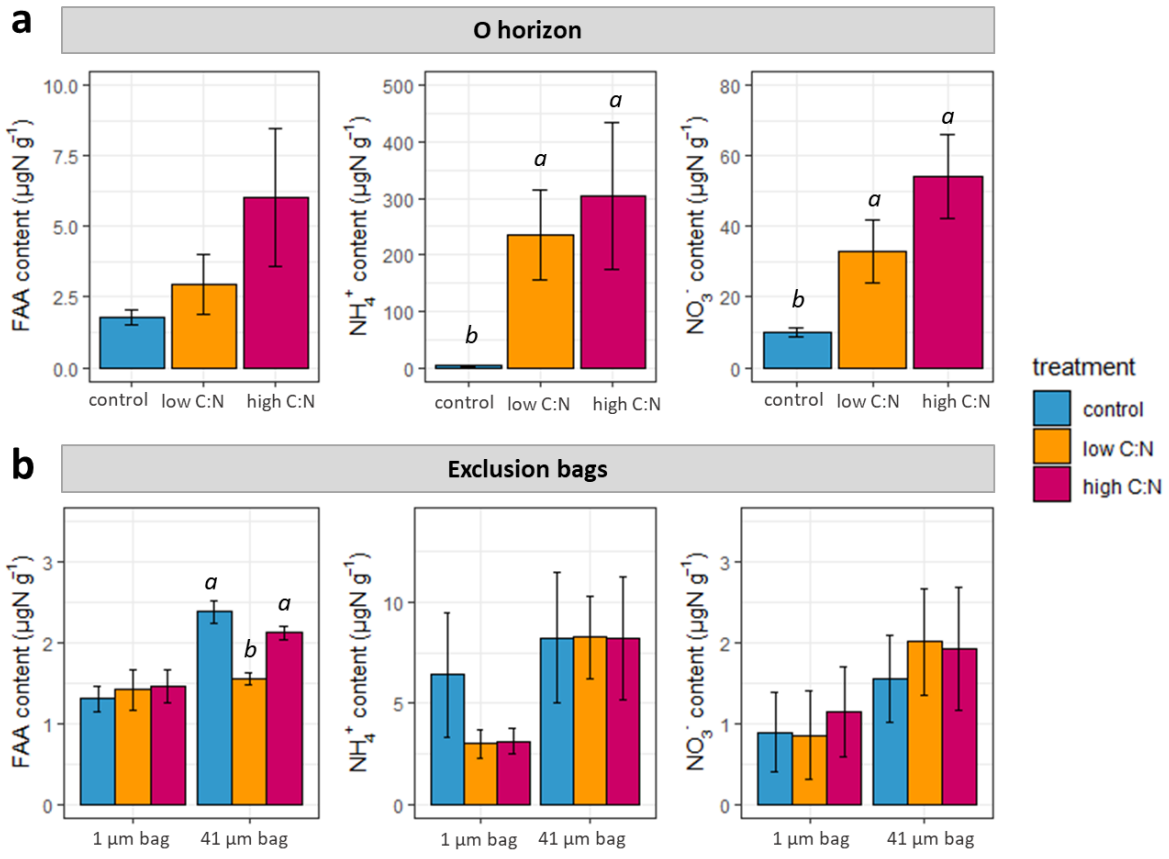

Figure 4.2: *Nitrogen concentrations in experimental exudate treatments a) in the O-horizon soil and b) in exclusion bags. Letters (a,b) indicate significant difference between treatment for this type soil micro-habitat. Values are means ± SE for n = 4 per treatment. Note the difference in y axis ranges among panels.*

4.3.2. Effect of exudates on N cycling rates

The high C:N exudate treatment enhanced gross N mineralization and NH_4^+ immobilization ($P < 0.05$) compared to the control, especially in the O-horizon, where gross N mineralization was two times higher relative to the control. The high C:N exudate treatment also enhanced gross nitrification in the 41 µm bags (root exclusion; + 95% relative to the control; $P < 0.05$) but not in the O horizon soils or 1 µm bags (Fig. 4.3). By contrast, the low C:N exudate treatment slightly reduced gross mineralization and gross nitrification compared to the control (— 46% and — 40% respectively; Fig. 4.3). As a result of the lower mineralization and nitrification activity in the low C:N exudate treatment, the mean residence times of both NH_4^+ and NO_3^- were higher compared to the control ($P = 0.005$; $P = 0.09$ respectively; Fig 4.3). The

ratio of immobilization to mineralization (I:Mi ratio) was unaffected by treatments (Fig. 4.4a). By contrast, the ratio NO_3^- immobilization to nitrification (I:Ni) was lower in the two exudate treatments compared to control ($P < 0.05$), indicating that less NO_3^- was immobilized for the same amount nitrified under exudate treatments (Fig. 4.4b).

4.3.3. Effect of microbial exclusion on N cycling rates

Gross mineralization, NH_4^+ immobilization rates and NH_4^+ mean residence times were two to five times higher in the O-horizon compared to the 1 µm and 41 µm exclusion bags ($P < 0.05$; Table 4.2). Conversely, gross nitrification and NO_3^- immobilization rates were almost always undetectable in the O-horizon but were detectable in all exclusion bag samples ($P < 0.05$; Fig. 4.3). Furthermore, the I:Mi ratio was twice as high in the 1 µm bag ($P < 0.05$) compared to the O-horizon soil, indicating that more NH_4^+ was immobilized per amount of NH_4^+ mineralized when roots and fungi were excluded (Fig. 4.4a).

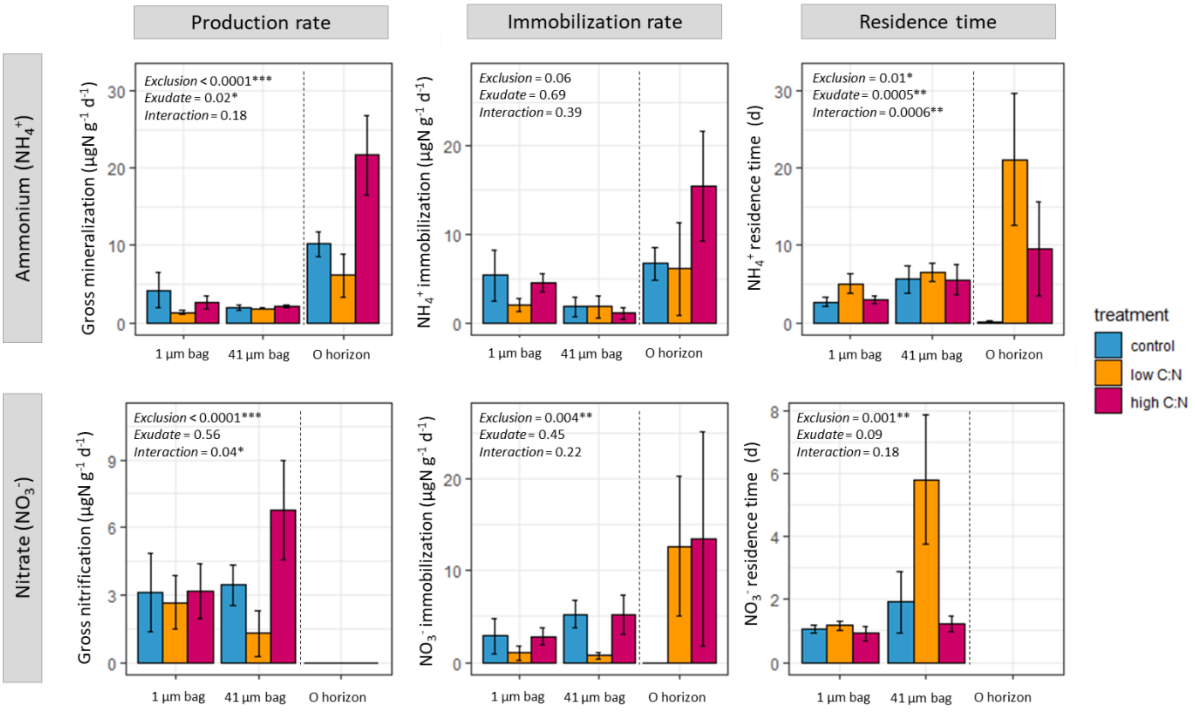

Figure 4.3: *Ammonium and nitrate production rates, immobilization rates and mean residence time in experimental exudate treatments and exclusion bags. A dashed line separates the O-horizon and exclusion bag soils. Gross nitrification and NO_3^- residence time were not detectable in the O-horizon. Significant effects of treatment, exclusion bags or their interaction at p < 0.05 are indicated by an asterisk. Values are mean ± SE for n = 4 per treatment.*

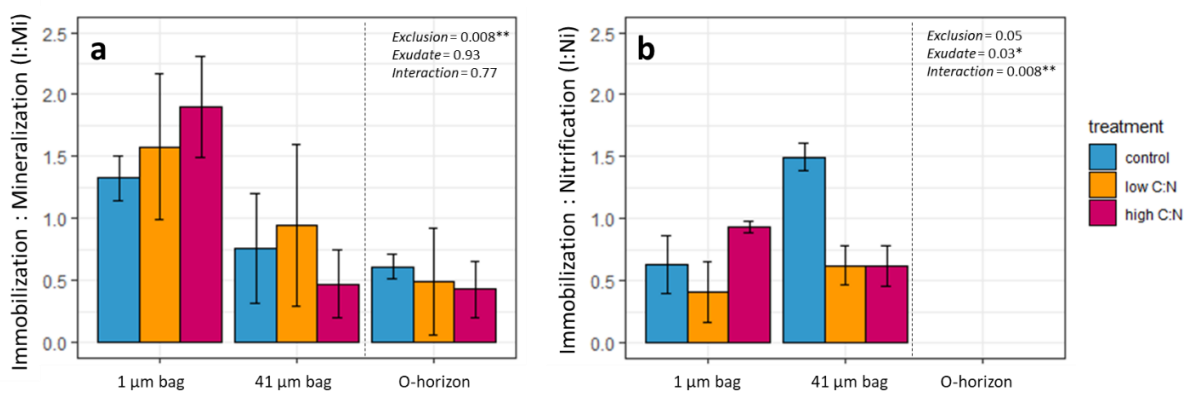

Figure 4.4: *Ratio between consumption and production rates for NH_4^+ (NH_4^+ immobilization / gross mineralization) and NO_3^- (NO_3^- immobilization / gross nitrification). A dash line separates the O-horizon soil and the exclusion bag soils. Significant effect of treatment, exclusion bags or their interactions are indicated by a p-value below 0.05 with an asterisk. Values are mean (n=4) ± SE.*

4.3.4. Comparison of the effect of exudate quantity vs quality

Response ratios revealed the effects of increasing exudate quantity (low C:N vs control) and increasing C:N ratio (low C:N vs high C:N) across exclusion bags (Fig. 4.5). On average, N availability increased to the same extent in both exudate treatments in the O-horizon. However, a greater quantity of exudates generally reduced N cycling rates (mineralization, nitrification, and immobilization) across the three exclusion treatments. Conversely, a high exudate C:N ratio increased N cycling rates. Gross mineralization and NH_4^+ immobilization were predominantly enhanced in the O-horizon and in the presence of bacteria only (1 µm bags), whereas nitrification and NO_3^- immobilization were mainly enhanced in the presence of fungi but in the absence of roots (41 µm bags; Fig. 4.5).

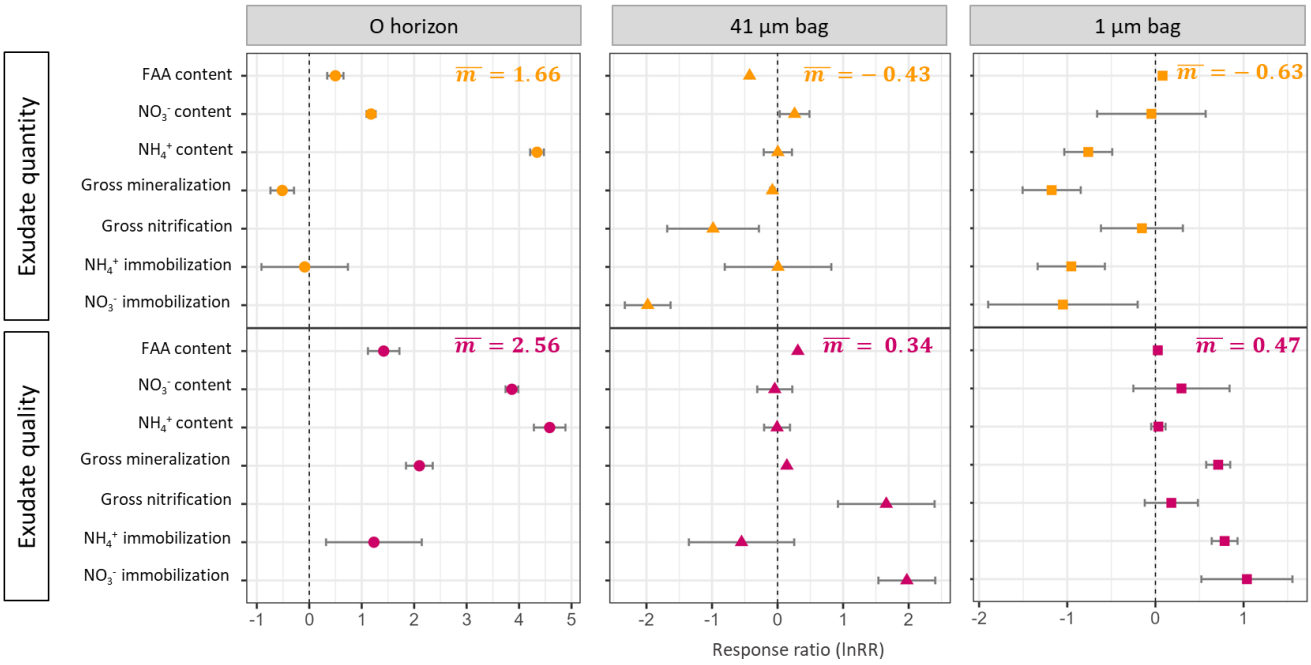

Figure 4.5: *Response ratio of N availability and processes to exudate quantity change (low C:N vs control) and to exudate quality change (high C:N vs low C:N).*

Table 4.2: *Statistics from two-way analyses of variance testing the effects of exclusion bag (O-horizon, 41-micron and 1-micron exclusion bags), exudate treatment (low C:N, high C:N, control) and their interactions on soil N pools and transformation rates. Bold typing indicates a significant effect (P < 0.05) and underline indicates a marginal effect (0.1 > P > 0.05).*

Factors	Exclusion treatment		Exudate treatment		Exclusion * Exudate	
DF	2		2		4	
Analysis of variance	F statistic	*P*	F statistic	*P*	F statistic	*P*
Gravimetric moisture	127.1	**<0.0001**	0.8	0.45	1.17	0.32
NH_4^+	16.1	**<0.0001**	4.8	**0.01**	6.5	**0.0008**
NO_3^-	83.1	**<0.0001**	6.6	**0.005**	1.2	0.33
FAA	7.7	**0.002**	2.6	0.09	2.2	0.09
Gross mineralization	30.8	**<0.0001**	4.4	**0.02**	1.7	0.18
Gross nitrification	30.5	**<0.0001**	0.57	0.56	2.87	**0.04**
NH_4^+ immobilization	3	0.06	0.37	0.69	1.05	0.39
NO_3^- immobilization	6.8	**0.004**	0.7	0.45	1.5	0.22
NH_4^+ residence time	5.6	**0.01**	10.2	**0.0005**	7.11	**0.0006**
NO_3^- residence time	9.7	**0.001**	2.8	0.09	1.9	0.18

4.4. Discussion

We assessed the effect of root exudation quality and quantity on N transformations using an experimental exudate cocktail. By simulating changes in root exudate composition under

eCO_2, we were able to isolate the specific effects of altered root exudation on N transformations and determine the organism groups mediating these N transformations. Thus, our approach enabled us to disentangle the mechanisms driving the acceleration of mineralization and the downregulation of nitrification previously observed under eCO_2 (Rumeau et al., 2024).

Higher exudate C:N stimulated N mineralization

Higher gross mineralization under the high C:N treatment but not under the low C:N exudate treatment suggests that gross mineralization is stimulated by N limitation in the high C:N treatment rather than by the amount of C supplied to microbes. This observation supports the "microbial N mining theory" suggesting that mineralisation of SOM in response to C addition (i.e. priming) occurs under low N availability as a strategy for microbes to acquire additional N (Chen et al., 2014; Craine et al., 2007; Dijkstra et al., 2013) and maintain their C:N stoichiometry (Hessen et al., 2004). That suggests that both C and N are essential regulators of N release from SOM, challenging the original theory focusing mainly on energy input from C (Jones et al., 2009, 2004). Mineralisation of SOM to acquire N is further supported by laboratory studies where priming effects were lower under combined C and N addition compared to C alone (L. Du et al., 2020; Jílková et al., 2020; Liu et al., 2020). In our study, mineralization was five times faster both in the presence of roots and in the high C:N exudate treatment, which suggests that priming is initiated by the rhizosphere microbiome (i.e. ectomycorrhiza (ECM) fungi, rhizosphere bacteria) or by the competition for N between microbes and roots (Jilling et al., 2018). Our findings build on previous work that emphasizes the role of the rhizosphere in regulating N availability under eCO_2 (Meier et al., 2015; Rumeau et al., 2024) by demonstrating that N cycling is influenced not only by root exudates but also by the interaction between root exudates and rhizosphere communities. However, our experiment does not allow us to quantify the relative contribution of ECM fungi and rhizosphere bacteria in the enhanced mineralization. Although our exudate treatments did not prompt microbes to retain more N, the higher I:Mi ratio in the absence of roots and fungi suggest that

bacteria when alone retained N more efficiently, potentially due to reduced competition for N when roots are absent (Schimel and Bennett, 2004). Thus, lower competition for N may explain why N-mining in response to a high exudate C:N ratio was also lower in the absence of roots. These findings demonstrate that the increase in root exudate C:N ratio, previously observed under eCO_2 (Reay et. al, *in prep*), rather than the increase in the amount of root exudates, enhances gross N mineralization by the root microbiome without disrupting the balance between mineralization and immobilization, thereby resulting in greater N availability for trees.

Exudate C:N ratio shifted microbial nutrient acquisition strategies

The lower than expected concentration in amino acids in the low C:N exudate treatment, together with low inorganic N immobilization rates suggests that microbes preferentially immobilized the added organic N in this treatment. Our findings thus add to previous studies demonstrating that soil microbes prefer to assimilate amino acids over inorganic N (Knowles et al., 2010; Mooshammer et al., 2014). Hence, increasing exudate stoichiometry, rather than the quantity of exudate-C, induced microbes to switch from preferential substrate utilization (Dijkstra et al. 2013) to a N-mining strategy, wherein microbes transition from utilizing exudates to decomposing SOM (Cheng, 1999), but without altering the relative contribution of bacteria and fungi to SOM decomposition. Changes in exudate quality could therefore have a negative impact on soil C storage by favouring SOM mining rather than SOM build-up (Guenet et al., 2010). Consequently, our results suggest that exudate composition could play a crucial role in determining microbial mechanisms of soil C storage, by prompting the switch from preferential substrate utilization and SOM accumulation at high amino acid concentrations (relative to C) to SOM decomposition due to N mining at low amino acid concentrations.

High exudate C:N ratio and root exclusion stimulated nitrification

Although downregulation of nitrification has been observed under eCO_2 (Rumeau et al., 2024) we measured greater nitrification rates in the root exclusion bags under the high C:N exudate

treatment. As higher nitrification rates were only measured in the 41 µm bags, they indicate increased fungal nitrification, as hypothesized, due to the high contribution of fungal activity in nitrification in acidic forest soils (Li et al., 2018). Root exclusion stimulated gross nitrification compared to the O-horizon where nitrification was suppressed by the end of the experiment. However, high nitrate levels in the O-horizon soil under exudate treatments indicate nitrification wasn't fully suppressed across the experiment, but, since this inhibition occurred even in the water treatment, it is more likely due to the presence of roots rather than the high nitrate concentration specific to exudate treatments. Nitrification inhibition in the presence of roots could be due to root uptake of ammonium or the release of biological nitrification inhibitors by trees as a strategy to conserve N (Andrianarisoa et al., 2010; Florio et al., 2021; Paavolainen et al., 1998). Biological inhibitors are a likely explanation for lower overall nitrification rates, as our exudate cocktail did not include inhibitory compounds. Thus, our root exudate cocktails stimulated fungal nitrification when roots were excluded, likely as a response to the addition of labile C sources which are known to enhance heterotrophic nitrification (Zhang et al., 2019). However, increased fungal nitrification in response to altered exudate quality are unlikely to play a major role in N-limited forest soils under eCO_2, where trees invest in larger root biomass (Norby et al., 2004; Ziegler et al., 2023) mitigating nitrification.

4.5. Conclusion

Together our results demonstrate that N transformations are influenced more by the C:N stoichiometry than the quantity of root exudates and are largely dependent on the root microbiome. In response to increasing exudate C:N ratio, soil microbes adopted an "N mining strategy", using exudate C to mine for N via SOM decomposition. This shift was exacerbated by the presence of roots competing with microbes for available N. Our findings reveal that both C and N content in exudates are critical drivers of rhizosphere N cycling and unveil two coupled key mechanisms – root exudation composition and root exploration – by which trees regulate soil N availability under eCO_2. However, changes in the N acquisition strategies of trees and

soil microbes under eCO_2 are likely to affect above- and belowground C storage, which warrants further investigation.

The last three chapters bring to light the importance of plant-soil interactions for meeting higher tree N demand under eCO_2. Together these findings highlight that by expanding root biomass and exploration, trees under eCO_2 favour N-mining and N conservation by inhibiting nitrification. Additionally, by increasing the C:N ratio of the soil exudates, trees promote N-mining by microbes as a way to maintain their stoichiometry. These plant-soil interactions enable higher tree N demand to be met after six years of CO_2 enrichment. However, whether these mechanisms are unique to this site or if they could apply to another ecosystem and/or to another nutrient (i.e. P) is a question that the next chapter will explore.

Chapter 5. Soil microbial limitation shifts in response to elevated CO_2 and P fertilization in a Eucalyptus forest

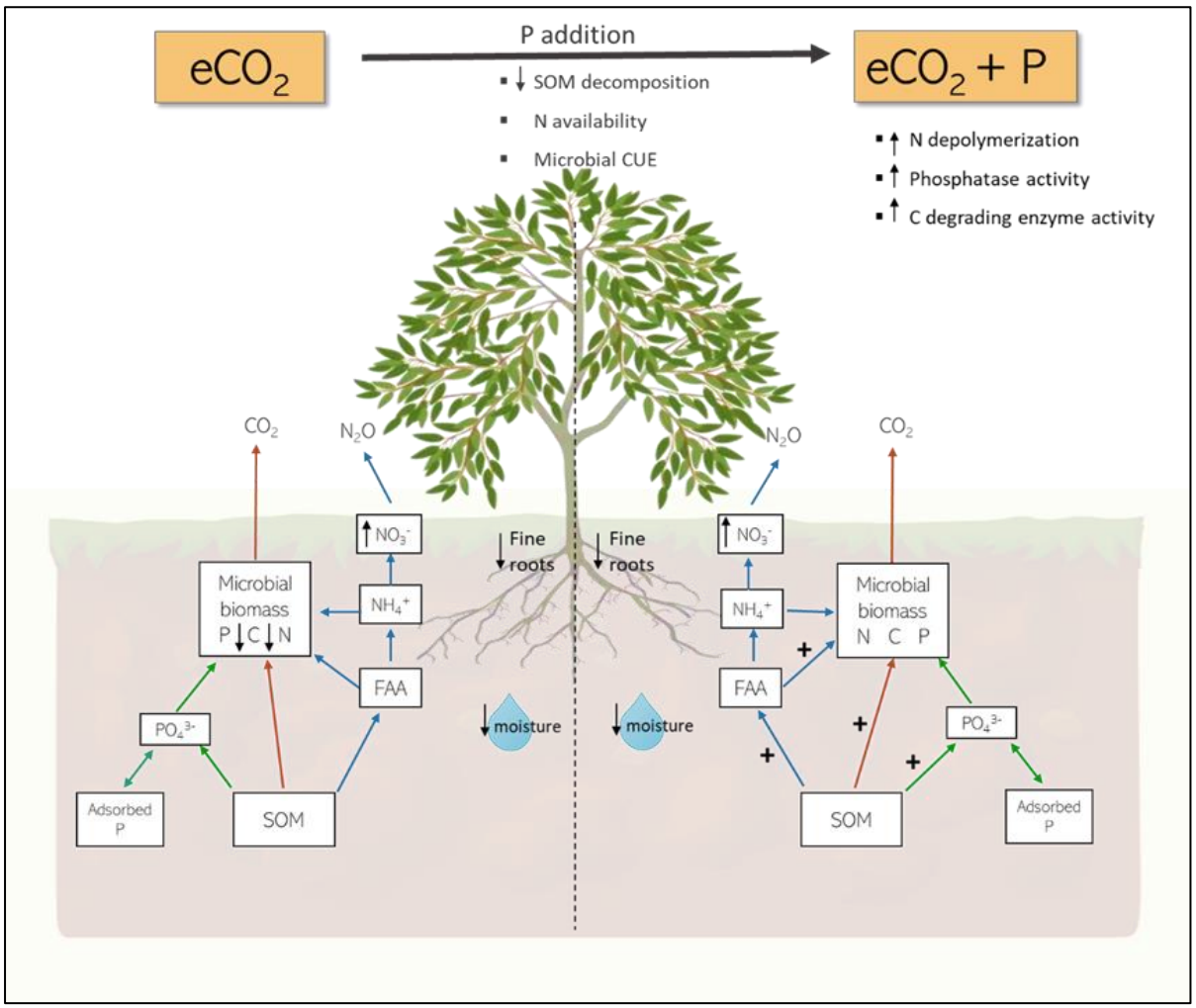

Soil microbial limitation shifts in response to elevated CO_2 and P fertilization in a Eucalyptus forest

Manon Rumeau[1,2*], Catriona Macdonald[3], Paola Pisetta Raupp[3], Charles Warren[4], Sami Ullah[1,2], Fotis Sgouridis[5], Michaela K. Reay[6], Rob Mackenzie[1,2], and Yolima Carrillo[3]

[1]*Birmingham Institute of Forest Research, University of Birmingham, Birmingham, UK*

[2]*School of Geography, Earth and Environmental Science, University of Birmingham, UK*

[3]*Hawkesbury Institute for the Environment (HIE), Western Sydney University Richmond, Australia*

[4] *School of Life and Environmental Sciences, University of Sydney, Australia*

[5]*School of Geographical Sciences, University of Bristol, Bristol, UK*

[6]*Organic Geochemistry Unit, School of Chemistry, University of Bristol, UK*

Corresponding author: Manon Rumeau (MLR094@student.bham.ac.uk)

Additional corresponding author: Yolima Carrillo (y.carrillo@westernsydney.edu.au)

Abstract

The ability of forests to store additional carbon (C) with increasing CO_2 concentration can be limited by phosphorus (P) availability. Given the widespread occurrence of P-limited forests, P fertilization can be employed to assess how enhanced soil P availability may support forest growth. However, the impact of P fertilization on forest C sinks in an ecosystem with other nutrient limitation remains unknown. This study assessed whether P fertilization induces a shift from P to nitrogen (N) limitation and if N limitation may be alleviated under elevated CO_2 (eCO_2) through a stimulation of N cycling. In April 2023, a mature Eucalyptus forest at Euc-FACE experiment in Australia for which the response to eCO_2 is limited by P, was fertilized with 1.75 kg P ha^{-1}. Enzyme activity, N cycling rates and nutrient pools in the top 10 cm of soil were investigated at three intervals: pre-fertilization, 10 days post-fertilization and 2 months post-fertilization. eCO_2 increased soil nitrate in the top 10 cm, likely associated to a shift in the understorey plant communities and root depth exploration. P fertilization decreased C-N-P-mining activities while increasing C and N recycling efficiency. However, eCO_2 partly offset this decrease, by enhancing C-P enzyme activities and protein depolymerization. This suggests faster nutrient cycling under eCO_2 compared to ambient CO_2 (aCO_2) once P limitation is reduced. Faster nutrient cycling may be targeting N-release from SOM however, the strong coupling between C, N and P cycling prevent a clear determination of the primary limiting nutrient. This study confirms that the stimulation of nutrient cycling under eCO_2 is constrained by P limitation in this forest but only long-term assessments will reveal changes in plant response and C stores.

Keywords: SOM decomposition; P fertilization; N depolymerization; gross mineralization; soil nitrate, P-limited soil

5.1. Introduction

Increasing atmospheric CO_2 concentrations due to human activities are projected to enhance photosynthesis, potentially mitigating climate change by storing carbon (C) in forest ecosystems (Norby and Zak, 2011). However, this CO_2 fertilization effect can be limited by soil nutrient availabilities, particularly nitrogen (N) and phosphorus (P) (Diaz et al., 1993; Reich et al., 2006; Terrer et al., 2018). Most research has focused on N-limited ecosystems in the northern hemisphere, while P-limited ecosystems in the southern hemisphere have received little attention (E. Du et al., 2020; Ellsworth et al., 2017). P availability is largely governed by abiotic factors (pH, sorption sites) making it less responsive to vegetation-driven changes compared to N (Castañeda-Gómez et al., 2022; Dijkstra et al., 2013). Although plants can release organic acids to mobilize P, it remains uncertain if this mechanism is sufficient to meet increased P demands under elevated CO_2 (eCO_2) (Jilling et al., 2018). Findings from a decade-long Free-Air CO_2 Enrichment (FACE) experiment conducted on a P-limited soil in Eastern Australia indicate that the ecosystem's growth response to eCO_2 is constrained by P availability (Ellsworth et al., 2017).This was confirmed by a P addition experiment outside of the FACE rings (Crous et al., 2015). Despite enhanced photosynthesis under eCO_2, C was allocated belowground and released via respiration instead of being converted into biomass due to P limitation (Ellsworth et al., 2017). These findings suggest that enhanced C allocation belowground may be insufficient to stimulate P availability on the long term (Hasegawa et al., 2016; Jiang et al., 2024; Ochoa-Hueso et al., 2017). But, further evidence is needed to understand the control of P limitation on plant response to eCO_2 (Jiang et al., 2020). Understanding the extent to which forest ecosystems are able to alleviate P limitation is crucial for predicting global response of forests to eCO_2, given the widespread occurrence of P limitation worldwide (E. Du et al., 2020).

Due to this widespread occurrence of P-limited forests and the observed constraining effect of P on plant response to eCO_2 (Cunha et al., 2022; Ellsworth et al., 2017), methods for enhancing soil P availability in order to optimize forest C sink are being explored. While

greenhouse experiments suggest that P fertilization could result in higher plant growth under eCO_2 (Jakobsen et al., 2016; Piñeiro et al., 2023), such response may be diminished or offset at the ecosystem level due to other nutrient limitation. C, N and P cycles are tightly coupled in soils because of microbial and plant C:N:P stoichiometry (Cleveland and Liptzin, 2007; Griffiths et al., 2012). Thus, alleviating P limitation in a highly P-limited ecosystem can increase the microbial demand for the other nutrients such as N, leading to a shift in microbial nutrient limitation. This could notably result in enhanced N retention by microbes and a decrease in N availability (Mooshammer et al., 2014). But, conversely, P fertilization may alleviate P limitation on N cycling and stimulate N release from SOM (Chen et al., 2016; Cheng et al., 2018). Forecasting the effect of P fertilization on N cycling is challenging due to the different responses and the limited number of studies. Furthermore, if N become the *new* limiting nutrient for plant and microbes, it is uncertain if eCO_2 will enhance plant C sink. In N-limited ecosystem, plant-soil interactions have been found to increase N mineralization to sustain higher N demand under eCO_2 as a consequence to higher C being allocated belowground (Phillips et al., 2011; Rumeau et al., 2024). At EucFACE, the higher C belowground was insufficient to stimulate P release for plant uptake or at least became insufficient with time after the initial stimulation (Hasegawa et al., 2016; Jiang et al., 2024). Whether higher C belowground can, however, stimulate N cycling when N becomes the limiting nutrient is this ecosystem remains to be observed.

To disentangle the nutrient limitation effect on microbial and plant nutrient supply and uptake processes under elevated CO_2, a 10-year-old Eucalyptus FACE experiment in Australia was fertilized with P (1.75 kg P ha^{-1}) in April 2023. By investigating the interplay between C, P and N dynamics under eCO_2, we aim to shed light on the complex interactions shaping nutrient availability and ecosystem responses to future climate. We monitored N depolymerisation, N mineralisation in soils before and after the P fertilization using a ^{15}N pool dilution approach. In order to reveal shifts in microbial nutrient limitation we measured soil enzyme activities involved in CNP cycling, microbial biomass CNP and calculated microbial nutrient use

efficiencies. We hypothesize that 1) eCO_2 has little to no impact of N cycling due to P-limitation. 2) P-fertilization will increase microbial N demand, thereby decreasing N availability and 3) eCO_2 will enhance N-mining in P-fertilized plots to meet higher plant N demand.

5.2. Materials and Methods

5.2.1. Experimental site

The study was performed at the EucFACE facility, located in a mature evergreen Eucalyptus forest within a Cumberland Plain Woodland in Western Sydney, New South Wales (NSW), Australia (33°61′S, 150°74′E). The vegetation is dominated by Eucalyptus trees (*Eucalyptus tereticornis L.*) and the understory is composed of a diverse mix of graminoids, forbs and shrubs (Hasegawa et al., 2018). Soil is classified as Aeric Podosol with areas of Densic Podosol (Australian soil classification; Ross et al., 2020). Soil texture is a loamy sand up to 50 cm followed by a sandy clay loam to about 300 cm deep. This soil is characterized by low fertility and a low phosphorus content. From March to May 2023, the site received a 149.1 mm of rain and the mean temperature was 16.5 °C. For a detailed site description, see Ellsworth et al. (2017).

The EucFACE facility is composed of six infrastructure arrays of 25 m diameter each. Three are fumigated with a concentration of 150 ppm of CO_2 above the ambient concentration (eCO_2) and three are fumigated with air (aCO_2) from soil level to the top of the canopy (Fig. S5-1). CO_2 enrichment started in September 2012 and reached the +150-ppm target in February 2013. CO_2 enrichment operates all year long during daylight.

5.2.2. Phosphorus fertilization treatment

On April 3rd 2023, four of the six rings, two ambient CO_2, two elevated CO_2, were fertilized with 1.75 kgP ha^{-1} of superphosphate fertilizer ($Ca(H_2PO_4)_2$) (Fig. S5-1). To ensure an even distribution of the fertilizer across the soil surface, the fertilizer was ground, blended with acid washed sand, split in weighed portions and manually applied to 2 x 2 m squares. In each ring, four 2 x 2 m plots were randomly pre-defined for soil sampling, and in each a section of 1 x 1

m was left unfertilized, receiving only acid-washed sand. In total four areas of 1 x 1 m were left unfertilized per ring and each one featured a square (0.5 x 0.5 m) made of aluminium sheet (~5 cm high) that was gently inserted into the soil to prevent horizontal fertilizer transfer without disturbing roots (Fig. 5.1B).

5.2.3. Sampling

Soil was sampled in the four rings that received P-fertilization (ring 1, 2, 3 and 4). Sampling was done three weeks before fertilization (March 13th), 10 days after fertilization (April 13th), and 7 weeks after fertilization (May 29th) in the four 2 x 2 m plots (Fig 5.1A). Prior to fertilization, four soil cores (5 cm diameter, 10 cm depth) were collected in each plot of each ring and bulked together to make up a total of four soil samples per ring. Post-fertilization, an additional four soil cores were collected from the unfertilized area delimited by aluminium sheets and bulked together to make up a total of four soil samples from fertilized area and four soil samples from unfertilized area per ring (Fig. 5.1B). Collected soil was placed in a cool box and brought back to the laboratory and was directly processed for ^{15}N incubation or stored at 4 °C.

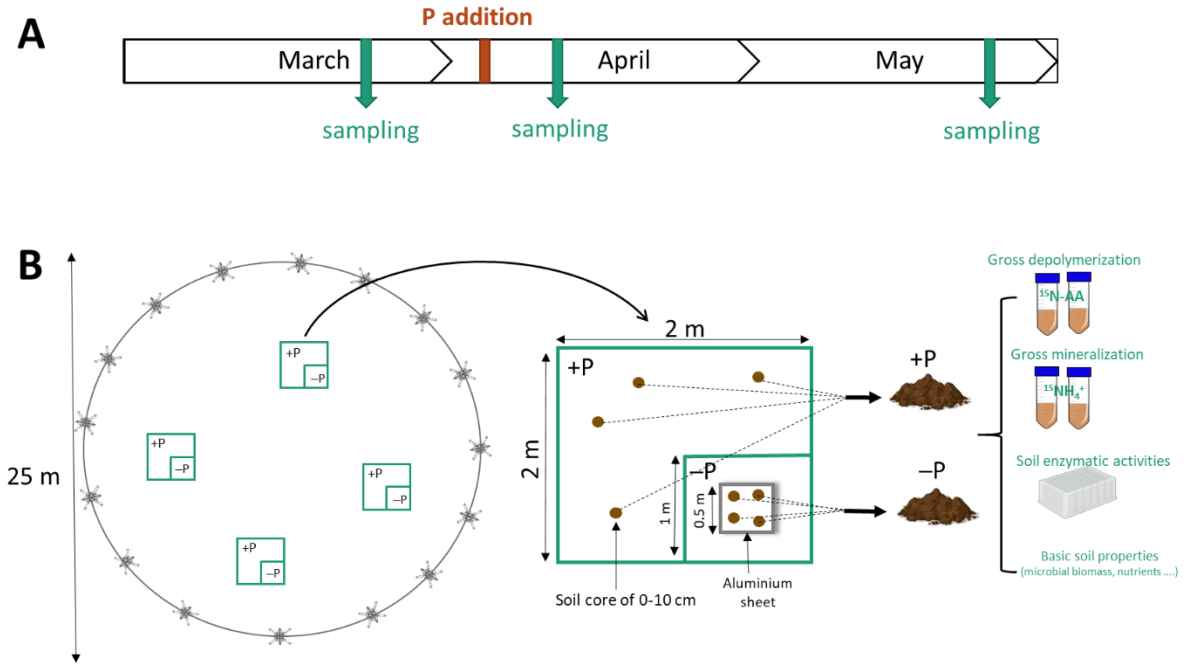

Figure 5.1: *Schematic of A) P addition and sampling time across the three months of the experiment B) the sampling and processing for one FACE ring.*

5.2.4. Soil and microbial nutrient pools

To determine soil nutrient pool contents, we quantified soil ammonium ($N\text{-}NH_4^+$), nitrate ($N\text{-}NO_3^-$), free amino acids (FAA), available P (Bray-P), dissolved organic C (DOC), dissolved organic N (DON) and microbial biomass C, N and P (MBC, MBN and MBP). All nutrient analyses were performed within a week after field collection. Gravimetric moisture was measured by drying ~ 5g of soil at 70°C for 48 h. The root biomass was assessed by collecting, washing and drying the roots at 60 °C for 48 h. Total root biomass was weighted and root below 2 mm diameter were re-weighted to assess the “fine root biomass” per volume of soil collected.

Soil NH_4^+ and NO_3^- were measured by extracting 20 g of soil with 60 ml of 1M potassium chloride (KCl). The extracts were filtered through a Whatman filter paper n°42 and analysed by continuous flow colorimetry (AQ2 discrete analyser; SEAL Analytical, Inc., Mequon, WI, USA). Soil free amino acid (FAA) concentration was determined on the same soil extract using the OPAME fluorescence assay described by Jones (2002) and adapted to a microplate assay by Darrouzet-Nardi et al. (2013). Fluorescence was read after one-hour incubation on a CLARIOstar plate reader (BMG LABTECH, Germany). Bray-P was measured by extracting 3.5 g of soil with 25 ml of Bray extracting solution (0.03 M NH4F, 0.025 M HCl). The extracts were filtered and analysed by continuous flow colorimetry (AQ2 discrete analyser; SEAL Analytical, Inc., Mequon, WI, USA). Dissolved organic C and N was measured after extraction with 0.05 M K_2SO_4 (1:3 (*w*/*v*)) and analysis on a TOC-TN analyser (total organic carbon analyser; Shimadzu Corporation, Japan). C, N and P microbial biomass was measured according to the chloroform extraction method (Brookes et al., 1985). For C and N microbial biomass, 2 subsamples of 10g each were weighed. One was directly extracted with 0.05 M K_2SO_4 while the other one was fumigated with chloroform for 4 days in a closed chamber before extraction. C and N were determined in the filtered extracts using a TOC-TN analyzer (total organic carbon analyser; Shimadzu Corporation, Japan). A similar method was applied for P microbial biomass at the difference that fumigation lasted for one day and extraction was

done using Bray extraction solution and analysed by colorimetry (AQ2 discrete analyser; SEAL Analytical, Inc., Mequon, WI, USA). Microbial C, N and P (MBC, MBN, MBP) were calculated as the difference in the C, N and P concentration between the fumigated and the non-fumigated samples. MBC, MBN and MBP were divided with the respective correction factors: K_{EC} = 0.45, K_{EN} = 0.54 and K_{EP} = 0.40 (Halbritter, 2020).

5.2.5. ^{15}N pool dilution assays

Gross rates of N mineralisation, depolymerisation, microbial immobilisation of NH_4^+ and amino acids were assessed by a ^{15}N pool dilution method as described by Hart et al. (1994) and Noll et al. (2019) within 1 week after sampling.

Gross mineralisation. Gross N mineralisation and NH_4^+ consumption rates were measured by a ^{15}N pool dilution method described Kirkham and Bartholomew (1954). Duplicates of fresh soils (20g) were labelled with 1 ml of ^{15}N enriched $(NH_4)_2SO_4$ (98 atom % ^{15}N, Sigma-Aldrich) solution targeting an enrichment of 0.7 µg ^{15}N per gram of soil corresponding to ~30% of the soil NH_4^+ pool. ^{15}N solution was added dropwise with a syringe and soil was stirred with a spatula to ensure even distribution. Immediately after labelling and following a 24 h incubation at 25°C in the dark, soil samples were extracted with 1 M KCl. Ammonium was diffused into acidified filter disks that was analysed for $^{15}N/^{14}N$ ratio analyses using an EA-IRMS (elemental analyser-IRMS: Elementar Isoprime Precision; Elementar Analysensysteme GmbH, Hanau, Germany).

Ammonium immobilization over a 24-hour period was determined by measuring the incorporation of ^{15}N into the microbial biomass. In order to do that, another set of soil sample was labelled with 1 ml of ^{15}N enriched $(NH_4)_2SO_4$ solution. After 24 h incubation, the $^{15}N/^{14}N$ ratio of the microbial biomass was determined using the chloroform method (as above) and 15 ml of the K_2SO_4 extracts were then dried, ground and encapsulated in tin boats and analysed with an EA-IRMS.

Bulk gross depolymerization. Gross depolymerisation and amino acid immobilization rates were measured by a ^{15}N pool dilution method described by Noll et al. (2019). Briefly, triplicates of fresh soils (5g) were labelled with a solution of ^{15}N enriched amino acids (20 AA mix, Cambridge) targeting an enrichment of 0.42 µg ^{15}N per gram of soil corresponding to ~30% of the soil FAA pool. Samples were incubated for 0 h, 45 min and 4 h at 25°C in the dark and extracted with 25 ml of 1 M KCl solution. 50 µl of the soil extract was used to quantify the total FAA concentration and the rest of the sample underwent the NH_4^+ diffusion procedure to remove NH_4^+ from the extract before converting FAA into N_2O (oxidation in nitrite and reduction in nitrous oxide). The ^{15}N content of the N_2O was then determined using a continuous flow isotope ratio mass spectrometer (IRMS; Elementar Isoprime Precision; Elementar Analysensysteme GmbH, Hanau, Germany) coupled with a trace-gas pre-concentrator inlet with autosampler (isoFLOW GHG; Elementar Analysensysteme GmbH, Hanau, Germany).

Gross rates of N mineralisation, NH_4^+ consumption, gross depolymerisation and FAA immobilization were calculated using equations developed by Kirkham and Bartholomew (1954) and modified by Wanek et al., (2010). Microbial N use efficiency was calculated as the amount of nitrogen used for growth (i.e. difference between AA immobilization and gross mineralization rate) over the amino acid uptake rate as described by Mooshammer et al., (2014).

Microbial NH_4^+ immobilization was calculated as follows:

$$NH_4^+ immobilization\ (\mu g\ g^{-1} d^{-1}) = \frac{MBN \times \frac{MBN_{15N\%excess}}{100}}{t} \times \frac{100}{NH4_{15N\%excess}} \qquad (5.1)$$

Where $MBN_{15N\%excess}$ and $NH4_{15N\%excess}$ are the %15N excess of the microbial biomass N and ammonium pool respectively.

Additionally, the recovery of the ^{15}N-NH_4^+ in the microbial biomass and ammonium pool was calculated to quantify the amount of ^{15}N recovered in each pool at the end of the incubation (Fig. S5-2).

Compound specific depolymerization rates. Compound specific depolymerization rates were measured solely on soil sampled 10 days after fertilization. After incubation with solution of ^{15}N enriched amino acids (20 AA mix, Cambridge), 2 ml aliquots of KCl extracts were transferred in an ultrafiltration spin column which was centrifuged at 3000 rpm for 5 min and ultra-filtered samples were kept frozen for LC-MS analysis. Before analysis, amino acids were derivatized to increase their volatility and increase their separation. Derivatization was performed using the AccQ-Tag Ultra Derivatization Kit. Briefly, 200 µl of KCl extracted were dried with 10 µl of $U^{13}C^{15}N$ Alanine standard (1µl ml^{-1}). Dried extracts were re-dissolved in 20 µl of 20 mM HCl and 60 µl of borate buffer before adding 20 µl of derivatization agent and heated for 10 minutes. As KCl solubility decreases in acetonitrile, samples were centrifuged to pellet the salts and the supernatant was transferred to a second vial and analysed on a LC-MS instrument. The LC-MS system comprised a nano-LC system (Ultimate 3000 RSLCnano, Thermo Scientific Dionex, Sunnyvale, USA) interfaced via a CaptiveSpray ion source (20 µm tip) to a mass spectrometer (AmaZon SL, Bruker Daltonics, Bremen, Germany). All specifications of the LC-MS characteristics are specified in (Warren, 2019). Amino acids and their isotopomers were detected by their difference in molar mass. As most amino acids contain only one atom of N, their ^{15}N isotopomer has the same molar mass as a C isotopomer. Therefore, we calculated the isotope distribution of each amino acids using an online isotope distribution calculator (https://www.sisweb.com/mstools/isotope.htm) to account for natural abundance.

5.2.6. Soil enzyme activities and microbial C and P use efficiency

The potential activity of seven hydrolytic soil enzymes that degrade C-rich substrates (β-1,4-glucosidase, β-d-cellubiosidase, α-glucosidase, and β-xylosidase), N-rich substrates (β-1,4-N-acetylglucosaminidase and leucine aminopeptidase) and P (phosphatase) were measured. Enzyme assays were conducted using standard fluorometric techniques described by Bell et al. (2013). In brief, 2 g of frozen soil was blended with 60 ml of 50 mM sodium acetate buffer (pH=5.2) for 1 minute. 800 µl of soil slurry was transferred on duplicate to a 96-deep-well

microplate containing 200µl of substrate solution. Duplicate quenched standards were made by adding 800 µl of soil slurry to 200 µl of either 4 methylumbelliferone (MUB), or 7-amino-4-methyl coumarin (MUC) at different concentration from 0 µM to 100 µM for each soil. Soil slurries with fluorometric substrates were incubated for 3 h at 25°C. After the incubation period, plates were centrifuged for 2 min at 2000 x g, after which 250 µl of soil slurry was transferred from the deep well plate into corresponding wells in black flat-bottomed 96-well plate and then scanned on a CLARIOstar plate reader (BMG LABTECH, Germany) using excitation at 365 nm and emission at 450 nm. Units for all enzyme nutrient acquisition activities are expressed as nmol activity g^{-1} dry soil h^{-1}.

Microbial carbon use efficiency (CUE) and phosphorus use efficiency (PUE) were calculated from enzyme activities. This calculation uses the elemental stoichiometry of organic matter and microbial biomass, and the ratios of C to N-acquiring ecoenzymatic activities (Sinsabaugh et al., 2016) (Equations 5.2 and 5.3). This method assesses how microbes shift their resource use efficiency in response to substrate stoichiometry (Schimel et al., 2022).

$$CUE_{C:N} = CUE_{max}\left(\frac{S_{C:P}}{(S_{C:P}+K)}\right) \quad where\ S_{C:N} = \frac{1}{EEA_{C:P}} \times \frac{B_{C:P}}{L_{C:P}} \qquad (5.2)$$

$$PUE_{P:C} = PUE_{max}\left(\frac{S_{P:C}}{S_{P:C}+K}\right) \quad where\ S_{N:C} = (1 - EEA_{P:C}) \times \frac{B_{P:C}}{L_{P:C}} \qquad (5.3)$$

Where $S_{C:P}$ is a scalar that quantifies how ecoenzymatic activities allocate resources to mitigate differences between the elemental composition of available resources and that of microbial biomass. CUE_{max} is set at 0.6, PUE_{max} is set at 1.0 and K is the half saturation constant set at 0.5 (Sinsabaugh et al., 2016). $EEA_{C:P}$ refers to the enzymatic BG:Pho ratio, $B_{C:P}$ is the microbial C:P ratio and $L_{C:P}$ is the soil DOC:Bray-P ratio.

5.2.7. Ion-exchange resins

Soil NH_4^+, NO_3^- and PO_4^{3-} availabilities was also assessed using ion-exchange resin bags to obtain integrative measurements over a period of more than two years, from December 2021 to May 2023. Resin bags contained ~ 15 g of ion exchange resin beads (Dowex Marathon

MR-3 hydrogen and hydroxide form; Sigma Aldrich) enclosed in nylon fabric. The bags were acid-washed before used. In each plot, 2 resins bags were gently inserted in the soil upper layer (0-5 cm). After an incubation time ranging from few days to few months – depending on the campaigns – resins bags were retrieved and stored at ─20 °C until extraction. Then, resins bags were washed with DI water and extracted with 100 ml of an extraction solution (2M NaCl, 0.088 M HCl). Extracts were shaken, filtered and stored at ─20°C until analysis. Extracts were analysed by continuous flow colorimetry (AQ2 discrete analyser; SEAL Analytical, Inc., Mequon, WI, USA). Concentration in NH_4^+, NO_3^- and PO_4^{3-} were corrected by the mass of resin beads by bag and by the time of incubation to be expressed in ng per mg of resin beads per day.

5.2.8. Statistical analyses

Statistical analyses were carried out with Rstudio software (version 4.1.0, R Core Team, 2021). Linear mixed effect models were used to evaluate eCO_2 effect, P fertilization effect, time effect and their interactions set as fixed effects, with ring set as random effect ("lmer" function, lme4 package; Bates et al., 2015). For each variable, two linear mixed models were produced. One with the effect of eCO_2 and time as fixed factors over the three sampling times (March, April and May). And one with the additional effect of P fertilization over two sampling times (April and May). Significance was determined using ANOVA tests and a Tukey's multi-comparison test was performed when eCO_2 or P fertilization had an effect. Log transformations were performed when the assumptions of normality and variance were not met. The logarithm response ratio of P fertilization effect ($lnRR_{Ferti}$) and eCO_2 effect ($lnRR_{eCO2}$) were calculated using May data with equations 5.4 and 5.5. Its corresponding pool variance was calculated with the formula from Hedges et al. (1999)

$$lnRR_{Ferti} = \ln\left(\frac{X_{aco2+P}}{X_{-P}}\right) \quad (5.4)$$

$$lnRR_{eCO2} = \ln\left(\frac{X_{eco2+P}}{X_{-P}}\right) \quad (5.5)$$

Where $X_{\_P}$ is the mean value of the variable in unfertilized plots under both aCO_2 and eCO_2, X_{aco2+P} is the mean value of the variable under aCO_2 after P fertilization and X_{eco2+P} is the mean under eCO_2 after P fertilization.

5.3. Results

5.3.1. Effect of eCO_2

5.3.1.1. Nutrient pools

Over the different nutrient pools measured, eCO_2 had only a significant effect on nitrate soil content (+27) and microbial biomass C (MBC; ─15%; Fig. 5.3). NH_4^+ and PO_4^{3-} availabilities measured by ion exchange resins (IER) over two years were not significantly affected by eCO_2 but fluctuated with time (p < 0.05; Fig. 5.2). However, nitrate availability from IER measurements showed a time dependant effect of eCO_2 (p = 0.07). From December 2021 to October 2022, and from March to May 2023, nitrate concentration was ~100% higher under eCO_2. This is in accordance with the concentration of nitrate measured in soil samples that was significantly higher from March to May 2023 (+ 27%; p < 0.05; Fig. 5.3). Fine root biomass was 30% lower under eCO_2 (p < 0.05; Fig. 5.3) and soil gravimetric moisture was consistently lower under eCO_2 (─14%; p > 0.05) and was negatively correlated with soil nitrate (Fig. S5-3). Finally, eCO_2 had a negative effect on MBC (─15%; p = 0.01). Lower MBC led to lower microbial C:N and C:P ratios under eCO_2 (p = 0.18; p = 0.11 respectively; Fig. 5.4).

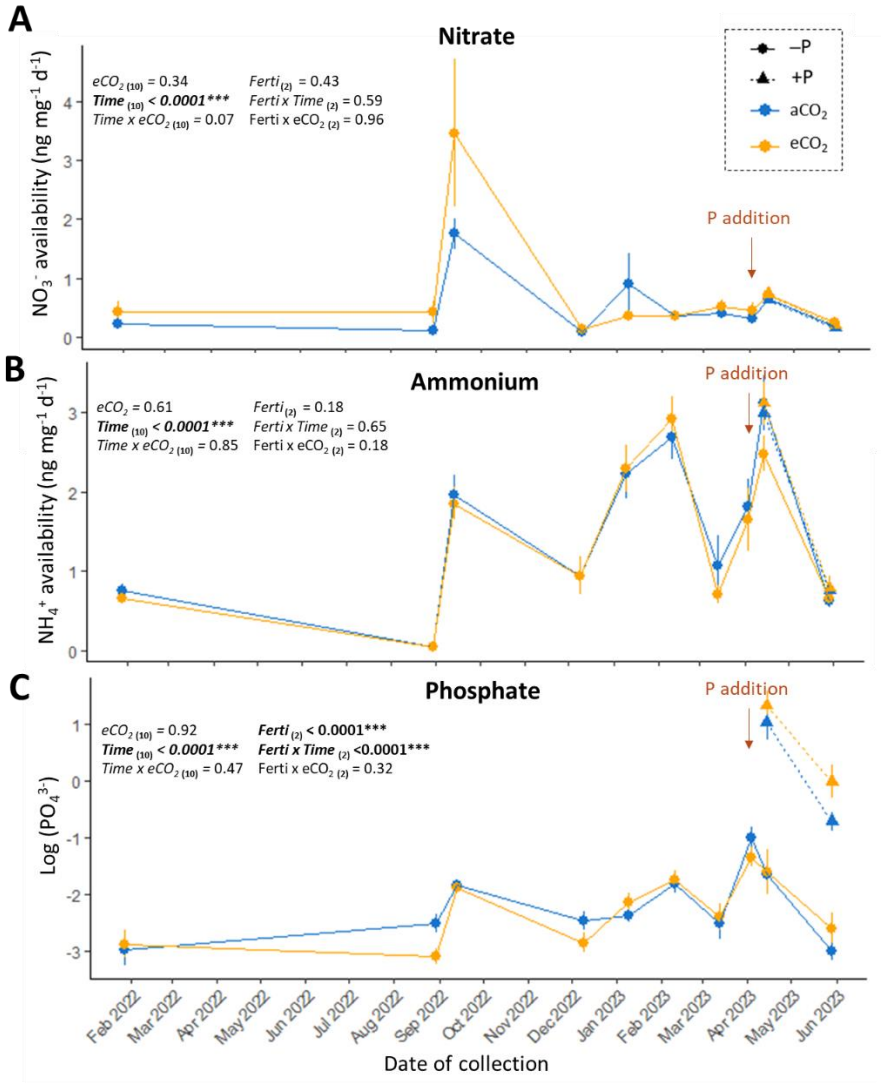

Figure 5.2: *(A) Nitrate, (B) ammonium and (C) phosphate availabilities measured by IER from December 2021 to June 2023 in the six rings under eCO_2 (orange) and aCO_2 (blue) in both unfertilized (–P) and fertilized (+P) areas. ANOVA p-values are detailed for the effect of eCO_2, time and P-fertilization (Ferti) their interactions. Number in subscript indicate the number of time points considered in the ANOVA. Data are means + SE (n=12).*

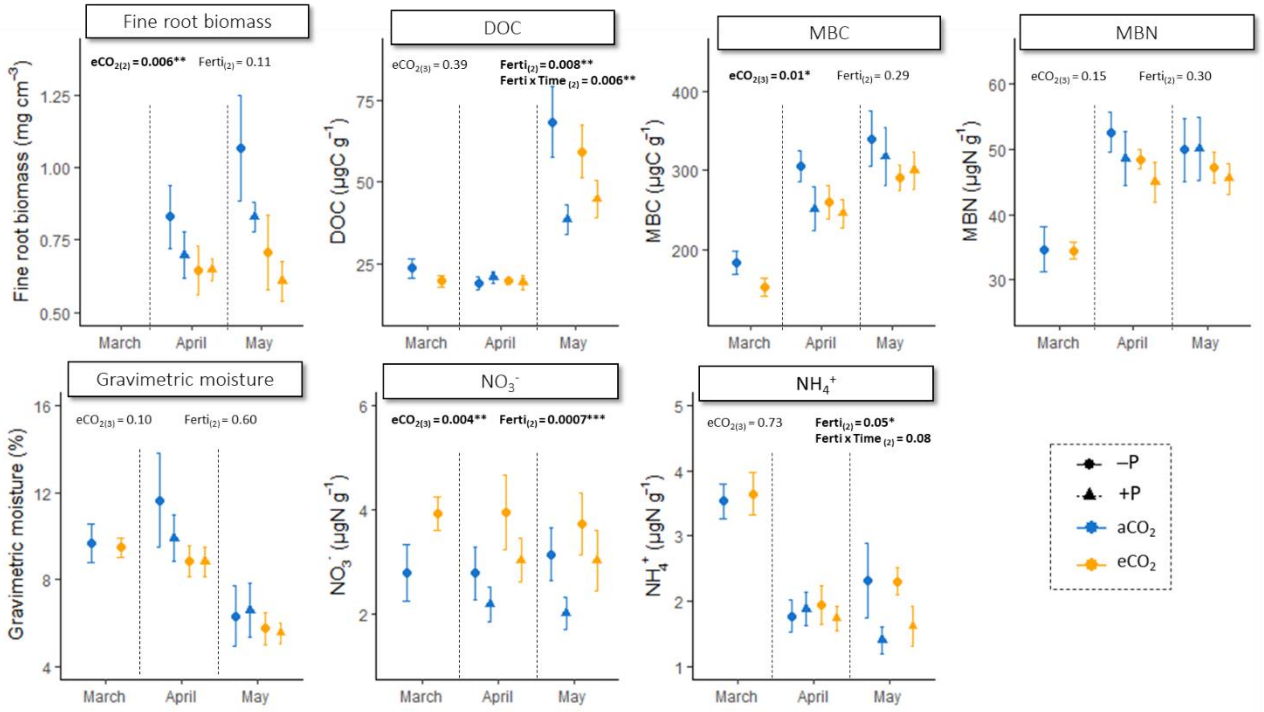

***Figure 5.3**: Fine root biomass, soil dissolved organic carbon (DOC), soil microbial biomass C (MBC) and N (MBN), gravimetric moisture and inorganic nitrogen content (NH_4^+ and NO_3^-) measured at three times: before fertilization (March), 10 days after fertilization (April) and two months after fertilization (May). ANOVA p-values for the effect of eCO_2 (eCO_2), fertilization (Ferti) and significant interactions are provided for each variable. Number in subscripts indicate the number of time points considered in the ANOVA. Data are means + SE (n=8).*

5.3.1.2. Nitrogen fluxes and enzyme activities

eCO_2 had no effect on N cycling rates or on enzyme activities. Gross mineralization and NH_4^+ immobilization rates were unaffected by eCO_2 but showed a strong effect of time, with gross mineralization and NH_4^+ immobilization rates being five times higher in March (Fig. 5.6). Gross depolymerization and FAA immobilization were approximatively ten times higher than mineralization rates. Microbial NUE was around 0.80 in March but very high (0.95) in April and May (Fig. 5.6). Out of the seven enzymes measured related to C, N and P metabolisms, none of them showed a significant effect of eCO_2 (Fig. 5.7) and were all positively correlated together (Fig. S5-6).

5.3.2. Effect of P fertilization

5.3.2.1. Nutrient pools and ratios

P addition increased P pools while decreasing most nutrients pools (DOC, NH_4^+, NO_3^-, FAA) in soil independently from eCO_2 effect. P addition increased soil Bray-P and MBP pool by 211% and 16%, respectively, after 10 days and by 195% and 27%, respectively, after two months ($p < 0.05$; Fig. 5.4). IER measurements showed a 14-fold difference in PO_4^{3-} concentration between unfertilized and fertilized plots (Fig. 5.2). Total soil P increased by ~ 8 µg g^{-1} of soil after fertilization, with 60% of this increase found in the microbial biomass (MBP) after 10 days and ~ 80% after 2 months (Fig. 5.4). MBC and MBN were not significantly increased by P fertilization leading to lower microbial biomass N:P and C:P ratios in fertilized plots ($p < 0.05$). Finally, soil DOC, ammonium and nitrate pools were significantly decreased by fertilization after two months, independently from eCO_2 effect (Fig. 5.3). Most of the effects of P fertilization were independent of eCO_2, expect for the microbial C:N ratio for which eCO_2 had a positive effect in P-fertilized plots but a negative effect in unfertilized plots ($p_{interaction} <$ 0.04).

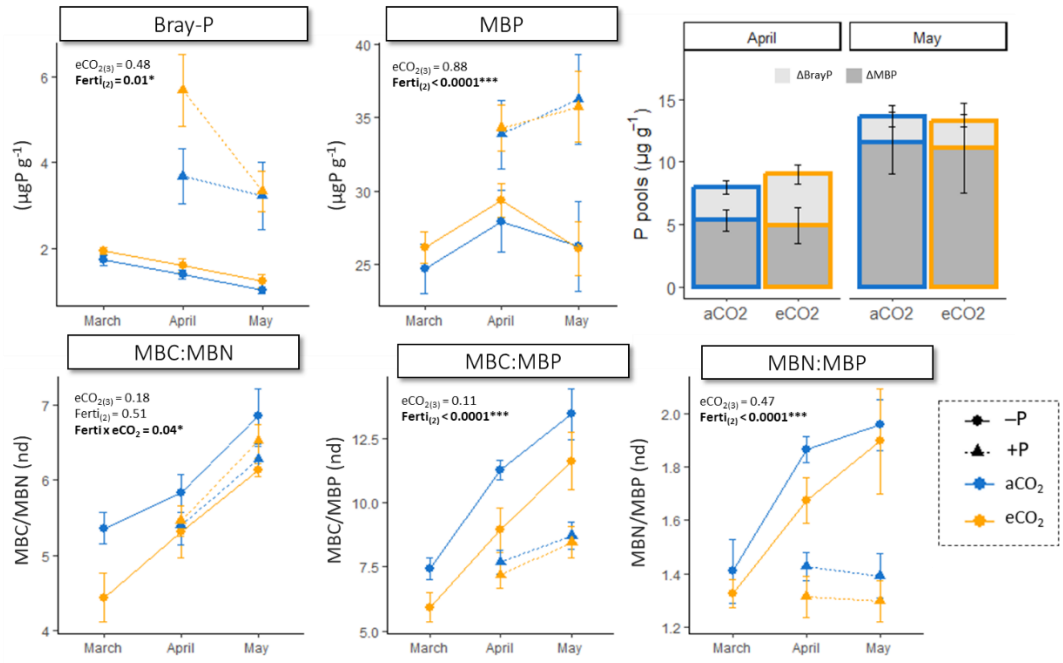

***Figure 5.4**: A) Bray-P concentration, microbial biomass P concentration at three collection times (means +SE). B) Difference in P pools between fertilized and unfertilized plots calculated per plot*

(ΔBray-P, ΔMBP). C) Microbial biomass ratios: C:N, C:P and N:P. ANOVA p-values for the effect of eCO_2 (eCO_2), fertilization (Ferti) and significant interactions are provided for each variable. Number in brackets indicate the number of time points considered in the ANOVA.

Compound specific analyses performed 10 days after fertilization and targeting 13 amino acids indicated a lower soil concentration of amino acids in P-fertilized plots ($p < 0.05$; Fig. 5.5). This lower total concentration in AA was observed in 7 out 13 amino acids (aspartic acid, glutamic acid, glycine, serine, threonine, tyrosine and valine). The rest of the amino acids were not affected by fertilization except for asparagine which was conversely higher in P-fertilized plots ($p = 0.09$; Fig. 5.5).

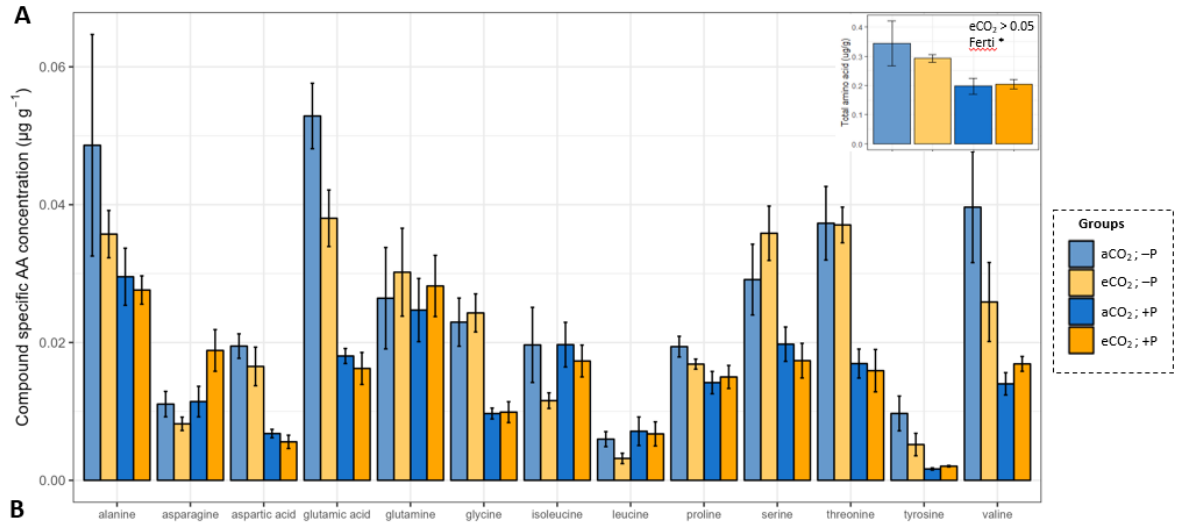

B

p	alanine	asparagine	aspartic acid	glutamic acid	glutamine	glycine	isoleucine	leucine	proline	serine	threonine	tyrosine	valine
eCO_2	> 0.05	> 0.05	> 0.05	> 0.05	> 0.05	> 0.05	> 0.05	> 0.05	> 0.05	> 0.05	> 0.05	> 0.05	> 0.05
Ferti	> 0.05	= 0.09	***	***	> 0.05	**	> 0.05	> 0.05	> 0.05	*	**	*	*

Figure 5.5: *A) Concentration of 13 amino acids in April and total of the 13 amino acids on the upper right part of the figure (data are means + SE). B) ANOVA test results where asterisk indicate level of significance for each amino acid.*

5.3.2.2. Nitrogen fluxes

P fertilization increased microbial N retention through opposing effects on N-mining and N immobilization. Gross mineralization rates were 13% lower in the P-fertilized plots in April and May ($p = 0.04$) while NH_4^+ immobilization was 27% higher ($p = 0.11$; Fig. 5.6). Consequently, microbial NH_4^+ retention (NH_4^+ immobilization : gross mineralization ratio) was significantly higher in P-fertilized plots, in line with lower NH_4^+ content. After 10 days, fertilization had no

detectable effect on gross depolymerization and FAA immobilization, but AA retention (FAA immobilization : depolymerization ratio) increased (p = 0.002). Two months post-fertilization, gross depolymerization and FAA immobilization decreased in P-fertilized plots, but only under aCO_2. Consequently, depolymerization and FAA immobilization were 14% higher under eCO_2 in P-fertilized plots (p > 0.05; Fig. 5.6). Despite this difference, microbial NUE remained unaffected as gross mineralization followed the same pattern but to a smaller extent.

Surprisingly, a similar pattern to bulk gross depolymerization in May was observed on total compound specific depolymerization in April (Fig. 5.7). Higher N depolymerization under eCO_2 in P-fertilized plots was mainly driven by higher alanine, glycine and glutamic acid production/immobilization rates (Fig. S5-4). However, compound specific rates revealed that several AA production and/or immobilization rates treatment decreased after P fertilization under both aCO_2 and eCO_2 (serine, threonine, valine, aspartic acid; Fig. S5-4) and few remained unaffected (proline, isoleucine, leucine; Fig. S5-4). The compound specific method accurately targeted 13 amino acids, representing approximately 50% of the bulk depolymerization rate.

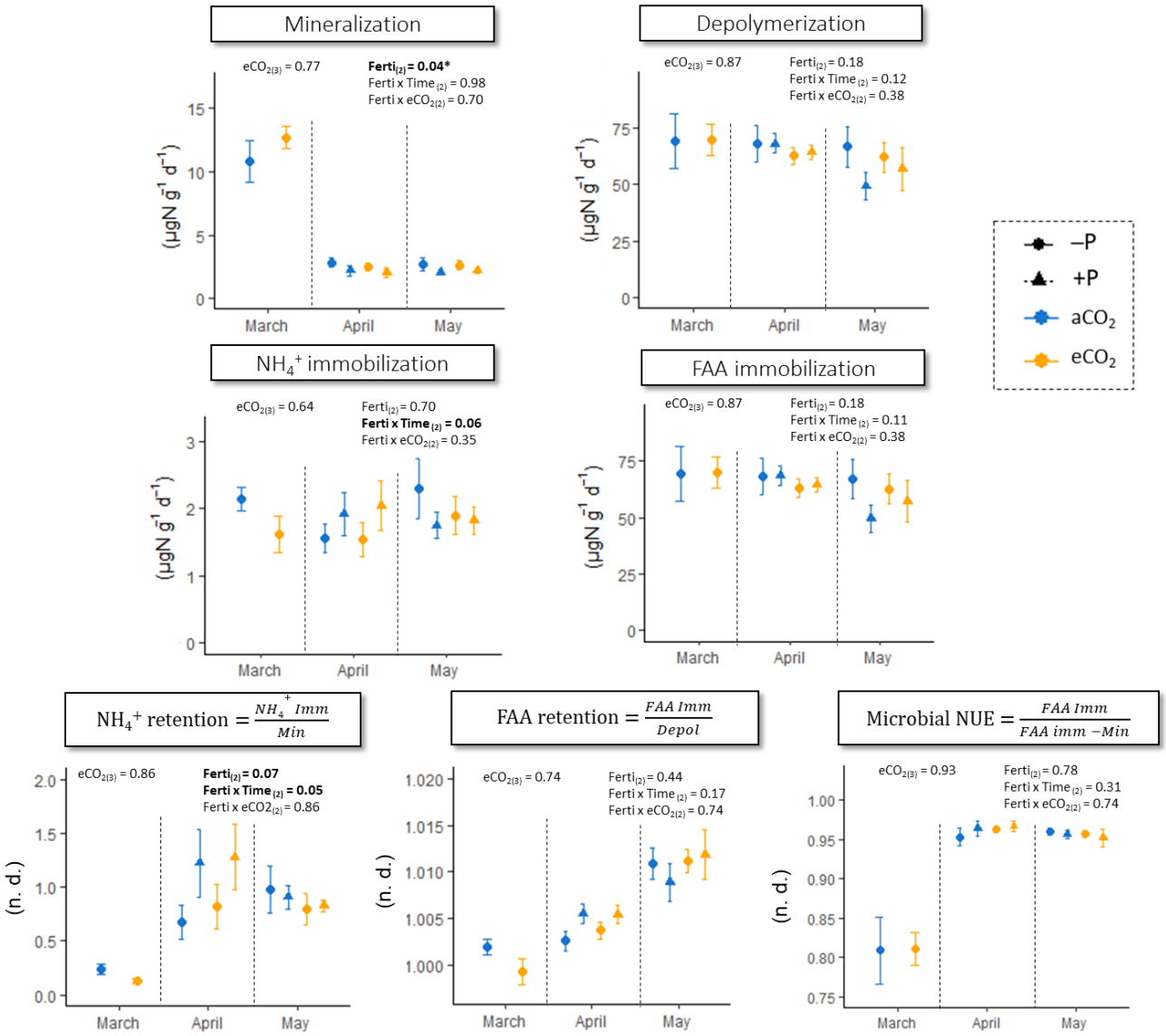

Figure 5.6: *Ammonium and amino acids production, immobilization, microbial retention and microbial N use efficiency (NUE) in P-fertilized (+P) and non-P-fertilized (-P) plots under aCO_2 (blue) and eCO_2 (yellow) in March, April and May. Data are means + SE (n=8). Min = Mineralization, Imm= Immobilization, Depol = Depolymerization and n.d. = non dimensional.*

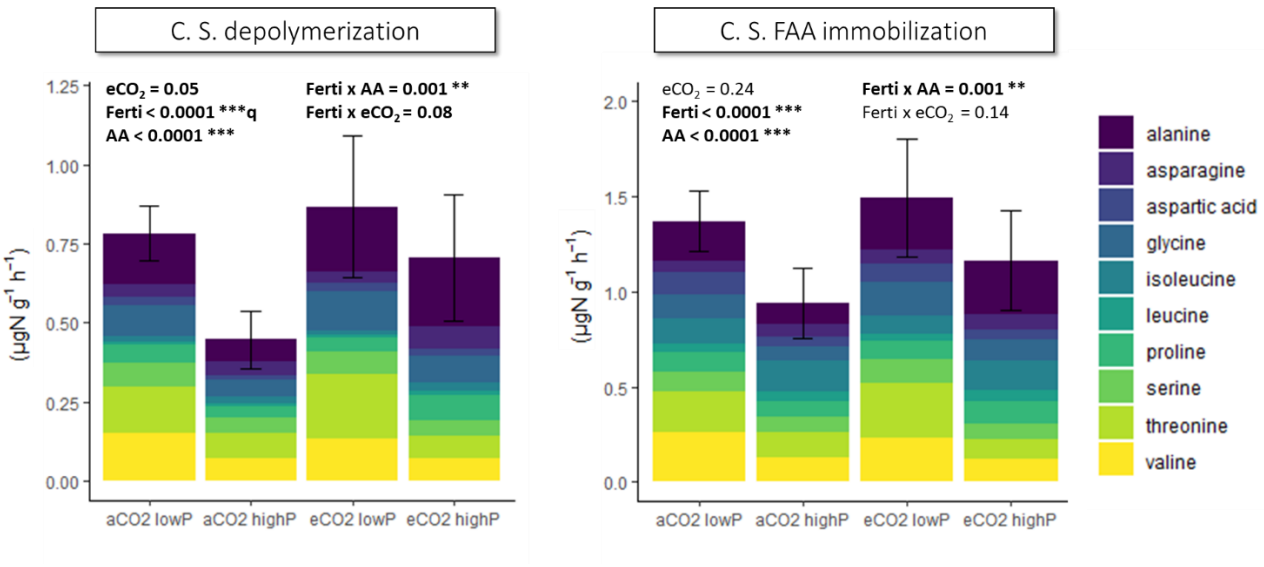

Figure 5.7: *Compound specific depolymerization and AA immobilization rates in April. Data are means + SE (n=4). C. S. = compound specific.*

5.3.2.3. *Enzyme activities*

P fertilization had no immediate effect on enzyme activities after 10 days; however, it reduced all seven enzyme activities after two months (Fig S5). N-targeting enzymes was reduced more strongly under eCO_2 (p = 0.08; Fig. 5.8). However, C-targeting enzymes (BG, Bxyl, AG, CB) were reduced more strongly under aCO_2 than eCO_2 (–79% under aCO_2 compared to –44% under eCO_2) with P-targeting enzyme (Pho) showing a similar pattern (–45% under aCO_2 compared to –30% under eCO_2). Microbial PUE decreased under P fertilization (p < 0.05) and varied over time, being lower in April compared to March and May. Microbial CUE increased with P fertilization, particularly after two months (Fig. 5.8).

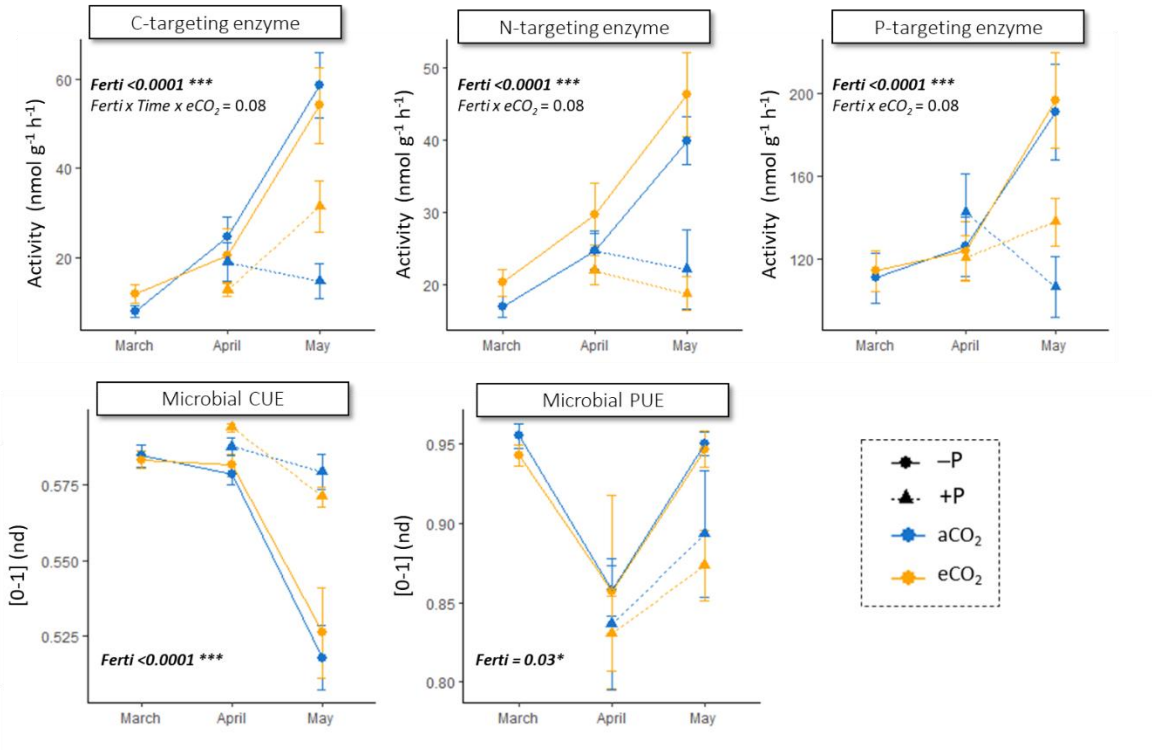

Figure 5.8: *Soil enzymatic activities associated with C (BG, AG, CB, Bxyl), N (NAG, LAP) and P (Pho) cycling before (April) and after P-fertilization (April and May) in P-fertilized (+P) and non-P-fertilized (-P) plots under aCO_2 and eCO_2. Data are means + SE (n=8).*

5.4. Discussion

5.4.1. eCO_2 increases soil nitrate pool in the top 10 cm

Nitrate concentration in soils increased under eCO_2, as shown by two-year ion-exchange resin (IER) measurements and three months of soil sampling. This aligns with the higher nitrate concentration during the first six months of the experiment (Hasegawa et al., 2016) and after five years in the upper soil layer (Pihlblad et al., 2023). These results suggest a persistent increase in nitrate concentration over 12 years, despite some seasonal variations (Andresen et al., 2020; Hasegawa et al., 2016). An accumulation of nitrate in soils was also observed after eight years of CO_2 treatment in a deciduous temperate forest (canopy FACE; Schleppi et al., 2012). In that same forest, the fine root biomass was also reduced under eCO_2 as detected in this experiment in the 0-10 cm layer. Hence a decrease in N uptake due to less root biomass in this horizon may explain the accumulation of nitrate under eCO_2. Nonetheless, it is important to note that previous studies at EucFACE found diverging effect of eCO_2 on root

biomass depending on soil depth, with a higher root biomass detected in the 10-30 cm soil layer (Piñeiro et al., 2020). Additionally, a shift was observed in the understorey community after three years of CO_2 enrichment, favouring C3 (N-rich) plants over C4 plants. This community shift may have enriched the soil with N via litter production (Hasegawa et al., 2018) and may have also contributed to change in root profile. Hence, a shift in plant community due to a stronger P limitation under eCO_2 may have prompted plants to explore deeper soil layers resulting in a faster production and/or accumulation of nitrates in the upper layer.

5.4.2. P fertilization reduce SOM and N availability

P fertilization induced a reduction of SOM decomposition, as evidenced by the decrease in all seven enzyme activities and N cycling rates, noticeable two months after P application. This suggests that microbial demand for P drives SOM decomposition under low P conditions (Rosinger et al., 2019)**.** This contrasts with several studies reporting an upregulation of C and N cycling after P fertilization as P availability may limit SOM decomposition (Castañeda-Gómez et al., 2022; Chen et al., 2016; Cheng et al., 2018; Cui et al., 2022). This discrepancy might be due to the dose of P applied in this experiment (1.75 kg ha^{-1}) which was lower than for those studies as it was chosen to be only sufficient to increase availability to all ecosystem components. Thus, the observed reduction in SOM decomposition with no specific difference between C, N or P targeting decomposition indicates a strong coupling of C, N and P cycling in soils due to substrate stoichiometry (Manzoni et al., 2021; Spohn, 2015).

Moreover, P fertilization increased microbial CUE and N retention suggesting a more efficient recycling of C and N, while it decreased microbial PUE. Increased CUE suggests that reducing P limitation allowed microorganisms to allocate more C to microbial growth rather than P acquisition (X. Wang et al., 2022). In contrast, NUE was not affected by P fertilization but microbial NH_4^+ and FAA retention increased with P fertilization, aligning with enhanced N retention reported in previous studies (Mehnaz et al., 2019; R. Wang et al., 2022). Higher N retention limited N release for plants as it was observed by lower soil N availability. Contrary to our second hypothesis, P fertilization reduced N mineralization and depolymerization and

increased microbial N retention. Thus, P fertilization may lead to reduced N availability in soils on the long term due to decreased SOM decomposition, increased microbial N retention, and increased plant uptake. Thus, long-term changes in N availability after P fertilization may elicit changes in the response of trees to eCO_2 that might not be detectable in the short term (Terrer et al., 2018).

5.4.3. Faster nutrient cycling under eCO_2 after P addition

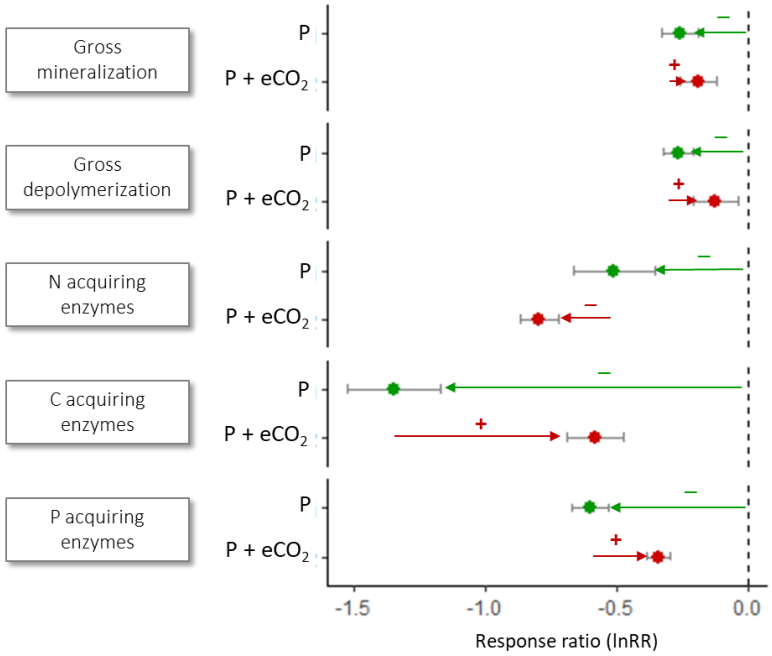

Figure 5.9: *Response ratio (lnRR) indicating the effect of P addition (P) and eCO_2 in P-fertilized plots (P + eCO_2) compared to the average between aCO_2 and eCO_2 under no fertilization in May. Green and red arrows represent the direction of P-addition and eCO_2 effects respectively for each variable where a ─ represent a negative effect and a + represent a positive effect.*

As discussed earlier, nutrient cycling slowed down after P fertilization. However, this effect was partly offset under eCO_2. In P-fertilized plots, C and P-targeting enzyme activities as well as protein depolymerization rates were higher under eCO_2 compared to aCO_2 (Fig. 8). Interestingly, the initially lower microbial C:N ratio under eCO_2 reversed after P addition. These findings suggest that despite the dampening effect of P addition on SOM decomposition, P addition enabled the ecosystem to enhance C cycling under eCO_2. This likely led to increased C immobilization and increased microbial C:N ratio. Phosphatase activity followed the same

pattern as C-acquiring enzymes, indicating a coupling between C and P cycling when P is sufficient as observed in Castañeda-Gómez et al. (2022). Hence, the enzyme responses under eCO_2 might have also been driven by P demand. The modest P addition (1.75 kg P ha^{-1}) likely only reduced P limitation without alleviating it, especially for plants given that ~ 70% of the P is locked away in the microbial biomass, and microbial competition for P is fierce in this ecosystem (Jiang et al., 2024). This would imply that reducing P limitation allowed eCO_2 to stimulate P cycling, as it was observed the first six months of CO_2 enrichment (Hasegawa et al., 2016).

Furthermore, the increase in protein depolymerization and AA immobilization rates (i.e. glycine, alanine and glutamic acid rates) under eCO_2 after P addition can be driven by an increase in C or N demand as AA serve as both C and N sources for microbes (Adour et al., 2006; Aliashkevich et al., 2018; Geisseler and Horwath, 2014). Increased C demand would support the observed enzymatic responses. Conversely, increased N demand was expected in this experiment, particularly given the higher microbial N retention and reduced organic and inorganic N availability following P addition. However, there was no other strong evidence indicating an increase in microbial N demand under eCO_2, thus preventing a definite conclusion on a shift towards N limitation. A longer time scale is needed for the ecosystem to acclimate to greater P availability and increases growth under eCO_2, which should theoretically exacerbate N demand. Despite this, the observed interactive effects between P fertilization and eCO_2 over just two months are encouraging. It suggests that the ecosystem may quickly respond to eCO_2 once P limitation is alleviated or just reduced.

5.5. Conclusion

This study highlights that alleviating/reducing P limitation in this Eucalyptus forest soil reduces SOM decomposition and increase C and N retention in the microbial biomass, potentially limiting N supply in the long term. P fertilization also initiated a response of the ecosystem to eCO_2 over just two months, enhancing soil C-N-P cycling. However, identifying the primary limiting nutrient after P addition is challenging due to strong C-N-P coupling in this system. A

longer time scale and possibly repeated P additions are needed for plants to acclimate to greater P availability and to let the time for N limitation to manifest under eCO_2.

5.6. Supplementary materials

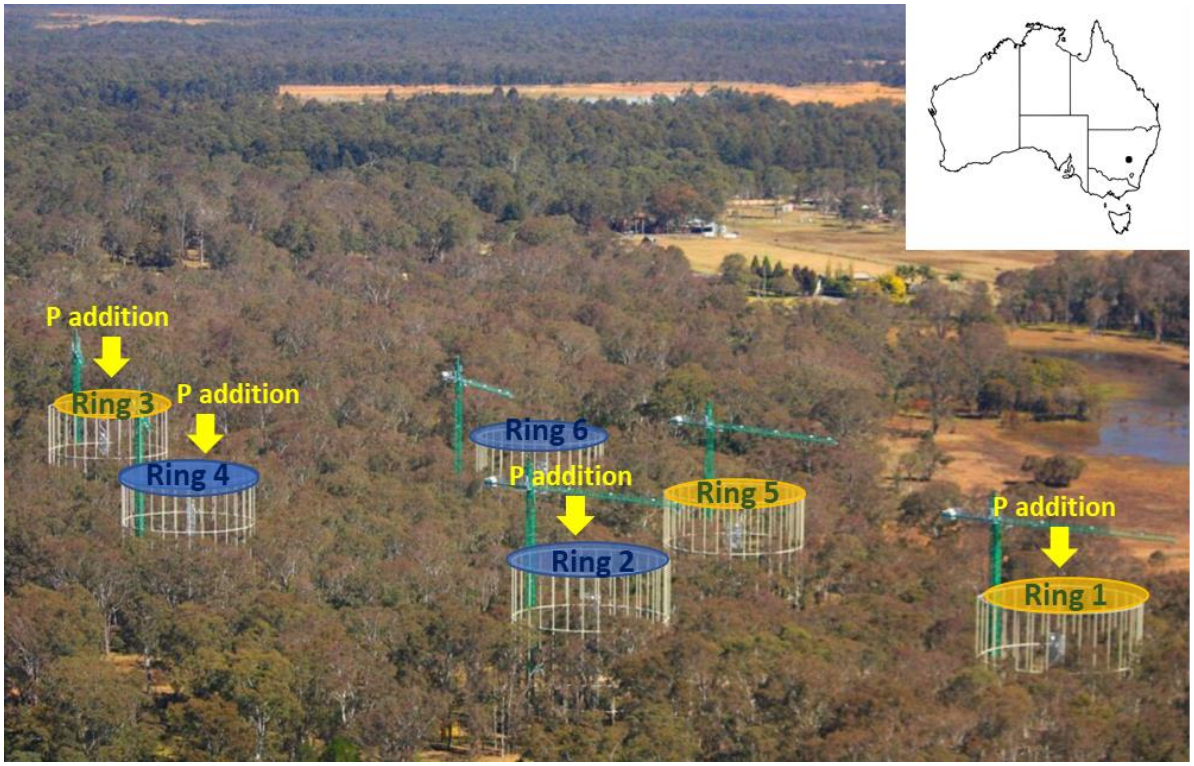

Figure S 5-1*: Schematic of EucFACE experimental design where aCO_2 ring are represented in orange and eCO_2 ring are in blue. Rings that received P addition in April are pointed with a yellow arrow.*

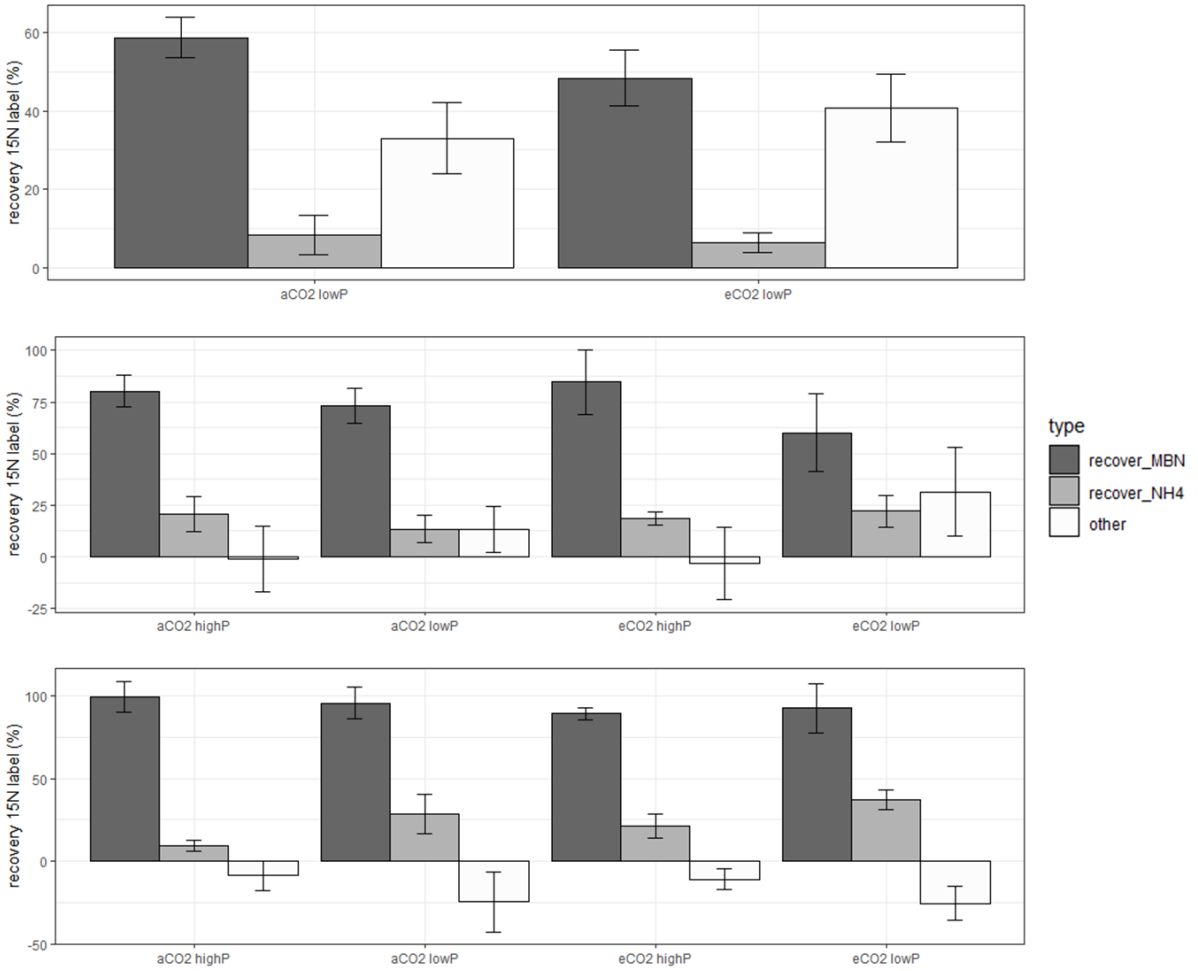

Figure S 5-2: *15N label recovery in the microbial biomass N (recovery_MBN) and in the ammonium pool (recover_NH4). The resulting balance (i.e. transfer in other pools or errors) is indicated by the white bar (other).*

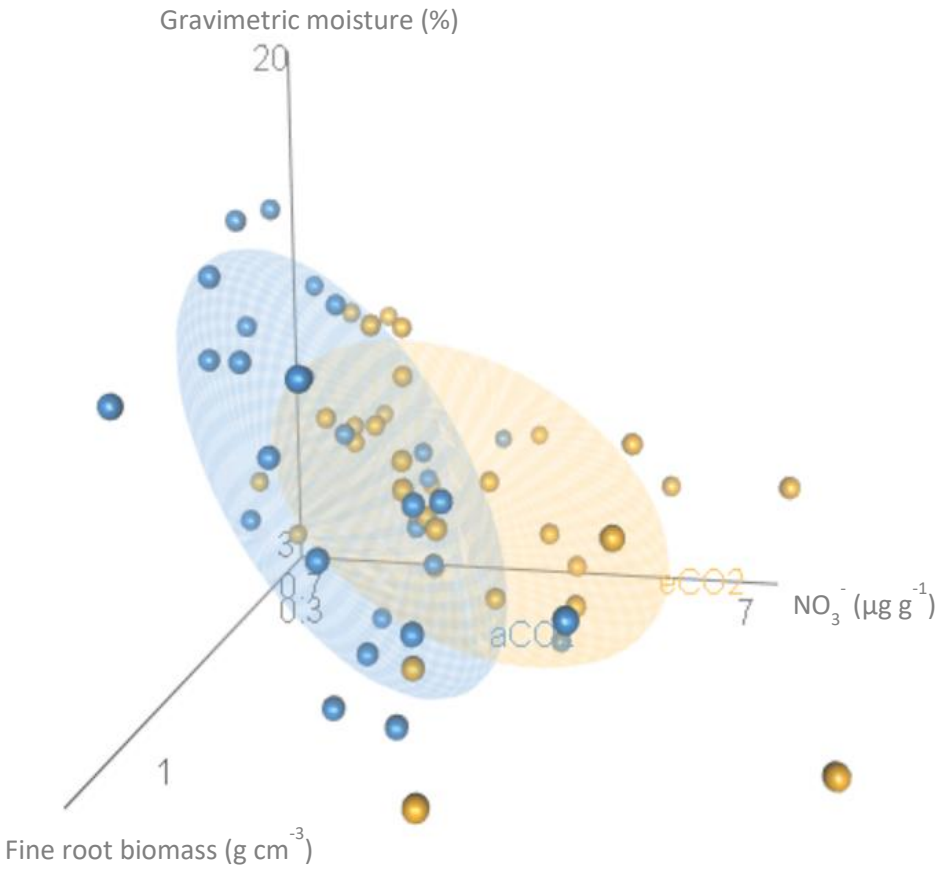

Figure S 5-3: *3D scatterplot representing the distribution of the samples according to gravimetric moisture, nitrate content and fine root biomass.*

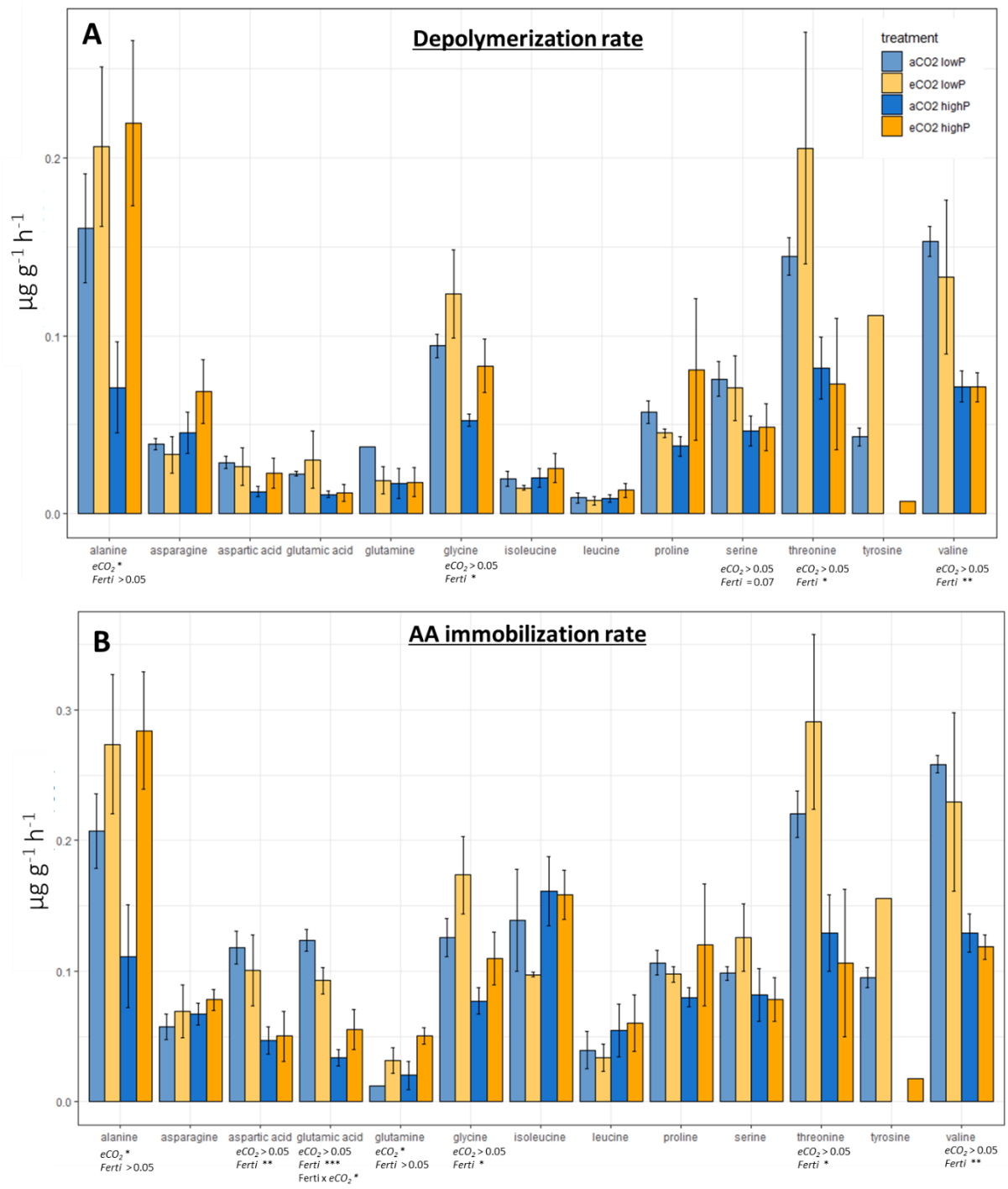

Figure S 5-4: *Compound specific depolymerization and amino acid uptake rate 10 days after P-fertilization (April) under aCO_2 (blue) and eCO_2 (orange) and in P-fertilized (clear tone) and non-P-fertilized plots (darker tone). Data are means +SE (n=4). P-value associated with the effect of eCO_2 and P-fertilized for each amino acid are indicated below the plots.*

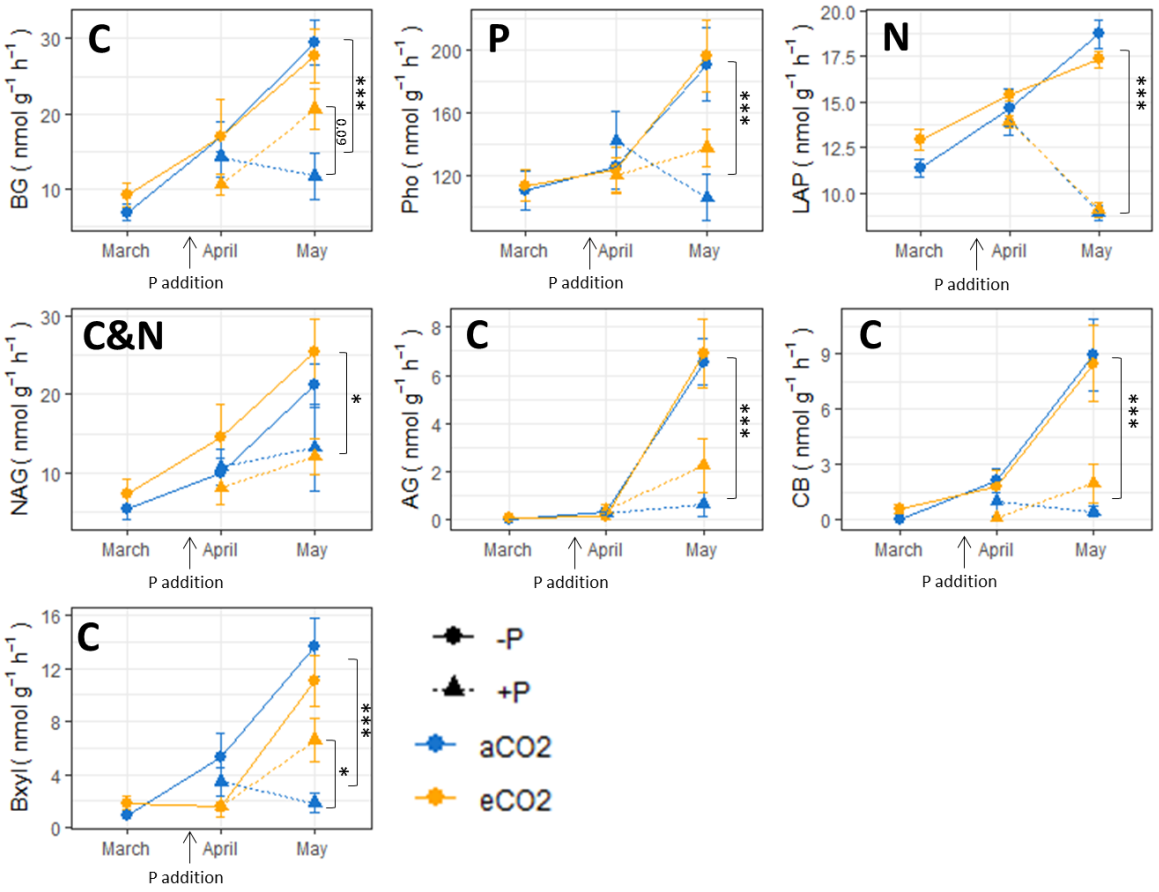

Figure S 5-5: *Soil enzymatic activities associated with C (BG, AG, CB, Bxyl), N (NAG, LAP) and P (Pho) cycling before (April) and after P-fertilization (April and May) in P-fertilized (+P) and non-P-fertilized (-P) plots under aCO_2 and eCO_2. Data are means + SE (n=8).*

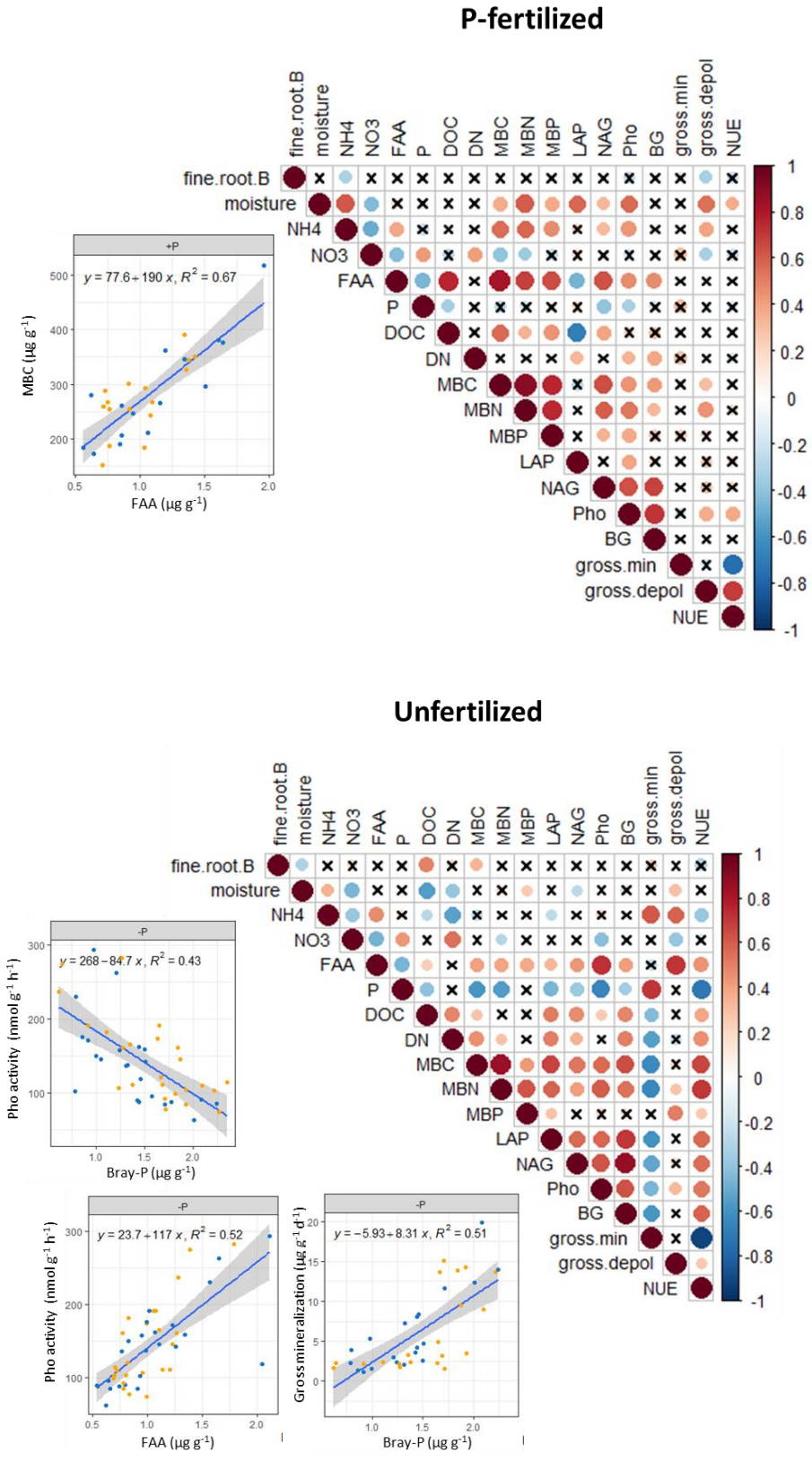

***Figure S 5-6**: Correlation matrix showing Pearson correlation between all variables in P-fertilized plots and unfertilized plots. A cross indicate a non-significant correlation while red and blue circles indicate a positive and negative correlation respectively.*

Chapter 6.Conclusion and outlook

6.1. Aims and hypothesis

The aims of this research were to identify the mechanisms by which forest ecosystems may stimulate N availability under eCO_2, understand the interactions between C, N and P cycling and provide grounded and *in situ* experimental data when possible to predict future nutrient constraints in mature forests. In this research, we combined *in-situ*, long-term measurements (Chap 2 and 5) with mechanistic studies in the laboratory (Chap 3 and 4) to successfully reached our aims.

The key scientific questions addressed in this research were:

1. **Does eCO_2 increase C allocation belowground?**

BIFoR-FACE	
EucFACE	

At BIFoR-FACE, there was clear evidence of increased C allocation belowground, demonstrated by the observed increase in soil DOC, MBC pools and root biomass. This was further supported by the doubling of the root C exudation rate (Norby et al., 2024). In contrast, no such evidence was found at EucFACE as root biomass and MBC were lower under eCO_2 in the top 10 cm layer. These results are surprising, especially given the higher C uptake by trees that was assumed to be allocated belowground (Jiang et al., 2020). However, if 50% the C from exudation is respired in soil as suggested in Jiang et al. (2020), it might explain the lack of effect on soil C pools. Nonetheless it raises the question: where does the rest of the C go, and what is its role in nutrient availability? One hypothesis is that this C may be allocated to deeper soil layers, but this remains to be confirmed.

2. Are N supplies via N fixation and mineralization fluxes enhanced under eCO_2?

BIFoR-FACE	N fixation	
	N mineralization	
EucFACE	N fixation	
	N mineralization	

At BIFoR-FACE, N fixation was unaffected by eCO_2 despite the higher C availability belowground. Likely, N fixation in soils was suppressed by the high Nr atmospheric deposition at site (~ 16 kg ha^{-1} y^{-1}) as evidenced by spatial variations in N fixation rates. However, N supplies via N mineralization were enhanced under eCO_2. Both gross and net mineralization methods point toward an increase in net mineralization of ~26 kg N ha^{-1} y^{-1} in 2022, meeting the higher tree N demand estimated at ~ 10 kgN ha^{-1} y^{-1} that year. At EucFACE, N fixation was not measured but N mining via mineralization and protein depolymerization remained largely unaffected by eCO_2. This suggests that the increase soil respiration at site (Jiang et al., 2020) does not result from N-mining but rather from P-mining or from degradation of exudate compounds.

3. Does increased C availability belowground under eCO_2 enhance nitrification and denitrification leading to greater N losses?

BIFoR-FACE	
EucFACE	

At BIFoR-FACE, despite higher dissolved organic C and N under eCO_2, nitrification was suppressed, especially in the rhizosphere. Multiple lines of evidence from Chapters 2 and 4 support the statement that eCO_2 has an indirect effect on nitrification via the negative effect of increased root biomass on nitrification. However, eCO_2 had no measurable effect on N_2O emissions or on the partitioning of N_2O from nitrification and denitrification. Interestingly, in laboratory incubations, N_2O emissions from sieved soil were almost always upregulated (Sgouridis et al., 2023), whereas there was no effect on rhizosphere soil or on intact soil cores. These findings suggest a mitigating effect of root biomass on N_2O emissions, although the data do not confirm a reduction in atmospheric N losses. Therefore, this study was unable to fully constrain the effects of eCO_2 on N losses, which would require continuous measurements of N_2O emissions and N leaching.

At EucFACE, we did not measure nitrification or dentification rates, however, we observed an accumulation of nitrates in the soils at various times. Nonetheless, it remains unclear if higher nitrate concentrations stem from higher nitrification activity, lower nitrate uptake or lower N losses via denitrification or leaching.

4. What mechanisms are behind the response of N cycling to eCO_2?

At BIFoR FACE, eCO_2 altered N cycling through two main pathways. First, by increasing root biomass, it stimulated gross ammonification by expanding rhizosphere area, where ammonification is ten times faster. Increased root biomass also suppressed nitrification by reducing nitrification hotspots, where nitrifying bacteria do not compete with root uptake, and by enlarging the area affected by biological nitrification inhibitors released as exudates. Second, by increasing the exudate C:N ratio, eCO_2 shifted microbial nutrient acquisition from “preferential substrate utilization” to an “N-mining strategy” stimulating as well gross ammonification.

5. Is the N response to eCO_2 consistent among ecosystems with different nutrient limitation status?

This research together with other findings at these two sites indicate that neither N nor P limited photosynthesis activity. However, P scarcity at EucFACE appeared to have prevented the extra C taken up to be stored as biomass. Despite the enhancement in nutrient cycling and availability detected six months into CO_2 enrichment at EucFACE (Hasegawa et al., 2016), nutrient cycling was not affected ten years into CO_2 enrichment. But the faster nutrient cycling initiated under eCO_2, two months after P fertilization, confirm that strong P scarcity at EucFACE prevent the ecosystem to respond to eCO_2. In contrast, at BIFoR-FACE, only a portion of the extra C taken-up by trees is allocated belowground as root biomass and C exudation. This effectively influences the N cycle by enhancing N-mining and downregulating N losses, thereby meeting the higher N demand and allowing C storage in biomass (Fig. 6.1).

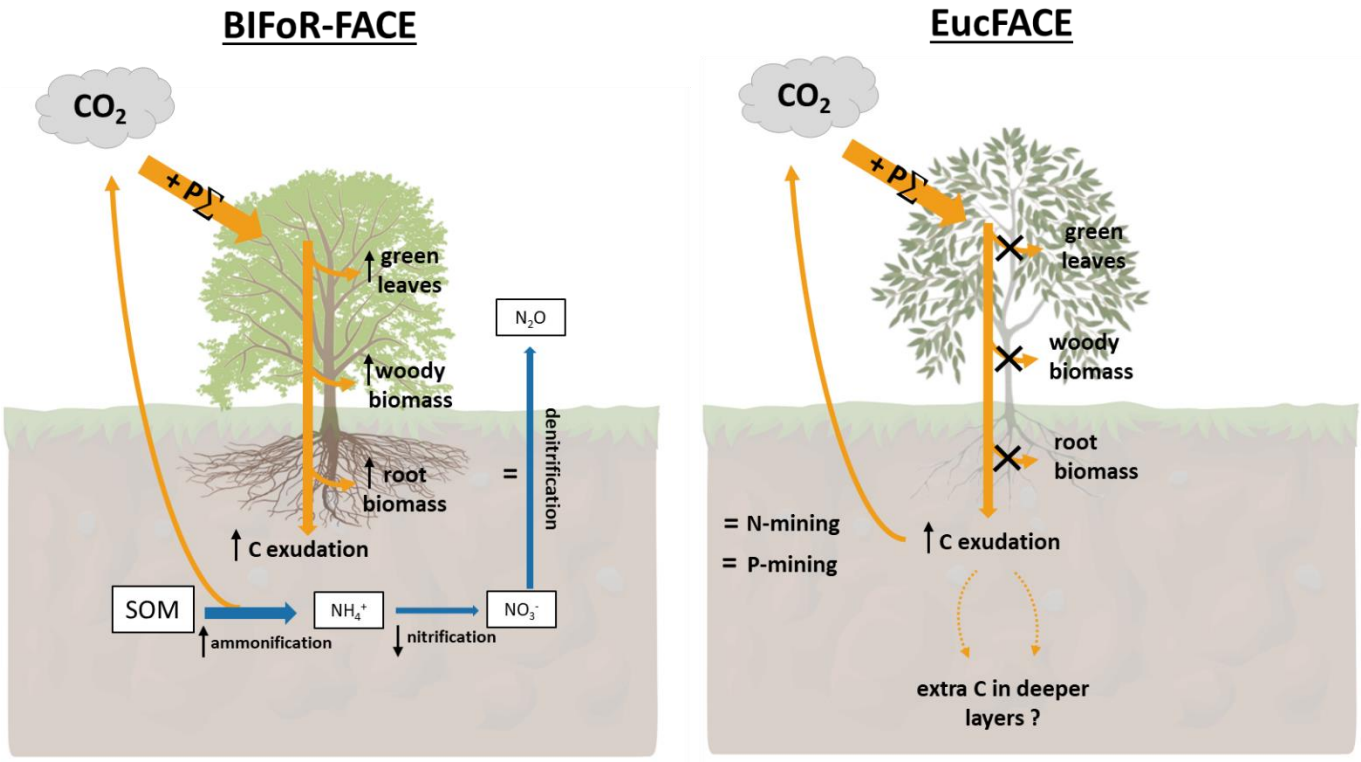

Figure 6.1: *Conceptual representation of C allocation and feedback on nutrient cycling between at BIFoR-FACE and EucFACE.*

Thus, this research highlights the divergence in the response of the two temperate forests to eCO_2 enrichment. Few reasons may explain the divergence observed regarding tree growth, C allocation and N cycling. The primary hypothesis is that ecosystem responses depend on

the limiting nutrient. N-limited ecosystems appear to be more responsive to eCO_2 due to tree's ability to influence the N cycle through soil-plant interactions while P availability is mainly controlled by abiotic factors (Dijkstra et al., 2013). However, the degree of nutrient limitation may also play a crucial role (Fig. 6.2). At BIFoR-FACE, N limitation may only hinder optimal growth without creating an intense competition between trees and microbes, as 200 years of high Nr atmospheric deposition have partially alleviated N constraint (Tipping, 2017). Conversely, trees at EucFACE experienced severe P limitation. This difference in the degree of limitation may explain why, after six years of CO_2 enrichment, plant-soil interactions (i.e., the trade-off of C for N) sustained higher productivity at BIFoR-FACE while a C to P trade-off at EucFACE was initiated but diminished six months into the experiment. This suggests that the nature and extent of nutrient limitations critically influence the long-term responses of forest ecosystems to eCO_2. Future research at the Amazon FACE facility, located in a P-limited forest, should help understanding if the diverging response between BIFoR-FACE and EucFACE is only driven by the difference in the limiting nutrient or if other factors may be at play.

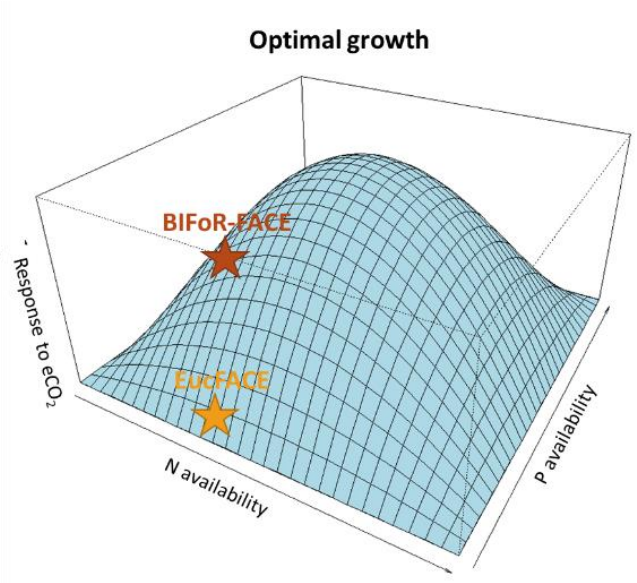

Figure 6.2: *Conceptual diagram representing the growth response of trees depending on N and P availability. EucFACE is located on severely low P soil constraining plant growth while BIFoR-FACE is located on low N soils only preventing optimal growth.*

6.2. Limitation and future work

One of the main questions emerging from this research is the soil C cost associated with this N-mining enhancement at BIFoR-FACE. According to Terrer et al. (2021), increased aboveground growth can negatively impact soil C stocks due to soil nutrient mining. BIFoR-FACE appears to fit in this scenario, where N-mining is linked to higher soil respiration, potentially offsetting 30% of the increased NPP. However, this estimation is subject to several critical considerations. First, microbial respiration may have been enhanced by the addition of a ^{15}N label and thus does not accurately represent basal respiration. Secondly, heterotrophic respiration may be underestimated due to root cutting. Therefore, more accurate estimations of soil respiration and partitioning of autotrophic and heterotrophic respiration are needed. Additionally, to understand the effect of N-mining on soil C storage, further research is required to identify which SOM pools are being targeted. Shifts in enzyme activities in the rhizosphere suggested that easily degradable pools are prioritized. Confirming this with confidence will necessitates to conduct labelling experiments coupled with C fractionation assessments.

Additionally, constraining the effect of eCO_2 on soil total C has proven challenging. From the start of the experiment, soil total C was 50% higher under eCO_2, likely due to an initial spatial effect (Sgouridis et al., 2023). After six years of CO_2 enrichment, soil total C was 20% higher under eCO_2 but, measurements were not performed exactly on the same layer of soil (different depths) to confirm that the initial enhancement decreased over time. However, lower total C in the rhizosphere also points toward a negative effect of eCO_2 on total C due to higher priming. Thus, continuous assessments of total C in bulk and rhizosphere soils are needed to identify the trajectory of eCO_2's effect on soil C. In addition, precise assessments of SOM pools and stability, using C fractionation methods and chemical structure assessments with spectroscopy or nuclear magnetic resonance methods, could also be crucial indicators to assess the effect of eCO_2 on soil C stocks.

Another question emerging from this study is the effect of eCO_2 on soil water, which is an essential regulator of nutrient cycling. Although initial assumptions about tree physiological

response assumed an increase in water use efficiency leading to higher soil water content eCO_2 (Medlyn et al., 2001; Schäfer et al., 2002). Evidence from both FACE experiments, particularly BIFoR-FACE, indicated the opposite response. This can be explained by higher aboveground water storage and higher canopy transpiration under eCO_2 that reduced soil water content (Donohue et al., 2017; Gardner et al., 2023; Medlyn et al., 2001; Tor-ngern et al., 2015; Uddling et al., 2009; Ward et al., 2018). Water-use efficiency was also not found to be affected by eCO_2 confirming that initial assumptions may be inaccurate in mature forests (Mayoral et al., *in prep*). At BIFoR-FACE, a relatively humid forest, this effect was only detectable in the summer (summer 2022), supporting that higher aboveground water storage might drive this phenomenon. Due to the pivotal role of soil water content in nutrient availability and C storage, it is imperative to revisit initial assumptions regarding the water budget under eCO_2. This is especially crucial as eCO_2 effects on water availability may be a consistent response observed across ecosystems.

While this research attempt to elucidate how changes in exudate quantity and composition affect N dynamics, we did not examine the exact composition of root exudates to detect if any secondary metabolites may be released in higher concentrations. For instance, we found an inhibitory effect of tree roots under eCO_2 on nitrification, suggesting that biological nitrification inhibitors may be released in higher concentrations under eCO_2 as a strategy to compete for ammonium and conserve N. Confirming this hypothesis would require sampling oak root exudate solutions and analysing them for metabolites. Such analysis is challenging but could significantly advance our understanding of the modulation of plant-soil interactions in the context of climate change or nutrient limitations.

References

Adour, L., Aziza, M., Couriol, C., Amrane, A., 2006. Amino acids as carbon, energy and nitrogen sources for *Penicillium camembertii*. J. Chem. Technol. Biotechnol. 81, 573–579. https://doi.org/10.1002/jctb.1431

Aliashkevich, A., Alvarez, L., Cava, F., 2018. New Insights Into the Mechanisms and Biological Roles of D-Amino Acids in Complex Eco-Systems. Front. Microbiol. 9, 683. https://doi.org/10.3389/fmicb.2018.00683

Amann, M., Kiesewetter, G., Schöpp, W., Klimont, Z., Winiwarter, W., Cofala, J., Rafaj, P., Höglund-Isaksson, L., Gomez-Sabriana, A., Heyes, C., Purohit, P., Borken-Kleefeld, J., Wagner, F., Sander, R., Fagerli, H., Nyiri, A., Cozzi, L., Pavarini, C., 2020. Reducing global air pollution: the scope for further policy interventions. Philos. Trans. R. Soc. Math. Phys. Eng. Sci. 378, 20190331. https://doi.org/10.1098/rsta.2019.0331

Ambus, P., Robertson, G.P., 1999. Fluxes of CH4 and N2O in aspen stands grown under ambient and twice-ambient CO2. Plant Soil 209, 1–8. https://doi.org/10.1023/A:1004518730970

Anderson, T., Domsch, K., 1993. The metabolic quotient for CO2 (qCO2) as a specific activity parameter to assess the effects of environmental conditions, such as ph, on the microbial biomass of forest soils. Soil Biol. Biochem. 25, 393–395. https://doi.org/10.1016/0038-0717(93)90140-7

Andresen, L.C., Carrillo, Y., Macdonald, C.A., Castañeda-Gómez, L., Bodé, S., Rütting, T., 2020. Nitrogen dynamics after two years of elevated CO2 in phosphorus limited Eucalyptus woodland. Biogeochemistry 150, 297–312. https://doi.org/10.1007/s10533-020-00699-y

Andrianarisoa, K.S., Zeller, B., Poly, F., Siegenfuhr, H., Bienaimé, S., Ranger, J., Dambrine, E., 2010. Control of nitrification by tree species in a common-garden experiment. Ecosystems 13, 1171–1187. https://doi.org/10.1007/s10021-010-9390-x

Anthony, M.A., Crowther, T.W., Van Der Linde, S., Suz, L.M., Bidartondo, M.I., Cox, F., Schaub, M., Rautio, P., Ferretti, M., Vesterdal, L., De Vos, B., Dettwiler, M., Eickenscheidt, N., Schmitz, A., Meesenburg, H., Andreae, H., Jacob, F., Dietrich, H.-P., Waldner, P., Gessler, A., Frey, B., Schramm, O., Van Den Bulk, P., Hensen, A., Averill, C., 2022. Forest tree growth is linked to mycorrhizal fungal composition and function across Europe. ISME J. 16, 1327–1336. https://doi.org/10.1038/s41396-021-01159-7

Armstrong, A., Ullah, S., Hamilton, L., Vanguelova, E., Morecroft, M., Basiliko, N., MacKenzie, R., McNamara, N., Douwes Dekker, N., 2024. Flux of CO2, CH4 and N2O from temperate woodland soil under elevated CO2. https://doi.org/10.5194/egusphere-egu24-16689

Bais, H.P., Weir, T.L., Perry, L.G., Gilroy, S., Vivanco, J.M., 2006. The role of root exudates in rhizosphere interactions with plants and other organisms. Annu. Rev. Plant Biol. 57, 233–266. https://doi.org/10.1146/annurev.arplant.57.032905.105159

Barnard, R., Leadley, P.W., Hungate, B.A., 2005. Global change, nitrification, and denitrification: A review. Glob. Biogeochem. Cycles 19. https://doi.org/10.1029/2004GB002282

Bates, D., Mächler, M., Bolker, B., Walker, S., 2015. Fitting linear mixed-effects models using lme4. J. Stat. Softw. 67. https://doi.org/10.18637/jss.v067.i01

Berntson, G.M., Bazzaz, F.A., 1997. Regenerating temperate forest mesocosms in elevated CO 2 : belowground growth and nitrogen cycling. Oecologia 113, 115–125. https://doi.org/10.1007/s004420050359

Berthrong, S.T., Yeager, C.M., Gallegos-Graves, L., Steven, B., Eichorst, S.A., Jackson, R.B., Kuske, C.R., 2014. Nitrogen Fertilization Has a Stronger Effect on Soil Nitrogen-Fixing Bacterial Communities than Elevated Atmospheric CO $_2$. Appl. Environ. Microbiol. 80, 3103–3112. https://doi.org/10.1128/AEM.04034-13

Bottomley, P.J., Taylor, A.E., Myrold, D.D., 2012. A consideration of the relative contributions of different microbial subpopulations to the soil N cycle. Front. Microbiol. 3. https://doi.org/10.3389/fmicb.2012.00373

Bradford, M.A., Keiser, A.D., Davies, C.A., Mersmann, C.A., Strickland, M.S., 2013. Empirical evidence that soil carbon formation from plant inputs is positively related to microbial growth. Biogeochemistry 113, 271–281. https://doi.org/10.1007/s10533-012-9822-0

Brookes, P.C., Landman, A., Pruden, G., Jenkinson, D.S., 1985. Chloroform fumigation and the release of soil nitrogen: A rapid direct extraction method to measure microbial biomass nitrogen in soil. Soil Biol. Biochem. 17, 837–842. https://doi.org/10.1016/0038-0717(85)90144-0

Brooks, P.D., Stark, J.M., McInteer, B.B., Preston, T., 1989. Diffusion Method To Prepare Soil Extracts For Automated Nitrogen-15 Analysis. Soil Sci. Soc. Am. J. 53, 1707–1711. https://doi.org/10.2136/sssaj1989.03615995005300060016x

Brunn, M., Hafner, B.D., Zwetsloot, M.J., Weikl, F., Pritsch, K., Hikino, K., Ruehr, N.K., Sayer, E.J., Bauerle, T.L., 2022. Carbon allocation to root exudates is maintained in mature temperate tree species under drought. New Phytol. 235, 965–977. https://doi.org/10.1111/nph.18157

Carney, K.M., Hungate, B.A., Drake, B.G., Megonigal, J.P., 2007. Altered soil microbial community at elevated CO_2 leads to loss of soil carbon. Proc. Natl. Acad. Sci. 104, 4990–4995. https://doi.org/10.1073/pnas.0610045104

Carrillo, Y., Dijkstra, F., LeCain, D., Blumenthal, D., Pendall, E., 2018. Elevated CO_2 and warming cause interactive effects on soil carbon and shifts in carbon use by bacteria. Ecol. Lett. 21, 1639–1648. https://doi.org/10.1111/ele.13140

Carrillo, Y., Dijkstra, F.A., Pendall, E., LeCain, D., Tucker, C., 2014. Plant rhizosphere influence on microbial C metabolism: the role of elevated CO2, N availability and root stoichiometry. Biogeochemistry 117, 229–240. https://doi.org/10.1007/s10533-014-9954-5

Castañeda-Gómez, L., Powell, J.R., Pendall, E., Carrillo, Y., 2022. Phosphorus availability and arbuscular mycorrhizal fungi limit soil C cycling and influence plant responses to elevated CO2 conditions. Biogeochemistry 160, 69–87. https://doi.org/10.1007/s10533-022-00939-3

Chari, N.R., Taylor, B.N., 2022. Soil organic matter formation and loss are mediated by root exudates in a temperate forest. Nat. Geosci. 15, 1011–1016. https://doi.org/10.1038/s41561-022-01079-x

Chari, N.R., Tumber-Dávila, S.J., Phillips, R.P., Bauerle, T.L., Brunn, M., Hafner, B.D., Klein, T., Obersteiner, S., Reay, M.K., Ullah, S., Taylor, B.N., 2024. The global root exudate carbon flux. https://doi.org/10.1101/2024.02.01.578470

Chen, R., Senbayram, M., Blagodatsky, S., Myachina, O., Dittert, K., Lin, X., Blagodatskaya, E., Kuzyakov, Y., 2014. Soil C and N availability determine the priming effect: microbial N mining and stoichiometric decomposition theories. Glob. Change Biol. 20, 2356–2367. https://doi.org/10.1111/gcb.12475

Chen, Y., Sun, T.-T., Qian, H.-Y., Fan, J.-B., He, Y.-Q., Sun, B., 2016. Nitrogen mineralization as a result of phosphorus supplementation in long-term phosphate deficient soil. Appl. Soil Ecol. 106, 24–32. https://doi.org/10.1016/j.apsoil.2016.04.019

Cheng, W., 1999. Rhizosphere feedbacks in elevated CO2. Tree Physiol. 19, 313–320. https://doi.org/10.1093/treephys/19.4-5.313

Cheng, Y., Wang, J., Sun, N., Xu, M., Zhang, J., Cai, Z., Wang, S., 2018. Phosphorus addition enhances gross microbial N cycling in phosphorus-poor soils: a 15N study from two long-term fertilization experiments. Biol. Fertil. Soils 54, 783–789. https://doi.org/10.1007/s00374-018-1294-5

Churchland, C., Grayston, S.J., 2014. Specificity of plant-microbe interactions in the tree mycorrhizosphere biome and consequences for soil C cycling. Front. Microbiol. 5. https://doi.org/10.3389/fmicb.2014.00261

Cleveland, C.C., Liptzin, D., 2007. C:N:P stoichiometry in soil: is there a “Redfield ratio” for the microbial biomass? Biogeochemistry 85, 235–252. https://doi.org/10.1007/s10533-007-9132-0

Cleveland, C.C., Townsend, A.R., Schimel, D.S., Fisher, H., Howarth, R.W., Hedin, L.O., Perakis, S.S., Latty, E.F., Von Fischer, J.C., Elseroad, A., Wasson, M.F., 1999. Global patterns of terrestrial biological nitrogen (N_2) fixation in natural ecosystems. Glob. Biogeochem. Cycles 13, 623–645. https://doi.org/10.1029/1999GB900014

Craine, J.M., Morrow, C., Fierer, N., 2007. Microbial nitrogen limitation increases decomposition. Ecology 88, 2105–2113. https://doi.org/10.1890/06-1847.1

Crous, K.Y., Ósvaldsson, A., Ellsworth, D.S., 2015. Is phosphorus limiting in a mature Eucalyptus woodland? Phosphorus fertilisation stimulates stem growth. Plant Soil 391, 293–305. https://doi.org/10.1007/s11104-015-2426-4

Cui, Y., Moorhead, D.L., Wang, Xiangxiang, Xu, M., Wang, Xia, Wei, X., Zhu, Z., Ge, T., Peng, S., Zhu, B., Zhang, X., Fang, L., 2022. Decreasing microbial phosphorus limitation increases soil carbon release. Geoderma 419, 115868. https://doi.org/10.1016/j.geoderma.2022.115868

Cunha, H.F.V., Andersen, K.M., Lugli, L.F., Santana, F.D., Aleixo, I.F., Moraes, A.M., Garcia, S., Di Ponzio, R., Mendoza, E.O., Brum, B., Rosa, J.S., Cordeiro, A.L., Portela, B.T.T., Ribeiro, G., Coelho, S.D., De Souza, S.T., Silva, L.S., Antonieto, F., Pires, M., Salomão, A.C., Miron, A.C., De Assis, R.L., Domingues, T.F., Aragão, L.E.O.C., Meir, P., Camargo, J.L., Manzi, A.O., Nagy, L., Mercado, L.M., Hartley, I.P., Quesada, C.A., 2022. Direct evidence for phosphorus limitation on Amazon forest productivity. Nature 608, 558–562. https://doi.org/10.1038/s41586-022-05085-2

Darrouzet-Nardi, A., Ladd, M.P., Weintraub, M.N., 2013. Fluorescent microplate analysis of amino acids and other primary amines in soils. Soil Biol. Biochem. 57, 78–82. https://doi.org/10.1016/j.soilbio.2012.07.017

Davidson, E.A., Hart, S.C., Shanks, C.A., Firestone, M.K., 1991. Measuring gross nitrogen mineralization, and nitrification by 15 N isotopic pool dilution in intact soil cores. J. Soil Sci. 42, 335–349. https://doi.org/10.1111/j.1365-2389.1991.tb00413.x

Davidson, E.A., Keller, M., Erickson, H.E., Verchot, L.V., Veldkamp, E., 2000. Testing a Conceptual Model of Soil Emissions of Nitrous and Nitric Oxides. BioScience 50, 667. https://doi.org/10.1641/0006-3568(2000)050[0667:TACMOS]2.0.CO;2

De Graaff, M.-A., Van Groenigen, K.-J., Six, J., Hungate, B., Van Kessel, C., 2006. Interactions between plant growth and soil nutrient cycling under elevated CO_2: a meta-analysis. Glob. Change Biol. 12, 2077–2091. https://doi.org/10.1111/j.1365-2486.2006.01240.x

Decina, S.M., Hutyra, L.R., Templer, P.H., 2020. Hotspots of nitrogen deposition in the world's urban areas: a global data synthesis. Front. Ecol. Environ. 18, 92–100. https://doi.org/10.1002/fee.2143

Diaz, S., Grime, P., McPhersont, E., 1993. mechanism limiting plant response to elevated carbon dioxide. Nature 364.

Dijkstra, F.A., Carrillo, Y., Pendall, E., Morgan, J.A., 2013. Rhizosphere priming: a nutrient perspective. Front. Microbiol. 4. https://doi.org/10.3389/fmicb.2013.00216

Directive EU, 2024. Directive (EU) 2016/2284 of the European Parliament and of the Council of 14 December 2016 on the reduction of national emissions of certain atmospheric pollutants (OJ L 344 17.12.2016, p. 1).

Dong, J., Hunt, J., Delhaize, E., Zheng, S.J., Jin, C.W., Tang, C., 2021. Impacts of elevated CO2 on plant resistance to nutrient deficiency and toxic ions via root exudates: A review. Sci. Total Environ. 754, 142434. https://doi.org/10.1016/j.scitotenv.2020.142434

Donohue, R.J., Roderick, M.L., McVicar, T.R., Yang, Y., 2017. A simple hypothesis of how leaf and canopy-level transpiration and assimilation respond to elevated CO_2 reveals distinct response patterns between disturbed and undisturbed vegetation. J. Geophys. Res. Biogeosciences 122, 168–184. https://doi.org/10.1002/2016JG003505

Dorodnikov, M., Kuzyakov, Y., Fangmeier, A., Wiesenberg, G.L.B., 2011. C and N in soil organic matter density fractions under elevated atmospheric CO2: Turnover vs. stabilization. Soil Biol. Biochem. 43, 579–589. https://doi.org/10.1016/j.soilbio.2010.11.026

Drake, J.E., Darby, B.A., Giasson, M.-A., Kramer, M.A., Phillips, R.P., Finzi, A.C., 2013. Stoichiometry constrains microbial response to root exudation- insights from a model and a field experiment in a temperate forest. Biogeosciences 10, 821–838. https://doi.org/10.5194/bg-10-821-2013

Drake, J.E., Macdonald, C.A., Tjoelker, M.G., Crous, K.Y., Gimeno, T.E., Singh, B.K., Reich, P.B., Anderson, I.C., Ellsworth, D.S., 2016. Short-term carbon cycling responses of a mature eucalypt woodland to gradual stepwise enrichment of atmospheric CO_2 concentration. Glob. Change Biol. 22, 380–390. https://doi.org/10.1111/gcb.13109

Du, E., Terrer, C., Pellegrini, A.F.A., Ahlström, A., Van Lissa, C.J., Zhao, X., Xia, N., Wu, X., Jackson, R.B., 2020. Global patterns of terrestrial nitrogen and phosphorus limitation. Nat. Geosci. 13, 221–226. https://doi.org/10.1038/s41561-019-0530-4

Du, L., Zhu, Z., Qi, Y., Zou, D., Zhang, G., Zeng, X., Ge, T., Wu, J., Xiao, Z., 2020. Effects of different stoichiometric ratios on mineralisation of root exudates and its priming effect in paddy soil. Sci. Total Environ. 743, 140808. https://doi.org/10.1016/j.scitotenv.2020.140808

Dynarski, K.A., Houlton, B.Z., 2018. Nutrient limitation of terrestrial free-living nitrogen fixation. New Phytol. 217, 1050–1061. https://doi.org/10.1111/nph.14905

Ellsworth, D.S., Anderson, I.C., Crous, K.Y., Cooke, J., Drake, J.E., Gherlenda, A.N., Gimeno, T.E., Macdonald, C.A., Medlyn, B.E., Powell, J.R., Tjoelker, M.G., Reich, P.B., 2017. Elevated CO2 does not increase eucalypt forest productivity on a low-phosphorus soil. Nat. Clim. Change 7, 279–282. https://doi.org/10.1038/nclimate3235

Fender, A.-C., Leuschner, C., Schützenmeister, K., Gansert, D., Jungkunst, H.F., 2013. Rhizosphere effects of tree species – Large reduction of N2O emission by saplings of ash, but not of beech, in temperate forest soil. Eur. J. Soil Biol. 54, 7–15. https://doi.org/10.1016/j.ejsobi.2012.10.010

Feng, J., Zhu, B., 2021. Global patterns and associated drivers of priming effect in response to nutrient addition. Soil Biol. Biochem. 153, 108118. https://doi.org/10.1016/j.soilbio.2020.108118

Finzi, A.C., DeLucia, E.H., Hamilton, J.G., Richter, D.D., Schlesinger, W.H., 2002. The nitrogen budget of a pine forest under free air CO2 enrichment. Oecologia 132, 567–578. https://doi.org/10.1007/s00442-002-0996-3

Finzi, A.C., Moore, D.J.P., DeLucia, E.H., Lichter, J., Hofmockel, K.S., Jackson, R.B., Kim, H.-S., Matamala, R., McCarthy, H.R., Oren, R., Pippen, J.S., Schlesinger, W.H., 2006a. Progressive nitrogen limitation of ecosystem processes under elevated CO2 in a warm-temperate forest. Ecology 87, 15–25. https://doi.org/10.1890/04-1748

Finzi, A.C., Sinsabaugh, R.L., Long, T.M., Osgood, M.P., 2006b. Microbial community responses to atmospheric carbon dioxide enrichment in a warm-temperate forest. Ecosystems 9, 215–226. https://doi.org/10.1007/s10021-005-0078-6

Fleischer, K., Dolman, A.J., Van Der Molen, M.K., Rebel, K.T., Erisman, J.W., Wassen, M.J., Pak, B., Lu, X., Rammig, A., Wang, Y., 2019. Nitrogen deposition maintains a positive effect on terrestrial carbon sequestration in the 21st century despite growing phosphorus limitation at regional scales. Glob. Biogeochem. Cycles 33, 810–824. https://doi.org/10.1029/2018GB005952

Florio, A., Marechal, M., Legout, A., Creuse Des Chatelliers, C., Gervaix, J., Didier, S., Zeller, B., Le Roux, X., 2021. Influence of biological nitrification inhibition by forest tree species on soil denitrifiers and N2O emissions. Soil Biol. Biochem. 155, 108164. https://doi.org/10.1016/j.soilbio.2021.108164

Fowler, D., Coyle, M., Skiba, U., Sutton, M.A., Cape, J.N., Reis, S., Sheppard, L.J., Jenkins, A., Grizzetti, B., Galloway, J.N., Vitousek, P., Leach, A., Bouwman, A.F., Butterbach-Bahl, K., Dentener, F., Stevenson, D., Amann, M., Voss, M., 2013. The global nitrogen cycle in the twenty-first century. Philos. Trans. R. Soc. B Biol. Sci. 368, 20130164. https://doi.org/10.1098/rstb.2013.0164

Franklin, O., Näsholm, T., Högberg, P., Högberg, M.N., 2014. Forests trapped in nitrogen limitation – an ecological market perspective on ectomycorrhizal symbiosis. New Phytol. 203, 657–666. https://doi.org/10.1111/nph.12840

Friedlingstein, P., O'Sullivan, M., Jones, M.W., Andrew, R.M., Gregor, L., Hauck, J., Le Quéré, C., Luijkx, I.T., Olsen, A., Peters, G.P., Peters, W., Pongratz, J., Schwingshackl, C., Sitch, S., Canadell, J.G., Ciais, P., Jackson, R.B., Alin, S.R., Alkama, R., Arneth, A., Arora, V.K., Bates, N.R., Becker, M., Bellouin, N., Bittig, H.C., Bopp, L., Chevallier, F., Chini, L.P., Cronin, M., Evans, W., Falk, S., Feely, R.A., Gasser, T., Gehlen, M., Gkritzalis, T., Gloege, L., Grassi, G., Gruber, N., Gürses, Ö., Harris, I., Hefner, M., Houghton, R.A., Hurtt, G.C., Iida, Y., Ilyina, T., Jain, A.K., Jersild, A., Kadono, K., Kato, E., Kennedy, D., Klein Goldewijk, K., Knauer, J., Korsbakken, J.I., Landschützer, P., Lefèvre, N., Lindsay, K., Liu, J., Liu, Z., Marland, G., Mayot, N., McGrath, M.J., Metzl, N., Monacci, N.M., Munro, D.R., Nakaoka, S.-I., Niwa, Y., O'Brien, K., Ono, T., Palmer, P.I., Pan, N., Pierrot, D., Pocock, K., Poulter, B., Resplandy, L., Robertson, E., Rödenbeck, C., Rodriguez, C., Rosan, T.M., Schwinger, J., Séférian, R., Shutler, J.D., Skjelvan, I., Steinhoff, T., Sun, Q., Sutton, A.J., Sweeney, C., Takao, S., Tanhua, T., Tans, P.P., Tian, X., Tian, H., Tilbrook, B., Tsujino, H., Tubiello, F., Van Der Werf, G.R., Walker, A.P., Wanninkhof, R., Whitehead, C., Willstrand Wranne, A., Wright, R., Yuan, W., Yue, C., Yue, X., Zaehle, S., Zeng, J., Zheng, B., 2022. Global Carbon Budget 2022. Earth Syst. Sci. Data 14, 4811–4900. https://doi.org/10.5194/essd-14-4811-2022

Gahrooee, F.R., 1998. Impacts of elevated atmospheric CO_2 on litter quality, litter decomposability and nitrogen turnover rate of two oak species in a Mediterranean

forest ecosystem. Glob. Change Biol. 4, 667–677. https://doi.org/10.1046/j.1365-2486.1998.00187.x

Galloway, J.N., Aber, J.D., Erisman, J.W., Seitzinger, S.P., Howarth, R.W., Cowling, E.B., Cosby, B.J., 2003. The Nitrogen Cascade. BioScience 53, 341. https://doi.org/10.1641/0006-3568(2003)053[0341:TNC]2.0.CO;2

Galloway, J.N., Cowling, E.B., 2021. Reflections on 200 years of Nitrogen, 20 years later: This article belongs to Ambio's 50th Anniversary Collection. Theme: Eutrophication. Ambio 50, 745–749. https://doi.org/10.1007/s13280-020-01464-z

Galloway, J.N., Townsend, A.R., Erisman, J.W., Bekunda, M., Cai, Z., Freney, J.R., Martinelli, L.A., Seitzinger, S.P., Sutton, M.A., 2008. Transformation of the Nitrogen Cycle: Recent Trends, Questions, and Potential Solutions. Science 320, 889–892. https://doi.org/10.1126/science.1136674

Garcia-Montiel, D.C., Steudler, P.A., Piccolo, M., Neill, C., Melillo, J., Cerri, C.C., 2003. [No title found]. Biogeochemistry 64, 319–336. https://doi.org/10.1023/A:1024968802018

Gardner, A., Ellsworth, D.S., Crous, K.Y., Pritchard, J., MacKenzie, A.R., 2021. Is photosynthetic enhancement sustained through three years of elevated CO2 exposure in 175-year-old *Quercus robur*? Tree Physiol. 42, 130–144. https://doi.org/10.1093/treephys/tpab090

Gardner, A., Ellsworth, D.S., Pritchard, J., MacKenzie, A.R., 2022. Are chlorophyll concentrations and nitrogen across the vertical canopy profile affected by elevated CO2 in mature Quercus trees? Trees 36, 1797–1809. https://doi.org/10.1007/s00468-022-02328-7

Gardner, A., Jiang, M., Ellsworth, D.S., MacKenzie, A.R., Pritchard, J., Bader, M.K., Barton, C.V.M., Bernacchi, C., Calfapietra, C., Crous, K.Y., Dusenge, M.E., Gimeno, T.E., Hall, M., Lamba, S., Leuzinger, S., Uddling, J., Warren, J., Wallin, G., Medlyn, B.E., 2023. Optimal stomatal theory predicts CO_2 responses of stomatal conductance in both gymnosperm and angiosperm trees. New Phytol. 237, 1229–1241. https://doi.org/10.1111/nph.18618

Gaudel, G., Xing, L., Raseduzzaman, M., Poudel, M., Dong, W., Hu, C., 2024. Soil microbes, carbon, nitrogen, and the carbon to nitrogen ratio indicate priming effects across terrestrial ecosystems. J. Soils Sediments 24, 307–322. https://doi.org/10.1007/s11368-023-03609-5

Geisseler, D., Horwath, W.R., 2014. Investigating amino acid utilization by soil microorganisms using compound specific stable isotope analysis. Soil Biol. Biochem. 74, 100–105. https://doi.org/10.1016/j.soilbio.2014.02.024

Griffiths, B.S., Spilles, A., Bonkowski, M., 2012. C:N:P stoichiometry and nutrient limitation of the soil microbial biomass in a grazed grassland site under experimental P limitation or excess. Ecol. Process. 1, 6. https://doi.org/10.1186/2192-1709-1-6

Griscom, B.W., Adams, J., Ellis, P.W., Houghton, R.A., Lomax, G., Miteva, D.A., Schlesinger, W.H., Shoch, D., Siikamäki, J.V., Smith, P., Woodbury, P., Zganjar, C., Blackman, A., Campari, J., Conant, R.T., Delgado, C., Elias, P., Gopalakrishna, T., Hamsik, M.R., Herrero, M., Kiesecker, J., Landis, E., Laestadius, L., Leavitt, S.M., Minnemeyer, S., Polasky, S., Potapov, P., Putz, F.E., Sanderman, J., Silvius, M., Wollenberg, E., Fargione, J., 2017. Natural climate solutions. Proc. Natl. Acad. Sci. 114, 11645–11650. https://doi.org/10.1073/pnas.1710465114

Groffman, P.M., Tiedje, J.M., 1989. Denitrification in north temperate forest soils: Spatial and temporal patterns at the landscape and seasonal scales. Soil Biol. Biochem. 21, 613–620. https://doi.org/10.1016/0038-0717(89)90053-9

Guenet, B., Neill, C., Bardoux, G., Abbadie, L., 2010. Is there a linear relationship between priming effect intensity and the amount of organic matter input? Appl. Soil Ecol. 46, 436–442. https://doi.org/10.1016/j.apsoil.2010.09.006

Guyonnet, J.P., Vautrin, F., Meiffren, G., Labois, C., Cantarel, A.A.M., Michalet, S., Comte, G., Haichar, F. el Z., 2017. The effects of plant nutritional strategy on soil microbial denitrification activity through rhizosphere primary metabolites. FEMS Microbiol. Ecol. 93. https://doi.org/10.1093/femsec/fix022

Hagen-Thorn, A., Varnagiryte, I., Nihlgård, B., Armolaitis, K., 2006. Autumn nutrient resorption and losses in four deciduous forest tree species. For. Ecol. Manag. 228, 33–39. https://doi.org/10.1016/j.foreco.2006.02.021

Haichar, F.E.Z., Santaella, C., Heulin, T., Achouak, W., 2014. Root exudates mediated interactions belowground. Soil Biol. Biochem. 77, 69–80. https://doi.org/10.1016/j.soilbio.2014.06.017

Halbritter, 2020. The handbook for standardised field and laboratory measurements in terrestrial climate-change experiments and observational studies (ClimEx). Methods in Ecology and Evolution, 11 (1):22–37. URL https://climexhandbook.w.uib.no/2019/11/06/soil-microbial-biomass-c-n-and-p/ (accessed 7.15.24).

Hamilton, J.G., DeLucia, E.H., George, K., Naidu, S.L., Finzi, A.C., Schlesinger, W.H., 2002. Forest carbon balance under elevated CO2. Oecologia 131, 250–260. https://doi.org/10.1007/s00442-002-0884-x

Hanson, H.I., Wickenberg, B., Alkan Olsson, J., 2020. Working on the boundaries—How do science use and interpret the nature-based solution concept? Land Use Policy 90, 104302. https://doi.org/10.1016/j.landusepol.2019.104302

Hart, K.M., Curioni, G., Blaen, P., Harper, N.J., Miles, P., Lewin, K.F., Nagy, J., Bannister, E.J., Cai, X.M., Thomas, R.M., Krause, S., Tausz, M., MacKenzie, A.R., 2020. Characteristics of free air carbon dioxide enrichment of a northern temperate mature forest. Glob. Change Biol. 26, 1023–1037. https://doi.org/10.1111/gcb.14786

Hart, S.C., Nason, G.E., Myrold, D.D., Perry, D.A., 1994. Dynamics of Gross Nitrogen Transformations in an Old-Growth Forest: The Carbon Connection. Ecology 75, 880–891. https://doi.org/10.2307/1939413

Hasegawa, S., Macdonald, C.A., Power, S.A., 2016. Elevated carbon dioxide increases soil nitrogen and phosphorus availability in a phosphorus-limited *Eucalyptus* woodland. Glob. Change Biol. 22, 1628–1643. https://doi.org/10.1111/gcb.13147

Hasegawa, S., Piñeiro, J., Ochoa-Hueso, R., Haigh, A.M., Rymer, P.D., Barnett, K.L., Power, S.A., 2018. Elevated CO_2 concentrations reduce C_4 cover and decrease diversity of understorey plant community in a *Eucalyptus* woodland. J. Ecol. 106, 1483–1494. https://doi.org/10.1111/1365-2745.12943

Hasegawa, S., Ryan, M.H., Power, S.A., 2023. CO2 concentration and water availability alter the organic acid composition of root exudates in native Australian species. Plant Soil 485, 507–524. https://doi.org/10.1007/s11104-022-05845-z

Haverd, V., Smith, B., Canadell, J.G., Cuntz, M., Mikaloff-Fletcher, S., Farquhar, G., Woodgate, W., Briggs, P.R., Trudinger, C.M., 2020. Higher than expected CO_2 fertilization inferred from leaf to global observations. Glob. Change Biol. 26, 2390–2402. https://doi.org/10.1111/gcb.14950

Hedges, L.V., Gurevitch, J., Curtis, P.S., 1999. The meta-analysis of response ratios in experimental ecology. Ecology 80, 1150–1156. https://doi.org/10.1890/0012-9658(1999)080[1150:TMAORR]2.0.CO;2

Hessen, D.O., Ågren, G.I., Anderson, T.R., Elser, J.J., De Ruiter, P.C., 2004. Carbon sequestration in ecosystems: the role of stoichiometry. Ecology 85, 1179–1192. https://doi.org/10.1890/02-0251

Hickler, T., Rammig, A., Werner, C., 2015. Modelling CO2 Impacts on Forest Productivity. Curr. For. Rep. 1, 69–80. https://doi.org/10.1007/s40725-015-0014-8

Hofmockel, K.S., Schlesinger, W.H., 2007. Carbon Dioxide Effects on Heterotrophic Dinitrogen Fixation in a Temperate Pine Forest. Soil Sci. Soc. Am. J. 71, 140–144. https://doi.org/10.2136/sssaj2006.110

Hofmockel, K.S., Zak, D.R., Moran, K.K., Jastrow, J.D., 2011. Changes in forest soil organic matter pools after a decade of elevated CO2 and O3. Soil Biol. Biochem. 43, 1518–1527. https://doi.org/10.1016/j.soilbio.2011.03.030

Hollis, J., Jones, B., Ullah, S., MacKenzie, R., Hart, K., 2021. Soil Profile Pit at BIFoR-FACE, Norbury Junction, Staffordshire.

Holmes, W.E., Zak, D.R., Pregitzer, K.S., King, J.S., 2006. Elevated CO2 and O3 Alter Soil Nitrogen Transformations beneath Trembling Aspen, Paper Birch, and Sugar Maple. Ecosystems 9, 1354–1363. https://doi.org/10.1007/s10021-006-0163-5

Hu, S., Firestone, M.K., Chapin, F.S., 1999. Soil microbial feedbacks to atmospheric CO2 enrichment. Trends Ecol. Evol. 14, 433–437. https://doi.org/10.1016/S0169-5347(99)01682-1

Hungate, B.A., Duval, B.D., Dijkstra, P., Johnson, D.W., Ketterer, M.E., Stiling, P., Cheng, W., Millman, J., Hartley, A., Stover, D.B., 2014. Nitrogen inputs and losses in response to chronic CO₂ exposure in a sub-tropical oak woodland. Biogeosciences Discuss. 11, 61–106. https://doi.org/10.5194/bgd-11-61-2014

Hyvönen, R., Ågren, G.I., Linder, S., Persson, T., Cotrufo, M.F., Ekblad, A., Freeman, M., Grelle, A., Janssens, I.A., Jarvis, P.G., Kellomäki, S., Lindroth, A., Loustau, D., Lundmark, T., Norby, R.J., Oren, R., Pilegaard, K., Ryan, M.G., Sigurdsson, B.D., Strömgren, M., Van Oijen, M., Wallin, G., 2007. The likely impact of elevated [CO_2], nitrogen deposition, increased temperature and management on carbon sequestration in temperate and boreal forest ecosystems: a literature review. New Phytol. 173, 463–480. https://doi.org/10.1111/j.1469-8137.2007.01967.x

Inatomi, M., Hajima, T., Ito, A., 2019. Fraction of nitrous oxide production in nitrification and its effect on total soil emission: A meta-analysis and global-scale sensitivity analysis using a process-based model. PLOS ONE 14, e0219159. https://doi.org/10.1371/journal.pone.0219159

Ipcc, 2022. Global Warming of 1.5°C: IPCC Special Report on Impacts of Global Warming of 1.5°C above Pre-industrial Levels in Context of Strengthening Response to Climate Change, Sustainable Development, and Efforts to Eradicate Poverty, 1st ed. Cambridge University Press. https://doi.org/10.1017/9781009157940

Iversen, C.M., Hooker, T.D., Classen, A.T., Norby, R.J., 2011. Net mineralization of N at deeper soil depths as a potential mechanism for sustained forest production under elevated [CO_2]. Glob. Change Biol. 17, 1130–1139. https://doi.org/10.1111/j.1365-2486.2010.02240.x

Iversen, C.M., Norby, R.J., 2008. Nitrogen limitation in a sweetgum plantation: implications for carbon allocation and storage. Can. J. For. Res. 38, 1021–1032. https://doi.org/10.1139/X07-213

Jacoby, R., Peukert, M., Succurro, A., Koprivova, A., Kopriva, S., 2017. The Role of Soil Microorganisms in Plant Mineral Nutrition—Current Knowledge and Future Directions. Front. Plant Sci. 8, 1617. https://doi.org/10.3389/fpls.2017.01617

Jakobsen, I., Smith, S.E., Smith, F.A., Watts-Williams, S.J., Clausen, S.S., Grønlund, M., 2016. Plant growth responses to elevated atmospheric CO_2 are increased by phosphorus sufficiency but not by arbuscular mycorrhizas. J. Exp. Bot. 67, 6173–6186. https://doi.org/10.1093/jxb/erw383

Jiang, M., Crous, K.Y., Carrillo, Y., Macdonald, C.A., Anderson, I.C., Boer, M.M., Farrell, M., Gherlenda, A.N., Castañeda-Gómez, L., Hasegawa, S., Jarosch, K., Milham, P.J., Ochoa-Hueso, R., Pathare, V., Pihlblad, J., Piñeiro, J., Powell, J.R., Power, S.A., Reich, P.B., Riegler, M., Zaehle, S., Smith, B., Medlyn, B.E., Ellsworth, D.S., 2024. Microbial competition for phosphorus limits the CO2 response of a mature forest. Nature. https://doi.org/10.1038/s41586-024-07491-0

Jiang, M., Medlyn, B.E., Drake, J.E., Duursma, R.A., Anderson, I.C., Barton, C.V.M., Boer, M.M., Carrillo, Y., Castañeda-Gómez, L., Collins, L., Crous, K.Y., De Kauwe, M.G., Dos Santos, B.M., Emmerson, K.M., Facey, S.L., Gherlenda, A.N., Gimeno, T.E., Hasegawa, S., Johnson, S.N., Kännaste, A., Macdonald, C.A., Mahmud, K., Moore, B.D., Nazaries, L., Neilson, E.H.J., Nielsen, U.N., Niinemets, Ü., Noh, N.J., Ochoa-Hueso, R., Pathare, V.S., Pendall, E., Pihlblad, J., Piñeiro, J., Powell, J.R., Power, S.A., Reich, P.B., Renchon, A.A., Riegler, M., Rinnan, R., Rymer, P.D., Salomón, R.L., Singh, B.K., Smith, B., Tjoelker, M.G., Walker, J.K.M., Wujeska-Klause, A., Yang, J., Zaehle, S., Ellsworth, D.S., 2020. The fate of carbon in a mature forest under carbon dioxide enrichment. Nature 580, 227–231. https://doi.org/10.1038/s41586-020-2128-9

Jílková, V., Straková, P., Frouz, J., 2020. Foliage C:N ratio, stage of organic matter decomposition and interaction with soil affect microbial respiration and its response to C and N addition more than C:N changes during decomposition. Appl. Soil Ecol. 152, 103568. https://doi.org/10.1016/j.apsoil.2020.103568

Jilling, A., Keiluweit, M., Contosta, A.R., Frey, S., Schimel, J., Schnecker, J., Smith, R.G., Tiemann, L., Grandy, A.S., 2018. Minerals in the rhizosphere: overlooked mediators of soil nitrogen availability to plants and microbes. Biogeochemistry 139, 103–122. https://doi.org/10.1007/s10533-018-0459-5

Johansson, E.M., Fransson, P.M.A., Finlay, R.D., Van Hees, P.A.W., 2009. Quantitative analysis of soluble exudates produced by ectomycorrhizal roots as a response to ambient and elevated CO2. Soil Biol. Biochem. 41, 1111–1116. https://doi.org/10.1016/j.soilbio.2009.02.016

Johnson, D.W., 2006. Progressive N limitation in forests: Review and implications for long-term responses to elevated CO2. Ecology 87, 64–75. https://doi.org/10.1890/04-1781

Jones, D., 2002. Simple method to enable the high resolution determination of total free amino acids in soil solutions and soil extracts. Soil Biol. Biochem. 34, 1893–1902. https://doi.org/10.1016/S0038-0717(02)00203-1

Jones, D.L., Hodge, A., Kuzyakov, Y., 2004. Plant and mycorrhizal regulation of rhizodeposition. New Phytol. 163, 459–480. https://doi.org/10.1111/j.1469-8137.2004.01130.x

Jones, D.L., Nguyen, C., Finlay, R.D., 2009. Carbon flow in the rhizosphere: carbon trading at the soil–root interface. Plant Soil 321, 5–33. https://doi.org/10.1007/s11104-009-9925-0

Karnosky, D.F., 2003. Impacts of elevated atmospheric CO2 on forest trees and forest ecosystems: knowledge gaps. Environ. Int. 29, 161–169. https://doi.org/10.1016/S0160-4120(02)00159-9

Kirkham, D., Bartholomew, W.V., 1954. Equations for Following Nutrient Transformations in Soil, Utilizing Tracer Data1. Soil Sci. Soc. Am. J. 18, 33. https://doi.org/10.2136/sssaj1954.03615995001800010009x

Knowles, T.D.J., Chadwick, D.R., Bol, R., Evershed, R.P., 2010. Tracing the rate and extent of N and C flow from 13C,15N-glycine and glutamate into individual de novo synthesised soil amino acids. Org. Geochem. 41, 1259–1268. https://doi.org/10.1016/j.orggeochem.2010.09.003

Körner, C., Asshoff, R., Bignucolo, O., Hättenschwiler, S., Keel, S.G., Peláez-Riedl, S., Pepin, S., Siegwolf, R.T.W., Zotz, G., 2005. Carbon Flux and Growth in Mature Deciduous Forest Trees Exposed to Elevated CO_2. Science 309, 1360–1362. https://doi.org/10.1126/science.1113977

Kuzyakov, Y., 2002. Review: Factors affecting rhizosphere priming effects. J. Plant Nutr. Soil Sci. 165, 382–396. https://doi.org/10.1002/1522-2624(200208)165:4<382::AID-JPLN382>3.0.CO;2-#

Kuzyakov, Y., Blagodatskaya, E., 2015. Microbial hotspots and hot moments in soil: Concept & review. Soil Biol. Biochem. 83, 184–199. https://doi.org/10.1016/j.soilbio.2015.01.025

Kuzyakov, Y., Horwath, W.R., Dorodnikov, M., Blagodatskaya, E., 2019. Review and synthesis of the effects of elevated atmospheric CO2 on soil processes: No changes in pools, but increased fluxes and accelerated cycles. Soil Biol. Biochem. 128, 66–78. https://doi.org/10.1016/j.soilbio.2018.10.005

Lacis, A.A., Schmidt, G.A., Rind, D., Ruedy, R.A., 2010. Atmospheric CO_2: Principal Control Knob Governing Earth's Temperature. Science 330, 356–359. https://doi.org/10.1126/science.1190653

Larcher, W., 2003. Physiological plant ecology: ecophysiology and stress physiology of functional groups, 4th ed. ed. Springer, Berlin ; New York. http://dx.doi.org/10.1007/978-3-662-05214-3

Lauriks, F., Salomón, R.L., De Roo, L., Steppe, K., 2021. Leaf and tree responses of young European aspen trees to elevated atmospheric CO2 concentration vary over the season. Tree Physiol. 41, 1877–1892. https://doi.org/10.1093/treephys/tpab048

Lavallee, J.M., Soong, J.L., Cotrufo, M.F., 2020. Conceptualizing soil organic matter into particulate and mineral-associated forms to address global change in the 21st century. Glob. Change Biol. 26, 261–273. https://doi.org/10.1111/gcb.14859

Le Quéré, C., Andrew, R.M., Friedlingstein, P., Sitch, S., Pongratz, J., Manning, A.C., Korsbakken, J.I., Peters, G.P., Canadell, J.G., Jackson, R.B., Boden, T.A., Tans, P.P., Andrews, O.D., Arora, V.K., Bakker, D.C.E., Barbero, L., Becker, M., Betts, R.A., Bopp, L., Chevallier, F., Chini, L.P., Ciais, P., Cosca, C.E., Cross, J., Currie, K., Gasser, T., Harris, I., Hauck, J., Haverd, V., Houghton, R.A., Hunt, C.W., Hurtt, G., Ilyina, T., Jain, A.K., Kato, E., Kautz, M., Keeling, R.F., Klein Goldewijk, K., Körtzinger, A., Landschützer, P., Lefèvre, N., Lenton, A., Lienert, S., Lima, I., Lombardozzi, D., Metzl, N., Millero, F., Monteiro, P.M.S., Munro, D.R., Nabel, J.E.M.S., Nakaoka, S., Nojiri, Y., Padin, X.A., Peregon, A., Pfeil, B., Pierrot, D., Poulter, B., Rehder, G., Reimer, J., Rödenbeck, C., Schwinger, J., Séférian, R., Skjelvan, I., Stocker, B.D., Tian, H., Tilbrook, B., Tubiello, F.N., Van Der Laan-Luijkx, I.T., Van Der Werf, G.R., Van Heuven, S., Viovy, N., Vuichard, N., Walker, A.P., Watson, A.J., Wiltshire, A.J., Zaehle, S., Zhu, D., 2018. Global Carbon Budget 2017. Earth Syst. Sci. Data 10, 405–448. https://doi.org/10.5194/essd-10-405-2018

Li, Y., Chapman, S.J., Nicol, G.W., Yao, H., 2018. Nitrification and nitrifiers in acidic soils. Soil Biol. Biochem. 116, 290–301. https://doi.org/10.1016/j.soilbio.2017.10.023

Li, Y., Yu, Z., Liu, X., Mathesius, U., Wang, G., Tang, C., Wu, J., Liu, J., Zhang, S., Jin, J., 2017. Elevated CO2 Increases Nitrogen Fixation at the Reproductive Phase Contributing to Various Yield Responses of Soybean Cultivars. Front. Plant Sci. 8, 1546. https://doi.org/10.3389/fpls.2017.01546

Li, Z., Tian, D., Wang, B., Wang, J., Wang, S., Chen, H.Y.H., Xu, X., Wang, C., He, N., Niu, S., 2019. Microbes drive global soil nitrogen mineralization and availability. Glob. Change Biol. 25, 1078–1088. https://doi.org/10.1111/gcb.14557

Liu, Chong, Ding, T.-X., Van Der Ent, A., Liu, Chang, Morel, J.L., Sirguey, C., Liu, W.-S., Tang, Y.-T., Qiu, R.-L., 2024. A novel method for in situ imaging of root exudates and labile elements reveals phosphorus deficiency-induced mobilization of rare earth elements in the rhizosphere of Phytolacca americana. Plant Soil 495, 13–26. https://doi.org/10.1007/s11104-023-06146-9

Liu, W., Jiang, Y., Su, Y., Smoak, J.M., Duan, B., 2022. Warming Affects Soil Nitrogen Mineralization via Changes in Root Exudation and Associated Soil Microbial Communities in a Subalpine Tree Species Abies fabri. J. Soil Sci. Plant Nutr. 22, 406–415. https://doi.org/10.1007/s42729-021-00657-z

Liu, Y., Ma, W., Kou, D., Niu, X., Wang, T., Chen, Y., Chen, D., Zhu, X., Zhao, M., Hao, B., Zhang, J., Yang, Y., Hu, H., 2020. A comparison of patterns of microbial C : N : P stoichiometry between topsoil and subsoil along an aridity gradient. Biogeosciences 17, 2009–2019. https://doi.org/10.5194/bg-17-2009-2020

Lopez-Sangil, L., George, C., Medina-Barcenas, E., Birkett, A.J., Baxendale, C., Bréchet, L.M., Estradera-Gumbau, E., Sayer, E.J., 2017. The Automated Root Exudate System (ARES): a method to apply solutes at regular intervals to soils in the field. Methods Ecol. Evol. 8, 1042–1050. https://doi.org/10.1111/2041-210X.12764

Lundberg, J., Moberg, F., 2003. Mobile Link Organisms and Ecosystem Functioning: Implications for Ecosystem Resilience and Management. Ecosystems 6, 0087–0098. https://doi.org/10.1007/s10021-002-0150-4

Luo, Y., Hui, D., Zhang, D., 2006. Elevated CO_2 stimulates net accumulations of carbon and nitrogen in land ecosystems: a meta-analysis. Ecology 87, 53–63. https://doi.org/10.1890/04-1724

Luo, Y., Su, B., Currie, W.S., Dukes, J.S., Finzi, A., Hartwig, U., Hungate, B., Mc Murtrie, R.E., Oren, R., Parton, W.J., Pataki, D.E., Shaw, M.R., Zak, D.R., Field, C.B., 2004. Progressive Nitrogen Limitation of Ecosystem Responses to Rising Atmospheric Carbon Dioxide. BioScience 54, 731. https://doi.org/10.1641/0006-3568(2004)054[0731:PNLOER]2.0.CO;2

MacKenzie, A.R., Krause, S., Hart, K.M., Thomas, R.M., Blaen, P.J., Hamilton, R.L., Curioni, G., Quick, S.E., Kourmouli, A., Hannah, D.M., Comer-Warner, S.A., Brekenfeld, N., Ullah, S., Press, M.C., 2021. BIFOR FACE : Water–soil–vegetation–atmosphere data from a temperate deciduous forest catchment, including under elevated CO_2. Hydrol. Process. 35, e14096. https://doi.org/10.1002/hyp.14096

Manzoni, S., Chakrawal, A., Spohn, M., Lindahl, B.D., 2021. Modeling Microbial Adaptations to Nutrient Limitation During Litter Decomposition. Front. For. Glob. Change 4, 686945. https://doi.org/10.3389/ffgc.2021.686945

Matejko, M., Dore, A.J., Hall, J., Dore, C.J., Błaś, M., Kryza, M., Smith, R., Fowler, D., 2009. The influence of long term trends in pollutant emissions on deposition of sulphur and nitrogen and exceedance of critical loads in the United Kingdom. Environ. Sci. Policy 12, 882–896. https://doi.org/10.1016/j.envsci.2009.08.005

Matsui, M., Fowler, J.H., Walling, L.L., 2006. Leucine aminopeptidases: diversity in structure and function. Biol. Chem. 387. https://doi.org/10.1515/BC.2006.191

Maxwell, T.L., Canarini, A., Bogdanovic, I., Böckle, T., Martin, V., Noll, L., Prommer, J., Séneca, J., Simon, E., Piepho, H., Herndl, M., Pötsch, E.M., Kaiser, C., Richter, A., Bahn, M., Wanek, W., 2022. Contrasting drivers of belowground nitrogen cycling in a montane grassland exposed to a multifactorial global change experiment with elevated CO_2, warming, and drought. Glob. Change Biol. 28, 2425–2441. https://doi.org/10.1111/gcb.16035

McInturf, A.G., Pollack, L., Yang, L.H., Spiegel, O., 2019. Vectors with autonomy: what distinguishes animal-mediated nutrient transport from abiotic vectors? Biol. Rev. 94, 1761–1773. https://doi.org/10.1111/brv.12525

McMurtrie, R.E., Norby, R.J., Medlyn, B.E., Dewar, R.C., Pepper, D.A., Reich, P.B., Barton, C.V.M., 2008. Why is plant-growth response to elevated CO2 amplified when water is limiting, but reduced when nitrogen is limiting? A growth-optimisation hypothesis. Funct. Plant Biol. 35, 521. https://doi.org/10.1071/FP08128

Medlyn, B.E., Barton, C.V.M., Broadmeadow, M.S.J., Ceulemans, R., De Angelis, P., Forstreuter, M., Freeman, M., Jackson, S.B., Kellomäki, S., Laitat, E., Rey, A., Roberntz, P., Sigurdsson, B.D., Strassemeyer, J., Wang, K., Curtis, P.S., Jarvis, P.G., 2001. Stomatal conductance of forest species after long-term exposure to elevated CO_2 concentration: a synthesis. New Phytol. 149, 247–264. https://doi.org/10.1046/j.1469-8137.2001.00028.x

Medlyn, B.E., Zaehle, S., De Kauwe, M.G., Walker, A.P., Dietze, M.C., Hanson, P.J., Hickler, T., Jain, A.K., Luo, Y., Parton, W., Prentice, I.C., Thornton, P.E., Wang, S., Wang, Y.-P., Weng, E., Iversen, C.M., McCarthy, H.R., Warren, J.M., Oren, R., Norby, R.J., 2015. Using ecosystem experiments to improve vegetation models. Nat. Clim. Change 5, 528–534. https://doi.org/10.1038/nclimate2621

Mehnaz, K.R., Corneo, P.E., Keitel, C., Dijkstra, F.A., 2019. Carbon and phosphorus addition effects on microbial carbon use efficiency, soil organic matter priming, gross nitrogen mineralization and nitrous oxide emission from soil. Soil Biol. Biochem. 134, 175–186. https://doi.org/10.1016/j.soilbio.2019.04.003

Meier, I.C., Pritchard, S.G., Brzostek, E.R., McCormack, M.L., Phillips, R.P., 2015. The rhizosphere and hyphosphere differ in their impacts on carbon and nitrogen cycling in forests exposed to elevated CO_2. New Phytol. 205, 1164–1174. https://doi.org/10.1111/nph.13122

Melillo, J.M., 1981. Nitrogen cycling in deciduous forests. Ecol. Bull. 427–442.

Meyerholt, J., Sickel, K., Zaehle, S., 2020. Ensemble projections elucidate effects of uncertainty in terrestrial nitrogen limitation on future carbon uptake. Glob. Change Biol. 26, 3978–3996. https://doi.org/10.1111/gcb.15114

Meyerholt, J., Zaehle, S., Smith, M.J., 2016. Variability of projected terrestrial biosphere responses to elevated levels of atmospheric CO2 due to uncertainty in biological nitrogen fixation. Biogeosciences 13, 1491–1518. https://doi.org/10.5194/bg-13-1491-2016

Micucci, G., Sgouridis, F., McNamara, N.P., Krause, S., Lynch, I., Roos, F., Pereira, M.G., Ullah, S., 2024. Towards enhanced sensitivity of the 15N gas flux method for quantifying denitrification in soil. Soil Biol. Biochem. 109421. https://doi.org/10.1016/j.soilbio.2024.109421

Micucci, G., Sgouridis, F., McNamara, N.P., Krause, S., Lynch, I., Roos, F., Well, R., Ullah, S., 2023. The 15N-Gas flux method for quantifying denitrification in soil: Current progress and future directions. Soil Biol. Biochem. 184, 109108. https://doi.org/10.1016/j.soilbio.2023.109108

Moorhead, D.L., Rinkes, Z.L., Sinsabaugh, R.L., Weintraub, M.N., 2013. Dynamic relationships between microbial biomass, respiration, inorganic nutrients and enzyme activities: informing enzyme-based decomposition models. Front. Microbiol. 4. https://doi.org/10.3389/fmicb.2013.00223

Mooshammer, M., Wanek, W., Hämmerle, I., Fuchslueger, L., Hofhansl, F., Knoltsch, A., Schnecker, J., Takriti, M., Watzka, M., Wild, B., Keiblinger, K.M., Zechmeister-Boltenstern, S., Richter, A., 2014. Adjustment of microbial nitrogen use efficiency to carbon:nitrogen imbalances regulates soil nitrogen cycling. Nat. Commun. 5, 3694. https://doi.org/10.1038/ncomms4694

Morley, N., Baggs, E.M., 2010. Carbon and oxygen controls on N2O and N2 production during nitrate reduction. Soil Biol. Biochem. 42, 1864–1871. https://doi.org/10.1016/j.soilbio.2010.07.008

Mylona, P., Pawlowski, K., Bisseling, T., 1995. Symbiotic Nitrogen Fixation. Plant Cell 869–885. https://doi.org/10.1105/tpc.7.7.869

Nadelhoffer, K.J., Emmett, B.A., Gundersen, P., Kjønaas, O.J., Koopmans, C.J., Schleppi, P., Tietema, A., Wright, R.F., 1999. Nitrogen deposition makes a minor contribution to carbon sequestration in temperate forests. Nature 398, 145–148. https://doi.org/10.1038/18205

Nardi, P., Laanbroek, H.J., Nicol, G.W., Renella, G., Cardinale, M., Pietramellara, G., Weckwerth, W., Trinchera, A., Ghatak, A., Nannipieri, P., 2020. Biological nitrification inhibition in the rhizosphere: determining interactions and impact on microbially mediated processes and potential applications. FEMS Microbiol. Rev. 44, 874–908. https://doi.org/10.1093/femsre/fuaa037

Noll, L., Zhang, S., Zheng, Q., Hu, Y., Wanek, W., 2019. Wide-spread limitation of soil organic nitrogen transformations by substrate availability and not by extracellular enzyme content. Soil Biol. Biochem. 133, 37–49. https://doi.org/10.1016/j.soilbio.2019.02.016

Norby, R.J., 1987. Nodulation and nitrogenase activity in nitrogen-fixing woody plants stimulated by CO_2 enrichment of the atmosphere. Physiol. Plant. 71, 77–82. https://doi.org/10.1111/j.1399-3054.1987.tb04620.x

Norby, R.J., Hanson, P.J., O'Neill, E.G., Tschaplinski, T.J., Weltzin, J.F., Hansen, R.A., Cheng, W., Wullschleger, S.D., Gunderson, C.A., Edwards, N.T., Johnson, D.W., 2002. Net primary productivity of a CO2 -enriched deciduous forest and the implications for carbon storage. Ecol. Appl. 12, 1261–1266. https://doi.org/10.1890/1051-0761(2002)012[1261:NPPOAC]2.0.CO;2

Norby, R.J., Ledford, J., Reilly, C.D., Miller, N.E., O'Neill, E.G., 2004. Fine-root production dominates response of a deciduous forest to atmospheric CO_2 enrichment. Proc. Natl. Acad. Sci. 101, 9689–9693. https://doi.org/10.1073/pnas.0403491101

Norby, R.J., Loader, N.J., Mayoral, C., Ullah, S., Curioni, G., Smith, A.R., Reay, M.K., Van Wijngaarden, K., Amjad, M.S., Brettle, D., Crockatt, M.E., Denny, G., Grzesik, R.T., Hamilton, R.L., Hart, K.M., Hartley, I.P., Jones, A.G., Kourmouli, A., Larsen, J.R., Shi, Z., Thomas, R.M., MacKenzie, A.R., 2024. Enhanced woody biomass production in a mature temperate forest under elevated CO2. Nat. Clim. Change 14, 983–988. https://doi.org/10.1038/s41558-024-02090-3

Norby, R.J., Warren, J.M., Iversen, C.M., Medlyn, B.E., McMurtrie, R.E., 2010. CO2 enhancement of forest productivity constrained by limited nitrogen availability. Proc. Natl. Acad. Sci. 107, 19368–19373. https://doi.org/10.1073/pnas.1006463107

Norby, R.J., Wullschleger, S.D., Gunderson, C.A., Johnson, D.W., Ceulemans, R., 1999. Tree responses to rising CO_2 in field experiments: implications for the future forest. Plant Cell Environ. 22, 683–714. https://doi.org/10.1046/j.1365-3040.1999.00391.x

Norby, R.J., Zak, D.R., 2011. Ecological lessons from Free-Air CO2 Enrichment (FACE) experiments.

Norton, J., Schimel, J., 2011. Nitrogen mineralization-immobilization turn-over. In: Huang PM, Li Y, Summers ME (eds) Handbook of soil science, Second edn. CRC Press, Boca Raton, FL, pp 8–18.

Ochoa-Hueso, R., Hughes, J., Delgado-Baquerizo, M., Drake, J.E., Tjoelker, M.G., Piñeiro, J., Power, S.A., 2017. Rhizosphere-driven increase in nitrogen and phosphorus availability under elevated atmospheric CO2 in a mature Eucalyptus woodland. Plant Soil 416, 283–295. https://doi.org/10.1007/s11104-017-3212-2

Paavolainen, L., Kitunen, V., Smolander, A., 1998. Inhibition of nitrification in forest soil by monoterpenes. Plant Soil 205, 147–154. https://doi.org/10.1023/A:1004335419358

Pathare, V.S., Crous, K.Y., Cooke, J., Creek, D., Ghannoum, O., Ellsworth, D.S., 2017. Water availability affects seasonal CO_2 -induced photosynthetic enhancement in herbaceous species in a periodically dry woodland. Glob. Change Biol. 23, 5164–5178. https://doi.org/10.1111/gcb.13778

Pellitier, P.T., Ibáñez, I., Zak, D.R., Argiroff, W.A., Acharya, K., 2021. Ectomycorrhizal access to organic nitrogen mediates CO2 fertilization response in a dominant temperate tree. Nat. Commun. 12, 5403. https://doi.org/10.1038/s41467-021-25652-x

Pendall, E., Osanai, Y., Williams, A.L., Hovenden, M.J., 2011. Soil carbon storage under simulated climate change is mediated by plant functional type. Glob. Change Biol. 17, 505–514. https://doi.org/10.1111/j.1365-2486.2010.02296.x

Peng, C., Apps, M.J., 1999. Modelling the response of net primary productivity (NPP) of boreal forest ecosystems to changes in climate and fire disturbance regimes. Ecol. Model. 122, 175–193. https://doi.org/10.1016/S0304-3800(99)00137-4

Philippot, L., Hallin, S., Börjesson, G., Baggs, E.M., 2009. Biochemical cycling in the rhizosphere having an impact on global change. Plant Soil 321, 61–81. https://doi.org/10.1007/s11104-008-9796-9

Phillips, R.L., Whalen, S.C., Schlesinger, W.H., 2001. Influence of atmospheric CO_2 enrichment on nitrous oxide flux in a temperate forest ecosystem. Glob. Biogeochem. Cycles 15, 741–752. https://doi.org/10.1029/2000GB001372

Phillips, R.P., Bernhardt, E.S., Schlesinger, W.H., 2009. Elevated CO2 increases root exudation from loblolly pine (Pinus taeda) seedlings as an N-mediated response. Tree Physiol. 29, 1513–1523. https://doi.org/10.1093/treephys/tpp083

Phillips, R.P., Brzostek, E., Midgley, M.G., 2013. The mycorrhizal-associated nutrient economy: a new framework for predicting carbon-nutrient couplings in temperate forests. New Phytol. 199, 41–51. https://doi.org/10.1111/nph.12221

Phillips, R.P., Erlitz, Y., Bier, R., Bernhardt, E.S., 2008. New approach for capturing soluble root exudates in forest soils. Funct. Ecol. 22, 990–999. https://doi.org/10.1111/j.1365-2435.2008.01495.x

Phillips, R.P., Finzi, A.C., Bernhardt, E.S., 2011. Enhanced root exudation induces microbial feedbacks to N cycling in a pine forest under long-term CO2 fumigation: Rhizosphere feedbacks in CO2-enriched forests. Ecol. Lett. 14, 187–194. https://doi.org/10.1111/j.1461-0248.2010.01570.x

Phillips, R.P., Meier, I.C., Bernhardt, E.S., Grandy, A.S., Wickings, K., Finzi, A.C., 2012. Roots and fungi accelerate carbon and nitrogen cycling in forests exposed to

elevated CO_2. Ecol. Lett. 15, 1042–1049. https://doi.org/10.1111/j.1461-0248.2012.01827.x

Pihlblad, J., Andresen, L.C., Macdonald, C.A., Ellsworth, D.S., Carrillo, Y., 2023. The influence of elevated CO_2 and soil depth on rhizosphere activity and nutrient availability in a mature *Eucalyptus* woodland. Biogeosciences 20, 505–521. https://doi.org/10.5194/bg-20-505-2023

Piñeiro, J., Ochoa-Hueso, R., Drake, J.E., Tjoelker, M.G., Power, S.A., 2020. Water availability drives fine root dynamics in a *Eucalyptus* woodland under elevated atmospheric CO_2 concentration. Funct. Ecol. 34, 2389–2402. https://doi.org/10.1111/1365-2435.13660

Piñeiro, J., Ochoa-Hueso, R., Serrano-Grijalva, L., Power, S.A., 2023. Phosphorus and water supply independently control productivity and soil enzyme activity responses to elevated CO2 in an understorey community from a Eucalyptus woodland. Plant Soil 483, 643–657. https://doi.org/10.1007/s11104-022-05763-0

Prosser, J.I., 2005. Nitrogen in soils: Nitrification, in: Encyclopedia of Soils in the Environment. Elsevier, pp. 31–39. https://doi.org/10.1016/B0-12-348530-4/00512-9

Quan, Q., Wang, C., He, N., Zhang, Z., Wen, X., Su, H., Wang, Q., Xue, J., 2014. Forest type affects the coupled relationships of soil C and N mineralization in the temperate forests of northern China. Sci. Rep. 4, 6584. https://doi.org/10.1038/srep06584

Quentin, A.G., Crous, K.Y., Barton, C.V.M., Ellsworth, D.S., 2015. Photosynthetic enhancement by elevated CO_2 depends on seasonal temperatures for warmed and non-warmed *Eucalyptus globulus* trees. Tree Physiol. tpv110. https://doi.org/10.1093/treephys/tpv110

R Core Team, 2021. R: A language and environment for statistical computing. R Foundation for Statistical Computing, Vienna, Austria.

Rastetter, E.B., Kling, G.W., Shaver, G.R., Crump, B.C., Gough, L., Griffin, K.L., 2021. Ecosystem Recovery from Disturbance is Constrained by N Cycle Openness, Vegetation-Soil N Distribution, Form of N Losses, and the Balance Between Vegetation and Soil-Microbial Processes. Ecosystems 24, 667–685. https://doi.org/10.1007/s10021-020-00542-3

Reed, S.C., Cleveland, C.C., Townsend, A.R., 2011. Functional Ecology of Free-Living Nitrogen Fixation: A Contemporary Perspective. Annu. Rev. Ecol. Evol. Syst. 42, 489–512. https://doi.org/10.1146/annurev-ecolsys-102710-145034

Reich, P.B., Grigal, D.F., Aber, J.D., Gower, S.T., 1997. Nitrogen mineralization and productivity in 50 hardwood and conifer stands on diverse soils. Ecology 78, 335–347. https://doi.org/10.1890/0012-9658(1997)078[0335:NMAPIH]2.0.CO;2

Reich, P.B., Hobbie, S.E., Lee, T., Ellsworth, D.S., West, J.B., Tilman, D., Knops, J.M.H., Naeem, S., Trost, J., 2006. Nitrogen limitation constrains sustainability of ecosystem response to CO2. Nature 440, 922–925. https://doi.org/10.1038/nature04486

Rennenberg, H., Dannenmann, M., 2015. Nitrogen Nutrition of Trees in Temperate Forests—The Significance of Nitrogen Availability in the Pedosphere and Atmosphere. Forests 6, 2820–2835. https://doi.org/10.3390/f6082820

Richter, M., Hartwig, U.A., Frossard, E., Nösberger, J., Cadisch, G., 2003. Gross fluxes of nitrogen in grassland soil exposed to elevated atmospheric pCO2 for seven years. Soil Biol. Biochem. 35, 1325–1335. https://doi.org/10.1016/S0038-0717(03)00212-8

Rogers, A., Ainsworth, E.A., Leakey, A.D.B., 2009. Will Elevated Carbon Dioxide Concentration Amplify the Benefits of Nitrogen Fixation in Legumes? Plant Physiol. 151, 1009–1016. https://doi.org/10.1104/pp.109.144113

Rosinger, C., Rousk, J., Sandén, H., 2019. Can enzymatic stoichiometry be used to determine growth-limiting nutrients for microorganisms? - A critical assessment in two subtropical soils. Soil Biol. Biochem. 128, 115–126. https://doi.org/10.1016/j.soilbio.2018.10.011

Ross, G.M., Horn, S., Macdonald, C.A., Powell, J.R., Reynolds, J.K., Ryan, M.M., Cook, J.M., Nielsen, U.N., 2020. Metabarcoding mites: Three years of elevated CO2 has no effect on oribatid assemblages in a Eucalyptus woodland. Pedobiologia 81–82, 150667. https://doi.org/10.1016/j.pedobi.2020.150667

RStudio Team, 2021. RStudio: Integrated Development Environment for R. RStudio, PBC, Boston, MA URL http://www.rstudio.com/.

Rubin, H.J., Fu, J.S., Dentener, F., Li, R., Huang, K., Fu, H., 2023. Global nitrogen and sulfur deposition mapping using a measurement–model fusion approach. Atmospheric Chem. Phys. 23, 7091–7102. https://doi.org/10.5194/acp-23-7091-2023

Rumeau, M., Sgouridis, F., MacKenzie, R., Carrillo, Y., Reay, M.K., Hartley, I.P., Ullah, S., 2024. The role of rhizosphere in enhancing N availability in a mature temperate forest under elevated CO2. Soil Biol. Biochem. 197, 109537. https://doi.org/10.1016/j.soilbio.2024.109537

Rummel, P.S., Well, R., Pfeiffer, B., Dittert, K., Floßmann, S., Pausch, J., 2021. Nitrate uptake and carbon exudation – do plant roots stimulate or inhibit denitrification? Plant Soil 459, 217–233. https://doi.org/10.1007/s11104-020-04750-7

Rütting, T., Andresen, L.C., 2015. Nitrogen cycle responses to elevated CO2 depend on ecosystem nutrient status. Nutr. Cycl. Agroecosystems 101, 285–294. https://doi.org/10.1007/s10705-015-9683-8

Rütting, T., Huygens, D., Boeckx, P., Staelens, J., Klemedtsson, L., 2013. Increased fungal dominance in N2O emission hotspots along a natural pH gradient in organic forest soil. Biol. Fertil. Soils 49, 715–721. https://doi.org/10.1007/s00374-012-0762-6

Saiz, E., Sgouridis, F., Drijfhout, F.P., Peichl, M., Nilsson, M.B., Ullah, S., 2021. Chronic Atmospheric Reactive Nitrogen Deposition Suppresses Biological Nitrogen Fixation in Peatlands. Environ. Sci. Technol. acs.est.0c04882. https://doi.org/10.1021/acs.est.0c04882

Saiz, E., Sgouridis, F., Drijfhout, F.P., Ullah, S., 2019. Biological nitrogen fixation in peatlands: Comparison between acetylene reduction assay and 15N2 assimilation methods. Soil Biol. Biochem. 131, 157–165. https://doi.org/10.1016/j.soilbio.2019.01.011

Salem, M.A., Wang, J.Y., Al-Babili, S., 2022. Metabolomics of plant root exudates: From sample preparation to data analysis. Front. Plant Sci. 13, 1062982. https://doi.org/10.3389/fpls.2022.1062982

Schäfer, K.V.R., Oren, R., Lai, C., Katul, G.G., 2002. Hydrologic balance in an intact temperate forest ecosystem under ambient and elevated atmospheric CO_2 concentration. Glob. Change Biol. 8, 895–911. https://doi.org/10.1046/j.1365-2486.2002.00513.x

Scheer, C., Fuchs, K., Pelster, D.E., Butterbach-Bahl, K., 2020. Estimating global terrestrial denitrification from measured N2O:(N2O + N2) product ratios. Curr. Opin. Environ. Sustain. 47, 72–80. https://doi.org/10.1016/j.cosust.2020.07.005

Schimel, Bennett, J., 2004. Nitrogen mineralization: challenges of a changing paradigm. Ecology 85, 591–602. https://doi.org/10.1890/03-8002

Schimel, J., Weintraub, M.N., Moorhead, D., 2022. Estimating microbial carbon use efficiency in soil: Isotope-based and enzyme-based methods measure fundamentally

different aspects of microbial resource use. Soil Biol. Biochem. 169, 108677. https://doi.org/10.1016/j.soilbio.2022.108677

Schimel, J.P., Bennett, J., 2004. Nitrogen mineralization: Challenges of a changing paradigm Ecology. 85. 591–602. https://doi.org/10.1890/03-8002

Schleppi, P., Bucher-Wallin, I., Hagedorn, F., Körner, C., 2012. Increased nitrate availability in the soil of a mixed mature temperate forest subjected to elevated CO2 concentration (canopy FACE). Glob. Change Biol. 18, 757–768. https://doi.org/10.1111/j.1365-2486.2011.02559.x

Sgouridis, F., Reay, M., Cotchim, S., Ma, J., Radu, A., Ullah, S., 2023. Stimulation of soil gross nitrogen transformations and nitrous oxide emission under Free air CO2 enrichment in a mature temperate oak forest at BIFoR-FACE. Soil Biol. Biochem. 184, 109072. https://doi.org/10.1016/j.soilbio.2023.109072

Shi, S., Richardson, A.E., O'Callaghan, M., DeAngelis, K.M., Jones, E.E., Stewart, A., Firestone, M.K., Condron, L.M., 2011. Effects of selected root exudate components on soil bacterial communities: Root exudate components and soil microbial communities. FEMS Microbiol. Ecol. 77, 600–610. https://doi.org/10.1111/j.1574-6941.2011.01150.x

Sinsabaugh, R.L., 2010. Phenol oxidase, peroxidase and organic matter dynamics of soil. Soil Biol. Biochem. 42, 391–404. https://doi.org/10.1016/j.soilbio.2009.10.014

Sinsabaugh, R.L., Turner, B.L., Talbot, J.M., Waring, B.G., Powers, J.S., Kuske, C.R., Moorhead, D.L., Follstad Shah, J.J., 2016. Stoichiometry of microbial carbon use efficiency in soils. Ecol. Monogr. 86, 172–189. https://doi.org/10.1890/15-2110.1

Smercina, D.N., Evans, S.E., Friesen, M.L., Tiemann, L.K., 2019. To Fix or Not To Fix: Controls on Free-Living Nitrogen Fixation in the Rhizosphere. Appl. Environ. Microbiol. 85, e02546-18. https://doi.org/10.1128/AEM.02546-18

Socci, A.M., Templer, P.H., 2011. Temporal patterns of inorganic nitrogen uptake by mature sugar maple (*Acer saccharum* Marsh.) and red spruce (*Picea rubens* Sarg.) trees using two common approaches. Plant Ecol. Divers. 4, 141–152. https://doi.org/10.1080/17550874.2011.624557

Son, Y., 2001. Non-symbiotic nitrogen fixation in forest ecosystem. Ecol Res 16, 183–196. https://doi.org/10.1046/j.1440-1703.2001.00385.x

Spohn, M., 2015. Microbial respiration per unit microbial biomass depends on litter layer carbon-to-nitrogen ratio. Biogeosciences 12, 817–823. https://doi.org/10.5194/bg-12-817-2015

Stadler, J., Gebauer, G., Schulze, E.-D., 1993. The Influence of Ammonium on Nitrate Uptake and Assimilation in 2-Year-Old Ash and Oak Trees - A Tracer-Study with ^{15} N. Isot. Isot. Environ. Health Stud. 29, 85–92. https://doi.org/10.1080/10256019308046139

Steffen, W., Richardson, K., Rockstrom, J., Cornell, S.E., Fetzer, I., Bennett, E.M., Biggs, R., Carpenter, S.R., de Vries, W., de Wit, C.A., Folke, C., Gerten, D., Heinke, J., Mace, G.M., Persson, L.M., Ramanathan, V., Reyers, B., Sorlin, S., 2015. Planetary boundaries: Guiding human development on a changing planet. Science 347, 1259855–1259855. https://doi.org/10.1126/science.1259855

Steidinger, B.S., Crowther, T.W., Liang, J., Van Nuland, M.E., Werner, G.D.A., Reich, P.B., Nabuurs, G.J., de-Miguel, S., Zhou, M., Picard, N., Herault, B., Zhao, X., Zhang, C., Routh, D., Peay, K.G., 2019. Climatic controls of decomposition drive the global biogeography of forest-tree symbioses. Nature 569, 404–408. https://doi.org/10.1038/s41586-019-1128-0

Strauss, E.A., Lamberti, G.A., 2002. Effect of dissolved organic carbon quality on microbial decomposition and nitrification rates in stream sediments. Freshw. Biol. 47, 65–74. https://doi.org/10.1046/j.1365-2427.2002.00776.x

Strock, J.S., 2008. Ammonification, in: Encyclopedia of Ecology. Elsevier, pp. 162–165. https://doi.org/10.1016/B978-008045405-4.00256-1

Stuart, E.K., Plett, K.L., 2020. Digging Deeper: In Search of the Mechanisms of Carbon and Nitrogen Exchange in Ectomycorrhizal Symbioses. Front. Plant Sci. 10, 1658. https://doi.org/10.3389/fpls.2019.01658

Subbarao, G.V., Rondon, M., Ito, O., Ishikawa, T., Rao, I.M., Nakahara, K., Lascano, C., Berry, W.L., 2007. Biological nitrification inhibition (BNI)—is it a widespread phenomenon? Plant Soil 294, 5–18. https://doi.org/10.1007/s11104-006-9159-3

Tang, Y., Yu, G., Zhang, X., Wang, Q., Tian, D., Tian, J., Niu, S., Ge, J., 2019. Environmental variables better explain changes in potential nitrification and denitrification activities than microbial properties in fertilized forest soils. Sci. Total Environ. 647, 653–662. https://doi.org/10.1016/j.scitotenv.2018.07.437

Terrer, C., Phillips, R.P., Hungate, B.A., Rosende, J., Pett-Ridge, J., Craig, M.E., Van Groenigen, K.J., Keenan, T.F., Sulman, B.N., Stocker, B.D., Reich, P.B., Pellegrini, A.F.A., Pendall, E., Zhang, H., Evans, R.D., Carrillo, Y., Fisher, J.B., Van Sundert, K., Vicca, S., Jackson, R.B., 2021. A trade-off between plant and soil carbon storage under elevated CO2. Nature 591, 599–603. https://doi.org/10.1038/s41586-021-03306-8

Terrer, C., Vicca, S., Hungate, B.A., Phillips, R.P., Prentice, I.C., 2016. Mycorrhizal association as a primary control of the CO_2 fertilization effect. Science 353, 72–74. https://doi.org/10.1126/science.aaf4610

Terrer, C., Vicca, S., Stocker, B.D., Hungate, B.A., Phillips, R.P., Reich, P.B., Finzi, A.C., Prentice, I.C., 2018. Ecosystem responses to elevated CO_2 governed by plant–soil interactions and the cost of nitrogen acquisition. New Phytol. 217, 507–522. https://doi.org/10.1111/nph.14872

Thornton, P.E., Lamarque, J., Rosenbloom, N.A., Mahowald, N.M., 2007. Influence of carbon-nitrogen cycle coupling on land model response to CO_2 fertilization and climate variability. Glob. Biogeochem. Cycles 21, 2006GB002868. https://doi.org/10.1029/2006GB002868

Tipping, E., 2017. Long-term increases in soil carbon due to ecosystem fertilization by atmospheric nitrogen deposition demonstrated by regional-scale modelling and observations. Sci. Rep. 11. https://doi.org/10.1038/s41598-017-02002-w

Tipping, E., Somerville, C.J., Luster, J., 2016. The C:N:P:S stoichiometry of soil organic matter. Biogeochemistry 130, 117–131. https://doi.org/10.1007/s10533-016-0247-z

Tobita, H., Yazaki, K., Harayama, H., Kitao, M., 2016. Responses of symbiotic N2 fixation in Alnus species to the projected elevated CO2 environment. Trees 30, 523–537. https://doi.org/10.1007/s00468-015-1297-x

Tor-ngern, P., Oren, R., Ward, E.J., Palmroth, S., McCarthy, H.R., Domec, J., 2015. Increases in atmospheric CO_2 have little influence on transpiration of a temperate forest canopy. New Phytol. 205, 518–525. https://doi.org/10.1111/nph.13148

Uddling, J., Teclaw, R.M., Pregitzer, K.S., Ellsworth, D.S., 2009. Leaf and canopy conductance in aspen and aspen-birch forests under free-air enrichment of carbon dioxide and ozone. Tree Physiol. 29, 1367–1380. https://doi.org/10.1093/treephys/tpp070

Ullah, S., Moore, T.R., 2009. Soil drainage and vegetation controls of nitrogen transformation rates in forest soils, southern Quebec. J. Geophys. Res. Biogeosciences 114, 2008JG000824. https://doi.org/10.1029/2008JG000824

Ullah, S., Saiz Val, E., Sgouridis, F., Drijfhout, F., 2020. Early response of biological nitrogen fixation in a mature oak dominated forest to elevated atmospheric CO2 fumigation at BIFoR-FACE (other). oral. https://doi.org/10.5194/egusphere-egu2020-8678

Uri, V., Lõhmus, K., Tullus, H., 2003. Annual net nitrogen mineralization in a grey alder (Alnus incana (L.) moench) plantation on abandoned agricultural land. For. Ecol. Manag. 184, 167–176. https://doi.org/10.1016/S0378-1127(03)00210-X

US Department of Commerce, N., n.d. Global Monitoring Laboratory - Carbon Cycle Greenhouse Gases. URL https://gml.noaa.gov/ccgg/trends/ (accessed 2.20.24).

U.S. DOE, 2020. U.S. Department of Energy Free-Air CO2 Enrichment Experiments: FACE Results, Lessons, and Legacy. U.S. Department of Energy Office of Science.

Van Der Woude, A.M., Peters, W., Joetzjer, E., Lafont, S., Koren, G., Ciais, P., Ramonet, M., Xu, Y., Bastos, A., Botía, S., Sitch, S., De Kok, R., Kneuer, T., Kubistin, D., Jacotot, A., Loubet, B., Herig-Coimbra, P.-H., Loustau, D., Luijkx, I.T., 2023. Temperature extremes of 2022 reduced carbon uptake by forests in Europe. Nat. Commun. 14, 6218. https://doi.org/10.1038/s41467-023-41851-0

van Groenigen, K.-J., de Graaff, M.-A., Six, J., Harris, D., Kuikman, P., van Kessel, C., 2006. The Impact of Elevated Atmospheric [CO2] on Soil C and N Dynamics: A Meta-Analysis, in: Nösberger, J., Long, S.P., Norby, R.J., Stitt, M., Hendrey, G.R., Blum, H. (Eds.), Managed Ecosystems and CO2, Ecological Studies. Springer Berlin Heidelberg, Berlin, Heidelberg, pp. 373–391. https://doi.org/10.1007/3-540-31237-4_21

Verburg, P.S.J., Cheng, W., Johnson, D.W., Schorran, D.E., 2004. Nonsymbiotic nitrogen fixation in 3-year-old Jeffrey pines and the role of elevated [CO2]. Canadian Journal of Forest Research, 34, 1979-1984. https://doi.org/10.1139/x04-077

Verchot, L.V., Holmes, Z., Mulon, L., Groffman, P.M., Lovett, G.M., 2001. Gross vs net rates of N mineralization and nitrification as indicators of functional differences between forest types. Soil Biol. Biochem. 33, 1889–1901. https://doi.org/10.1016/S0038-0717(01)00095-5

Vitousek, P.M., Hedin, L.O., Matson, P.A., Fownes, J.H., Neff, J., 1998. Within-System Element Cycles, Input-Output Budgets, and Nutrient Limitation, in: Pace, M.L., Groffman, P.M. (Eds.), Successes, Limitations, and Frontiers in Ecosystem Science. Springer New York, New York, NY, pp. 432–451. https://doi.org/10.1007/978-1-4612-1724-4_18

Vitousek, P.M., Menge, D.N.L., Reed, S.C., Cleveland, C.C., 2013. Biological nitrogen fixation: rates, patterns and ecological controls in terrestrial ecosystems. Philos. Trans. R. Soc. B Biol. Sci. 368, 20130119. https://doi.org/10.1098/rstb.2013.0119

Wanek, W., Mooshammer, M., Blöchl, A., Hanreich, A., Richter, A., 2010. Determination of gross rates of amino acid production and immobilization in decomposing leaf litter by a novel 15N isotope pool dilution technique. Soil Biol. Biochem. 42, 1293–1302. https://doi.org/10.1016/j.soilbio.2010.04.001

Wang, C., Wan, S., Xing, X., Zhang, L., Han, X., 2006. Temperature and soil moisture interactively affected soil net N mineralization in temperate grassland in Northern China. Soil Biol. Biochem. 38, 1101–1110. https://doi.org/10.1016/j.soilbio.2005.09.009

Wang, R., Bicharanloo, B., Hou, E., Jiang, Y., Dijkstra, F.A., 2022. Phosphorus Supply Increases Nitrogen Transformation Rates and Retention in Soil: A Global Meta-Analysis. Earths Future 10, e2021EF002479. https://doi.org/10.1029/2021EF002479

Wang, X., Cui, Y., Wang, Y., Duan, C., Niu, Y., Sun, R., Shen, Y., Guo, X., Fang, L., 2022. Ecoenzymatic stoichiometry reveals phosphorus addition alleviates microbial nutrient limitation and promotes soil carbon sequestration in agricultural ecosystems. J. Soils Sediments 22, 536–546. https://doi.org/10.1007/s11368-021-03094-8

Ward, E.J., Oren, R., Seok Kim, H., Kim, D., Tor-ngern, P., Ewers, B.E., McCarthy, H.R., Oishi, A.C., Pataki, D.E., Palmroth, S., Phillips, N.G., Schäfer, K.V.R., 2018. Evapotranspiration and water yield of a pine-broadleaf forest are not altered by long-term atmospheric [CO_2] enrichment under native or enhanced soil fertility. Glob. Change Biol. 24, 4841–4856. https://doi.org/10.1111/gcb.14363

Warren, C.R., 2019. Isotope pool dilution reveals rapid turnover of small quaternary ammonium compounds. Soil Biol. Biochem. 131, 90–99. https://doi.org/10.1016/j.soilbio.2019.01.004

Webb, G.A., 1999. Nitrogen NMR*, in: Encyclopedia of Spectroscopy and Spectrometry. Elsevier, pp. 1790–1799. https://doi.org/10.1016/B978-0-12-374413-5.00219-0

Wen, T., Yu, G.-H., Hong, W.-D., Yuan, J., Niu, G.-Q., Xie, P.-H., Sun, F.-S., Guo, L.-D., Kuzyakov, Y., Shen, Q.-R., 2022. Root exudate chemistry affects soil carbon mobilization via microbial community reassembly. Fundam. Res. 2, 697–707. https://doi.org/10.1016/j.fmre.2021.12.016

Xiao, W., Chen, X., Jing, X., Zhu, B., 2018. A meta-analysis of soil extracellular enzyme activities in response to global change. Soil Biol. Biochem. 123, 21–32. https://doi.org/10.1016/j.soilbio.2018.05.001

Xu, X., Hui, D., King, A.W., Song, X., Thornton, P.E., Zhang, L., 2015. Convergence of microbial assimilations of soil carbon, nitrogen, phosphorus and sulfur in terrestrial ecosystems. Sci. Rep. 5, 17445. https://doi.org/10.1038/srep17445

Yan, S., Yin, L., Dijkstra, F.A., Wang, P., Cheng, W., 2023. Priming effect on soil carbon decomposition by root exudate surrogates: A meta-analysis. Soil Biol. Biochem. 178, 108955. https://doi.org/10.1016/j.soilbio.2023.108955

Yin, L., Dijkstra, F.A., Phillips, R.P., Zhu, B., Wang, P., Cheng, W., 2021. Arbuscular mycorrhizal trees cause a higher carbon to nitrogen ratio of soil organic matter decomposition via rhizosphere priming than ectomycorrhizal trees. Soil Biol. Biochem. 108246. https://doi.org/10.1016/j.soilbio.2021.108246

Yu, L., Zhang, Q., Tian, Y., Sun, W., Scheer, C., Li, T., Zhang, W., 2022. Global variations and drivers of nitrous oxide emissions from forests and grasslands. Front. Soil Sci. 2, 1094177. https://doi.org/10.3389/fsoil.2022.1094177

Yu, W., Huang, W., Weintraub-Leff, S.R., Hall, S.J., 2022. Where and why do particulate organic matter (POM) and mineral-associated organic matter (MAOM) differ among diverse soils? Soil Biol. Biochem. 172, 108756. https://doi.org/10.1016/j.soilbio.2022.108756

Zak, D.R., Holmes, W.E., Finzi, A.C., Norby, R.J., Schlesinger, W.H., 2003. Soil nitrogen cycling under elevated CO_2: a synthesis of forest face experiments. Ecol. Appl. 13, 1508–1514. https://doi.org/10.1890/03-5055

Zhalnina, K., Louie, K.B., Hao, Z., Mansoori, N., Da Rocha, U.N., Shi, S., Cho, H., Karaoz, U., Loqué, D., Bowen, B.P., Firestone, M.K., Northen, T.R., Brodie, E.L., 2018. Dynamic root exudate chemistry and microbial substrate preferences drive patterns

in rhizosphere microbial community assembly. Nat. Microbiol. 3, 470–480. https://doi.org/10.1038/s41564-018-0129-3

Zhang, Q., Li, Y., Wang, M., Wang, K., Meng, F., Liu, L., Zhao, Y., Ma, L., Zhu, Q., Xu, W., Zhang, F., 2021. Atmospheric nitrogen deposition: A review of quantification methods and its spatial pattern derived from the global monitoring networks. Ecotoxicol. Environ. Saf. 216, 112180. https://doi.org/10.1016/j.ecoenv.2021.112180

Zhang, Y., Wang, J., Dai, S., Zhao, J., Huang, X., Sun, Y., Chen, J., Cai, Z., Zhang, J., 2019. The effect of C:N ratio on heterotrophic nitrification in acidic soils. Soil Biol. Biochem. 137, 107562. https://doi.org/10.1016/j.soilbio.2019.107562

Zhang, Z., Qiao, M., Li, D., Yin, H., Liu, Q., 2016. Do warming-induced changes in quantity and stoichiometry of root exudation promote soil N transformations via stimulation of soil nitrifiers, denitrifiers and ammonifiers? Eur. J. Soil Biol. 74, 60–68. https://doi.org/10.1016/j.ejsobi.2016.03.007

Zheng, M., Zhang, W., Luo, Y., Wan, S., Fu, S., Wang, S., Liu, N., Ye, Q., Yan, J., Zou, B., Fang, C., Ju, Y., Ha, D., Zhu, L., Mo, J., 2019. The Inhibitory Effects of Nitrogen Deposition on Asymbiotic Nitrogen Fixation are Divergent Between a Tropical and a Temperate Forest. Ecosystems 22, 955–967. https://doi.org/10.1007/s10021-018-0313-6

Zheng, M., Zhou, Z., Zhao, P., Luo, Y., Ye, Q., Zhang, K., Song, L., Mo, J., 2020. Effects of human disturbance activities and environmental change factors on terrestrial nitrogen fixation. Glob. Change Biol. 26, 6203–6217. https://doi.org/10.1111/gcb.15328

Zheng, Q., Ding, J., Lin, W., Yao, Z., Li, Q., Xu, C., Zhuang, S., Kou, X., Li, Y., 2022. The influence of soil acidification on N2O emissions derived from fungal and bacterial denitrification using dual isotopocule mapping and acetylene inhibition. Environ. Pollut. 303, 119076. https://doi.org/10.1016/j.envpol.2022.119076

Zheng, X., Liu, Q., Ji, X., Cao, M., Zhang, Y., Jiang, J., 2021. How do natural soil NH_4^+, NO_3^- and N_2O interact in response to nitrogen input in different climatic zones? A global meta-analysis. Eur. J. Soil Sci. 72, 2231–2245. https://doi.org/10.1111/ejss.13131

Zhu, X., Liu, D., Yin, H., 2021. Roots regulate microbial N processes to achieve an efficient NH4+ supply in the rhizosphere of alpine coniferous forests. Biogeochemistry 155, 39–57. https://doi.org/10.1007/s10533-021-00811-w

Ziegler, C., Kulawska, A., Kourmouli, A., Hamilton, L., Shi, Z., MacKenzie, A.R., Dyson, R.J., Johnston, I.G., 2023. Quantification and uncertainty of root growth stimulation by elevated CO2 in a mature temperate deciduous forest. Sci. Total Environ. 854, 158661. https://doi.org/10.1016/j.scitotenv.2022.158661

Zwetsloot, M.J., Kessler, A., Bauerle, T.L., 2018. Phenolic root exudate and tissue compounds vary widely among temperate forest tree species and have contrasting effects on soil microbial respiration. New Phytol. 218, 530–541. https://doi.org/10.1111/nph.15041